THE OXIDATIVE STORAGE AND REDUCTIVE RELEASE OF SULPHUR COMPOUNDS BY AUTOMOBILE CATALYTIC CONVERTERS

A. P. HARVEY

PhD.

The University of Edinburgh

1998

Acknowledgements

I would like to thank Mike Davidson, my supervisor.

I would like to thank all those in this Department who have helped me in this work; Des Costello, Matthew Rea, Tom Pringle, and Kenny, Rab and Bobby in the workshop. In addition, I'd like to thank my friends here in the Department, whose moral support has been invaluable.

I'd like to thank my parents for remembering, occasionally, not to ask if I'd finished yet.

I'd like to thank all those at Johnson Matthey, that's Neil, Bob, Martyn and Chris (and, no doubt others) for their good ideas.

Most of all, thanks to Katie for her support and patience.

Abstract

Hydrogen sulphide emission by catalytic converter-fitted automobiles is a problem, because the gas has an extremely unpleasant odour, which is detectable by the human nose at concentrations below 1 ppm.

The problematic hydrogen sulphide emissions are produced by the "storage release" mechanism, in which the catalyst adsorbs sulphur dioxide during net oxidising conditions and releases it very rapidly as hydrogen sulphide when the stoichiometry of the exhaust gas changes to net reducing. After a prolonged period of oxidative storage the peak emission of hydrogen sulphide by "storage release" can greatly exceed that possible by direct conversion of sulphur dioxide during net reducing conditions (termed the "steady state" mode of emission).

Components of the formulation of typical TWCs (Three Way Converters), as well as iron, nickel and barium doped analogues, were prepared. Storage-release sequences were then simulated on the samples at a number of different temperatures on purpose-built 'catalyst test apparatus'. Temperature programmed reductions were performed in the same apparatus by dosing the samples with sulphur dioxide in oxidising conditions at 500 °C (the temperature at which the emission of hydrogen sulphide is conventionally said to become a problem). The TPR spectra exhibited sulphur dioxide and hydrogen sulphide peaks, the hydrogen sulphide peak always occurring at the higher temperature.

The addition of platinum to various oxides and oxide mixtures was shown to increase the proportion of stored sulphur emitted as hydrogen sulphide and to lower the temperature at which storage-release effects occur. These effects were evident in the lowered temperatures at which the TPR spectra peak maxima occurred and the increased size of hydrogen sulphide peaks relative to those of sulphur dioxide.

Iron and nickel doping was demonstrated to greatly attenuate hydrogen sulphide emissions. The TPR spectra of these samples exhibited pronounced 'tailing' of the hydrogen sulphide peaks, which was attributed to the decomposition of sulphide species. Their *modus operandi* was to form sulphates, which decompose to the oxide (and sulphur dioxide) or a sulphide, which decomposes more slowly with the release of hydrogen sulphide. The net effect was that most of the adsorbed sulphur dioxide was emitted as sulphur dioxide, and the relatively small amount that was emitted as hydrogen sulphide was emitted slowly. Barium doping attenuated hydrogen sulphide emission to a much lesser extent, and is not considered a viable alternative to nickel or iron, which are used in practice.

Table of Contents

Tables

Table of Figures

Symbols and Abbreviations Used

β	Linear Heating Rate	(^{o}C/min.)
ν	Kinematic viscosity	(m^2/s)
ν_a	Pre-exponential factor for adsorption	
ν_δ	Pre-exponential factor for desorption	
λ	Wavelength.	(m)
ϕ	Thiele modulus.	
θ	Fractional Surface Coverage	
A/F	Air-Fuel (ratio)	
BEI	Backscattered Electron Imaging	
C_g	Concentration of gas	(mol/m^3)
D	Diffusivity	(m^2/s)
DRIFTS	Diffuse Reflectance Infrared Fourier Transform Spectroscopy	
d_e	Effective particle diameter	(m)
E_a	Activation energy	(J)
E_d	Desorption energy	(J/mol)
F	Volumetric flowrate	(m^3/s)
FTIR	Fourier Transform Infrared.	
GIV	Gas Injection Valve	
I	Amplitude of adsorbate pulse	(mol/m^3)
k_a	Rate constant of adsorption	(m^3/mol.s)
k_d	Rate constant of desorption	(s^{-1})
$k_d(\theta)$	Rate constant of desorption as function of θ	(s^{-1})
l	Bed depth	(m)
NDIR	Non-Dispersive Infrared	
NMHC	Non-Methane Hydrocarbon	
NOx	Oxides of nitrogen	
p	Power dependence of the adsorption kinetics	
Pe	Peclet number	
PAH	Polycyclic Aromatic Hydrocarbon	
PGM	Platinum Group Metal.	
R_a	Rate of adsorption	(s^{-1})
R_d	Rate of desorption	(s^{-1})
Re	Reynolds number	
Re_p	Particle Reynolds number	
S	External surface area	(m^2)
S_0	Initial amount of reducible species	(μmol)

SEM	Scanning Electron Microscopy.	
Sh	Sherwood number.	
SOx	Sulphur oxides	
t	Time	(s)
T	Temperature	(^{o}C)
T_o	Initial temperature	(^{o}C)
T_{max}	Temperature at which TPR peak maximum occurs	(^{o}C)
TCD	Thermal Conductivity Detector.	
TEM	Transmission Electron Spectroscopy	
THC	Total Hydrocarbons.	
TPD	Temperature Programmed Desorption.	
TPR	Temperature Programmed Reduction or Reaction	
TPSR	Temperature Programmed Surface Reaction	
TPO	Temperature Programmed Oxidation	
TWC	Three Way Catalyst	
u	Interstitial gas velocity	(m/s)
V*	Total flowrate of reducing gas	(cm^3(NTP)/s)
V_c	Total solid volume	(m^3)
V_m	Moles of surface sites per unit volume	(mol/m^3)
VOC	Volatile Organic Compounds	
W	Width of adsorbate pulse	(m)
W1/2	Half width of TPR peak	(^{o}C)
W3/4	Three quarters width of TPR peak	(^{o}C)
XPS	X-ray Photoelectron Spectrometry.	
XRD	X-ray Diffraction/Diffractometry	
XRPD	X-ray Powder Diffraction/Diffractometry	
WDS	Wavelength Dispersive Spectroscopy.	
z	Axis along bed of reactant particles	

1. Introduction

Automobile catalytic converters will, in certain circumstances, produce malodorous hydrogen sulphide. In this thesis the results of investigations into the process by which the hydrogen sulphide is emitted are reported. The role of automobile catalytic converters is reviewed in this chapter. An overview of catalysis, with emphasis on heterogeneous catalysis, is also given.

1.1 The Autocatalyst

The most widely used heterogeneous catalyst is the automobile three-way converter (TWC), which has been fitted to all new cars in Europe since January 1993 (Henssler, 1991). The contribution of all other catalysts to the world market is dwarfed by that of the 'autocatalyst'. Hence, a problem with the 'autocatalyst', is very significant: firstly, because there are so many converter-fitted vehicles and, secondly, because any problems are noticeable by, and directly affect, the general public.

1.1.1 Pollution by Automobiles

Ideally, the combustion of petroleum to provide the power requirement for automobiles would proceed as follows;

$$\text{Petroleum Hydrocarbons} + O_2 \rightarrow CO_2 + H_2O(+ Energy)$$

i.e., with *no* partial combustion products. In reality, combustion in petrol-fuelled vehicles is seldom complete. One of the main reasons for this is that engines are often designed to be run on a fuel/air mixture which is close to stoichiometric. Increased 'performance' is said to result from running the vehicle slightly below stoichiometry. This decreases the fuel economy, as there is not sufficient oxygen present for complete combustion. Automobiles running substantially fuel-lean (i.e., 'lean-burn') produce much fewer partial combustion products, and have increased fuel economy.

The major products of incomplete combustion of petroleum are:

CO	1 - 2 vol. %
Hydrocarbons	500 - 1000 vppm

(Heck and Farrauto (1993))

The lack of oxygen in the mixture means that the hydrocarbons cannot form fully oxidised products. Instead they remain unreacted (hydrocarbons) or partially reacted (CO and various hydrocarbon byproducts, e.g., alkenes, aldehydes). Combustion of other fuels, such as diesel, takes place in excess oxygen, leading to lower CO and hydrocarbon emissions, but there are other pollution problems associated with diesel vehicles (see 'Literature Survey').

Both species are pollutants; CO, because of its direct toxicity, replacing oxygen in haemoglobin, and hydrocarbons, primarily because of their contribution to photochemical smog, but also because of direct health effects; hydrocarbons are suspected carcinogens and can cause headaches, nausea and respiratory problems.

The third major pollutant produced by automobiles is NO_x (100 - 3000 vppm), a collective term for nitrogen's oxides (mainly nitric oxide, NO, with some nitrogen dioxide, NO_2). The NO_x from automobiles is not formed by incomplete combustion, but by thermal fixation of N_2 at the extremely high temperatures occurring inside the combustion chamber (typically > 1500°C (Warr (1994)). This 'thermal NO_x' is formed by the Zel'dovich mechanism. NO_x is a greater environmental problem than hydrocarbons and CO, for the following reasons:

- It leads to the formation of NO_2, a brown gas that decreases visibility and reduces air quality. NO_2 decreases lung function and increases susceptibility to respiratory diseases (Radojevic (1998)).
- It contributes to acid rain. Currently its contribution is similar to that of sulphur dioxide, but in some areas of the USA it is the principal cause[1].
- It participates in the formation of ozone at ground level (ozone acts to impair lung function, irritates the eyes, nose and throat, and causes coughing and chest discomfort).

---

[1] Western U.S.A. has many vehicles and fewer fossil fuel burning power stations (to produce SO_2).

- It participates, along with hydrocarbons, in the cycle of reactions which produce peroxyacyl nitrates (principally peroxyacetyl nitrate, PAN), which are powerful lachrymators.
- Formation of nitrate aerosols which disperse light, decreasing visibility further during photochemical smogs
- NO_x and ozone damage vegetation

Hydrocarbons and CO also participate in the cycle of reactions which lead to the formation of photochemical smog, but NO_x is the main contributor.

An idea of the amounts of pollution produced by road transport relative to other anthropogenic sources of pollution is given by the following table;

Source	SO_2	NO_x	CO	VOC	Black Smoke
Road Transport	2	51	90	41	46
Power	72	28	1	-	6
Other Industry	19	9	4	52	14
Domestic	3	2	4	2	33
Other	7	9	-	4	1
Total (kT)	3774	2719	6659	2396	453

Table 1: Contributions of various sources to primary air pollutants as % of total, (Dept. of Environment, (1992))

The table demonstrates that automobiles are one of the major contributors to carbon monoxide and hydrocarbon emission. Their detrimental effect on human health is greater than other sources, because of the geography of the emissions, in that emissions are localised in the areas of greatest population density. Another problem is that it is more difficult to tackle the emissions from automobiles, because the emissions are not centralised, as they are for power stations; the responsibility lying instead in the hands of individuals. This tends to slow down the progress of legislation for preventative measures, and render it more difficult to enforce. A symptom of this is research by Calvert *et al.* (1993), which has shown that some of the largest contributions to automobile generated pollution in the USA are 'super-emitters'; the 5% of the car owning population who do not maintain their converters.

Anthropogenic sources of NOx, are far outweighed by natural sources (bacteria, volcanoes and lightning), but are a greater pollution problem, because the emissions are localised in areas of high population density. The greatest problems due to NOx occur when a meteorological phenomenon known as a 'temperature inversion' occurs. This is when a cooler layer of air is trapped beneath a warmer layer causing the pollutants to be trapped (see diagram), leading to 'photochemical smog'. The situation occurs frequently in Los Angeles, because of its bowl-shaped topography, prompting the region to enforce the most stringent and far-reaching emissions legislation in the World

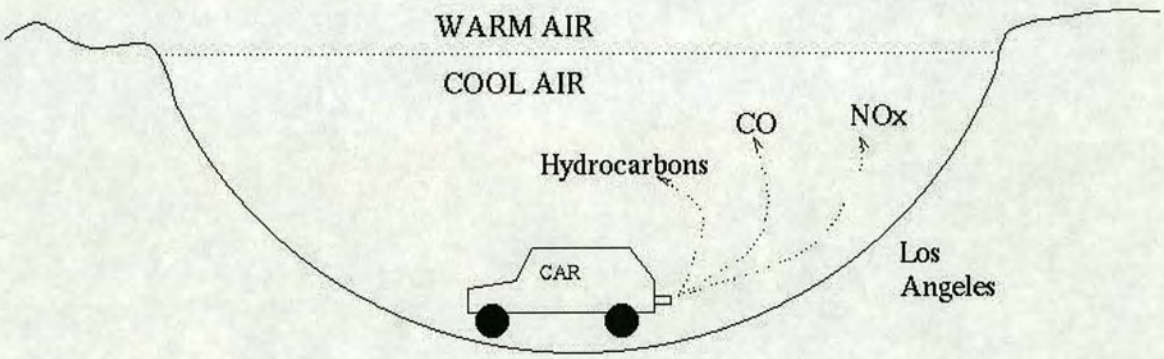

Figure 1: A Temperature Inversion

The concentration of pollutants and their derivatives builds up in the atmosphere, causing lower air quality and visibility. The link between poor air quality and hospital admissions for respiratory illnesses has long been established (e.g., Viala (1989)).

1.1.2 Legislation

Since the invention of automobile catalytic converters in the early 1970s (for a comprehensive review see Heck and Farrauto (1993)), legislation has been the driving force behind the development of the autocatalyst. It has dictated the speed and direction of every technological advance. California's serious problems with photochemical smog caused the region to introduce the first automobile emissions legislation in 1971, and ever since it has led the way, in terms of increasingly stringent emissions legislation. The standards brought in by California have, so far, been followed a few years later by the rest of the United States, and later again by Europe.

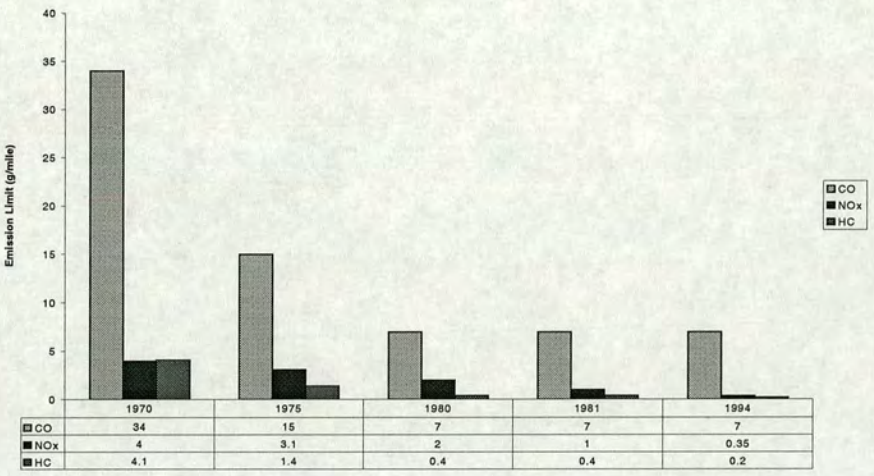

	1970	1975	1980	1981	1994
CO	34	15	7	7	7
NOx	4	3.1	2	1	0.35
HC	4.1	1.4	0.4	0.4	0.2

Figure 2: US Emissions Legislation (Warr et al. (1994))

The histogram below illustrates how emission standards have changed in the European Union. Recently European legislation has been catching up with that of the USA.

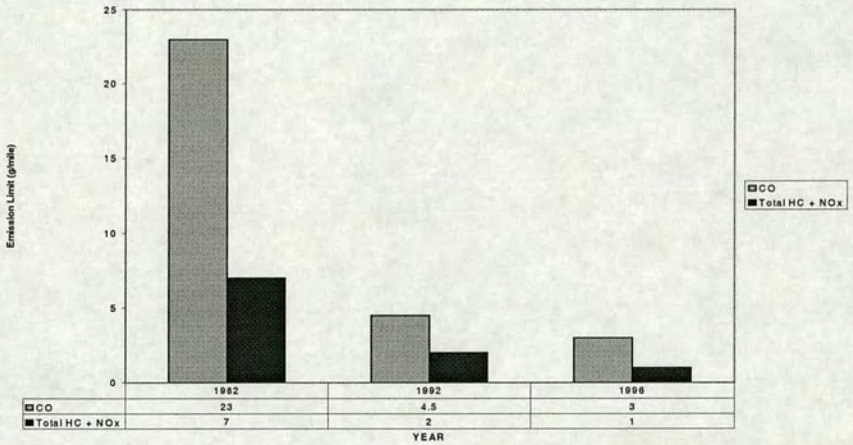

	1982	1992	1996
CO	23	4.5	3
Total HC + NOx	7	2	1

Figure 3: The Development of EEC Emission Legislation (Warr et al. (1994))

In the EEC all new cars have been legally required to be fitted with catalytic converters since January 1993 (Henssler (1991)).

1.1.3 The Hydrogen Sulphide Problem

As the number of catalytic converter-equipped vehicles on the road increases, one of their drawbacks is becoming more apparent; that is, that they produce malodorous hydrogen sulphide .

Hydrogen sulphide *is* a pollutant; its acid rain - forming potential is essentially the same as sulphur dioxide and it is described as a "a very poisonous gas", Sharp (1983). The amounts emitted, though, are small compared to the main pollutants from automobiles and, consequently, there are no legal limits for hydrogen sulphide production by automobiles. Much of the sulphur will be emitted as sulphur dioxide and, as can be seen in Table 1, automobiles are far from being the greatest producers.

The main problem with hydrogen sulphide emission is that, even at very low concentrations (see table below), well before its toxicity becomes an issue, it has a distinctive, unpleasant odour.

Concentration (ppm)	**Effect on Humans**
0.02 - 0.03	Odour threshold[2]
0.15 - 0.20	Offensive odour
10	Threshold limit
15	Short time exposure
50	Eye irritation
100 - 200	Loss of smell
300 - 500	Threat to life
500 - 1000	Unconsciousness

Figure 4: The Effect of Hydrogen Sulphide at Various Concentrations, Gottberg et al. *(1989)*

The odour threshold should be compared with the lower smell limits for the sulphur oxides (10 ppm and 280 ppb for the dioxide and trioxide, respectively) to give some idea of just how pungent hydrogen sulphide is.

So, although modern TWCs convert almost all of the toxic or environmentally detrimental gases into less harmful species, the exhaust gas mixture can smell *much* worse than it did before their introduction. This is a serious problem for autocatalyst manufacturers.

---

[2] In Lox *et al.* (1989) the 'lower smell limit' is given even lower, as 1 ppb

1.1.4 The Objectives of this Research

The objectives of this research are:

1. To simulate the storage-release mode of hydrogen sulphide emission in the laboratory.
2. To investigate the temperature dependence of the storage-release mechanism.
3. To investigate the effect of platinum on the storage-release behaviour.
4. To investigate the effects of dopants on the storage-release behaviour.
5. To investigate the *modus operandi* of known hydrogen sulphide emission attenuators and use the knowledge gained to suggest new additives.

1.2 Heterogeneous Catalysis

A catalyst can be simply defined as "a species which can alter the rate of a chemical process whilst undergoing no permanent chemical change itself". The catalyst participates in the reaction by becoming part of a transition state of lower energy than that by which the reaction normally proceeds. Hence, the activation energy is lowered and the reaction rate increased. It should be noted that the catalyst does not alter the *thermodynamics* of the reaction, only the kinetic rate. The catalyst can also be said to lower the temperature required for a reaction to proceed at a given rate.

Industrially there are many advantages to catalysing a chemical process;

- The energy and, therefore, cost savings due to lower temperature requirements.
- There may be increased product selectivity. Many industrial processes cannot work without the correct catalyst (e.g. enzyme-catalysed reactions, some polymerisation reactions).

It has been estimated (Harrison (1997)) that approximately 80% of new processes in the chemical industry involve some form of catalyst. Catalysis has been said to 'underpin 20% of world GNP' (Hutchings (1997)). This gives some idea of the importance of catalysis to today's chemical industry. Indeed, the UK Government's 'Foresight Initiative' identified catalysis as one of the most important areas for new research. To quote from the report:

> "The Chemicals Panel consider this area to be of key importance to the future success of the UK chemical industry and commends it as a key priority"

This is particularly important in the UK, as the chemical industry is one of the country's largest wealth generators.

The main distinction to be made in the field of catalysis is that between homogeneous and heterogeneous catalysis. Catalysis is said to be homogeneous when all the catalysed reactions occur in the same phase. The majority of these reactions are in the liquid phase, although others are known, e.g.;

- gas phase, $SO_2 \xrightarrow{NO} SO_3$

- solid phase, $KClO_3 \xrightarrow{MnO_2} KCl + \frac{3}{2}O_2$

Heterogeneous catalysis refers to catalysis where any of the phases present differ from one another. This is usually gas-solid, although other types are possible:

- Liquid-catalysed gas reactions, $C_2H_4 \xrightarrow{H_3PO_4} [CH_2CH_2]_n$
- Solid-catalysed liquid reactions, $H_2O_2 \xrightarrow{Au} H_2O + \frac{1}{2}O_2$
- Solid-catalysed gas-liquid reaction $ArNO_2 + H_2 \xrightarrow{Pd} ArNH_2$

Heterogeneous catalysts are used in many industrial processes e.g.,

- ammonia synthesis
- methanol production
- nitric acid production
- crude oil cracking
- sulphuric acid manufacture

Heterogeneous catalytic processes are usually preferred by industry for a number of reasons:

- Higher activity
- Ease of separation of products (as they are in different phases).
- Robustness

Given that catalysis is such an important part of one of the UK's leading industries, and that heterogeneous catalysis is industrially preferred, it seems strange to note that, in general, heterogeneous catalysis is much less well understood than homogeneous catalysis. The explanation lies in the fact that heterogeneous catalysis is a considerably more complex process, involving as it does many more processes (particularly mass transfer processes) than is the case in homogeneous catalysis. In addition, homogeneous catalysis is much more easily studied than heterogeneous; there are more direct means of studying solutions than there are of studying surfaces.

1.2.1 Reaction Kinetics

The reaction kinetics for heterogeneous reactions become much more complicated than for homogeneous systems, because of the added mass transfer step between phases. The mass transfer can dictate the rate of the reaction. If it is relatively slow compared to the reaction rate it can become the *rate determining step.* It is very important to recognise when a heterogeneous reaction is 'diffusion-controlled'. Possible symptoms of diffusion control are:

- Reaction rate being proportional to catalyst concentration to a power less than one.
- Rate being changed by altering the rate of gas flow relative to the catalyst.
- Apparent activation energy being low (e.g. 10-15 kJ/mol).

Most of the surface area of a typical oxide or supported oxide catalyst is internal, so the pore diffusion resistance can be very important.

Mass transfer is not only important prior to formation of products, but also afterwards. The surface must be freed of product, before further reactions can take place. It has been seen (Iwasawa (1997)) that fresh reactant may be required to displace the product from the surface. Like the reactant(s), the product(s), may have to overcome pore diffusion resistance and the surface gas film resistance.

1.2.2 Adsorption

The process of bringing the gas molecule into contact with the catalytic site and, for multimolecular reactions, the other reactant, occurs by two distinct processes; *physisorption* and *chemisorption*. Physisorption is the process whereby the gas molecule is first held at the solid surface. The molecule is attached by weak attractive forces due to polarisation of electron clouds (van der Waals forces). This does not form a chemical bond, but a weak, non-specific interaction and, consequently, desorption of physisorbed species is facile. Physisorption can be quantitatively described by equations such as the Langmuir or BET isotherms. These isotherms can be very important to the kinetics of many heterogeneous catalytic processes, as they give some idea of the rate of the adsorption process, which may determine the rate of the entire process.

Physisorption is a step on the way to chemisorption. The diagram below illustrates this process:

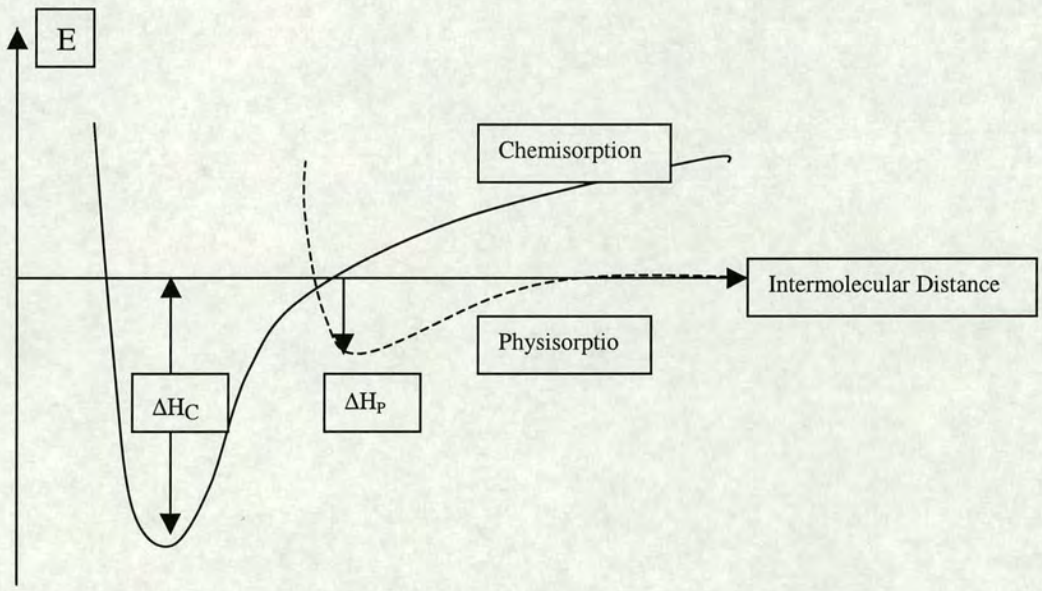

Figure 5: Physisorption aids Chemisorption

It can be seen that physisorption renders the energetics of chemisorption more favourable by bringing the reactants into close contact (ΔH_p is heat of physisorption, ΔH_c heat of chemisorption).

Chemisorption differs from physisorption in that strong chemical bonds are formed; the two forms of adsorption can only reliably be distinguished by their heats of desorption. Chemisorption in heterogeneous catalysis can be either dissociative, in which the bonds of the adsorbate molecule are broken, or associative in which the molecule retains its integrity. Chemisorption, as can be seen in the previous diagram, is a shorter range interaction. It differs from physisorption in that it cannot form surface multilayers, although chemisorbed species can penetrate the surface to form 'bulk' layers. Chemisorption is also more specific than physisorption, in that it will only take place between specific species at the correct site.

Much research has been conducted into reactions on the surfaces of single crystals, where specific active sites can be identified on well characterised surfaces, but for understanding real catalysts in use today these results may not be applicable. Oxide-supported catalyst surfaces do not have perfect surfaces; they consist of a number of categories of defects, dislocations and discontinuities, such as steps and vacancies. A surface itself is a discontinuity and, consequently has unbalanced molecular forces at the surface leading to a *surface energy*. Many heterogeneous reactions are site-specific, and this has led to increasing amounts of research into the types of sites present on real catalyst surfaces.

The entropy change of adsorption is always negative, meaning that for all adsorption processes where $\Delta G < 0$, ΔH is also negative (i.e., the process is exothermic), by the equation:

$$\Delta G = \Delta H - T\Delta S \qquad \text{Equation 1}$$

Hence, there is always a driving force for adsorption of species onto a surface.

One of the greatest practical problems in heterogeneous catalysis is poisoning; a good laboratory catalyst may prove impractical in the field if it is too sensitive to poisoning by feedstream impurities. During early research into autocatalysts one of the main reasons that platinum was preferred to certain base metal oxide catalysts was that it was less easily poisoned by impurities such as lead and sulphur.

2. Literature Survey

2.1 Introduction

This chapter reviews the background literature to all aspects of the interactions of autocatalysts with sulphur compounds. This will entail a description of the developments in the design of automobile catalytic converters, since their proposal in 1968. It will also cover the background literature to the experimental techniques used in this research and their application.

2.2 Autocatalyst Structure and Composition

2.2.1 Development of Autocatalysts

The first autocatalysts were oxidation catalysts designed to combat carbon monoxide and hydrocarbon emissions only. Legislation was later (USA, 1980) brought in to lower NOx emissions. This necessitated the use of so-called 'three-way catalysts' (TWCs) which could oxidise some components (CO, hydrocarbons), whilst reducing others (NOx).

The original European three-way catalyst, proposed in 1968, consisted of "a cordierite[3] monolith with 400 passages per square inch", (Gross *et al.* (1968)), coated with "20 wt. % pseudo-boehmite[4] with . . . lanthanides, to improve the high temperature stability and the adhesion to the carrier". The coating contained 35 - 40 g/ft^3 platinum and rhodium as the catalytic ingredients. Since that time catalytic converters have undergone a number of changes; Heck and Farrauto (1993) term today's autocatalysts "4th generation".

PGMs (platinum group metals) are the catalytic ingredients, with various metal oxides[5] forming a high surface area, thermally stable substrate. In the case of "90% of world market", (Beckwith *et al.* (1994)) the formulations are platinum/rhodium or platinum/rhodium/nickel to a PGM weighting of typically

---

[3] Cordierite : "Magnesium aluminium silicate with some iron", (Walker (1988)).
[4] Boehmite is a form of aluminium hydroxide.
[5] In the autocatalyst industry these are referred to by somewhat archaic names such as ceria and zirconia, hence they are referred to as such in this text.

0.5 wt.%. The PGMs function by catalysing reactions which render the exhaust gases harmless to the environment or to humans. The reactions catalysed (in a simplified form) are as follows:

$$\text{Hydrocarbons} + O_2 \rightarrow H_2O + CO_2$$

$$CO + 1/2O_2 \rightarrow CO_2$$

$$NO_x + xH_2 \rightarrow N_2 + xH_2O$$

2.2.1.1 The Oxidation Catalyst

Early catalytic converters in the USA (1976 - 1979)[6] were required to oxidise CO and hydrocarbons. There *were* NO_x emission standards, but these could be more easily achieved by a technique called Exhaust Gas Recirculation (EGR), which simply involved returning a certain portion of the exhaust gas to the combustion chamber, thereby cooling the chamber and reducing the production of 'thermal NOx'.

The converter was simply a washcoat of γ-alumina containing ~0.5 wt. % Pt on a cordierite monolith. Air was injected before the oxidation catalyst to ensure that the exhaust gas mixture had sufficient oxygen.

2.2.1.2 The Dual – Bed Autocatalyst

The dual-bed converter was the first response to legislation demanding lower NO_x emissions, which could no longer be achieved by EGR. The converter consisted, firstly, of a reduction catalyst containing rhodium. Rhodium had been found to have a lower ammonia-forming capability in reducing conditions than Pt or Pd (Heck and Farrauto (1993)). The formation of ammonia in the reducing bed was undesirable, partly because of the possibility of ammonia emission, but mainly because it tended to be oxidised back to NO_x in the oxidation catalyst.

The second part of the converter was an oxidation catalyst which was essentially the same as that used previously. Between the two beds, air was injected to create the net oxidising conditions required for the oxidation catalyst.

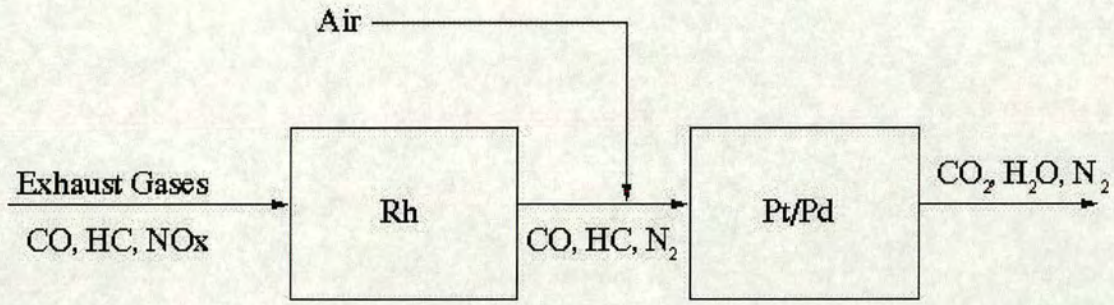

Figure 6: The dual bed converter

The reduction catalyst converted the nitric oxide (the major part of NO_x), by the following reactions:

$$2NO + 2CO \xrightarrow{Rh} N_2 + 2CO_2$$

$$2NO + 2H_2 \xrightarrow{Rh} N_2 + 2H_2O$$

The first reaction is particularly desirable in automobile exhaust catalysis, because two of the pollutants are made to cancel each other out.

The dual bed converter was soon superseded by the TWC, for reasons explained in the following section.

---

[6] There were emission standards prior to this, but they could be achieved by better tuning (CO, THC) and EGR (NOx).

2.2.1.3 The T.W.C.

Studies showed that in a narrow region around stoichiometry (where "air/fuel ratio", A/F = 14.7) all three pollutants could be converted (See Fig.).

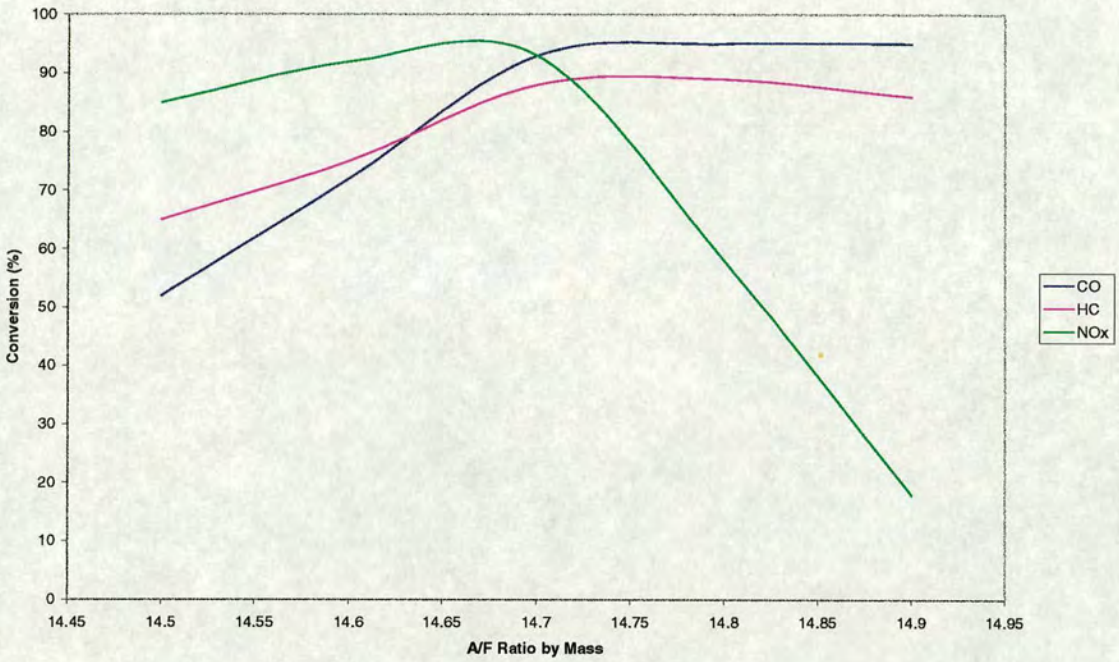

Figure 7: Conversion vs. Air/Fuel Ratio (Warr et al. *(1991))*

The significance was that, theoretically, one set of conditions, and therefore one bed, could be used to catalyse all three reactions. The greatest problem was the accurate control of the air/fuel ratio. The solution to that problem came with the invention of the Exhaust Gas Oxygen sensor (EGO)[7] which could monitor oxygen concentrations rapidly enough at the low levels required, to give feedback to the fuel injection system. It was found (Wotring *et al.* (1978)) that the use of feedback control had the added advantage that it improved road fuel economy.

It was later discovered (Wotring *et al.* (1978)) that TWCs were extremely sensitive to lead poisoning. This, along with the proven detrimental effect on human health of lead emission, was the reason for the development of 'lead-free' petrol.

---

[7] This was made from stabilised zirconia connected to a platinum electrode

An improvement in the performance of catalytic converters was achieved with the inclusion of an 'oxygen storage component' in the washcoat. Its function was to provide small amounts of O_2 when the engine was running rich to consume unreacted hydrocarbons and CO. The component would adsorb excess oxygen when the exhaust was running lean. A number of oxide systems were tried, including NiO/Ni and Fe_2O_3/FeO, but overall that with the best 'redox response' was found to be ceria. The addition of ceria rendered control easier as it effectively damped the oscillations of the A/F ratio. The oxygen storage reactions of ceria are believed to proceed thus:

Fuel - rich : $CeO_2 + CO \rightarrow Ce_2O_3 + CO_2$

Fuel - lean : $Ce_2O_3 + \frac{1}{2}O_2 \rightarrow CeO_2$ *(Oxygen storage)*

Oxygen storage is not the only useful attribute of ceria; it is also a good catalyst for the water-gas shift and steam reforming reactions.

Water-gas Shift : $CO + H_2O \rightarrow CO_2 + H_2$

Steam reforming : $C_xH_y + 2H_2O \rightarrow \left(2 + \frac{y}{2}\right)H_2 + xCO_2$

(H_2 formation leads to $NO_x + xH_2 \rightarrow N_2 + xH_2O$

These two reactions are important additional means for converting pollutants in a typical modern three-way catalyst.

Currently a typical European TWC consists of a honeycomb cordierite monolith, to which is applied a washcoat of various oxides, principally γ-alumina and ceria, impregnated with PGMs. The typical amounts are as follows (Heck and Farrauto (1993))

0.1 to 1.15 % precious metals (usually Pt:Rh in the ratio 5:1)

10 - 20 % CeO_2

Remainder γ-alumina washcoat, stabilised with 1 - 2 % La_2O_3 and/or BaO

The washcoat accounts for ~15% of the total weight of the converter and is applied to the monolith surface at 1.5 - 2.0 g/in.^{2}. The converter is typically 5 - 6" in diameter and 3 - 6" in length.

The rôles of the components are as follows:

Washcoat

γ – ***Alumina*** is a high surface area, thermally stable substrate.

Ceria, with alumina, forms the basis of the washcoat. It increases water-gas shift activity (thereby removing CO) and steam-reforming activity. It has a high oxygen storage capacity, thereby helping to maintain oxidation of pollutants during periods of fuel-rich running. It aids lower temperature CO, C_3H_6 and NO conversion. It is also a structural promoter of Pt and γ – alumina.

Lanthana and Baria are added as stabilisers to maintain surface area at high temperatures. They have been shown to inhibit ceria crystallite growth.

Zirconia may be added to perform the same role as lanthana and baria, but it has the advantage of preventing Rh-alumina interaction. At the higher temperatures that the latest catalysts are required to operate at[8], zirconia has a role in decreasing the formation of rhodium aluminates. The aluminate formation renders the rhodium inactive. Although the phenomenon is (mostly) reversible, it is still undesirable.

PGMs

Platinum is the principal noble metal catalyst for oxidative reactions.

Rhodium is the principal catalyst for $NO_x \rightarrow N_2$

Palladium is used in some formulations, having a similar role to platinum. There is evidence that it may cause reduced H_2S emissions (see sect. 2.4).

2.2.2 Current Challenges to Autocatalyst Technology

Researchers in the field of autocatalyst technology currently have many challenges to face. The most important are discussed in this section.

2.2.2.1 Increasingly Stringent Emissions Legislation.

Emissions legislation has decreased automobile emission so much, that other forms of pollution are becoming relatively important. For instance the diurnal 'breathing' of the car is now one of the main sources of emission. The greatest amount of emissions via a modern TWC are in the period before it has become warm enough to function (see following section 'Cold Start'). Nonetheless, emissions limits are being decreased further. The projected emission standards for California (see Calvert *et al.* (1996)) include, as well as lowering certain emission limits once again, recommendations for a certain number of cars on the road to be ZEV (Zero Emission Vehicles) (which would probably be battery-powered vehicles) and ULEV (Ultra-Low Emission Vehicles). Whether changing to electrically powered ZEVs lowers overall pollution is a point for debate. Overall, electrically powered vehicles would be an improvement for two reasons:

1. It is easier to treat the emissions in bulk at the power station rather than relying on individuals. Sulphur dioxide for instance is treated with scrubbers at the power station.
2. It reduces the problems of photochemical smog in urban areas, because the emissions from power stations tend to be in less urbanised areas, and the gases emitted do not cause the same problems. The vehicle would still cause pollution, except that it would be displaced to the vicinity of the power stations, and would now be in the form of NO_x, CO_2 and sulphur dioxide (see Table 2).

The environmental arguments against the use of ZEVs are:

1. They are less efficient, causing more fuel to be burnt and, consequently, greater emission of CO_2 leading to greater greenhouse effects.
2. The batteries that power the ZEVs are often made of toxic chemicals leading to disposal difficulties.

---

[8] Modern TWCs are exposed to higher temperatures due to being positioned closer to the engine. The purpose of this positioning is for the TWC to heat up more quickly, thereby lessening the problems of 'cold start' (see section 2.2.2.2).

2.2.2.2 The 'Cold Start' Problem.

For current autocatalysts a relatively large percentage of emissions occur during the warm-up phase (60-80% of total emissions (Heck and Farrauto (1993)). This is because, during the period prior to reaching light-off temperature, the catalyst is redundant and the pollutants created by the engine are released into the atmosphere unfettered. A number of strategies are currently being investigated to combat this problem;

1. **Positioning the catalyst closer to the engine.** This certainly reduces emissions, as the catalyst warms up much more quickly, but it leads to problems, because the maximum temperature to which the catalyst is exposed is increased as is the average running temperature. This causes problems with 'ageing' (sintering, and formation of inert compounds of some components). Zirconia may be added to the washcoat to decrease some of these problems. The close positioning of the catalyst also leads to problems with control because the feedback time is decreased.
2. **Self-heating TWCs.** Are currently under development. The idea is that the catalyst block itself is the heater, being composed of a material which conducts electricity (this could be either a metal or a ceramic). The TWC would heat up as soon as the ignition is started. (e.g. Chem & Ind. (1996)).
3. **Pre-heaters.** The idea of EHCs (electrically heated catalysts) is that a smaller catalyst heats the exhaust gas prior to contact with the main TWC. The pre-catalyst has a metallic support, which is heated by the automobile battery. Further heat is generated by the heat of reaction over the pre-catalyst, such that ignition at the main catalyst is achieved much earlier (e.g., Kirchner and Eigenberger (1996)).
4. **Sieve - traps.** The idea of sieve traps is to absorb the hydrocarbons etc. as they emerge, while the catalyst is still cold and release them onto the catalyst when it has achieved light-off temperature. The difficult part is matching the molecular sieve's regeneration temperature to the catalyst's light-off. Other difficulties lie in finding a sieve which can withstand the combination of high temperatures and poisons.
5. **Insulation.** Volvo are currently conducting research into double-walled catalysts which would retain more of their heat, thereby heating up more quickly.

The solution is likely to be a combination of some of these ideas.

2.2.2.3 Lean Burn Engines

Increasingly motorists want greater fuel efficiency from their cars and one of the most likely ways that this will be achieved is via lean-burn engines, in which fuel combustion takes place in excess air. Lean burn is a problem for catalyst manufacturers, because these engines operate at an air/fuel ratio of greater than 17:1, whereas today's catalysts are designed to operate at around stoichiometry (14.7:1).

Although use of lean-burn engines decreases the amounts of hydrocarbons and CO produced, due to the more complete combustion taking place, NO_x reduction is rendered much more difficult. The reduction of NO_x to nitrogen in oxidising atmospheres is one of the most difficult challenges facing autocatalyst manufacturers today.

Sulphur poisoning could well prove more of a problem in lean-burn automobiles, because sulphur dioxide tends to deposit in oxidising conditions. In conventional vehicles, the deposits are released as sulphur dioxide or H_2S when the air/fuel ratio becomes fuel-rich (because it is a reversible poison), whereas in a lean-burn exhaust there could be no such release mechanism.

2.2.2.4 Diesel Engines

The composition of diesel engine exhausts differs from that of petrol-driven vehicles in a number of ways:

- More particulates: diesel engines produce more smoke and soot than petrol engines, and require the use of a 'filter trap' which traps soot etc and oxidises it to CO_2 and water. Among the particulates are some of the most carcinogenic chemicals known (Pearce (1997)), species such as nitro – PAHs[9], particularly 3 – nitrobenzanthrone. Very small combustion particles, mostly from diesel combustion, are believed to be responsible for approximately 10,000 deaths in Britain each year (Brown (1998)).
- Different air/fuel ratio: diesel engines are lean - burn and therefore use oxidation catalysts. Hence, they have all the problems associated with lean-burn exhausts (see above).
- Diesel fuel contains considerably more sulphur than petroleum. For fuels of the early 1990s typical values for sulphur content would be 0.2 % for diesel and 0.03 % for petrol, (Johnson

[9] Polycyclic Aromatic Hydrocarbon

Matthey (1994)). Hence diesel engines produce more sulphur dioxide (but not H_2S because the conditions are always oxidising).

Diesel engines are often considered more 'environmentally friendly' than conventional petrol engines. This is not necessarily the case; diesel engines do have better fuel economies and, therefore, produce less CO_2 overall. They also produce much less CO and slightly less HC, because they operate in lean-burn. Against this, they produce far more particulates and sulphur dioxide and, when both have catalysts, more NO_x than a petrol engine; this is because the problems of reducing NO_x in an oxidising atmosphere have yet to be overcome (see 'lean-burn engines' above).

2.2.2.5 New Fuels

There are currently a number of natural gas-powered vehicles on the road and under development. As there is, as yet, no distribution infrastructure these vehicles are intended for large fleet use only. The advantage of natural gas is that it is a relatively inexpensive fuel. In terms of pollution it should be cleaner than petroleum. The particular demands of catalytic converters for natural gas exhausts are being investigated (White *et al.* (1993)). They already have their own emissions regulations.

2.2.2.6 The Environmental Cost of TWCs

As emissions legislation becomes stricter and increasing numbers of cars equipped with catalytic converters come into operation, questions must be asked about the environmental cost of the converters themselves. They *do* have a cost and, therefore, there must, at some point, be a balance.

Environmental problems associated with converters themselves are as follows:

1. *Platinum emission.* Concerns have been conceived over the safety of platinum in the atmosphere. A study by Barefoot (1997) has shown evidence of high concentrations of extremely fine platinum dust in the proximity of highways. It is unknown whether the platinum dust causes detrimental effects to human health, and because of this there are no limits for platinum concentration in the environment. It is known, though, that platinum is biologically active; many people are allergic to it ('platinum asthma'), and it is used in a number of anti-cancer drugs.
2. *The environmental cost of platinum production.* Mining and refining platinum can cause considerable environmental harm. The greatest problem is the amount of sulphur dioxide

produced in the refining process. This is dependent on the source of the platinum; the largest producers are Canada, South Africa and Russia. The differences between the amounts of sulphur dioxide produced per kg of platinum in these different countries are enormous. Indeed, it has been calculated (MacKenzie (1997)) that, in terms of the acid-rain causing potential, a converter containing Canadian platinum would have to be driven 4900 km to make up for the environmental harm caused by its production, whereas one containing Russian platinum would have to be driven 25,000 km. A solution to this, and to the problem of finite supplies of PGMs, is the 'recycling' of catalytic converters. This is currently being researched (Fierain (1991)).

3. *Nickel carbonyl emission.* As will be discussed in section 2.3, TWCs in the USA contain an amount of nickel which effectively attenuates H_2S emissions. This is proscribed in Europe over fears of emission of nickel carbonyl, a suspected carcinogen.

2.3 Sulphur Dioxide Adsorption by Metal Oxides

Numerous studies have been conducted into sulphur dioxide sorption and desorption by metal oxides[10]. The research has been conducted in a wide range of areas other than that of automotive catalysts, because the same, or similar, reactions are important in other industrially important areas, such as flue gas desulphurisation, environmental monitoring and in the Claus reaction[11]. One of the principal methods of investigation has been infrared spectroscopy, but other methods are mentioned here, where pertinent.

FTIR studies of sulphur dioxide adsorbed on metal oxides have identified four general bands, representing 4 types of adsorbed species. These have been characterised, as follows:

1. ~1060 cm^{-1}. Sulphite-type species formed by the adsorption of sulphur dioxide on 'basic O^{2-}' sites. Principally these have been characterised on alumina, but have also been observed on CaO and MgO (Schoonheydt and Lunsford (1972)).
2. 635 cm^{-1} and 660 cm^{-1}, frequencies due to interactions between basic -OH groups with sulphur dioxide. On alumina they are believed to be hydrogen-sulphite species. They have been assigned to hydrogen sulphite and disulphite species on sodium-doped silica, and have been seen on zeolites.
3. 1330 cm^{-1} and 1150 cm^{-1}: represent weakly bonded species (removed by evacuation). These bands are very close to those of gaseous sulphur dioxide (Karge (1984), Chang (1978)[12]) implying that they are physisorbed species.
4. Sulphate species have been observed on a number of oxides; CuO (Kent *et al.* (1977)), CaO (Low *et al.* (1971)), MgO (Schoonheydt and Lunsford (1972)). The frequencies attributed to the sulphates species vary, but some are given in the following reviews.

Khulbe and Mann (1977) showed the presence of SO_2^- ions on alumina due to sulphur dioxide absorption by means of ESR studies.

---

[10] Also carbon (chars etc.) and metal surfaces
[11] The Claus reaction is used to convert waste hydrogen sulphide into useful elemental sulphur by reaction with sulphur dioxide. The main catalyst of this process is alumina.
[12] Both for alumina

Chang (1978) studied the infrared spectroscopy of sulphur dioxide adsorption on γ-Al_2O_3. He identified three phases in which the sulphur dioxide was adsorbed, firstly as a sulphite species (at ~1080 cm^{-1}), secondly as "a different chemisorbed species" and, thirdly, as a physisorbed species. Experiments with the oxidation of these species showed that upon oxidation "aluminium sulphate-like" species were formed. This was deduced from spectra of γ-alumina doped with aluminium sulphate. Alumina requires oxygen to be present for aluminium sulphate to be formed when dosing with sulphur dioxide.

Karge and Dalla Lana (1984) identified weakly and strongly adsorbed sulphur dioxide species. They showed that the strongly held species was formed by interaction with basic sites on the alumina surface.

Datta *et al.* (1985) claimed that the adsorption process took place at Lewis acid and base sites, the basic sites adsorbing the sulphur dioxide relatively strongly. They proposed a mechanism for this adsorption which involved the sulphur dioxide's sorption at an exposed oxygen atom (a Lewis base) between two aluminium atoms, followed by the cleavage of an Al-O bond to form a sulphite species.

Saur *et al.* (1986) showed that sulphur dioxide on alumina, when oxidised at 450 °C, presents an identical spectrum to that produced by doping alumina with aluminium sulphate. They proposed a mechanism to explain the differences between the spectrum of anhydrously sulphur dioxide-treated alumina and aluminium sulphate, which involved the adsorbate becoming part of a SO_4 tetrahedral structure linked to the alumina by three of its four oxygens.

Berben *et al.* (1988) investigated the adsorption of sulphur dioxide on alumina (both α and γ). They identified a hydrogen-bonded bisulfite species as one of the adsorbate species from a broad band in the hydroxyl region. They observed the usual physisorbed species at ~1330 and ~1150 cm^{-1}. A weak chemisorbed species was seen at 1320 cm^{-1}. The sulphite species seen at 1090 cm^{-1} was seen to desorb at ~773 K. Bands at 1200 and 1245 cm^{-1} (attributed to the asymmetric SO vibration in octahedral and tetrahedral positions, respectively, on an aluminium cation) were seen to be disappear between 373 and 473 K.

Waqif *et al.* (1992) studied, by infrared spectroscopic means, the sorption of sulphur dioxide on a number of oxides with the intention of using sulphur dioxide as a 'basicity probe'. The oxides examined were MgO, CeO_2, ZrO_2, $MgAl_2O_4$, TiO_2 (anatase), TiO_2 (rutile), Al_2O_3 and Na-Al_2O_3 (with varying Na content). Ceria was cited as a 'special case', because it appeared to have the ability to thermally transform adsorbed sulphite species into sulphates. It should be noted that there are a number of differences between Waqif's experimental conditions and those employed in this study:

- The use of transmission infrared spectra with the sample pressed into discs. This has been observed (e.g., Mitchell *et al.* (1995)) to generate significantly different spectra to DRIFTS studies of powdered samples.
- The temperatures used in the gravimetric and TPD studies were not as high as those typically found in a catalytic converter, i.e., the temperatures used in this study.
- The IR spectra were not produced in flow conditions.
- All sulphur dioxide treatments were conducted at room temperature in non-oxidising conditions (this was often followed by heating).

Dalla Lana *et al.* (1993) used TPD-MS techniques to investigate the adsorption of sulphur dioxide by alumina. They concluded that it was chemisorbed by interaction of oxygen atoms of the sulphur dioxide with an oxygen vacancy. Oxygen vacancies would be able to exhibit a wide range of energies, depending upon their situations, and this would explain the broadness of the TPD peaks observed. By isotope labelling of the sulphur dioxide they showed that the sulphur dioxide can be adsorbed in either dissociated or undissociated form. The dissociated form had some degree of surface mobility as it was able to exchange oxygen isotopes with the alumina surface. The chemisorbed sulphur dioxide was shown to be desorbed as SO^{13} as well as SO_2. The peak maxima of the TPD spectra were shifted to higher temperature as the temperature at which the sulphur dioxide was adsorbed was increased. The adsorption was described as an "activated process" meaning that as the adsorption temperature increased higher adsorption energies became accessible. A "tentative" mechanism, in which the oxygen of the sulphur dioxide fills the oxygen vacancy, was given. A similar mechanism could be responsible for alumina's strong adsorption of water.

Mitchell *et al.* (1995) studied the adsorption of sulphur dioxide on alumina, with and without sodium impregnation, by DRIFTS and thermogravimetric techniques. The addition of sodium was investigated, because it can act as a promoter. They found that sulphur dioxide can chemisorb at basic

---

[13] This conclusion was arrived at by analysis of the mass fragment ratios.

sites on alumina to form a sulphite, which is converted to a sulphate upon oxidation, (although this can occur without an oxygen containing atmosphere).

Ziolek *et al.* (1996) studied the effects of sulphur dioxide adsorption on a number of metal oxides[14] at 623 K. They claim that the sulphur dioxide adsorption effect is explained by the formation of hydrogen sulphite species. Ceria is again (c.f. Waqif *et al.* (1992)) an exception, in that it forms sulphates as well as the hydrogen sulphites and sulphites formed on other oxides. The sulphur dioxide is seen to interact with the most basic hydroxyl sites and this is seen as evidence (as in Berben *et al.* (1988)) of hydrogen sulfite formation. They agree with previous researchers that the strongest adsorptions are on basic sites, with sulphur dioxide behaving as an electron acceptor. The form of the hydrogen sulphite species is discussed. They concluded that basicity is the key to sulphur dioxide adsorption, but that this is altered in the case of ceria by its redox character. Ceria was seen to adsorb the greatest amount of sulphur dioxide for this reason.

Waqif *et al.* (1997) studied the oxidative sulphation of ceria in detail by infrared spectroscopy and temperature-programmed and thermogravimetric techniques. They concluded that there are two main types of sulphate formed: surface and bulk-like, exhibiting absorbances at 1400-1340 cm^{-1} and 1200 cm^{-1} (broad), respectively. As seen previously, oxygen is not necessary for the formation of sulphates on ceria (this requires heating to at least 373 K). The consequent reduction of the ceria during such a reaction is shown by UV-vis spectroscopy. They studied the adsorption on two types of ceria, a high surface area (115 m^2/g) form and a low surface area (~5 m^2/g) form, which showed that the type of sulphate formed depended upon the amount of available surface area. They give decomposition temperatures of 600 – 700 °C for the species formed, and claim that they decompose in an atmosphere of hydrogen at temperatures above 500 °C.

The results of research into the interactions of sulphur dioxide with a number of other oxides is pertinent, as the interpretation of the results of work on alumina and ceria has developed from earlier works on other oxides:

1. Low *et al.* (1971) studied the adsorption by CaO at room temperature by means of transmission infrared spectroscopy, observing the formation of at least three adsorbed forms; a surface sulphite, a reversibly chemisorbed species and a physisorbed species. Sulphite was observed to be converted to bulk sulphate by the action of temperature or oxygen.

2. Goodsel *et al.* (1972) studied the adsorption of sulphur dioxide by MgO. They found that sulphur dioxide was adsorbed on MgO as both monodentate and bidentate sulphites. Unlike the species seen on CaO, these species were not converted to sulphate by heating.

3. Kent *et al.* (1977) studied adsorption of sulphur dioxide by CuO at room temperature, observing the formation of a number of different species, including chemisorbed sulphur dioxide[15], sulphites and sulphates.

4. Ghardaskani *et al.* (1990) studied the reaction between sulphur dioxide and calcium oxide, by thermogravimetry, infrared spectroscopy and XRD, in an inert atmosphere (nitrogen) at high temperature. They observed frequencies in the infrared which were assigned to sulphite and sulphate species.

5. Hedges and Yeh (1992) studied the adsorption of sulphur dioxide on CeO_2/Al_2O_3. Their findings are reviewed elsewhere (section 2.3.3.1).

2.4 Hydrogen Sulphide Formation by Autocatalysts

2.4.1 The Origin of the Sulphur

The main source of the sulphur is the "0.01 - 0.05 wt.% sulphur in the form of organosulphur compounds" (Truex *et al.* (1987)) present in ordinary automobile fuel. (there is also a contribution to the sulphur from oil additives (Lundgren *et al.* (1995)). Upon combustion, the sulphur compounds form mainly sulphur dioxide (Lox *et al.* (1989)). Thermodynamic calculations (Cadle and Murawa (1978)) have been performed which show that hydrogen sulphide and carbonyl sulphide (COS) can be formed during combustion in fuel-rich running, but there has been no evidence of this in practice.

The 1989 limit in West Germany for sulphur in fuel was 0.1 wt.%, which would correspond to 60 vppm of sulphur dioxide in the mixed exhaust gas (Lox *et al.* (1989)). Currently, the European limit

---

[14] Ceria, alumina, magnesia, zirconia, titania (anatase and rutile).

for sulphur content of gasoline is 500 ppm (Beckwith *et al.* (1994)), although decreasing this limit to 50 or 30 ppm is being discussed.

.

The sulphur dioxide is able to react on the autocatalyst surface to form hydrogen sulphide during net reducing conditions, but during oxidising conditions the catalyst has the ability to store sulphur which can be spontaneously released as hydrogen sulphide upon change to reducing conditions. Hence, hydrogen sulphide can be formed via one of two mechanisms, termed the "steady state" and "storage-release" mechanisms:

2.4.2 "Steady State" Hydrogen Sulphide Formation

There is a "steady-state" conversion of sulphur dioxide to hydrogen sulphide during fuel-rich (net reducing) conditions. Under these conditions the concentration of hydrogen sulphide out of the autocatalyst can never exceed the concentration of sulphur dioxide in. A rudimentary representation of the reaction is as follows:

$$SO_2 \xrightarrow{Pt} H_2S$$

Diwell *et al.* (1987) theorised that the role of the PGM was to absorb the sulphur dioxide and react with it in a redox manner to form the respective sulphide. This would then react with free hydrogen, which would be abundant in the combustion products, to form the hydrogen sulphide, e.g.;

$$Pt + SO_2 + 2H_2 \longrightarrow PtS + 2H_2O$$
$$PtS + H_2 \longrightarrow Pt + H_2S$$

It appears that other components of the washcoat make little contribution to this mode of hydrogen sulphide production. Dettling *et al.* (1990) demonstrated that "steady state H_2S is not greatly affected by the absence of either alumina or ceria in the washcoat". It is also unaffected by catalyst ageing (Rieck *et al.* (1989)).

Against this, Engler *et al.* (1991) found that the washcoat did have an effect on the steady state production of hydrogen sulphide. They showed that formulations of PGMs on ceria converted all sulphur dioxide to hydrogen sulphide during reducing conditions, whereas not all was converted when alumina was the substrate.

---

[15] Although, as its frequency is at 1361 cm^{-1}, this seems more like a physisorbed species.

2.4.3 "Storage-Release" Mechanism

The second mechanism of hydrogen sulphide emission has been termed "a rapid reductive release" (Truex *et al.* (1987)), occurring on changeover from fuel-lean (oxidising) to fuel-rich (reducing) conditions where $[H_2S]_{out}$ can greatly exceed $[SO_2]_{in}$.

The adoption of high cerium contents into the formulation of the TWC in the mid-1980s caused the catalysts to produce much greater amounts of hydrogen sulphide than had been the case previously (Bending *et al.* (1993)). This was particularly pronounced in automobiles with open loop or malfunctioning closed loop A/F ratio control (Lox *et al.* (1989)), where the exhaust was allowed to run fuel-lean for too long, thereby allowing build-up of stored sulphur in amounts sizeable enough to cause significant hydrogen sulphide 'spikes'.

This mode of H_2S formation is due to the sudden release of sulphur compounds, which have been stored on the surface of the catalyst, probably in the form of sulphates or oxysulphates, during fuel-lean conditions. This 'switchover' from oxidising to reducing conditions occurs in a number of real driving situations, where there is a prolonged period of fuel-rich running followed by a switch to fuel-lean. Common driving modes which have been observed to produce large "spikes" are:

- Acceleration after 'idling'
- Deceleration after cruising (Ernest (1989))
- "Low speed driving", i.e., continuous stopping and starting

During idling after deceleration the temperature of the engine increases greatly and the car tends to run fuel-lean; these are the ideal conditions for storage of sulphur in a form which will be released as hydrogen sulphide upon switchover to fuel-rich conditions.

Storage release "spikes" in outlet concentration are "the H_2S problem". They have been observed to be as high as 175 ppm (Truex *et al.* (1987)), in which case there would have to be a large amount of dispersion of the exhaust gases before the concentration fell below the odour threshold of 0.03 ppm (see 'Introduction').

2.4.3.1 Sulphur Storage

It is unlikely that bulk sulphates are formed with either alumina or ceria, hence this section concerns only surface phenomena. Henk *et al.* (1987) state that "the storage of sulfur on alumina is directly related to the surface area of the alumina".

The general form of the storage mechanism is believed to be:

Storage:

$$2SO_2 + O_2 \xrightarrow{Pt} 2SO_3$$

$$MO + SO_3 \longrightarrow MSO_4$$

Where M is a general metal, usually aluminium or cerium.

Other variants have been proposed for the sulphur storage mechanism:

Rieck *et al.* (1989) claim that storage is predominantly on the cerium as oxysulphates;

$$SO_2 + \frac{1}{2}O_2 \xrightarrow{"Noble-metal"} SO_3$$

$$SO_3 + CeO_2 \longrightarrow CeOSO_4$$

Truex *et al.* (1987) and Yamada *et al.* (1990) claim that sulphur dioxide can also react directly on the oxide surface to form sulphates;

$$MO + SO_3 \longrightarrow MSO_4 \text{ and}$$

$$MO + SO_2 + \frac{1}{2}O_2 \longrightarrow MSO_4$$

($MO = CeO_2$, Al_2O_3)

Waqif *et al.* (1992) have observed, by infrared spectroscopy, the adsorption of sulphur dioxide as 'sulphite-like' species, sulphates, hydrogen sulphites and physisorbed sulphur dioxide.

The PGMs do not retain any sulphur under fuel-lean conditions, but thermodynamic studies (e.g., Diwell *et al.* (1987)) have shown that sulphur dioxide can be adsorbed and stored by both ceria and alumina.

Chang (1978) found that sulphur dioxide chemisorbed on alumina only up to 200 °C, although his experiments were conducted *in vacuo* rather than in oxidising conditions. Lox *et al.* (1989) demonstrated "that H_2S can be formed from sulphur dioxide adsorbed on γ–Al_2O_3 by reduction with molecular hydrogen". Gottberg *et al.* (1989) claim that aluminium oxides react easily with sulphur trioxide and that the storage capacity increases to a maximum at approximately 500 °C. They claim that the sulphate decomposes at 600 °C.

Ceria is believed to be responsible for most hydrogen sulphide emissions. The cerium (III) sulphate is thermodynamically more likely to form than that of the aluminium (Diwell *et al.* (1987)). Studies (e.g., Rieck *et al.* (1989)) have shown that H_2S emissions increase with increasing 'rare earth'[16] content. Truex *et al.* (1987) claim that alumina catalysts release less than 35 % of the stored sulphur as H_2S, whereas ceria/alumina catalysts release greater than 70 % as H_2S.

XPS studies (Diwell *et al.* (1987), Lundgren *et al.* (1995) and Hedges and Yeh (1992)) have shown that cerium's oxidation state appears to change from IV to III during sulphur dioxide treatment, implying the formation of a cerium (III) sulphate species. At room temperature it is known that sulphur dioxide is chemisorbed onto ceria by the reaction:

$$6CeO_2 \longrightarrow Ce_2(SO_4)_3 + \text{"}Ce_2O_3\text{"}$$[17]

Although the precise form of the sulphate is unknown, it has been speculated (Diwell *et al.* (1987)) that it is amorphous or highly dispersed.

Hedges and Yeh (1992) conducted research on ceria/alumina as a sorbent for sulphur dioxide and NO_x produced by coal-fired boilers. They found, using gravimetric techniques, that the absorption followed "a simple kinetic model", which was first order with respect to both the pressure of sulphur dioxide and fractional unreacted ceria. Also they reported that the rate was unaffected by ;

- CO_2 in the range 0 - 15%,
- H_2O in the range 4 -18 %,
- NO between 0 and 500 ppm and

---

[16] Lanthana, another rare earth, makes up a very small weight percentage of a typical washcoat. Its contribution to hydrogen sulphide formation is negligible compared to that of ceria.

[17] "Ce_2O_3" represents reduced cerium sites

- O_2 in the range 2.8 - 12.7%.

Ceria was believed to react thus :

$$2CeO_2 + 3SO_2 + O_2 \rightarrow Ce_2(SO_4)_3$$

Their XPS studies showed that heavily sulphated samples contained "predominately Ce (III)".

Lundgren *et al.* (1995), dosed fully formulated ceria-alumina catalysts with sulphur dioxide and found emission of sulphur dioxide and hydrogen sulphide in the subsequent TPR spectra.

2.4.3.2 Hydrogen Sulphide Release

According to Yamada *et al.* (1990) the general form of the reaction which produces the hydrogen sulphide is:

$$MSO_x + H_2 \xrightarrow{reducing, \sim 500-550^o C} H_2S + MO + H_2O$$

Where M is, again, a general metal, usually either cerium or aluminium.

Diwell *et al.* (1987) believe that the PGMs participate to a greater extent than this. They claimed that rhodium or platinum form sulphides during this release.

In Henk *et al.* (1987) the hydrogen sulphide emission reaction is expressed as follows:

$$Ce(SO_4)_x \xrightarrow{FUEL-RICH} CeO_2 + SO_x(ad.)/SO_2(g)$$

Then :

$$SO_x(ad.)/SO_2(g) + H_2 \xrightarrow{Pt/Pd/Rh} H_2S + H_2O$$

OR

$$Ce(SO_4)_x + H_2 \xrightarrow{PT/Pd/Rh} CeO_2 + H_2S + H_2O$$

This assumes that cerium is the principal storage agent and there is much evidence to support this. Cerium sulphate is the compound which is thermodynamically the most likely to decompose to hydrogen sulphide in rich conditions (Gidney (1996)).

Lox *et al.* (1989) identify two distinct regions in a hydrogen sulphide spike due to a lean-rich transition on a platinum-containing catalyst. A sudden release resulting in a sharp spike is superimposed on a

slower, but longer lasting emission of hydrogen sulphide. They claim that this indicates that the sulphur oxides are stored on at least two types of site. They claim a correlation between the amount of hydrogen sulphide emitted in the initial 'spike' and the number of active platinum sites, implying that the sulphur is stored on the platinum or by some form of interaction between platinum sites and the surrounding ceria or alumina. However, thermodynamic studies by Diwell *et al.* (1991) suggest that platinum is not able to form compounds with sulphur in oxidising conditions (although this is possible in reducing conditions). Conventional wisdom (e.g., Warr *et al.* (1996)) has it that only catalytic converters which contain platinum can produce hydrogen sulphide. The question is; what role does the platinum have, if it is not able to store sulphur?

2.4.3.3 Catalyst Ageing and the Sulphur Storage-Release Mechanism

Hydrogen sulphide storage-release emissions decrease markedly with catalyst 'age'. Gottberg *et al.* (1989) report that the release of hydrogen sulphide requires a temperature of 450 °C for fresh catalysts and 550 °C for aged catalysts.

Lundgren *et al.* (1995) theorise that this is due to loss of surface precious metals to catalyse the reaction:

$$SO_2 + 3H_2 \xrightarrow{PM} H_2S + 2H_2O$$

They point out that sulphur dioxide is still produced by storage-release mechanisms, and this can be observed in their TPRs.

Rieck *et al.* (1989) conclude otherwise; that sintering of the noble metals reduces hydrogen sulphide emissions "by decreasing the activity of the catalyst for sulphur dioxide oxidation and thereby decreasing the quantity of sulfur stored". Their evidence for this is that hydrogen sulphide is still produced in steady state, but not in storage-release mode, therefore it is the storage facility which has decreased. They do not report whether or not sulphur dioxide is emitted upon switchover from oxidising to reducing in their experiments.

Bending *et al.* (1993) attribute the reduced tendency of aged catalysts to produce hydrogen sulphide to sintering of the ceria and "other morphological changes".

2.5 Strategies for the Attenuation of Hydrogen Sulphide Emissions

This section reviews all attempted methods for the attenuation of hydrogen sulphide. Many of these methods have been partially successful and are used in practice.

2.5.1 Vehicle Modification

A strategy in use is the modification of the engine behaviour or characteristics such that the "rich excursions" which cause the large hydrogen sulphide "spikes" do not occur (i.e., by tight control of the air/fuel ratio). According to Bending *et al.* (1993) the circumstances to avoid are running the car simultaneously hot and rich.

Potentially, this could prove a very complex procedure, because it has to be accomplished without compromising overall vehicle or catalyst performance. In fact the conditions required for the optimal performance of a catalytic converter are at approximately stoichiometry, as this is where the window for three-way conversion exists. If the automobile could run at, or around, stoichiometry constantly, there would be very little problem with hydrogen sulphide emission, because in these conditions the converter could not store enough sulphur to create large 'spikes' (Joy *et al.* (1979)). This is because in real situations, when the exhaust gas is said to be 'at stoichiometry', the air/fuel ratio is oscillating rapidly around the point of stoichiometry and small amounts of sulphur species are constantly being stored and emitted.

If the strategy of maintaining the A/F ratio fuel-lean was followed, to prevent hydrogen sulphide 'spikes', by preventing the sulphate's desorption, sulphate species would accumulate on the catalyst surface. This would adversely affect the operation of the catalyst and cause greater emission of other pollutants. This is because sulphur dioxide acts as a poison, albeit a reversible one, competing with all other species for sites.

The strategy of tighter air/fuel ratio control has considerably lessened hydrogen sulphide emissions over the last few years. It was desireable to develop this, regardless of the hydrogen sulphide issue, because it leads to better TWC performance and fuel economy.

There remain, inevitably, modes of driving which cause the automobile exhaust to move away from stoichiometry, despite the action of the air/fuel ratio controller, and hydrogen sulphide 'spikes' still occur.

2.5.2 Lowering Fuel Sulphur Levels.

Recently (1995), E.U. legislation has been introduced to lower the maximum level of sulphur in fuel from 1000 ppm to 500 ppm (Beckwith *et al.* (1994)). Although this will reduce the problem somewhat, when "rich excursions" occur there can still be enough sulphur stored to cause significant 'spikes'.

Reduction of sulphur levels in fuels decreases the frequency of spikes, but is beneficial for a number of other reasons:

1. *Decreased sulphur dioxide emissions.* Although only 2% of anthropogenic sulphur dioxide emissions are due to automobiles (see Table 2) and there is no sulphur dioxide legislation for automobiles, they are contributors to acid rain, which causes damage to trees, buildings and aquatic life. The gas itself is a lachrymator, and, in greater concentrations, poisonous. This can be more of a problem than other sulphur dioxide emission sources, because of the geography of the emissions, i.e., usually in the areas of greatest human population density. Sulphur dioxide causes secondary pollutants during photochemical smog in the form of sulphate aerosols (caused by photochemical oxidation of sulphur dioxide), which disperse light, thereby lowering visibility.
2. *Urban ozone levels would be reduced.* Schleyer *et al.* (1993) claim that peak ozone levels in a number of U.S. cities would be reduced by between 8 and 16 % if the fuel sulphur levels were reduced from 450 ppm to 50 ppm.
3. *Catalysts would become more efficient.* This is the most important of the consequences of fuel sulphur content being lowered. Sulphur poisoning affects the conversion of all three major pollutants (Beck and Sommers (1995)). For hydrocarbons and CO this is mostly because it poisons the water-gas shift and steam-reforming reactions, which are important for conversion under fuel-rich conditions. Sulphur dioxide has been seen to compete for sites with CO. Light-off temperatures are seen to be increased by the presence of sulphur dioxide in the exhaust gas (Beck and Sommers (1995)). Given that 80 % of emissions in short journeys are now due to the period

prior to the catalyst reaching light-off temperature (see 'Cold Start'), this is a major cause of pollution. Calvert *et al.* (1993) claim that lowering sulphur content and vapour pressure[18] are the two changes mooted for the proposed "reformulated gasoline" in the U.S.A. that will be of the greatest beneficial effect. They state that "the reduction of fuel sulphur increases catalyst efficiency for hydrocarbons, carbon monoxide and NO_x . The effect is immediate and reversible". This belief is reinforced by the findings of Mayotte *et al.* (1994) who claim that "sulphur concentration was found to have the greatest effect on hydrocarbon and NO_x emissions". The significance of the reversibility of the sulphur poisoning is that a reduction would achieve lower emissions of HC, CO and NO_x from vehicles *currently in use.*

Desulphurisation is prohibitively expensive, as it typically involves heating the fuel to 700 °C at 70 atm. The expense means that many fields of high sulphur content oil are not exploited. Recently (Coghlan (1998)), a new, less costly technique has been developed which could make these oil-fields economically viable, but more importantly, increase the likelihood of fuels with extremely low sulphur levels. This is the ideal solution, because, if the sulphur is present there is no completely inert gaseous species for it to be converted into. Conversion of the sulphurous exhaust compounds into non-gaseous species, e.g., by using some form of sulphur absorbent is impractical.

2.5.3 Additives.

A large amount of research has gone into the search for an additive which can simply be added to the catalyst formulation to attenuate hydrogen sulphide emissions. This is seen as the ideal solution, because it requires no modifications to car or fuel and would require little change in the catalyst production line. The additive must fulfil several other criteria, beyond that of attenuating the emissions:

1. It must be thermally stable.
2. It must not sinter, or aid sintering of other components.
3. It must not adversely affect the performance of the catalyst
4. It must not lead to the formation of any toxic products that can escape the converter.

---

[18] A large percentage of modern automobiles' hydrocarbon emissions occur when the car is stationary, due to the 'diurnal breathing', (Calvert *et al.*, (1993) of parked cars. These emissions occur when a parked car 'breathes' cool air in at night and breathes out air plus hydrocarbon vapours as it warms up

A number of effective additives have been identified, but have proved impractical as they did not fulfil all these criteria. These are reviewed in the following sections.

2.5.3.1 Nickel Oxide

A large amount of research has been conducted in the area of new components and in the case of nickel oxide has proved very successful. According to Dettling *et al.* (1990), "nickel suppresses 95% of the H_2S". This is achieved (unlike any other tried additive) without catalyst performance being significantly adversely affected in any way (Yamada *et al.* (1990)). The addition of nickel oxide successfully attenuates the emission of hydrogen sulphide, but there are serious doubts in Western Europe over its safety. This is because nickel can cause allergic reactions (Gottberg *et al.* (1990)), and because of the identification of one of nickels theoretical products as a suspected carcinogen. Hence, nickel use in catalytic converters in Europe is proscribed, despite the fact that there is no evidence that the carcinogenic compound, nickel carbonyl, is ever formed, or if it *is* formed, that it is ever emitted. There are no such doubts about nickel's safety in the USA where nickel is used in most catalytic converters.

The nickel oxide has been said to act as a "sulphur getter" or "H_2S scavenger" (Lox *et al.* (1989), Rieck *et al.* (1989)). The belief was that the nickel's *modus operandi* was to form a stable sulphide with released hydrogen sulphide during fuel-rich (reducing) conditions and to release the sulphur as sulphur dioxide in fuel-lean (oxidising) conditions. The reaction scheme is believed to be thus;

1. $NiO + H_2S \rightarrow NiS + H_2O$ (fuel-rich)

2. $NiS + \frac{3}{2} O_2 \rightarrow NiO + SO_2$ (fuel-lean)

---

during the day. On a hot day up to 50 g of fuel can be emitted. This is particularly serious given that much of this vapour is benzene, a known carcinogen.

Later studies disagree with the pure "H_2S scavenger" theory. Diwell *et al.* (1991) believe that the nickel also functions by reacting with sulphur dioxide during oxidising conditions to form a sulphate, which decomposes with the release of an excess of oxygen. They proposed that this would lead to the re-formation of species such as cerium (III) sulphate. They claim that "even if a catalyst additive forms sulphates under lean conditions, it may still be able to attenuate H_2S". There is an implicit assumption in this statement that the formation of sulphates by the additive is not a useful part of its attenuating effect, whereas this is not necessarily the case.

Golunski and Roth (1991) demonstrated that there was no simple relationship between hydrogen sulphide adsorption ("scavenging") by nickel oxide and the attenuation of hydrogen sulphide 'spikes'. They reasoned that this meant that nickel had more than one mode of attenuation and concluded from studies of that the nickel acts in two ways:

- It prevents the formation of the hydrogen sulphide, by forming nickel sulphate.
- It absorbs emitted hydrogen sulphide. This was demonstrated by dosing nickel-containing catalysts with hydrogen sulphide.

2.5.3.2 Iron Oxide

Bending *et al.* (1993) demonstrated that a fresh, iron oxide-containing catalyst exhibited similar control to that of a nickel-containing catalyst. The drawback was that the aged catalyst exhibited ~30% worse conversion of THC and NO_x than the catalyst without the additive. The reduced conversion was attributed to a decrease in surface area due to the reaction of the iron oxide with the alumina of the catalyst support. "A modified form of iron oxide" was then included in the formulation, which had none of the decreased surface area problems when aged.

The additive is currently in use, although its emission attenuation overall is not as good as that of nickel oxide, or of the unmodified iron oxide on fresh catalysts, because the improved aged performance was achieved at the cost of some of its ability to attenuate.

2.5.3.3 Other Additives

Rieck *et al.* (1989) conducted research into the feasibility of various ferrites (Ni, Co, Zn, Cu) as additives. The theory was that they had the same hydrogen sulphide adsorption capacity as the pure

metal oxides, but could regenerate more readily in oxidising conditions. Nickel, copper and cobalt ferrites were shown to be "as effective as NiO at reducing hydrogen sulphide emissions" in hydrogen sulphide emissions for fresh and aged catalysts. Further, cobalt and nickel ferrites had no adverse effect on three-way catalytic activity (fresh or aged). They also investigated certain aluminates, which were known to absorb hydrogen sulphide in other applications (Falconer and Schwarz (1983)), but they exhibited no activity for hydrogen sulphide emission attenuation whatsoever. They believed that this was due to differences between the electronic/structural qualities of the matrices of ferrites and aluminates.

Copper oxide was identified by Harkonen *et al.* (1990) as "an especially good H_2S scavenger", although their research also showed that some proven hydrogen sulphide suppressants (Ni, Fe) would actually *increase* spikes. According to Bending *et al.* (1993) the use of both copper ferrites and oxides is precluded by their detrimental effect on aged catalyst performance. Attempts to use a separate "getter brick" in a cooler part of the exhaust or "getter band" at the downstream end of the catalyst, which would not interfere with catalyst performance, were not successful due to copper's volatility.

According to Diwell *et al.* (1991) "in practice calcium has been used as an H_2S getter", although their thermodynamic models predicted that it should increase H_2S emission. This is in contrast to the work of Yamada *et al.* (1990) who showed that a calcium-doped formulation showed no hydrogen sulphide suppression activity (although they had predicted, thermodynamically, that it would).

Yamada *et al.* (1990) surveyed a number of base metal oxides[19], firstly by thermodynamic calculations to identify those most likely to be active, then by engine tests. The thermodynamic calculations did not always correspond with the real test data, because thermodynamic data does not necessarily predict reaction kinetics, and because of the assumptions made about the mechanism by which hydrogen sulphide emission attenuation is achieved. In the calculations it was assumed that the attenuating additive would have a smaller thermodynamic favourability for forming sulphates than ceria or alumina during oxidising conditions, and form a stable sulphide with hydrogen sulphide in reducing conditions. This is not necessarily the *modus operandi* of a successful attenuator, such as nickel oxide.

Yamada *et al.*'s calculations predicted that calcium, barium and strontium oxides would attenuate hydrogen sulphide emissions, but their engine tests showed that none of these oxides were effective.

---

[19] Al_2O_3, Ag_2O, BaO, Bi_2O_3, CaO, CeO_2, Co_3O_4, CuO, Fe_2O_3, GeO_2, K_2O, La2O3, MgO, MnO, MnO_2, MoO_3, Na_2O, Nd_2O_3, NiO, Sb_2O_3, SrO, TiO_2, V_2O_5, WO_2, ZnO.

They believed that this may be because these alkaline earths formed sulphates and sulphites directly during sulphur dioxide treatment in oxidising conditions, which would not be effective as "H_2S scavengers".

A question mark against their predictions and experimental runs is that they predict, and find, that iron oxide is not a hydrogen sulphide suppressant, although it is successfully used in practice (Bending *et al.* (1993)).

After taking other factors into account in the screening of potential additives, such as thermal stability of the oxide itself (this consideration ruling out the use of V_2O_5[20] and CuO[21]), Yamada *et al.* concluded that germanium dioxide (GeO_2) effectively attenuated emissions without adversely affecting catalyst function. The only problem with germanium oxide proves to be its relatively low melting point (1100°C) which causes losses of germanium of up to 40 % in typical TWC operating conditions (Bending *et al.* (1993)).

Manganese oxide has been identified by Dettling *et al.* (1990) as a suitable candidate for hydrogen sulphide suppression. They conducted research on manganese and copper only in the forms of "getter-bricks" or "-bands" to avoid "harmful precious metal interactions". The use of these bands or bricks is not the ideal solution, because it would call for significant changes in process and materials at the catalyst or automobile manufacturer. In Yamada *et al.* (1990) manganese oxide (as part of the catalyst formulation) is shown to suppress hydrogen sulphide formation, but to adversely affect light-off temperatures (to a large extent) and conversions (slightly). Manganese oxide has a considerably higher melting point (1650°C) than germanium oxide and may yet prove to be a more successful candidate.

2.5.4 Modification of Catalyst Morphology

Lox *et al.* (1989) attempted to prevent hydrogen sulphide emission by altering the structure of the catalyst. They observed that the amount of sulphur oxides stored could be reduced by increasing ceria crystallite size or by modifying surface hydroxyl groups. Their data shows that this can be achieved

---

[20] Melting Point, 800°C
[21] Melting Point, 1026°C

without detriment to the activity and durability of the catalyst. This seems unlikely, as they also show that the surface area and oxygen storage capacity of the catalyst are reduced. This strategy has never been used in practice. Yamada *et al.* (1990) state that "the TWC catalytic function is adversely effected".

2.5.5 Other Catalysts

Recently, interest has been expressed in high-loading palladium catalysts and Pd:Rh and Pt:Pd:Rh formulations. These new formulations "offer improved H_2S attenuation compared to current platinum rhodium catalysts with additives" (Brisley *et al.* (1995)). Without any additives to attenuate H_2S emissions they were shown to produce considerably less than a typical European Pt:Rh catalyst with hydrogen sulphide attenuating additives[22]. Comparisons in Brisley *et al.* (1995) in a standard test showed that the hydrogen sulphide peak area for:

- a Pd:Rh catalyst was ~10% that of the Pt:Rh catalyst,
- a Pt:Pd:Rh catalyst was ~2% that of the Pt:Rh catalyst and
- a high-loading, Pd-only catalyst was negligible.

The main attraction of high palladium loadings on catalysts was economic, in that world prices of palladium were considerably lower than either rhodium or platinum. However, the price of palladium has increased greatly, very recently (Nov. 1997) and high palladium loadings may no longer be economically viable. Palladium's other failing is that it is more susceptible to poisons, particularly sulphur (Beck and Sommers (1995)), although as the quality of fuels increases it may become the preferred PGM, due to its advantages over platinum:

- High palladium loadings can be used (Brisley *et al.* (1995)) as substitutes for rhodium.
- High hydrocarbon conversion (Summers *et al.* (1989)).
- Lower light-off temperatures (Heck and Farrauto (1993)).

---

[22] Presumably iron oxide.

The main performance disadvantage of using palladium is poorer rich-side NOx and CO conversion, but this can be overcome by tight A/F control or lean calibration.

2.5.6 Alternative Fuels

It is not suggested that alternative fuels should be introduced purely for reasons of reducing hydrogen sulphide emissions, but many other possible fuels do not have many of the environmental problems that petroleum has. Other fuels currently under consideration as alternatives to petroleum are;

- **Natural gas**. Ideally, natural gas would combust to form only water and carbon dioxide. Currently its use remains impractical due to the compression required to store it. It is currently not an environmentally friendly solution, as the gas, unavoidably, leaks and is not only a greenhouse gas, but an ozone-depletant. The solution is being looked for in the area of catalysis; research is going into catalysing reactions in which methane polymerises to C_{5+} chains, thereby undergoing conversion to a liquid. As a liquid fuel it would be easier to provide and would not leak. A number of compressed natural gas vehicles already exist and it is currently being considered as a fuel for buses and other large-fleet operations where the existing distribution infrastructure is not as important. Natural gas already has its own set of requirements for emission control (White *et al.* (1993), Subramanian *et al.* (1993)).

- **LPG**. LPG is increasingly being used on the roads in the UK. Petrol-driven vehicles can easily (but not inexpensively) be converted to run on it. LPG engines are currently used by a number of bus companies.

- **Alcohols**. Apart from reduced sulphur emissions alcohols have little advantage over petroleum in terms of air quality, other than a decrease in CO levels. Ethanol is successfully used as a fuel in Brazil, although at high cost.

- **Hydrogen.** Hydrogen, if it were practical, would be an ideal fuel in terms of the environment, because its only exhaust gas would be steam. Also, there is little danger of depleting world stocks of hydrogen. There are considerable safety concerns over its use, although progress is being made in the search for likely sorbents for storage. Daimler Benz are conducting research into powdered metal catalysts which store the hydrogen in the fuel tank as a hydride. Storage in this manner renders the fuel safe in collisions. The distance the vehicles can travel between each refuelling is still extremely low. Its other problem is the difficulty and energy intensity, and therefore cost, of production. Environmentally, it is not necessarily a good solution because of the source of the

hydrogen, i.e., normally from fossil fuels at a high energy cost. This year the first London taxis to be run on hydrogen fuel cells will be put into operation.

- **Methanol.** Methanol as a fuel is attractive because it is a liquid and therefore can use much of the same distribution infrastructure as petroleum. It is difficult to use as it is highly corrosive and very toxic. However, its greatest technological problem is that it requires temperatures of at least 7 °C for ignition. The solution to this has been to mix it with petrol, but the result of this is a fuel that is little better than petrol in terms of the pollutants emitted.

All these fuels exhibit little or no hydrogen sulphide emission as they do not contain significant levels of sulphur-containing compounds. They are unlikely to be used in the short term for reasons of cost, distribution infrastructure, availability and the lack of suitable engine technology.

2.6 Analytical Techniques

2.6.1 Temperature-Programming

Temperature-programming techniques developed from 'flash desorption' methods. The 'flash desorption' method was used to study metal filaments under very high vacuums. The filament was heated by passing a current directly through it. The resultant temperature increase and the species desorbed were analysed.

Temperature-programmed techniques differed from flash desorption in that the samples were externally heated and could be heated in any environment. The advantages of TPR over flash desorption methods for the study of catalysts were that the conditions required were more easily achieved and closer to real conditions of use, and that samples could be used which were not electrically conductive. Some of the earliest investigations into temperature-programmed methods were by Amenomiya and Cvetanovic (1963). An excellent review covering the theory, analysis and practice of temperature programmed techniques is by Falconer and Schwarz (1983). Elements of the theory can be found in more detail in appendix 7.2.

The basis of temperature-programmed analytical techniques, usually TPR (temperature-programmed reduction), TPD (temperature-programmed desorption) and TPSR (temperature–programmed surface reaction), is that the rate at which an adsorbed species will desorb or react will increase with increasing temperature. The spectrum produced is, essentially, a graph of reaction rate versus temperature. The temperature is increased linearly (although other heating strategies are possible[23]). The rate of desorption increases with temperature, but eventually decreases due to depletion of adsorbent, thereby creating a peak. Temperature programming is a versatile technique, which can be used to determine many different types of information about the samples. At its most basic, it generates simple, but in this research important, information about the temperatures at which a substance's various reactions/desorptions occur. In this research it is generally used as a tool with which to compare the effects of varying composition on peak temperatures and shapes.

Temperature-programmed techniques can generate more fundamental information e.g.;

- Reaction order.
- Heats of desorption
- Pre-exponential factors
- Surface site information
- Activation energies

There are a number of methods by which TPD and TPR data can be analysed. Some of these methods require sets of experiments in which the coverages or heating rates are varied. In this research there was not sufficient time to perform sets of temperature programmed experiments for every component. This was because there were so many different formulations investigated and other experiments to be conducted (principally simulated storage-release) and because the purpose of the temperature programmed experiments was principally comparative. Nonetheless, it is theoretically possible to derive most of the information from experiments with one initial coverage and ramp rate. Falconer and Schwarz (1983) detailed many methods of interpreting TPR and TPD data, some of which required the analysis of only one peak:

- *Redhead's method.* Redhead's method can be used to determine the pre-exponential factor if the activation energy of the desorption[24] or reaction is known (or vice versa). It can be used to determine the activation energy using an assumed pre-exponential factor. Other quantities that are required are the peak temperature and the initial coverage.
- *Peak Width Analysis.* This method requires prior knowledge of the reaction order. Using the half and three-quarter widths two separate measures of the activation energies can be determined for first and second order processes. The method is independent of heating rate.
- *Shape Index Analysis.* The shape index, S, is the ratio of the slopes of the peak at the inflection points. This can be used to determine the order of the desorption and the presence of readsorption effects. This analysis requires that the surface is saturated, except when readsorption is negligible. This technique is likely to have problems with accurate measurement of the slope at the inflection point.
- *Skewness Parameter Analysis.* Peak shapes due to second and first order desorptions/reactions are distinctly different, second order being close to symmetrical and first order distinctly

---

[23] The technique of interrupted linear temperature ramps is often used.
[24] If the desorption is not activated then the heat of desorption is equal to the heat of adsorption.

asymmetrical. This technique uses the half and three-quarter widths to determine whether the desorption/reaction is first or second order, by calculating a skew parameter. In practice these results are extremely prone to small experimental errors in the temperatures.

Methods of analysis of temperature programmed experiment can involve the variation of heating rate or surface coverage:

- *Variable heating rate (β).* Peaks shift to higher temperature and have larger amplitudes with increased heating rate. This analysis requires the heating rate to vary by a factor of ten, such that the graph to be plotted, which involves a logarithmic function of the peak maximum temperature, has a wide enough range to determine the reaction/desorption energy with any real degree of accuracy. This method has been noted to be very sensitive to minor experimental errors (Brenner and Hucul, (1979)), but this is counterbalanced by the fact that it generates two estimates of the activation energy and the correlation between these two estimates can be used to determine the reliability of the value. The reaction order does not need to be known in this method.
- *Variable coverage (θ).* Activation energy may be a function of coverage. This technique can be used to determine the reaction order. A large number of spectra are required. This technique takes into account coverage-dependant activation energies and can find activation energy at a specific coverage.

The multiple experiment techniques have not been the principal methods used in this research for the reasons stated above, but they have been used to a very limited extent.

Temperature programmed experiments on single crystals have provided much detailed information concerning surface sites. Peaks observed have been assigned to species desorbing from specific crystal planes. Readsorption effects, which can act to ruin data, should be negligible in single crystal experiments, as they are conducted at very low pressures.

The complex surface structure of supported metal particles makes interpretation of results considerably more difficult than those for single crystals. Peaks do not correspond to single sites and readsorption effects are very difficult to overcome. In this research interpretation is further complicated by the fact that the temperature programmed experiments are predominantly TPRs, rather than the simpler TPDs.

In summary, although further analysis of the peaks of temperature programmed spectra is theoretically possible and was performed, the principal aim of the TPRs performed in this research is comparative, and little store was set by the results of the analysis. This is one of the main applications of temperature programmed experiments; to assess the effect on reduction temperatures and peak characteristics of changing aspects of the formulations used (in this case mainly by addition of dopants or catalytic materials).

2.6.2 Use of Microreactors

The use of temperature-programmed methods and various other experiments performed in the course of this research required the use of a high temperature microreactor. Microreactors are becoming increasingly important, not only as laboratory-scale reactors in academic research, but in industry for 'sweeps' of possible new catalysts (Chopey *et al.* (1997)). The microreactor has a number of advantages over conventional reactors;

- Flexibility. It is much easier to vary the conditions under which a microreactor is operating. It takes less time and there is less risk involved than for conventional reactors.
- Specificity. The conditions of the reactor can be controlled to a much greater degree than is the case for conventional reactors.

Their design, particularly for high temperature and catalytic applications, is troublesome. The most important issues are:

1. *Temperature measurement.* Is the correct temperature measurement being taken? It is not uncommon to see flow reactor designs in published papers, in which the temperature is measured at the outflow or on the outside of the reactor, but is taken to be the same as that in the reactant bed. Brenner and Hucul (1979) claim that there may be significant errors in a lot of TPD data due to the use of glass-coated thermocouples, which have a significant thermal lag. The design employed in this research uses an axially mounted thermocouple with the tip immersed in the reactant bed (without touching the sinter). In many cases it is difficult to know whether the correct temperature is being measured, because there can be extreme temperature gradients between particle and fluid. To overcome this, relatively high flow rates of carrier gas were used in these experiments, to decrease the possibility of large temperature gradients (Vanhove (1996)). The gas

was preheated to some extent as it moved down the reactor and through the bed of quartz particles. The quartz bed was only of a similar depth to that of the sample itself, because it was found that using a greater mass of quartz had a cost in terms of temperature control. These concerns are addressed in more detail, for the specific reactor used, in 'Materials and Methods'.

2. *Flow regimes.* The flow regime in a reactor is always an issue, whether plug flow or perfect mixing is required. In this design, plug flow is desired, so that no information is lost due to axial dispersion, between reactor and detector, and to ensure flat temperature and concentration profiles across the bed. The axial dispersion was also reduced by keeping the volume of piping between reactor and detector as low as possible.

2.6.3 Fourier Transform Infrared Spectroscopy

Two forms of Fourier transform infrared spectroscopy have been used in this research; gas FTIR and DRIFTS (Diffuse Reflectance Infrared Fourier Transform Spectroscopy). The theory behind these two forms of infrared spectroscopy is now reviewed. The theory of the infrared spectroscopy of gases is treated as the same as fundamental infrared spectroscopy theory.

2.6.3.1 Theory

The theory of infrared spectroscopy is a staple of undergraduate chemistry teaching and, is therefore treated in detail in many undergraduate-level texts (e.g., Atkins (1997)). A more detailed text, concerning the infrared spectra of inorganic species is the book by Nakamoto (1986).

The basis of the theory is that when molecules vibrate they behave as coupled harmonic oscillators. The frequency of the vibration of a given chemical bond is determined by the stiffness of that bond and the masses of the atoms attached. The vibrations are quantised into a number of energy levels described by the solutions to the Schrodinger equation. A molecule is able to absorb radiation which corresponds to the frequency of an allowed[25] transition between vibrational energy levels. The molecules have a number of 'degrees of freedom' to their vibrations. The total number of degrees of

[25] Selection rules apply which are derived from the geometry of the molecule.

freedom for a molecule of N atoms is 3N. For a non-linear molecule three of these degrees of freedom are rotational and three are translational, leaving 3N-6 vibrational degrees of freedom. (A linear molecule exhibits 3N-5 vibrational degrees of freedom, as it has only 2 modes of rotation). For a non-linear triatomic molecule, such as sulphur dioxide or water[26] (shown below), there will be three modes of vibration. There are symmetric and assymmetric stretches, as well as 'bending' modes of vibration.

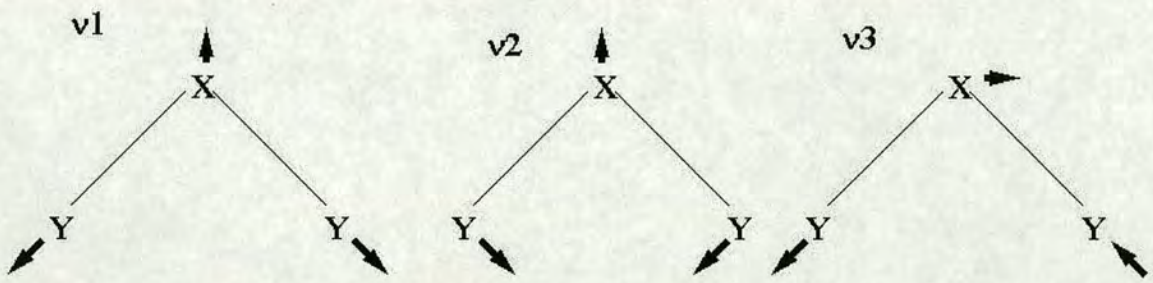

Figure 8 : The Three Fundamental Modes of Vibration for a Non-linear Triatomic Molecule, ν_1 Symmetric Stretch, ν_2 Bending and ν3 Asymmetric Stretch

These fundamental vibrations can lead to 'overtones' (multiples of fundamentals) and 'combination bands' (the sums or differences of two or more fundamentals).

The majority of infrared spectroscopy is conducted in the 'mid-IR' region, 4000 – 400 cm^{-1}. The major use of infrared spectroscopy in this region is the identification of functional groups. These groups have characteristic frequency ranges. The variation of a frequency within this range can lead to the determination of its local environment and to the identification of an unknown compound.

In the same way that the vibrations of the molecules are quantised, so are the rotations. The purely rotational spectrum can be seen in an entirely different part of the electromagnetic spectrum (1-100 cm^{-1}), but it affects the vibrational spectrum, in that, a vibrational energy level transition is often accompanied by a rotational energy level transition[27]. This leads to what is known as 'fine structure' within infrared absorbances, where the absorbance is split into 'branches' representing different rotational energy level changes. This can be seen very clearly in the infrared spectrum of water vapour.

---

[26] The infrared spectra of these species can be seen in the 'Results' section
[27] Again, this depends upon selection rules.

The quantitative analysis of gases by infrared spectroscopy is based upon the principle that the absorbance due to a gas is proportional to the concentration of that gas, by Beer's Law (see equation below). This absorbance can be calibrated from the absorbance peak using either the peak height at a specific wavenumber or the area of the peak.

Beer's law[28]:

$$A_i = \ln\left(\frac{I_o}{I_i}\right) = \varepsilon c_i l \qquad \textit{Equation 2}$$

Increased sensitivity can be achieved by maximising the path length, although for transient experiments this has a cost in terms of time resolution, as the residence time of the cell will be increased.

In the 1950s Fellgett determined that by use of an interferometer, rather than a diffraction grating, information from the entire infrared spectrum could be measured simultaneously. "Fellgett's advantage" was that not only could this technique produce spectra much more quickly, but the signal-to-noise ratio was considerably increased. The theoretical time advantage was proportional to the number of resolution elements of the spectrum, and the signal-to-noise ratio advantage was proportional to the square root of this value. For a typical spectrum of resolution 2 cm^{-1} over the range 4000 – 400 cm^{-1} FT-IR would (theoretically) be 1800 times as fast and have a signal-to-noise ratio 42 times greater than that of a grating spectrometer (Griffiths and de Haseth (1986)). The entirety of the theoretical advantages has not been realised in practice, but they are still considerable[29].

Initially the technique of FT-IR was not successful, because the analysis of the interferograms was very time-consuming. The advent of more powerful and readily available computers to perform the fast Fourier transforms required made the time advantages of the technique realisable. In this research the time advantage was important, as experiments were performed which involved recording the entire spectrum approximately every second.

---

[28] A – absorbance, I – intensity, ε - extinction coefficient, c – concentration, l – path length, suffix i – incident, suffix o – emergent.

[29] FT speeds up the collection of data by 10-1000 times (Banwell (1983)).

The simple theory of infrared spectroscopy is directly applicable to gas spectra. When applied to solids the interpretation of spectra becomes considerably more complicated.

2.6.3.2 Diffuse Reflectance Infrared Fourier Transform Spectroscopy (DRIFTS)

DRIFTS is a technique for studying solid samples by infrared spectroscopy using reflection-absorption rather than the transmitted infrared radiation. The theory of reflectance spectroscopy is treated in detail in Kortum (1969), and in a more abbreviated form in Delgass *et al.* (1979).

The basis of reflectance spectroscopy is that incident radiation upon a solid surface can undergo a number of processes before emerging from the surface. These processes include reflection, refraction and absorption. Solids are able to scatter photons as well as absorb them, so the amount of a species is no longer directly proportional to the amount of radiation absorbed. Hence, the interpretation and acquisition of reflectance spectra is greatly complicated and the path length is no longer known.

The Kubelka-Munk theory states that for an infinitely wide, flat, surface of depth X, the reflectance, R, is given by:

$$R = \frac{\left(1 - R_g\left[a - b\coth(bSX)\right]\right)}{\left(a - R_g + b\coth(bSX)\right)} \qquad \textit{Equation 3}$$

where $a = 1 + \frac{K}{S}$, and $b = \sqrt{a^2 - 1}$ and K and S are constants to account for radiation losses due to absorption and scattering, respectively.

The applicability of Kubelka–Munk theory to a specific sample is dependent upon a number of aspects of the experimental set-up. One of these is that the sample is sufficiently thick that the background reflectance is effectively zero. The reason for this is that, in the equation above, as $X \rightarrow \infty$ the equation can be simplified to yield the Kubelka-Munk remission function:

$$\frac{K}{S} = \frac{\left(1 - R_\infty\right)^2}{2R_\infty}$$

which is used in Kubelka-Munk spectra.

2.6.3.2.1 Infrared Analysis of Adsorbed Species

An adsorbed species confers its 3N degrees of freedom onto the adsorbent surface. Whether these extra degrees of freedom are exhibited depends upon the type and strength of the adsorption. The infrared spectrum of a physisorbed species can be very similar to that of the free molecule, due to the weakness of the interaction (van der Waals). This is not so for chemisorbed species, as they may have undergone substantial change; even if the adsorbate molecule has not been physically rearranged during the chemisorption, it is likely to have lost aspects of its symmetry, thereby changing its infrared absorbances. Whether a species can be distinguished from lattice vibrations, once chemisorbed, depends upon the species involved. If the bond formed is very similar to those of the lattice it will effectively become part of the lattice ('coupled') and therefore be indistinguishable by infrared spectroscopy from lattice vibrations. If the vibrations of the adsorbate molecule are very different to those of the lattice, this will not be the case.

Another complication is that there may be interactions between the adsorbate molecules, if the adsorbate surface density is great enough.

2.6.4 Electron Microscopy

A number of different techniques related to electron microscopy were used in the course of this research. An excellent book for an introduction to the theory and practice of most areas of electron microscopy is Flegler (1993). The following sections briefly detail the techniques used, their relative merits and objectives.

2.6.4.1 Scanning Electron Microscopy (SEM)

SEM has a higher resolution of image than optical microscopy and considerably greater magnification. This is because the wavelength of the particle/radiation used determines the lower limit of resolution and the effective wavelength of electrons is considerably smaller than that of visible light. The resolution of SEM is usually about 100 times greater than the highest resolution optical microscope can provide.

SEM detects low energy 'secondary' electrons[30]. The electron beam 'spot' is scanned over the surface and the secondary electrons detected, thereby generating a topographical image of the sample surface. The technique's depth of field[31] can be up to 1 mm, which is considerably more than that of optical microscopy.

SEM has produced evidence of surface species on solid absorbents (e.g., Sohail (1992), Bowker *et al.* (1981)). It can also be used as a means of characterising surfaces' topographies and textures. With these objectives, SEM was performed in this research on various oxide materials and oxide-supported catalysts before and after sulphur dioxide treatment.

2.6.4.2 Wavelength and Energy Dispersive Spectroscopies

When an atom is bombarded with electrons it emits X-rays of a characteristic frequency. The elements[32] present in a sample can be determined by measuring either the energy or the wavelength of the X-rays produced in this manner. This has resulted in two types of spectroscopy; energy-dispersive spectroscopy (EDS) and wavelength-dispersive spectrosopy (WDS). In general, EDS has a number of advantages over WDS:

- The cost of EDS systems may be only a quarter that of WDS (Flegler (1993))
- All elements can be determined in one spectrum by EDS, as opposed to a maximum of four by WDS giving EDS a large time advantage over WDS for elemental sweeps.
- WDS generally requires higher beam currents for sensitivity, which can destroy samples such as polymers and biological samples

WDS's greatest advantage over EDS is that it is more selective. The difference in energy of the emitted X-ray need only be 10 eV for this technique to be able to distinguish between two samples, whereas a difference of ~135 eV is required in EDS[33] (Flegler (1993)). For the purposes of this

---

[30] Electrons produced by interactions between incident electrons and sample electrons.
[31]. The highest resolution of an optical microscope is ~200 nm, whereas the highest resolution of a typical SEM is ~3 nm (Flegler (1993)).
[31] The amount of sample which can be in focus at one time.
[32] Elements with atomic numbers 8 to 99
[33] Overlaps often occur in EDS, i.e., differentiating between potassium and calcium is facile in WDS, but extremely difficult in EDS

research WDS was satisfactory, because there were very few elements of interest. The WDS, in tandem with SEM was used as a tool to map the distribution of elements (usually sulphur) at a microscopic level, rather than as a tool to identify which elements were present. Before attempting to perform WDS on the samples it had to be determined whether there was likely to be enough of the adsorbent to distinguish it from the inherent noise of the technique. Flegler (1993) states that, to be registered, the element must make up at least ~0.08 % of the sample by weight. This proved to be approximately the lower limit to the amount of sulphur adsorbed by the oxide samples in this research, hence, sulphur maps were obtained.

2.6.4.3 Backscatter Detection

Backscattered electrons can be used to detect areas of different atomic number within a sample. This is because the depth to which the incident electrons penetrate the surface prior to backscattering is inversely proportional to the atomic number of the atom by which they are scattered. The deeper they penetrate, the fewer escape. This results in a 'depth of penetration map', which is representative of the atomic numbers of the elements present, rather than a surface map.

2.6.5 X-Ray Powder Diffraction (XRPD)

The X-ray powder diffraction (XRPD) technique is used to identify different crystal phases within materials. It is often used as a tool of characterisation. A collimated X-ray beam is diffracted differently depending upon the crystal structure of the phase it is incident upon and the angle of incidence. Hence, a beam of X-ray radiation is directed onto an extremely flat surface of powdered sample over a range of angles. The diffracted signal received produces a pattern of signal versus angle, which can be used to determine the crystal phases present, usually by comparison with standards from a database. Goniometers are used to accurately determine the angles.

3. Materials and Methods

This chapter specifies the experimental apparatus used in this research and all procedures and analytical methods used. The principal piece of apparatus used in this research was the 'catalyst test apparatus'.

3.1 Catalyst Test Apparatus

3.1.1 Layout

The full layout of the catalyst test apparatus can be seen on the following page. The rig design is extremely flexible; a number of different experiments can be performed, without significant change to the arrangement. The following experiments can be performed:

- Dosing via a gas injection valve with sample gas in oxidising, reducing or inert conditions at a range of temperatures (ambient - 1000°C).
- Steady state treatment with sample gases.
- Temperature programmed experiments (e.g. TPD, TPR, TPO, TPSR).

In this research the main use was simulated storage and release of sulphur species involving dosing with sulphur dioxide in oxidising conditions, followed by a switch to reducing conditions to observe the release of the sulphur.

The rig was designed to minimise all the time lags between the reactor and the detection devices. The intention was to lessen the potential for axial dispersion of flows, which would lead to loss of information.

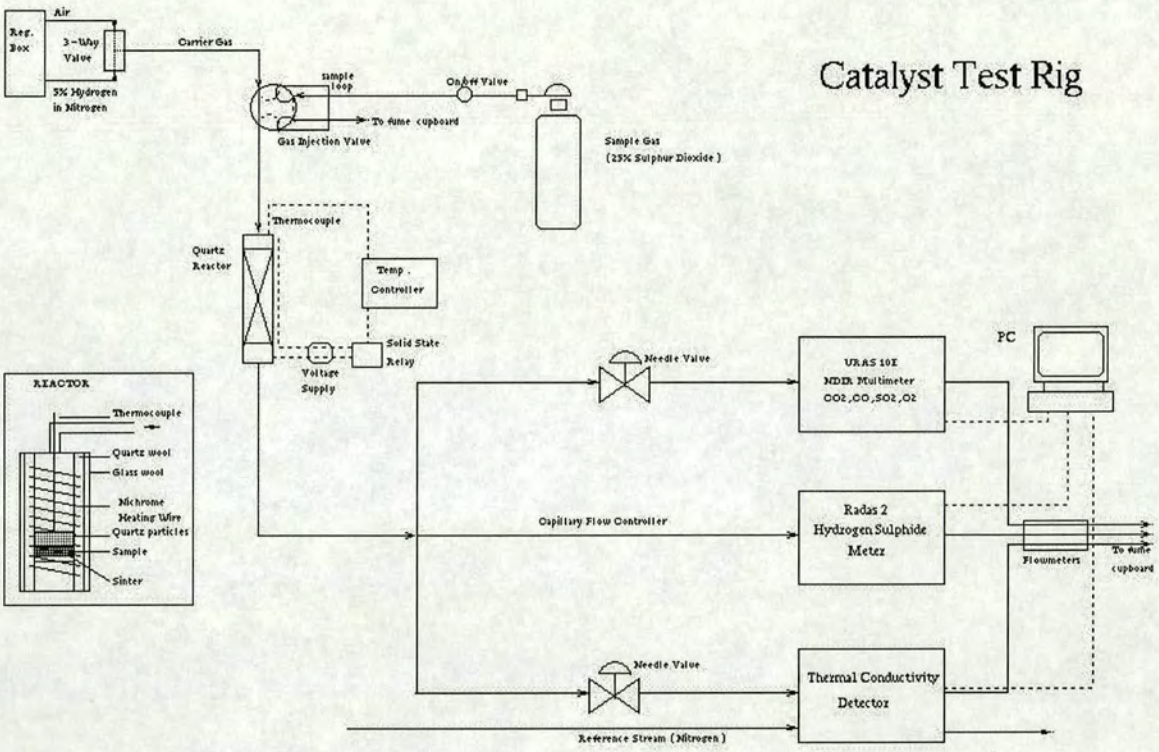

Figure 9: The Catalyst Test Rig

The pressure head of carrier gas was used to set the flow through a capillary restrictor to the hydrogen sulphide meter. Flows through the multimeter and the TCD were set using precision needle valves and variation of the total carrier gas pressure.

The Burkett three port, two position valve was computer-controlled to switch the carrier gas between air and 5% hydrogen in nitrogen. A Burkett two-way valve, also controlled by the computer, was used to ration the supply of sample gas to ensure that it was not flowing when unneeded. This considerably extended the period between refills of the sample gas cylinder.

3.1.2 Reactor Design

The reactor design was based upon a simple design in Bowker *et al.* (1981) and upon suggestions made in Amenomiya and Cvetanovic (1971), Falconer and Schwarz (1983) and Machiels (1982).

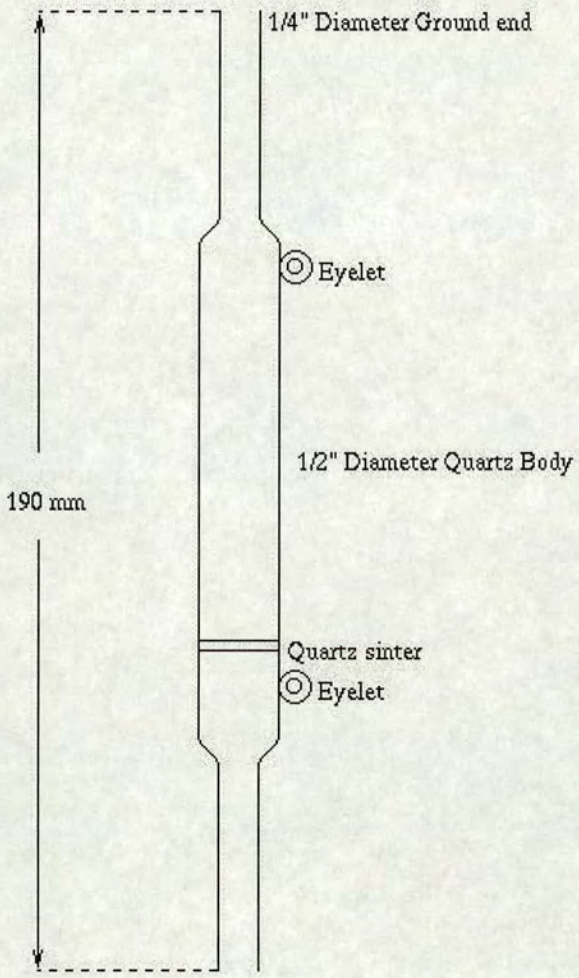

Figure 10: High Temperature Reactor

The reactor was fabricated at Cambridge Glass Blowing, Brookfield Ind. Est., Twentypence Rd., Cottenham, Cambs. It consisted of a quartz tube containing a quartz sinter. The sinter acted as a support for the reactants and quartz chips. The layer of quartz chips facilitated preheating and mixing of incoming gas. The reactor was heated by resistance wire ('Brightray', 24.7 Ω/m), surrounded by quartz wool wrapped in glass wool. The quartz wool was used as the inner insulant, rather than the glass, because the glass wool melted at the high temperatures used and fused with the quartz, damaging the reactor's outer surface. The glass wool used on the outside was in the form of a tape and, as such, could be wrapped around to hold the quartz wool in place, as well as providing extra

insulation. The power to the heating wire was provided by a variac set at ~40V, the output of which was controlled by a Eurotherm 902 temperature controller. The controller received feedback from a 0.5 mm diameter thermocouple in direct contact with the bed of particles (the head of the thermocouple was placed in the layer of particles, as close to the central axis as was possible). The thermocouple was the smallest diameter possible, so that its heat capacity has negligible bearing on the temperature recorded. The maximum temperature achieved on this rig was 1000°C and the temperature registered by the Eurotherm in the normal working range was always within 1 °C of the set-point temperature.

3.1.2.1 Developments in Reactor Design

The initial design required a few modifications over the course of its use:

- The original quarter inch ground-glass ends were found to be extremely prone to breaking, and the tubing was difficult for suppliers to obtain. The quarter inch diameter was originally specified so that the reactor could be attached via quarter inch Swagelok fittings. More robust 6 mm tubing without ground glass ends, connected to the Swagelok via a quarter inch to 6 mm conversion PTFE ferrule, was found to be an improvement.
- The main problem with the reactor itself was its fragility. This was mainly a problem at the ends, where the quartz was under stress where it connected with the large quarter inch 'Swagelok' fittings. There was a very small difference, when fitting the bolts, between overtightening, and thereby breaking the tubing, and undertightening, meaning that the seal was not air-tight and would leak. This problem was exacerbated initially by the use of graphite ferrules; it was found later on that PTFE ferrules were considerably more 'forgiving' on the quartz tubing.
- The heating wire was doubled over for a few cms between the eyelets, where it attaches to the reactor and the connectors to the power supply wire. This is because this portion of the wire was not in contact with the reactor and tended to burn out; doubling over effectively halved the current passing through any one part of the wire. Later, this part of the wire was also insulated by ceramic 'fish spines' for extra protection against burning out.
- The first heating wire, described in the previous section, was prone to burn out. This was because it tended to oxidise at the higher temperatures, and as the outer layer oxidised the cross-sectional area for the current decreased and this caused hot-spots', eventually leading to its failure. The area most prone to this was the portion of the wire not in contact with the quartz, (as mentioned

above). A number of different wires were used[34] before settling on Kanthal[35], a proprietary alloy, which was designed to operate at high temperatures and as such has fewer problems with oxidation.

3.1.3 Eurotherm 902

This was a controller/programmer, used in this experiment to control the power supply to the heating wire around the reactor to provide reliable steady temperatures and accurate linear temperature ramps. Once tuned to a specific system the controller uses derivative and proportional action algorithms to control the temperature of the reactor to a high degree of accuracy (all temperatures quoted here are to at least the nearest 1°C).

3.1.3.1 Tuning

The Eurotherm controller has a number of tuning options. The default values set at the factory ensure 'straight line control', but these values did not cope well with perturbations (such as a switch between carrier gases of greatly differing thermal conductivity[36]) and rapidly changing set-points (such as in the linear temperature ramps required); the controller required 'loop tuning'. This could be done manually or by using the 'self-tune' facility.

The self-tune facility overwrote certain default values. The problem with this facility, for temperature ramp purposes, was determining the tuning temperature. In most instances during this research it was tuned to 500°C. This tended to give good control (the measured temperature was +/-1°C of the set-point) in temperature programmed experiments from ~250°C onwards, but poor control beforehand (oscillating around the set point). This was acceptable in all experimental runs, as the temperature region in which all significant data were collected was above 400 °C.

A number of factors caused the tuning requirements to change over time:

- *Deterioration of heating wires.* As the heating wire reached very high temperatures in air its outer surface tended to oxidise. This causes its resistance to increase, causing greater power to be

---

[34] 'Brightray' and nichrome resistance wire.
[35] For which we are grateful to the Kanthal Company for complimentary samples
[36] Such as air and 5% hydrogen in nitrogen used in this research

required from the voltage supply to achieve the same temperature. The reverse was true when new wiring was installed

- *Reactor changeover.* Every time the reactor was changed over (when each new sample was installed) there were, inevitably, slight changes in the arrangement, such as a slightly different arrangement of insulation or wiring or a sample with a slightly different heat capacity. These caused slight differences to the amount and direction of the heat flux within the system.

The self-tuning algorithm used by the Eurotherm determines the optimal tuning parameters by observing the response (the temperature) of the system to certain power input values. The self-tuning procedure involves putting the system through a number of temperature variations, including a temperature increase to over 500 °C, thereby changing the temperature history of the sample and substantially altering the results of any subsequent experiment. For these reasons self-tuning cannot be done *in situ*, so the tuning parameters were not the best possible, although, generally they did give very good control.

3.1.4 Sulphur Dioxide Detection

A number of sulphur dioxide meters are mentioned in the literature for research in this area;

- The Siemens Ultramat 5E sulphur dioxide analyser (Gidney (1996)).
- Mass spectrometers (e.g. Lox *et al.* (1989), Kim and Juskelis (1996)). Mass spectrometry was not used in this research. It is preferable to the techniques used here on the grounds of greater specificity in the analysis of complex systems, but it is known that such high levels of sulphur would adversely affect the mass spectrometer signal, particularly when hydrogen sulphide is involved.
- The Uras 10E Industrial Photometer was used in this research. It was supplied by Hartmann and Braun (UK) Ltd., Moulton Park, Northampton. The Uras 10E is a 4-way gas analyser, configured to monitor CO_2, CO, SO_2 and O_2, although it can be configured for a number of other gases[37]. The principle of its operation is based upon the "property of heteroatomic gases to absorb infrared radiation in the wavelength range... ...λ = 2 - 8 μm", (Hartmann & Braun), using NDIR[38] in a system of filters. The meter gives a linear signal output derived from the I.R. absorbances by the

---

[37] CH_4, C_6H_{14}, NO, N_2O, various freons.
[38] Non-Dispersive Infrared

Lambert-Beer law. The meter readout is given to an accuracy of 1 ppm for CO_2, 2 ppm for SO_2 and CO and to 0.01 volume % for O_2.[39]

A significant drawback was discovered in the use of the Uras 10E for the purposes of this research; the fact that the I.R. band of sulphur dioxide used for detection overlapped with that of water (see following figure), thereby causing concentrations of water vapour to be registered as sulphur dioxide. This made it extremely difficult to conduct experiments in which water could be a major factor.

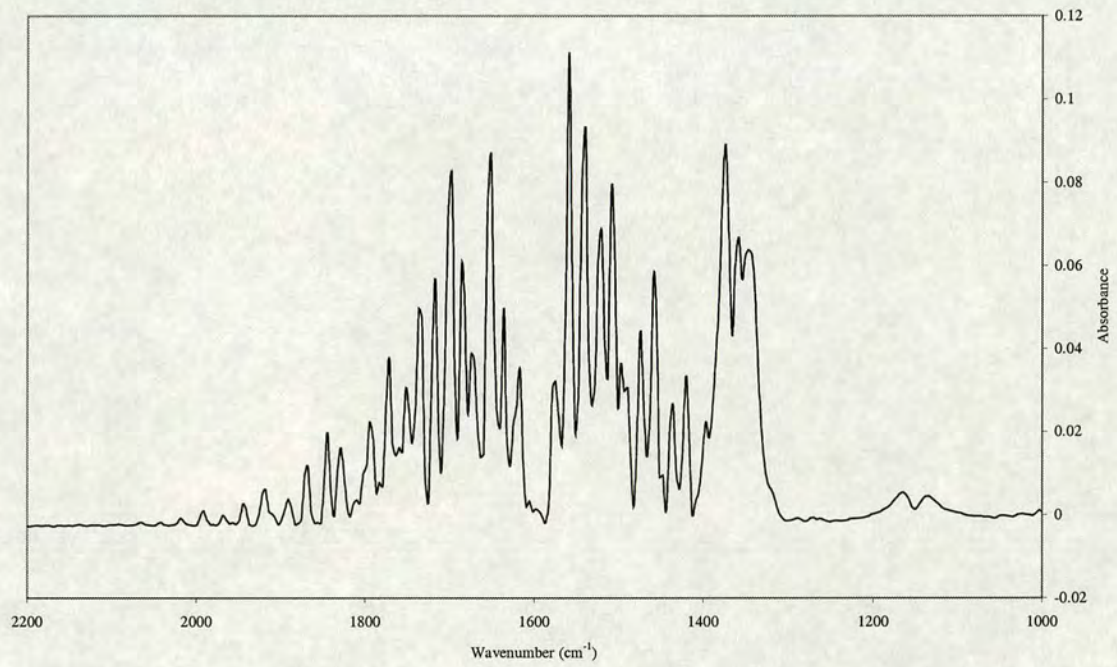

Figure 11: IR Spectrum of H_2O and SO_2

The multiplet centred at ~1600 cm^{-1} represents the water, and this can be seen to overlap with the sulphur dioxide ν_3 frequency centred at 1361 cm^{-1}. The peak centred at 1180 cm^{-1} represents the sulphur dioxide ν_1 vibration.

A number of trials of possible reactants and absorbents[40] to remove the water were conducted, but all either absorbed SO_2 to too great an extent or did not absorb water sufficiently. In any case the use of

---

[39] Greater accuracy for the Uras and Radas readings has been achieved using the data collection programs by averaging readings over 1 second (400 - 500 readings).

[40] Molecular sieves 3A, 4A, 5A, anhydrous calcium sulphate, silica, Tanax™ and phosphorus pentoxide.

an adsorbent would complicate the analysis of any data, as the reaction would now be 'coupled' to the response of the adsorbent.

Hartmann and Braun provide a condensing unit to remove the water for just this reason, but this was not a good solution to the problem in this research, as it would increase the amount of time between reactor and detector and, therefore, increase the amount of axial dispersion. An attempt to use D_2O instead of water proved unsuccessful, because the D_2O band overlapped with sulphur dioxide in the IR spectrum more than the H_2O.

Since the meter is relatively insensitive to the water concentration, the solution to the problem was to run experiments where the water concentration is effectively constant (either in excess or with no water at all), and then to correct for the water and thus deduce the sulphur dioxide concentration using the Lambert-Beer law. When ambient air (1 - 2 % water) flowed through the meter, it was registered as only ~70 ppm SO_2, so any changes in water concentration due to sorption or reaction with the sample were unlikely to affect the water concentration appreciably. Any water concentrations large enough to cause significant artefacts in the sulphur dioxide trace would be obvious in the TCD reading.

3.1.5 Hydrogen Sulphide Detection

A number of different methods of transient hydrogen sulphide concentration measurement have been tried:

- Mass spectrometry is normally cited as the ideal technique for temperature programmed experiments. Kim and Juskelis (1996), Lundgren (1995), and Lox *et al.* (1989) have all reported experiments involving hydrogen sulphide detection by this means. Nonetheless, it was believed that the concentrations of hydrogen sulphide used would lead to problems with decreasing response, due to sulphur contamination of the filament. Also there would be significant adsorption effects inside the spectrometer which would adversely effect the signal and the time resolution.
- Dettling, 1990, reported continuous monitoring of the hydrogen sulphide by use of an analyser produced by Horiba. Presumably this is the same as that used by Gidney (1996) "the Horiba 1120 cross-flow analyser", which uses NDIR.
- *Jerome gold film analysers* have been used (e.g., by Bending *et al.* (1993)). The time-resolution of this technique is unlikely to be sufficient for the experiments conducted in this research.

- *Drager tubes:* Gottberg *et al.* (1989). This method does not have the required time-resolution.
- *Gas chromatography:* Yamada *et al.* (1990) used a flame photometric detector This would be too slow a technique for this research.
- *EPA colorimetric* (Henk *et al.* (1987)): This involves bubbling exhaust gas through a zinc acetate solution to trap the hydrogen sulphide and reacting it to form methylene blue. This method would have neither the time resolution, nor the accuracy required.
- Lox *et al.* (1989) report the use of a technique using lead acetate tape as a colorimetric device. This is unlikely to be accurate enough for this research.
- Harkonen *et al.* (1990) used "a fluorescence based analyser" (Monitor Labs, Model 8850) to measure sulphur dioxide and hydrogen sulphide simultaneously.
- *Radas 2 Hydrogen Sulphide Meter.* The meter available for use in this research was the Radas 2, supplied by Hartmannn and Braun (UK) Ltd., Moulton Park, Northampton. The Radas 2 operates on ultraviolet absorption principles.

The Radas 2 readout gives a display accurate to 5 ppm over the range 0 - 2500 ppm. This meter also had problems with overlapping frequencies, in that its ultraviolet detection frequency overlaps with that of SO_2. This problem could be rectified, because, unlike the SO_2/H_2O overlap in the Uras 10E, the concentration of the other gas is known from the URAS 10E reading. Its contribution can, therefore, be subtracted from the H_2S reading during the data handling[41].

3.1.6 Thermal Conductivity Detector (TCD)

The TCD works on the principle that two resistance wires (one on-line the other immersed in the reference gas flow) conduct differently depending on their temperature. The temperature is dependant on the thermal conductivity of the gas surrounding them. This was used to distinguish between gases of differing thermal conductivity. The reference gas used for the thermal conductivity detector in this research was nitrogen. Oxygen has a thermal conductivity which is not significantly different from nitrogen's and is therefore not detected. Gases such as sulphur dioxide and hydrogen sulphide were never present in large enough quantities to be detected, taking into account the fact that their thermal

---

[41] The maximum amount of water artefact encountered in the SO_2 readings, when scaled down for the correction for H_2S would be smaller than the resolution of the H_2S meter and therefore negligible.

conductivities are relatively close to nitrogen. The TCD response is due to hydrogen, as hydrogen's thermal conductivity differs from that of the reference gas by much more than the other gases:

Gas	Thermal Conductivity at 26.7 °C (cal/s.cm^2) (°C/cm) x 10^{-6}
Nitrogen	62.40
Oxygen	63.64
Hydrogen	446.32
Water vapour	42.57
Carbon dioxide	39.67
Carbon monoxide	59.92

Table 2: The Thermal Conductivities of all gases present at Operating Temperature 28 °C (Weast (1981)).

In retrospect, the TCD data may have been improved by the use of a cold trap, to trap out all the gases except hydrogen and nitrogen. Due to the noise of the system and the relatively small amounts of other substances present (the thermal conductivities of which were much closer to the reference gas than hydrogen) this would have made little difference to the final results, but may have decreased the error margins slightly.

3.1.7 FTIR Gas Analysis

The catalyst test rig was set up with infrared gas analysis. The infrared spectrometer used was the Biorad FTS-7. The ability to observe the entire gas IR spectrum was useful for two main reasons:

- It enabled water and sulphur dioxide to be distinguished.
- It enabled sulphur trioxide to be observed.

Other advantages were:

- It enabled unanticipated species to be observed.
- It could back up the readings from the other meters.

The technique has a high sensitivity for sulphur dioxide and trioxide, and lower sensitivity for water (although it is one of the best techniques for transient water concentration measurement). However, hydrogen sulphide detection is extremely poor, and all homonuclear diatomic species are not detected, so this technique could not be used as the sole detection device. The FTIR spectrometer was not available throughout the investigation, but when in use, it contributed to a comprehensive quantitative gas analysis.

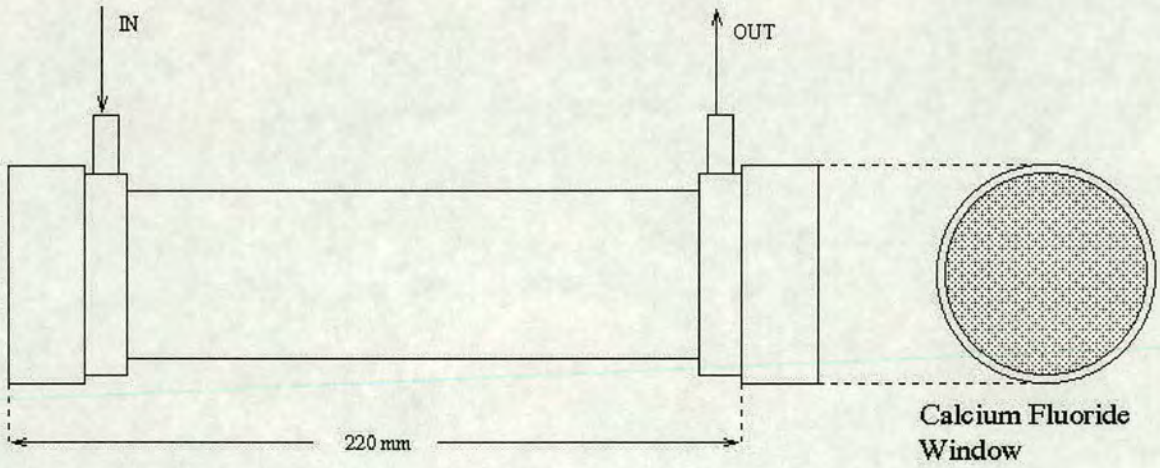

Figure 12: Gas IR Cell

The cell was designed to have as long a path length as possible (to maximise the IR absorption of the gases). The windows are made of calcium fluoride, which is water-resistant and has a wide spectral operating range. The cell was designed to be able to withstand high internal vacuums as these are a necessary part of the calibration process used here. The spectrometer was fitted with a moveable iris to

control the amount of infrared radiation through to the cell. This was particularly important to prevent saturation of the MCT[42] detector, which would lead to non-linearity.

3.1.7.1 The Formation of Sulphur Trioxide

The formation of sulphur trioxide was identified as, potentially, a large problem in this research, in that, it is not distinguished from sulphur dioxide by the photometer (the URAS 10E) and, more importantly, it would cause significant corrosion damage. Consequently, separate experiments were performed with IR gas analysis to assess the extent of sulphur trioxide formation. In general, it seems unlikely that sulphur trioxide would be evolved during TPRs or, indeed, any portions of experiments where hydrogen is present, as it is extremely reactive.

If the reaction taking place over a platinum catalyst in oxidising conditions in the presence of sulphur dioxide were the same as that over platinum metal (Bond (1962)):

$$SO_2 \xrightarrow{Pt} SO_3$$

as in the early 'Contact Process' for the production of sulphuric acid, there would be no doubt that sulphur trioxide would be one of the main products. In the late 1970s this was a major health concern, as it was believed that oxidation catalysts could cause the emission of sulphuric acid and various sulphates. The solution arrived at was to decrease the oxygen content of the exhaust gas. It was decreased to a level where the sulphate emissions were no longer significant, but the conversion of CO and hydrocarbons was not adversely affected.

This does not necessarily mean that today's catalysts do not produce sulphur trioxide (although it is to be hoped that they do not), as there have been many developments in catalyst design since those studies, but it does imply that the problem is not as significant as could be imagined.

Lox *et al.* (1989) used a mass spectrometer as the detector for all sulphur–containing species. During experiments on sulphur absorption and release by catalyst components they found that "no SO_3 was detected in any of these experiments", although they do not preclude the possibility that all the SO_3 has decomposed to sulphur dioxide and O_2.

---

[42] Mercury Cadmium Telluride, a fast, mid-range detector.

If it were the case that all the SO_3 formed decomposed, then, for the purposes of this research there would be no problem with SO_3, because the main reason that the question of SO_3 formation must be resolved is to account for all sulphur. The sulphur mole balances would obviously be inaccurate if the amount of one of the species formed could not be quantified due to its non-detection. The other possible explanation for the location of the trioxide if it is formed, is that all the sulphur trioxide formed on the surface goes on to react with the surface oxides to form the species in which the sulphur is stored (e.g., sulphates or oxysulphates).

Sellers and Shustorovich (1997) state that it may be impossible to desorb sulphur trioxide intact, as it will decompose to sulphur dioxide before desorption.

Engler *et al.* (1991), on the other hand, reported the detection of sulphur trioxide during investigations of the effect of sulphur in oxidising and reducing conditions on various PGMs supported on alumina and ceria. Their detection method involved passing the exhaust gas mixture through a mistcatcher maintained at 90 °C such that the sulphur trioxide reacts to form sulphuric acid and is condensed out and titrated against a barium acetate solution. Their method of determining the sulphur dioxide was similar, involving passing the gas from the mistcatcher into an "aqueous solution of H_2O_2" which oxidises the sulphur dioxide to the trioxide, the same titration being performed on the resultant sulphur dioxide.

3.1.7.2 Calibration Equipment

The apparatus shown below was used to calibrate the gas infrared cell for sulphur dioxide. All the lines used were glass.

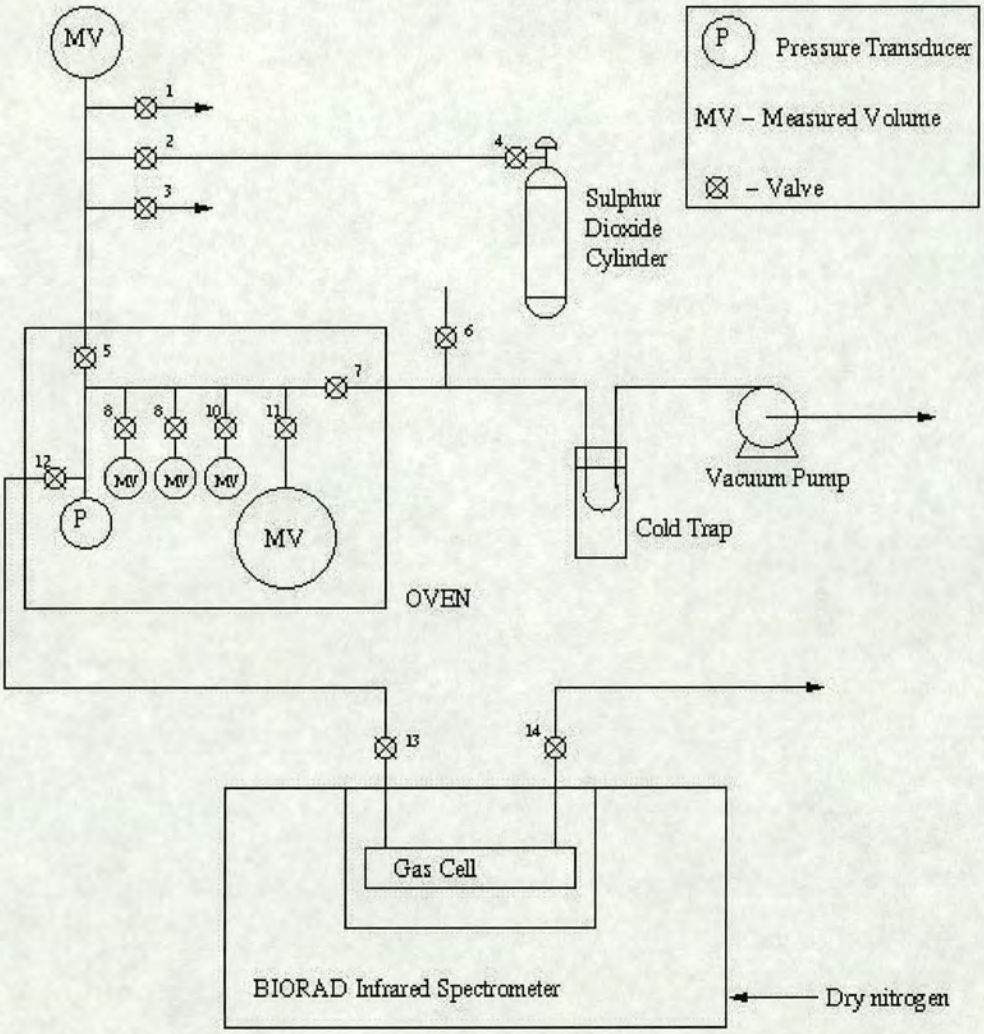

Figure 13: Calibration Equipment

Initially the entire system was evacuated and then filled with nitrogen and evacuated three times. The evacuation involved ensuring that valves 1, 3, 4 and 14 were closed and all others open with the pump warmed up and running. When the system had achieved a satisfactory level of vacuum, valves 8-10, 12 and 7 were closed. Valves 4 and 11 were then opened to allow sulphur dioxide to pass into the main measured volume (the largest one inside the oven). This volume was then isolated and the residual sulphur dioxide in the pipework pumped away to be caught by the cold trap, which was at liquid nitrogen temperature. Valves 7 and 5 were then closed and 12 opened so that sulphur dioxide could be bled into the gas infrared cell. When the desired pressure was achieved the bulb was again isolated.

Infrared spectra were then recorded, at a resolution of 2 cm^{-1} and with each spectrum consisting of 64 co-added scans. Each spectrum was repeated four times to identify any time-dependence of the reading which would indicate leakage or inherent activity of the system to sulphur dioxide. Once these had been taken the process was repeated with a different pressure of sulphur dioxide. The infrared peak areas were calculated using macros which made use of the 'WinIR' peak integration software. The calibration involved data from different initial fillings.

3.1.8 Driving Software

A number of programs were written to log and display the data and operate the valves in the system. The writing necessitated the learning of the computer language, C. The following programs were written in C with help from Dr. D. Costello. The functions of these programs (listed in Appendix 7.6) were as follows;

1. *observe.c* : As well as displaying the readings every second, this program logged all the gas concentrations, taking a data point every 10s (so as to reduce data-file size) and whenever a SO_2 or H_2S reading deviated from the previous one by a specified amount (this gave greater detail on peaks etc.). This program was used in slower TPRs and in pretreatment TPRs (where detailed peak information is less important than in standard TPRs).

2. *obstpr.c* : This program was designed to collect data every second. This was required for high heating rate[43] TPRs.

3. *3way.c*: This changed the position of the switchover valve (usually between 5%H_2 in N_2 and air).

4. *flush.c* : This program operated the sample gas cutoff valve, thereby flushing out the sample loop. This was performed prior to any dosing experiment.

---

[43] The higher the heating rate the greater the temperature difference per second, therefore the more rapid the data collection required for the same resolution.

5. *1pulse.c* : This program was designed specifically for peak analysis and consequently had data collection every 10s before gas injection (to examine for baseline drift) and every second thereafter. The program records the response to only one dose.

6. *nonavge.c* : This program functioned as per 1pulse.c, except with real-time data collection (as opposed to an average over the previous second[44]). From experiments conducted it has been found that real-time data can be preferable when observing rapid changes such as peaks, but that for small rates of change averaging was more accurate.

7. *switch.c* : This program performed 'switchover' experiments, i.e., simulated storage-release cycles, on autocatalyst components (see section 3.2.2.1 for the full procedure). The switchover experiment consisted of 1000s of dosing (one dose every 100 s) with data collection every 10 s, or when perturbations occur, followed by every-second data collection after 1000 s to observe the switchover peak in great detail. The program also operated all the valves involved; the GIV, the carrier gas switchover valve and the dosing cutoff valve (to reduce sample gas use).

8. *ambpulse.c* : This program kept the sample loop at ambient pressure during dosing, thereby giving smaller pulses when required. Otherwise it was identical to other dosing programs.

9. *sol-try.c* : This program performed gas injections every 100s and operated the sample gas cutoff valve such that the sample gas only flowed in an experiment when required (thereby increasing cylinder lifetime from a few days to a few weeks). Injections were performed every 100 s to ensure that concentrations returned to baseline levels between doses. This file was used to dose the sample during the dosing stage of standard TPRs and for prolonged sulphur dioxide treatments.

The relationship between the signal received at the computer and the gas concentrations was determined by comparison of the signal and the displayed meter readings for various constant concentrations of gas. A linear fit was applied.

---

[44] Of ~450 readings.

3.1.9 Peak Shape Analysis

The peak shape can give important information about the quality of the experimental system, particularly concerning the extent of axial dispersion. The amount of axial dispersion is important, because the greater the amount of dispersion between reactant bed and detector, the lower the quality and reliability of the data. If the amount of axial dispersion is known, then the degree of error in the results can be assessed. The peaks have been analysed by the methods and criteria described in Levenspiel (1962) and Westerterp *et al.* (1984).

The "vessel dispersion number" is a dimensionless group used to determine the amount of axial dispersion. The vessel dispersion number is 0 for plug flow and infinite for backmixed flow. Hence, it is desirable to obtain as small a value for this number as possible (perfect plug flow results in no loss of information). Levenspiel describes a value of the order of 0.002 as a "small amount of dispersion" and 0.025 as an "intermediate amount of dispersion". The vessel dispersion number is defined thus:

Vessel Dispersion Number[45]: $\frac{D}{uL}$ Equation 4

The problem with direct calculation of the vessel dispersion number is that it is difficult, if not impossible, to know D, the "effective longitudinal dispersion coefficient". Therefore the vessel dispersion number cannot be calculated for the system directly, but must be derived from peak shape data. The following two graphs are, firstly, a 'standard' pulse of sulphur dioxide passing through the multimeter and, secondly, the residence time distribution of the system, derived from that pulse.

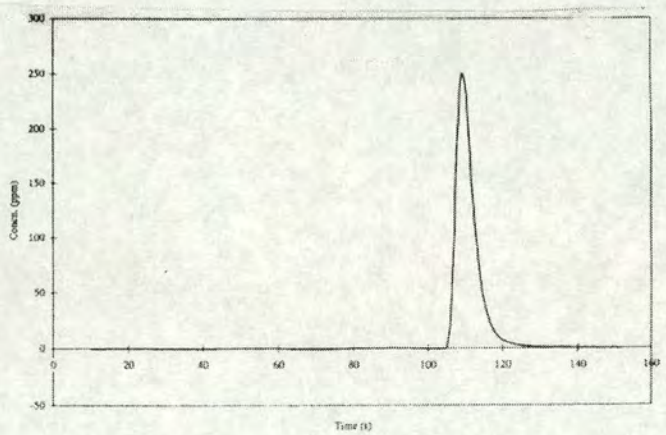

Figure 14: Pulse of Sulphur Dioxide detected by SO_2 Meter

[45] D - effective longitudinal dispersion coefficient (m^2/s). u - velocity (m/s), L - length (m).

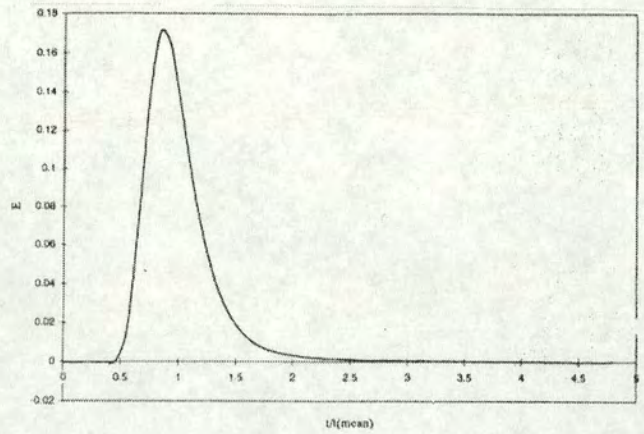

Figure 15: Apparent Residence Time Distribution

The data were analysed using an equation implemented on a spreadsheet. The variable "Var(Q)" on the spreadsheet is the variance, calculated using the equation (Levenspiel (1962):

$$Var(Q) = \frac{1}{\bar{t}^2}\left(\frac{\sum t_i^2 C_i}{\sum C_i} - \left(\frac{\sum t_i C_i}{\sum C_i}\right)^2\right) \qquad \text{Equation 5}$$

From the data of the residence time graph, the variance was calculated to be 0.0802.

Once the variance has been determined, the vessel dispersion number can be calculated, in one of two ways:

1. Using the equation: $$Var(Q) = 2\frac{D}{uL} - 2\left(\frac{D}{uL}\right)^2\left(1 - e^{-\frac{uL}{D}}\right) \qquad \text{Equation 6}$$

A trial and error method must then be employed to find $\frac{D}{uL}$, with a first guess of $\frac{Var(Q)}{2} = 0.04$ based upon ignoring the second term as an approximation.

2. Using the equation: $$Var(Q) = 2\frac{D}{uL} + 8\left(\frac{D}{uL}\right)^2 \qquad \text{Equation 7}$$

This is less accurate, as it is based upon the assumption that this is an ideal "open vessel", i.e., with no discontinuities in flow. This assumption becomes increasingly accurate as the vessel dispersion number decreases (as the vessel becomes more like the plug flow model).

The first method gave a value of 0.04185 for the vessel dispersion number. The second analysis generates a value of 0.0351, which differed by approximately 16% from the more accurate first method. Clearly the second method is not accurate enough for use in this system.

The value of 0.04185 is in the range termed by Levenspiel "an intermediate level of dispersion". This result could be worked with, but is not particularly good. The vessel dispersion number is actually considerably lower than this, because the analysis assumes an ideal Dirac δ input function, which is not the case. The input function in this system will have a peak-like shape, because it is a function of the manner in which the carrier gas flushes the sample gas out of the sample loop. The design was intended to minimise the duration of the input function as much as possible, but it was expected that the input function will still be considerably non-ideal. The aspects of the design which went towards minimising the input function duration were:

- Relatively large flow rate
- Relatively small sample loop

These design considerations had to be weighed against a number of other factors:

- The length of the sample loop was constrained by the minimum length needed to attach the loop at both ends of the gas injection valve.
- Too small a sample loop, would lead to smaller pulses, leading to detector sensitivity problems. As the pulse size diminishes the quality of the peak decreases, because the signal becomes of similar magnitude to the resolution of the meter, and the digitisation of the signal becomes apparent.
- The carrier gas flow rate was constrained by the pressure, which could be supplied by the regulator boxes used. In any case, too high a rate would lead to smaller peaks, leading to detectability problems, as mentioned above.

To obtain a more meaningful idea of the axial dispersion between the reactant bed and the detector (the section in which useful information would be lost), the outcome of this experiment needs to be compared to the input function. This was achieved by routing the piping from the gas injection valve

output into the detector as directly as was physically possible. In attempting to do this it was found to be very difficult to achieve a lower vessel dispersion number than that achieved already. Routing the pulse directly from the GIV to the Uras 10E via 1/16 inch diameter piping with a flow rate of over 800 cc/min actually led to a larger apparent vessel dispersion number. The experimental level of dispersion was comparable with that seen when the volumes of piping between the sample loop and detector were minimised. Hence, the apparent dispersion is mainly due to the non-ideal shape of the input function. It was expected that dispersion would be very small in this system, because the flow rates were large and the volumes of piping etc. were extremely small.

3.1.10 Particle and Sample Sizing

The autocatalyst component samples could not be used in their original form, that of very fine, free-flowing powders, for a number of practical reasons:

- The powder would tend to blow through the sinter and would have an adverse effect on all instrumentation downstream of the reactor, as well as constricting, and eventually blocking, pipes. Constrictions of the pipes would lead to changes in the flow resistance of the system thereby necessitating constant varying of the pressure head.
- The fine powders could make heat transfer and therefore temperature control more difficult. Transfer of heat through beds of small particles requires greater bed depths, as the main mechanism by which the heat is transferred is by stream-splitting, which increases with particle size and bed depth. This method of heat transfer is increased in the reactor used in this work by a layer of larger inert particles of quartz on top of the catalyst layer.

It was decided to compress the powders into discs, which would then be broken up into small particles and sieved into a specific size range. There were a number of factors that limitted the particle size:

- If the particles were too large, wall effects[46] become significant, leading to unequal flows through the bed.
- Intraparticle diffusion effects become significant for particles over a certain size.
- Larger particles have worse contact with the thermocouple, leading to inaccuracies in temperature measurement.

---

[46] The channeling of flow down the walls of the reactor due to having larger interstices between wall and particle than between particles.

Bed depth must be kept to a minimum to reduce readsorption effects, although this has a cost in terms of the flow characteristics, in that plug flow is more likely through deep beds. This is overcome to some extent by a layer of quartz particles above the catalyst layer; this layer improved the flow characteristics, without causing readsorption problems (as it is inert). The reactor diameter must be small to lessen the potential for thermal gradients across the bed (Falconer and Schwarz (1983)). These requirements can lead to very small amounts of particles, and so must be weighed against the requirements of the detectors.

A number of different criteria have been proposed for determining the optimum particle size of samples in TPD and TPR experiments. Fierro *et al.* (1994), claimed that, in general, a size of 400 μm or less would be acceptable in terms of avoiding intraparticle gradients. Their calculations were based upon the findings of Ibok and Ollis (1980) who found that "no appreciable diffusion gradients exist within the pellet" for $\phi < 0.3$. (where ϕ is the Thiele modulus[47]). The Thiele modulus for the system used here has been calculated to be considerably below this value.[48]

Monti and Baiker (1983) found that no intraparticle diffusion gradients or interparticle limitations (evaluated on the basis of Sh number) existed for sample sizes of radius <100 μm. They also defined a "characteristic number", $K = S_0/(V^*.c_0)$[49], which would provide optimal sensitivity in the range $55 < K < 140$ for heating rates of 6 - 18°C/min..

Gorte (1982) proposed a dimensionless group[50] for sample sizing:

$\frac{Ql}{DS} < 0.1$ - Intraparticle gradients negligible.

$\frac{Ql}{DS} > 20$ - Pore diffusion governs.

---

[47] Thiele modulus, $\phi = L\,(k/D)^{1/2}$; L = length of pore, K = reaction constant, D = diffusivity

[48] K was calculated from TPR data for ceria assuming first order kinetics, L ~ 150 μm, the effective radius, and the value of D used was the lowest possible, thereby giving the highest estimate for the Thiele modulus possible.

[49] S_0 - amount of reducible species initially (μmol), V^* - total flowrate of reducing gas (cm^3(NTP)/s), c_0 - concentration of hydrogen at outlet (μmol/cm^3)

[50] Q - volumetric flowrate (m^3/s), l - bed depth (m), D - effective diffusivity (m^2/s), S - external surface area (m^2)

Forzatti and Tronconi (1985) claim that "changes in temperature of the peak maximum ... as functions of the particle radius ... provide experimental criteria to detect the presence of intraparticle diffusional intrusions during TPD experiments".

Other workers in the field (e.g., Li *et al.* (1992) and Herz *et al.* (1982)) have performed similar analyses on differing chemical systems and created similar characteristic numbers or dimensionless groups.

Fierro *et al.*'s recommendation that particle diameters of less than 400 μm are used in TPR experiments has been observed in this research. Their work concerned oxide catalysts and was, therefore, applicable to this system.

The diameter of the reactor used in this research (0.01 m) will have no problems with wall effects as the particle sizes used were in the range 250 – 355 μm. The particle Reynolds number (defined below) was calculated to be 1.71 for this system at 500 °C.

$$^{51}\mathrm{Re}_p = \frac{d_e u}{\nu} \qquad \text{Equation 8}$$

Fierro *et al.* (1994) made a number of observations concerning the other variables in TPR experiments. They observed that broadening of TPR peaks occurs if the ratio of initial reducible species to feed rate is too high. For this reason, the design used in this research has a molar flow rate of hydrogen which was relatively large compared to the molar amount of sample. There are other reasons why a relatively high flow rate is desirable:

- It cuts down the potential for loss of information between reactor and detector by lowering the residence times for that section and flattening the velocity profile.
- According to Vanhove (1995), use of high gas velocity is the key to reducing the problems of fluid-particle thermal gradients in microreactors.

---

[51] d_e – effective particle diameter, u – superficial velocity, ν - kinematic viscosity

- According to Falconer and Schwarz (1983) low flow rates lead to problems with diffusion from catalyst surface to gas phase, longer time delay, increased temperature gradients and the increased likelihood of readsorption.

3.2 Experimental Procedures for Transient Reactions

3.2.1 Sample Preparation

The methods of preparation used were standard methods used at Johnson Matthey Technology Centre, Royston, Herts. The justification for this was that the intention of this research was that the results were applicable to real automobile catalytic converters.

3.2.1.1 General Method

The method of preparation was to duplicate as accurately as possible the preparation undergone by components of real autocatalysts. To this end the following substances were calcined for 1 hr. at 500°C[52];

1. *Cerium hydroxide:* Incorporated into commercial TWCs to improve long term catalyst performance and enhance noble metal utilization (Rieck *et al.* (1989)). The material was supplied, via Johnson Matthey, by Rhone-Poulenc. The hydroxide has the formula $Ce(OH)_2.nH_2O$. The material produced is of the formula CeO_{2-x}. Approximately 20 wt% of the sample is lost as water during the calcination.
2. *γ–Alumina (P_0)*: High surface area, thermally stable substrate. Provided by Condea Puralox, pH 4.5, surface area 138.6 m^2/g
3. *Ceria/alumina (P_{12})*: Johnson Matthey's current basic washcoat, a mixture of the two oxides above, with the composition 21.1 wt. % ceria, remainder alumina, pH 5.4, surface area 129.4 m^2/g.

These materials were all prepared by myself at Johnson Matthey Technology Centre, Royston, Herts. An XRPD was taken of the product of the cerium hydrate calcination, which proved that the compound was indeed ceria. The XRPDs of the other two products were in excellent agreement with powder patterns from the database, i.e., the XRPD of P_0 correlated with γ–alumina and that of P_{12} with a mixture of ceria and γ–alumina.

---

[52] This is a standard preparation of catalytic materials (Falconer and Schwarz (1983)).

3.2.1.2 Platinum-Doped Samples

Platinum-doped analogues of all the samples in the previous section were prepared. The doped samples were prepared in as similar a manner as was possible. The same starting materials were impregnated with platinum to 0.5 wt. %. The method used was to mix an amount of tetra-amine platinum (II) hydrogen carbonate ($Pt(NH_3)_4(HCO_3)_2$)[53], dissolved in the minimum quantity of citric acid, with an 'incipiently wet' slurry of the oxide powder and distilled water (the samples had already had incipient wetness factors[54] measured).

Hence, these samples had an additional drying step in their preparation. The drying step involved maintaining the sample at ~100°C for approximately 2 hrs. The samples were then calcined for one hour at 500°C, as in the preparation of the unplatinised materials. This heating regime is a standard procedure (Heck and Farrauto (1993)).

3.2.1.3 Nickel, Iron and Barium doped P_{12} and Platinised P_{12}

These samples were prepared by the "dry impregnation technique", as described in Aris (1985). After an incipient wetness test to determine the amount of distilled water required, the correct amount of nitrate of the dopant was dissolved in that amount of water and thoroughly mixed with the P_{12} or platinised P_{12}. After drying at ambient temperature the sample was calcined at 500°C for 1 hour.

The final weight percentages of nickel, iron and barium were 2.0, 1.9 and 4.7, respectively, i.e., equivalent molar amounts.

3.2.1.4 Preparation into a Form Suitable for the Catalyst Test Rig

After the preparatory steps described above, the samples were in the form of a very fine free-flowing powder. This could not be used in the catalyst test rig, as the powder would be able to move through the sinter. Hence, the powders were compressed under 8 tonnes pressure, crushed and screened into the size range 250 – 355 μm. The amount of sample used was 250 mg (+/- 0.1 mg), beneath a layer of 250 mg of quartz chips in the size range 355 – 850 μm.

---

[53] Chloroplatinic acid is often used to platinise samples, but this was not used here due to the tisk of chlorine contamination.

[54] The amount of distilled water per gram required to produce an incipiently wet slurry.

3.2.2 Experimental Procedures

3.2.2.1 'Switchover' Experiments

'Switchover' experiments on the catalyst test rig (section 3.1.1) were designed to simulate the fundamentals of the conditions in which it is believed that most storage-release H_2S emissions, or 'spikes', occur. Thus, exposure to sulphur species (as SO_2 in this simulation) in net oxidising conditions (dry air) was followed by a rapid switch to net reducing conditions (5% hydrogen in nitrogen).

Hydrogen was used as the reductant, because current research suggests that hydrogen is the main active reductant in real 'switchovers' (Yamada *et al.* (1990), Gidney (1996), Diwell *et al.* (1987), Lox *et al.* (1989) and Henk *et al.* (1987)). Gidney states that, "The reduction is attributed to the reaction with free hydrogen, which is readily available in fuel-rich combustion products".

The procedure was as follows;

Preliminary flow checks[55]:	TCD Measuring channel	25 cm^3/min.
	TCD Reference channel	25 cm^3/min
	Multimeter	225 cm^3/min
	H_2S Meter	800 cm^3/min

1: System flushing with 5% H_2 in N_2 at ambient temperature. This was continued until all monitored gas concentrations were stable at their baseline levels.

2: Heating to 50°C. This is the start temperature for the pretreatment TPR. The TPR did not begin until the temperature was reliably maintained and the monitored gas concentrations had returned to stable baseline values. The sample was allowed to stabilise at 50 °C for ~30 minutes. The TPR was started from 50 °C rather than ambient temperature, because maintenance at this temperature prior to the temperature ramp seemed to improve early temperature control. Another advantage was a standard starting temperature as opposed to the variable ambient value.

3. Pretreatment TPR. This was typically at a ramp rate of 50°C/min. to a maximum temperature of 900 °C. There were variations; a maximum temperature of 800 °C was used for some pure ceria samples due to the risk of sintering above this temperature. The pretreatment TPR is a standard procedure (Falconer and Schwarz (1983)), and is found to be very reproducible.

The ceiling of 900 °C was used, as this is a typical maximum temperature for conventional autocatalysts.

4. Cooling to run temperature. After a dwell period at 900 °C, during which all concentrations were seen to be stable at their respective baseline levels, the reactor was allowed to cool in 5% H_2 in N_2 to the desired temperature.

5. Switchover to dry air. All gas concentrations were observed during the switchover, because some small emissions do occur and the sample's temperature generally increases rapidly for a few seconds during the switch, before falling back to the setpoint, (this was due to the sudden change in thermal conductivity of the carrier gas).

6. Switchover run. When the gas concentrations return to the baseline once more the "switch file" was operated (see section, *'Driving Software'*). The sample was then treated with 10 doses of sulphur dioxide in air, followed by a switchover to 5% H_2 in N_2, at which point the switchover peak (if any) was observed with every-second data collection. Ten doses were used as the standard because this was found to be the greatest number that could be used without certain components causing some gas concentrations to go off-scale during the switchover.

7. Post-run TPR. This was performed so that all sulphur species could be accounted for. It was started about 500 s after the switch, when all gas levels had returned to their baseline levels, and was usually at a ramp rate of 50 °C/min.

---

[55] The errors for these readings are given in Appendix 7.4

3.2.2.2 'Standard TPR'

The 'standard TPR' involves heating a previously sulphur dioxide-treated sample at 50 °C/min from 50 °C to 900 °C in an atmosphere of 5 % hydrogen in nitrogen. The aims of the TPR are:

- To compare and contrast with the switchover data.
- As a means of comparing the strengths of adsorption of the sulphur species formed on different compounds and the form in which they are desorbed in reducing conditions.

TPRs performed by Kim and Juskelis (1996), showed that those performed in methane resulted in much higher peak maximum temperatures (~100–150°C higher) of both hydrogen sulphide and sulphur dioxide than when hydrogen was the reductant. Lundgren *et al.* (1995) performed TPRs on fully formulated fresh and aged catalysts in a number of reductants (H_2, CH_4, C_2H_2, C_3H_6, C_3H_8). They found that unsaturated hydrocarbons tended to cause peaks at much higher temperatures, but that saturated hydrocarbons could cause peaks to be even lower than those achieved with hydrogen. However, it is unlikely that hydrocarbons are significant reductants in real driving situations, as there are much lower levels of hydrocarbons than hydrogen in a typical automotive exhaust gas stream.

Experiments with other reductants were impractical with the available equipment, for reasons of their detection, and the detection of carbonyl sulphide (COS). All other likely reductants[56] contain carbon and would, therefore, be likely to emit COS. Lundgren *et al.* (1995) state that "COS desorption ...can contribute to the total sulfur desorption when carbon-containing reducing agents are used". Harkonen *et al.* (1990) reported that "COS formation (is observed)... at high temperature (700°C) during very rich conditions".

For these reasons the procedure decided upon as the 'standard TPR' involved hydrogen as the reductant and is as follows:

1 - 5: As switchover run.

6: Dosing. The sample was dosed to a much greater extent than during switchover runs to generate more detailed TPRs (without the peaks going off-scale). The 'standard' TPR performed lasted for 4000s (40 doses) at 500°C; the temperature at which the H_2S problem is conventionally said to occur (Gidney (1996), Lox *et al.* (1989)).

7: Cooling. The sample was then cooled in air to approximately ambient temperature, where the carrier gas was switched over to 5% H_2 in N_2. At this temperature there should be no switchover effects, either in temperature or gaseous emissions (and none were observed).

8: Heating to 50°C. This was carried out as per the pretreatment.

9: TPR. A temperature ramp to 900 °C at a linear heating rate of 50 °C/min, usually with more frequent data collection (every second) than the pretreatment, as the data were more important. There were variations to this procedure:

- Experiments were repeated with varying heating rate to assess the effect of this variable on the TPR spectra.
- In some instances, TPRs were conducted at 10 °C/min. for comparison with TPRs of pure compounds.
- Experiments have been conducted with varying surface coverage.

3.2.2.3 TPRs of Pure Compounds

A number of TPRs of pure compounds were performed for comparison with the catalyst components. The procedure was as follows:

1. Flushing at ambient temperature with 5 % hydrogen in nitrogen, until all other species had been expelled.
2. Slow heating to the start point of the TPR, 50 °C.
3. When all concentrations were stable at 50 °C, the temperature was ramped at a rate of 10 °C/min. Ideally, this rate would have been 50 °C/min for direct comparison with the component TPRs, but this was found to lead to gas concentrations going off-scale. The amounts required for the readings to remain on-scale at 50 °C/min would be too small for accurate weighing and for retrieval from the reactor, so a lower heating rate was opted for. Some standard TPRs have been performed at 10 °C/min for direct comparison.

---

[56] CO, hydrocarbons

3.2.2.4 Heavy Sulphur Dioxide Treatment

A number of heavily treated samples were produced, usually for DRIFTS, WDS and XRD analysis. The procedure was the same as the TPR steps 1 to 8 above, except that dosing was typically much longer (7000s, 70 doses) and there was no following temperature program, the sample was simply allowed to cool to ambient temperature when the dosing procedure was complete.

3.2.2.5 Glove Box Operation

Certain experiments[57] required the use of a glove box, because the materials were air-, or moisture-sensitive. A novel, fully evacuable glove box was custom-built for the laboratory, thus:

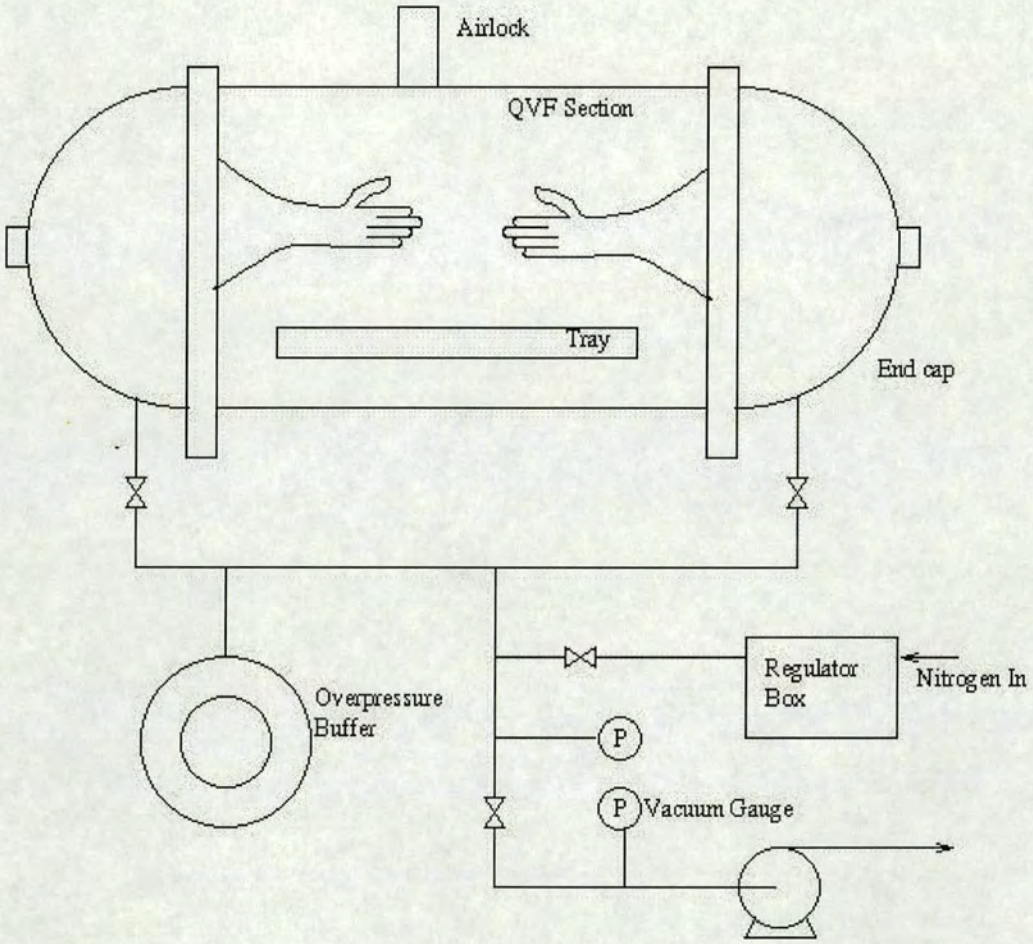

Figure 16: Glove Box

Operation typically involved evacuation to less than 5 mbar, followed by filling with nitrogen to approximately atmospheric pressure. This was repeated three times. The end-caps could then be removed and substances could be measured out, or the reactor loaded up, in an atmosphere of 99.999 % N_2. All vessels were sealed with 'Nesco' film, prior to exposure to air. A more detailed description of the design and use of this glove box is given in Pringle (1998).

---

[57] The TPR of aluminium sulphate for instance.

3.3 DRIFTS Analysis

The IR spectrometer used in this research was a BIO-RAD FTS-7, with DRIFTS accessories. DRIFTS was used in this research, because it has a number of advantages over transmission infrared spectroscopy for solid samples;

- DRIFTS does not require the sample to be pressed into a disc. This is a distinct advantage, as the sample can be investigated in the form in which it is used (or likely to be used).
- An environmental cell can be used to produce exactly the gaseous conditions of interest.

3.3.1 Mirror System

The DRIFTS cell mirror system is shown schematically below.

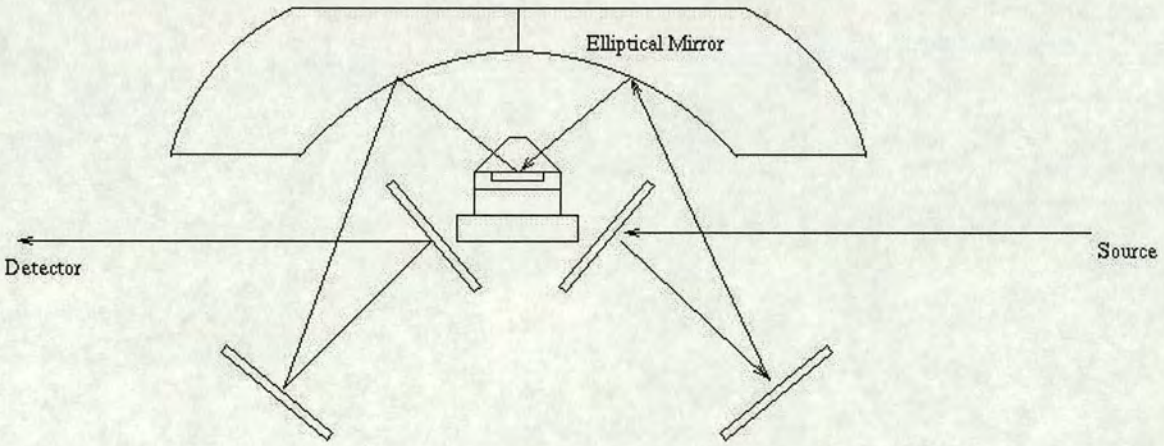

Figure 17: SpectraTech Mirror system "The Collector"

The chamber surrounding the mirror system and the inside of the entire IR spectrometer were flushed with dry nitrogen (99.999 % N_2) during operation. The mirror system depicted above reflects the infrared beam onto the sample via an ellipsoidal mirror which concentrates the beam in the centre of the sample. The opposing ellipsoidal mirror converts the diffusely reflected light back into a beam, which then passes to the detector of the interferometer. The elliptical mirrors could be slid apart for loading samples etc. All mirrors were uncoated aluminium.

When the DRIFTS cell is in use it is often advantageous to have infrared gas analysis available to identify any gas species which are desorbed or reacted. This was facilitated in this research by having the DRIFTS cell outflow passing through a gas infrared cell similar to that used for sulphur dioxide calibration, through which the infrared beam could be directed by use of a mirror system which could be slid into place:

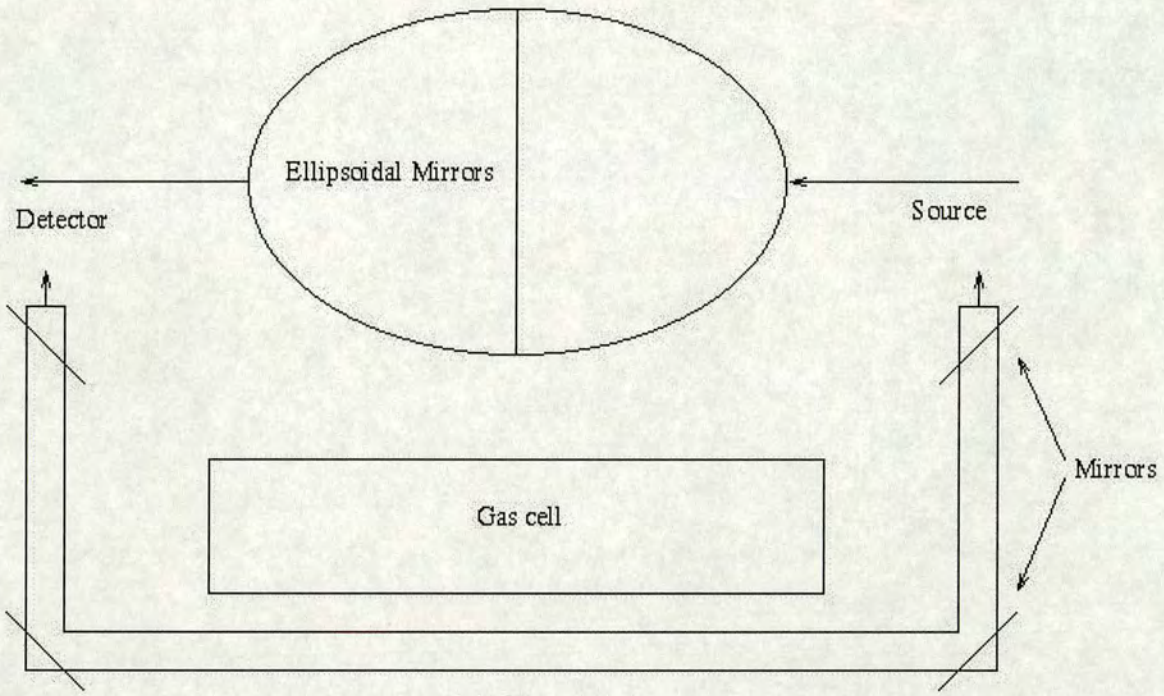

Figure 18: DRIFTS to Gas IR Mirror System: Plan View

3.3.2 DRIFTS Cell Design

The simplest DRIFTS cell used was an open cup. The design used was a detachable cup on a slider to facilitate quick and easy changeover of samples. The sample was prepared by grinding it to a fine powder using an agate mortar and pestle. The powder was then loaded into the cup and was smoothed horizontally with the minimum force possible, to ensure a flat surface with no compacting.

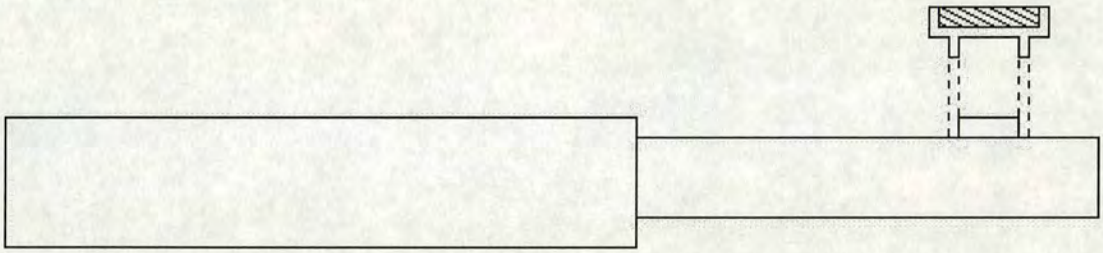

Figure 19: DRIFTS Open Cup

The environmental cell design evolved considerably during the course of the project. The first design used for *in situ* environmental DRIFTS work was a modification of that of SpectraTech.

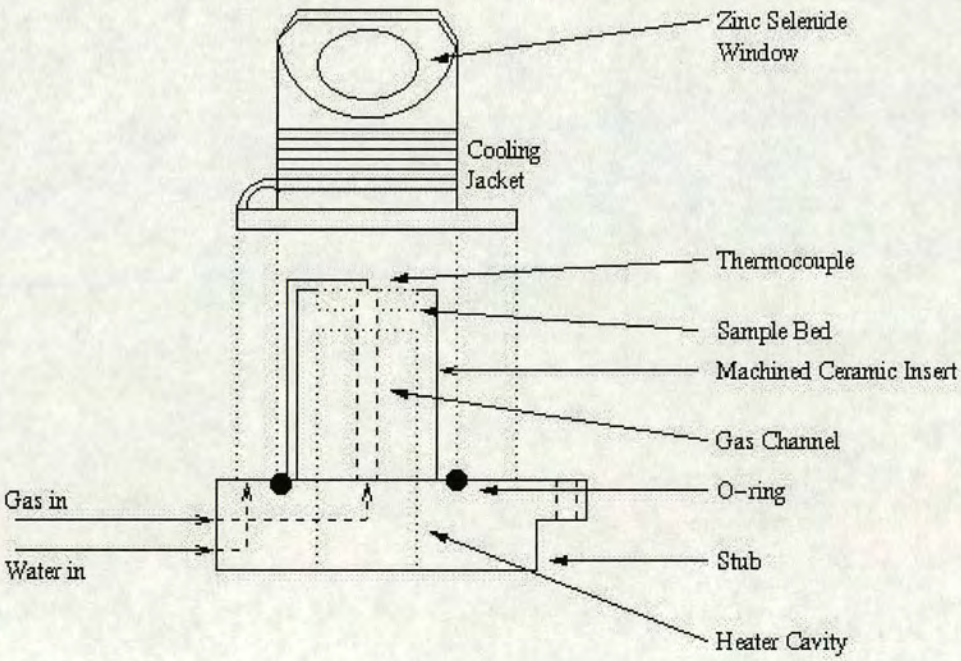

Figure 20: SpectraTech DRIFTS Cell

The cell was cooled by the water piped round the jacket (by a suction pump). This was principally to prevent heating of the windows, as the seals are temperature proof to less than 200°C. The zinc selenide windows are thermally stable.

The cell had a number of disadvantages;

- The path length inside the cell through which the infrared beam travels is quite large (~2 cm). This caused the DRIFTS spectra to register frequencies which were actually due to gases flowing over the sample (sometimes desirable, e.g., Sohail (1992), but not in this research).
- Inadequate heating. The system could not reliably reach and maintain the temperatures required in this research (500 °C - 600 °C).
- Inadequate flow characterisation.
- Condensation problems occur if the sample gas contains large enough concentrations of water, or if water is given off by the sample. The condensation occurs because the windows are much cooler than the gas. The temperature of the windows must be kept down because the rubber of the o-rings, which keep the windows air-tight and hold them in place, is only stable to ~200°C.

The first version of a new type of 'hot windows' cell was built (see following page):

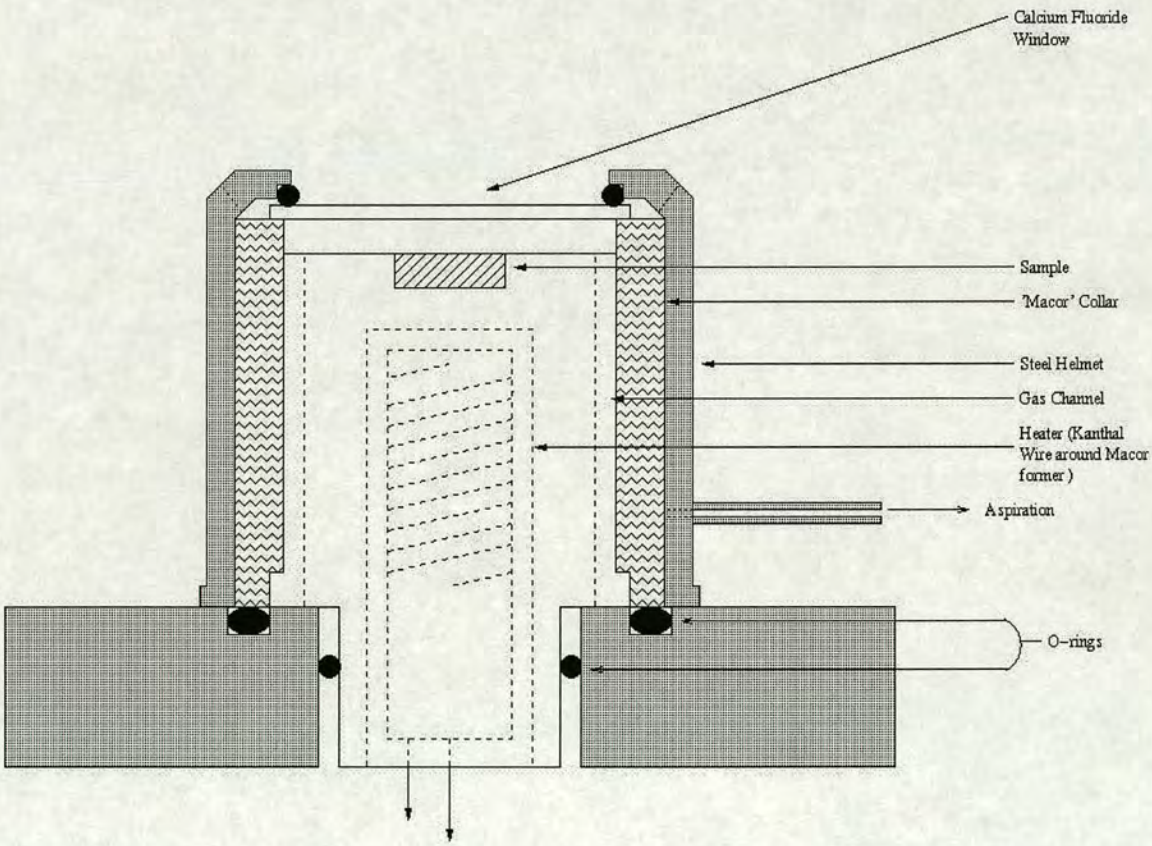

Figure 21: New design of Environmental DRIFTS cell

The new features incorporated were:

- Small free space between sample and window, due to the horizontal positioning of the window, resulting in a very short light path length such that IR absorption due to gases flowing over the sample is kept as low as is physically possible.
- The system is no longer sealed as this proved very difficult at the desired temperatures (up to 600 °C). the cell was designed to leak slightly, any leaked gas being aspirated as shown.
- Characterised flow; the flow of the gas is more tightly governed, because of the smaller volume above the sample and the shape (parallel sides) of the space through which it must flow.
- Fully heated body of the cell, so that there are fewer problems with water condensation on the windows of the cell.

In the first version of this design the helmet had 90° corners, but these were found to cut out a large amount of the infrared, significantly reducing the quality of any spectra.

The new parts for the cell were manufactured from Macor™, a machineable glass ceramic. The literature concerning Macor and our own tests on free standing machined parts showed that it can withstand temperatures in excess of 1100°C. However, the manufacture of materials in Macor proved to be problematic, as it tended to break when put under stress at high temperature. The stresses were usually due to unequal rates of expansion in the apparatus, usually between the sample holder and heater, but sometimes between the holder and the surrounding collar. The solution to this would be to allow more space between these parts, but, for the case of the heater and holder, increasing the clearance results in a decrease in the maximum temperature achievable, due to the decreased contact between the two and consequent increased heat loss. When the Macor pieces remain intact, the maximum temperature is dictated by the burning out of the heater wires. The use of more wire would decrease the likelihood of this, but the maximum amount possible had already been coiled onto the former.

An attempt to use a metal holder insulated from the wire of the heater by an internal silica liner liner proved unsuccessful, as the metal tended to conduct the heat away from the sample. However, the use of the silica liner prompted a further design development.

The problem was solved by redesigning the sample holder as a simple capped silica tube. The other problem this new design solved was that of very large temperature gradients which had been discovered through the samples: the difference between the temperature at the base of the sample and that at the upper surface could be ~100°C, when the lower temperature was ~400°C. This phenomenon

has been reported before in the field of reflectance spectroscopy (e.g., Kortum (1969)[58]). In this new design it was decided to apply samples to the ceramic as very thin washcoats. This required the manufacture of a new design of sample holder, which was no longer a cup or indentation, but merely a flat top.

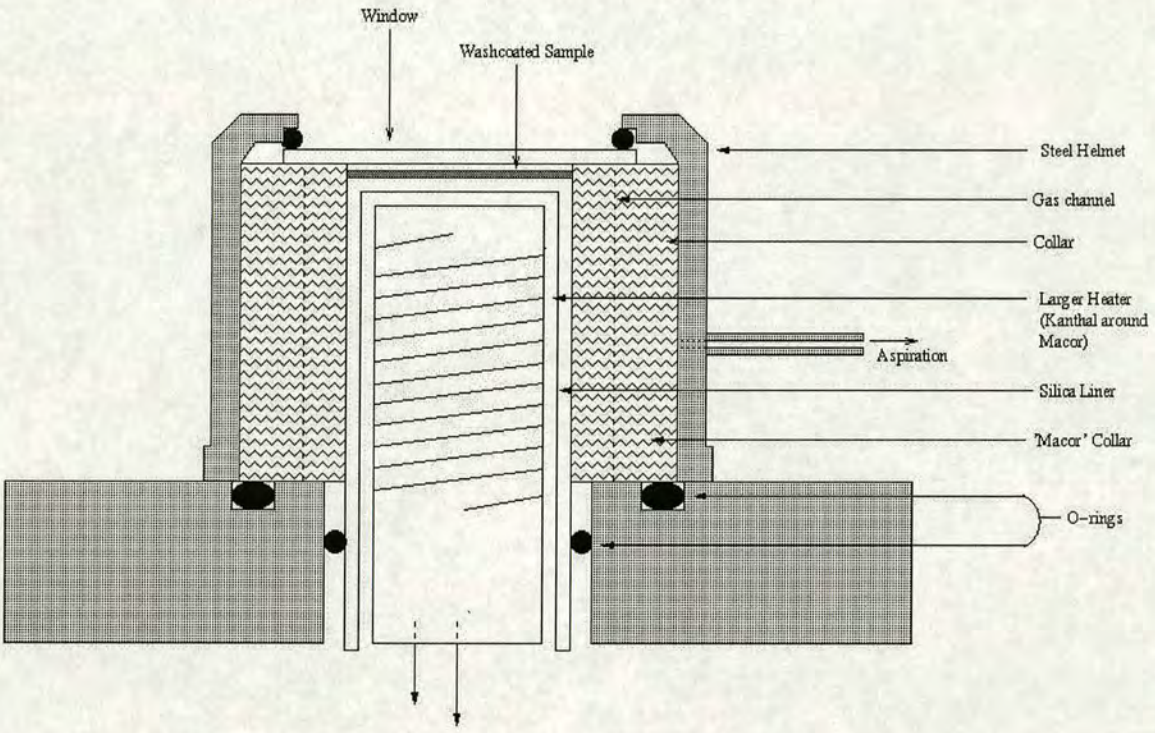

Figure 22: Latest Version of the High Temperature Environmental Cell

This latest version of the HTEC has the sample washcoated onto the top face of the silica liner. This simple design has proved to be the most effective. It achieved and maintained higher temperatures with less power input than any other design, because the distance between heater and sample has been substantially reduced. It also has considerably more reliable temperature measurement as the sample is so thin that significant temperature gradients within it cannot exist. Another advantage, for this particular research project, was the use of washcoats, as this means that the samples are in the same form as they would be in a real autocatalyst. The silica was an improvement over the Macor, because, even though its compressive strength is much lower[59], it has a much lower coefficient of thermal expansion[60] vastly reducing the stresses due to expansion.

---

[58] p 289
[59] 1200 as opposed to 50000 PSI
[60] 0.3 as opposed to 5.2 $^{\circ}F^{-1}$ ($x10^{-6}$)

The wiring of the heater had proved problematic throughout the development of this design. A number of different wires and connectors were used. One of the greatest difficulties was the proximity of the heating wires in and out. This meant that the wires had to be electrically insulated at every point prior to contact with the Macor of the heater. This was difficult because there was a very limited amount of space to work with below the heater, between the two lower mirrors of 'The Collector'. Insufficient insulation led to sparking and burn out of the wires. The connectors used, ultimately, were crimped electrical connectors surrounded by large ceramic 'fish spines'. The wire used was Kanthal (as for the microreactor). Kanthal proved to be able to reach higher temperatures without burn out. Attempts to use platinum wire failed as it was particularly prone to sparking.

3.3.3 Sample Preparation

The powdered samples for the open cup and earlier versions of the HTEC were prepared by grinding to an extremely fine powder in an agate mortar and pestle. If the particle size were smaller than the incident radiation, then the spectra produced would be very reliable.

For the washcoated samples a method of applying a reliable washcoat had to be developed. A number of simple techniques were attempted;

- Making the oxide sample into an incipiently wet slurry with distilled water, applying to the surface and allowing it to dry at ambient temperature.
- As above, except with drying for ~1 hr. at ~110°C.

The viscosity of the slurry proved to be crucial to the quality of the washcoat achieved on the liner. If the sample were much more than incipiently wet, no coherent layer of sample was formed. The washcoat could not be too thin, as this would lead to problems with Kubelka-Munk spectra; one of the assumptions of the Kubelka-Munk theory (see 'Literature Survey') is that the sample is sufficiently thick that the background reflectance is zero.

Ultimately, the development of satisfactory washcoating procedures proved difficult and time-consuming. Instead, an extremely shallow sample bed was opted for (0.5 mm deep), the circular bed being machined out of the top of the silica liner.

3.4 Scanning Electron Microscopy

A number of S.E.M. sessions were undertaken at the University of Edinburgh SEM Facility. The S.E.M. was a Cambridge Stereoscan 250 with an MSCOPE SC500A gold coater. The aim of performing SEM was to examine the components for microscopic evidence of morphological changes due to treatment with sulphur dioxide. This method has been seen to yield results before (Sohail (1992), Bowker *et al.* (1983)).

3.4.1 Sample Preparation

Fine powders were prepared for S.E.M. analysis by applying a mixture of acetone and the powder to a metallic S.E.M. stub and allowing the acetone to evaporate. Larger samples, such as the chips used in the catalyst test rig, which have a size range of 250 - 355 μm, had to be fixed to the stub using a graphite paste.

These larger samples were prone to 'charging', rendering good definition at large magnifications rather difficult. Charging is simply the build-up of electrons on the sample. The increased charging on larger samples was due to the smaller available earthing area of gold relative to the volume of the particles, as illustrated below.

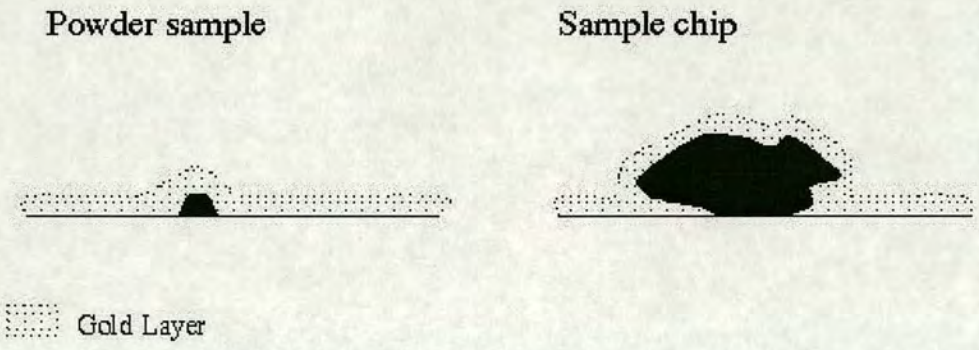

Figure 23: SEM Samples (stubs 1:1)

The samples were gold-sputtered and placed in the microscope at the facility by Mr J. Findlay.

3.4.2 W.D.S.

Wavelength Dispersive Spectroscopy (with SEM) was performed on a number of samples at Johnson Matthey Technology Centre, Royston, Herts.

The preparation of samples in the form of small chips was different at Johnson Matthey, involving a similar stub, but, instead of graphite paste, a carbon sticker was used to affix the samples.

After checking that none of the other elements present (Al, Ce, O) would present any problems of interference, i.e., that their characteristic frequencies were not close to that of sulphur, the spectrometer was calibrated for sulphur with an FeS_2 sample. The sample was then scanned at this frequency to produce a 'sulphur map' of individual sample chips, recorded as a photograph or videographic printout.

3.4.3 B.E.I.

The microscope was also fitted with a backscattered electron detector, which gives a map of the atomic number of the sample, thereby identifying which areas of any one chip were rich in aluminium or cerium. WDS could not do this as the detector would be saturated by such high element densities.

Backscattered electron images were taken of a number of sample chips. The images were, again, recorded as photographs or videographic printouts.

3.5 X.R.P.D.

X-ray powder diffraction was performed at Johnson Matthey Technology Centre, Royston, Herts. The diffractometer was a Siemens model D5000 equipped with a θ/θ goniometer. The radiation was Cu K-α of wavelength 1.5406 A. It was controlled by the Diffrac – AT software. The resulting powder patterns were compared with the JCPDS database of standard patterns kept on CD-ROM.

3.6 Surface Area Analysis

Surface area analysis was performed at Johnson Matthey Technology Centre, Herts. on the Micromeritics 'Digisorb 2500'. The equipment generates information on B.E.T. isotherms, surface areas and pore size distributions. B.E.T. surface areas were also obtained at the University of Edinburgh Department of Chemistry. The procedure was as follows:

1. Degassing of sample by subjecting to heat and vacuum, typically taking 1/2 - 1 day (longer for a few samples of heavily SO_2 treated samples).
2. Nitrogen absorption at liquid nitrogen temperatures.
3. Equilibration.
4. Heating.

The output gave the following data:

- surface areas (BET and single point),
- adsorption and desorption pore surface areas,
- micropore areas and volumes,
- adsorption and desorption pore volumes,
- average pore diameter

4. Results

4.1 Standard Matrix of Experiments

A standard set of experiments[61] was performed on a number of autocatalyst components to form a matrix of results. The set was as follows:

- 400°C, 500°C, 600°C and 700°C standard 'switchover' experiments (see section 3.2.2.1)
- 500°C, 4000s SO_2 dosing (40 doses) in air, followed by TPR (i.e., a 'Standard TPR' – see section 3.2.2.1).[62]

The autocatalyst components were:

1. γ – alumina
2. Platinised γ – alumina (0.5 wt. % Pt)
3. Ceria
4. Platinised Ceria (0.5 wt. % Pt)
5. P_{12}, Ceria/Alumina
6. Platinised P_{12} (0.5 wt. % Pt)
7. Nickel Doped P_{12}, Platinised P_{12} and alumina (2.0 and 10.0 wt. % Ni)
8. Iron Doped P_{12} and Platinised P_{12} (1.9 wt. % Fe)
9. Barium Doped P_{12} and Platinised P_{12} (4.7 wt. % Ba)

A number of samples were heavily dosed with sulphur dioxide at 500 °C. This procedure comprised of a pretreatment, followed by cooling to 500 °C, then treatment with 70 standard doses of SO_2, without a subsequent temperature ramp. The intention of performing these runs was to have a large enough amount of the surface sulphur species that it would be possible to identify the species formed by analytical techniques such as WDS, XRPD and DRIFTS.

---

[61] All experiments were repeated at least once to ensure reproducibility of results.
[62] This temperature (500 °C) also correlates with the highest working temperature of the DRIFTS cell.

4.1.1 Pretreatments

The pretreatment employed as the first step in all experiments reported here is a 50°C/min. temperature ramp in 5 % hydrogen in nitrogen from 50°C to 900°C, as described in 'Materials and Methods'. The purpose of this step is to ensure the removal of unwanted species from the formulations, without altering the composition or form of the component. It was decided not to use oxidising conditions, as they would inevitably lead to sintering and/or alteration of the crystal structure of the oxide mixtures. Reducing conditions are recommended as the best means of ensuring a uniform state of the material (Falconer and Schwarz (1983)).

The most commonly seen feature of a pretreatment TPR was the emission of carbon dioxide. The origin of the carbon dioxide was thought to be physisorption of ambient carbon dioxide. Examination of the preparation procedures shows that there is no other likely source of this carbon dioxide for unplatinised samples.

The efficacy of the pretreatment can be demonstrated by comparing a first pretreatment with a successive one (see following page):

(a.) First pretreatment of a platinised P_{12} sample.

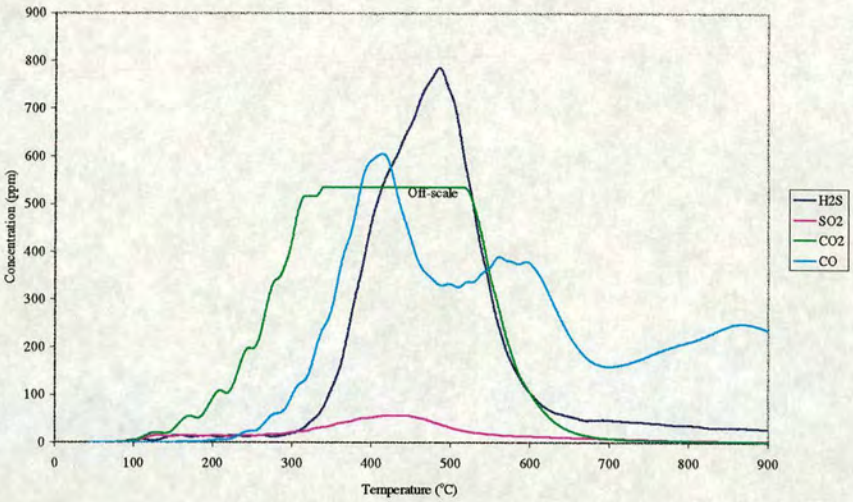

(b) Second pretreatment of a platinised P_{12} sample.

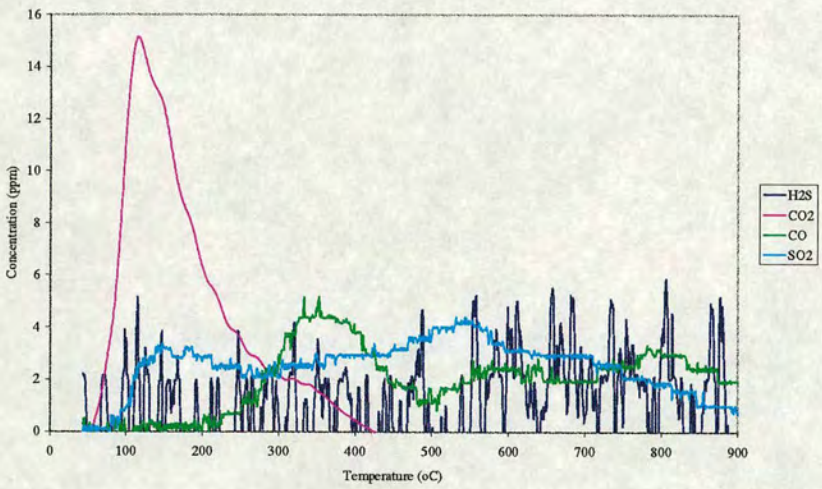

Figure 24: Efficacy of Pretreatments

The sample of platinised P_{12} used in this experiment underwent no treatments between the first and second pretreatment. It can be seen that scarcely any of the species emitted in the first pretreatment remain; the second pretreatment TPR spectrum is virtually featureless. The concentrations seen in the second pretreatment would scarcely be noticeable in the first pretreatment TPR spectrum. The signal in the second pretreatment spectrum appears noisy, because the gases' concentrations were close to the resolutions of the meters involved.

A noticeable feature of the pretreatment TPRs was that platinised and unplatinised samples gave significantly different traces. There are two possible explanations for this:

- The sources of the platinum contain various other functional groups and/or contaminants.
- The platinum causes increased adsorption of ambient species either at ambient temperature during storage or, as seems more likely during the 500 °C calcination step in the preparation.

(a) First pretreatment of an alumina sample

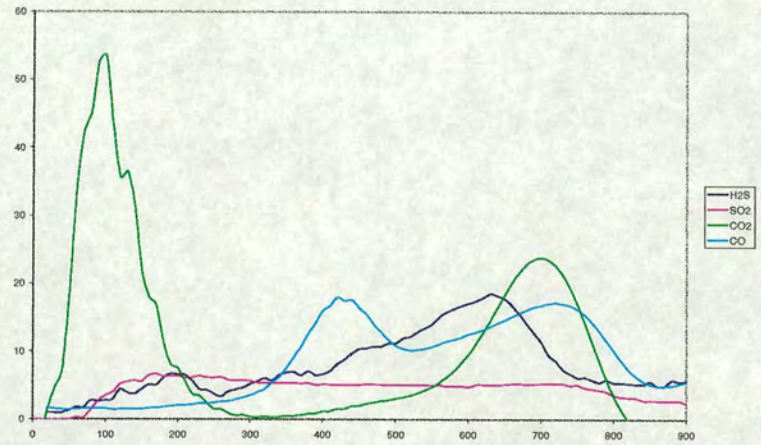

(b) First pretreatment of a platinised alumina sample

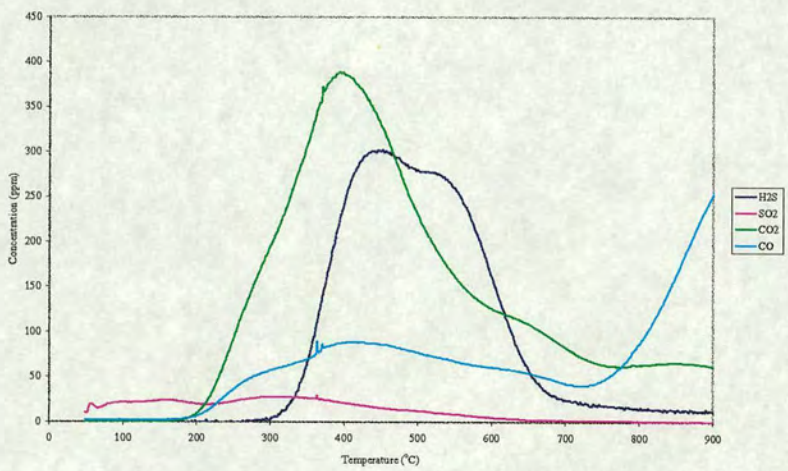

Figure 25: Pretreatment TPRs (Platinised and Unplatinised samples)

The large desorption of carbon dioxide by the platinised sample could be due to the platinum tetra-amine hydrogen carbonate or the citric acid, $C_6H_8O_7$, used in its preparation. These species should have been removed during the calcination, although Waqif *et al.* (1997) report residual carbonate

species on their samples of ceria[63] (which were also provided by Rhone-Poulenc) after calcination to 600 °C. They report that the species were displaced by sulphur dioxide treatment.

The carbon monoxide could be generated by the same source. The large breadth of the CO peaks is typical of experiments seen elsewhere (Herz *et al.* (1982)), where the CO peak was believed to be broadened and shifted to higher temperatures due to readsorption effects.

The presence of hydrogen sulphide in the pretreatment is difficult to explain: no sulphur-containing species were involved in the preparation of these compounds. A possible explanation is that the substance had adsorbed ambient sulphur dioxide, although there is an extremely large amount evolved considering that sulphur dioxide makes up such a small part of the atmosphere (approximately 2×10^{-8} % vol. in the absence of local pollution). It is also possible that this is some other species with a similar ultraviolet absorption frequency as hydrogen sulphide, although no such species were observed in the infrared gas cell.

The pretreatment TPR spectra can be used as a form of 'fingerprint' of a catalyst sample. In this research the pretreatment TPR spectra proved to be very reproducible.

---

[63] Identical to the material used in this research

4.1.2 General Shape of TPRs

The main features of the TPR profile for the majority of the sulphur dioxide treated components (the exceptions will be addressed later) are:

- That they exhibit two peaks; a sulphur dioxide and a hydrogen sulphide peak, the hydrogen sulphide peak always occurring at the higher temperature
- The ratio of sulphur dioxide peak size to hydrogen sulphide peak size tended to increase with increasing dosage
- The fully developed peaks have an approximately Gaussian profile. See comparison below:

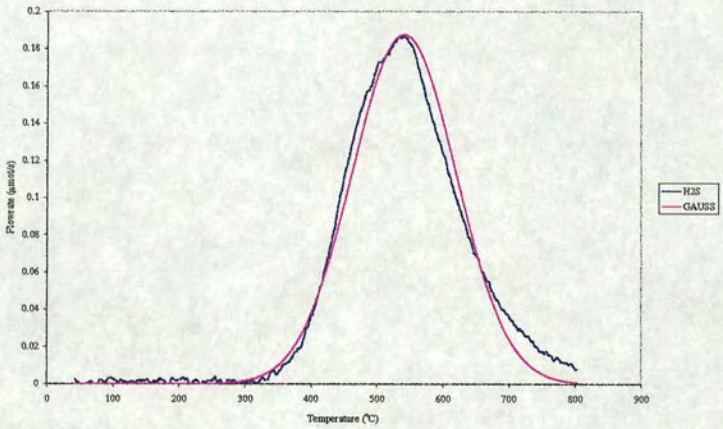

Figure 26: Standard TPR of Platinised P_{12}, compared to simple Gaussian Fit

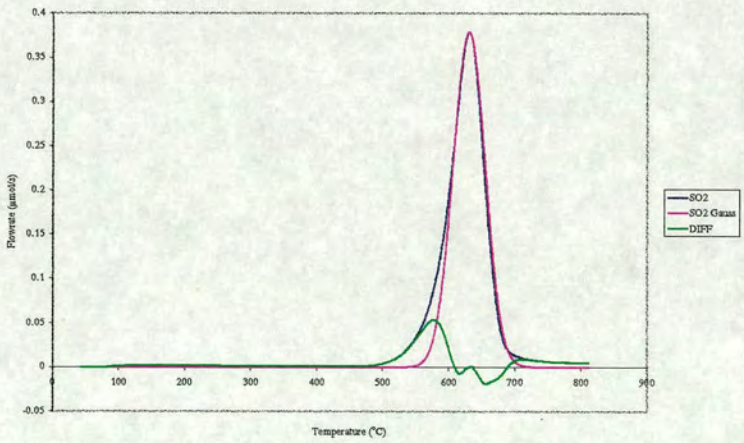

Figure 27: Standard TPR of Ceria, compared to simple Gaussian Fit

Similar TPR spectra were produced by Lundgren *et al.* (1995) and Kim and Juskelis (1996).

4.1.3 Washcoat Materials

4.1.3.1 Alumina

Undoped alumina was the least active of the components tested; it adsorbed considerably less sulphur dioxide than any other compound of comparable surface area.[64] All other formulations contained ceria or platinum. Despite the relatively small amount adsorbed, alumina exhibited distinct H_2S and SO_2 peaks in the standard TPR spectrum:

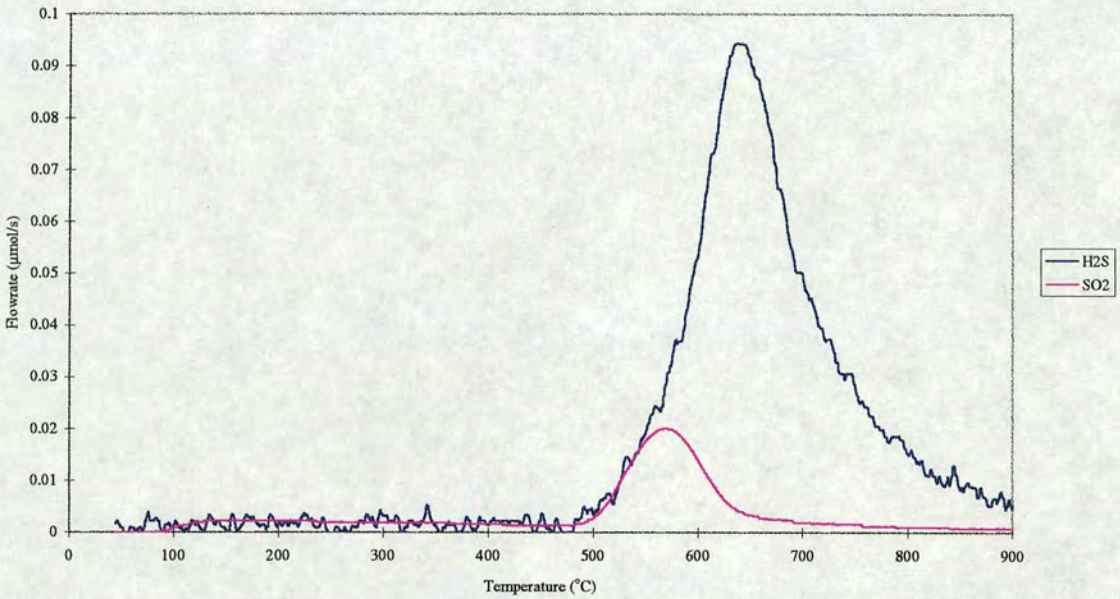

Figure 28: Standard TPR of Alumina

The principal species evolved was hydrogen sulphide, with the peak maximum occurring at 643 °C, and representing 9.5 µmol. The emission of sulphur dioxide was not negligible: its peak occurs at approximately 575°C and represents 3.7 µmol. These molar amounts should be compared to the amount adsorbed, 29 µmol.

Lox *et al.* (1989) who also found that sulphur dioxide-treated alumina could evolve hydrogen sulphide when exposed to hydrogen, found that the hydrogen sulphide maximum occurred at ~550 °C on fully

---

[64] Platinised ceria adsorbed less, but has a surface area of ~2.9 m^2/g as opposed to alumina's surface area of ~170 m^2/g.

formulated catalysts. However, they dosed the components with sulphur dioxide in helium at 60 °C, which would give rise to physisorption or weaker chemisorption.

Chang (1978) investigated the adsorption of sulphur dioxide on alumina in detail by infrared spectroscopic means, including studies of sulphur trioxide adsorption and the effects of doping the alumina with aluminium sulphate. When the adsorption was carried out in an atmosphere containing oxygen, he observed that no oxidation reaction occurred until 400 °C, When it did occur the infrared bands arising were not removed until heating to ~800 °C, which is indicative of aluminium sulphate formation.[65] Clearly, the species formed here decompose well below this temperature.

The results of storage-release switchover experiments on alumina showed that very little hydrogen sulphide was emitted even at high temperatures. The temperature dependence is illustrated below:

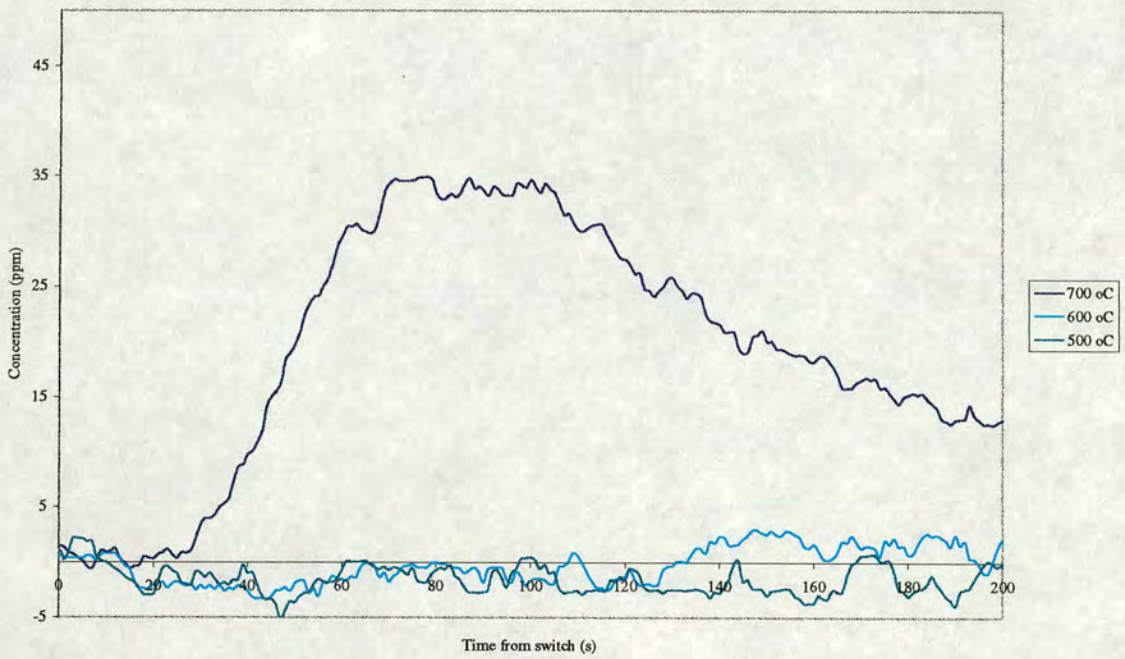

Figure 29: Hydrogen Sulphide Switchover peaks on Alumina

At 600 °C a small amount of hydrogen sulphide is emitted over a relatively long time The only significant amounts of hydrogen sulphide are emitted at 700 °C and are delayed and emitted over a relatively long time.[66] The hydrogen sulphide peaks occur after the sulphur dioxide peaks (shown

---

[65] See 'Temperature Programmed Reductions of Pure Compounds' section in this chapter.

[66] It should be pointed out that a certain part (~15s) of the period prior to any switchover peak is systemic.

below). This phenomenon is in keeping with the results of the standard TPR, where the hydrogen sulphide is emitted at a higher temperature than the sulphur dioxide. At 700 °C a larger amount of hydrogen sulphide is emitted, but this peak is still very small compared to that from platinised alumina.

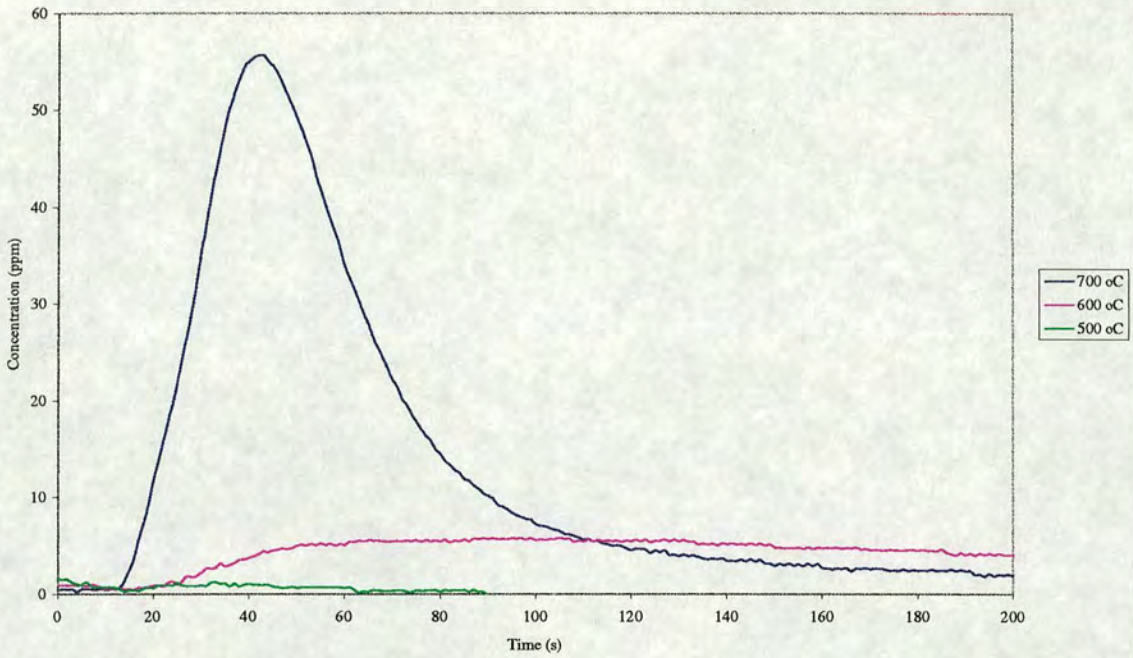

Figure 30: Sulphur Dioxide Switchover Peaks on Alumina

The emission of sulphur dioxide parallels that of hydrogen sulphide in that the emission increases with temperature and is only significant at the highest temperature. The emission at 600 °C is extremely persistent, emitting at a low level (>5ppm) for over 400 s. In general, hydrogen sulphide is emitted more slowly than sulphur dioxide. This correlates with its higher temperature peaks in the TPR. From this it may be inferred that this is a reaction phenomenon rather than a desorption phenomenon.

It was observed that if the temperature is too low for the sulphur species to be emitted in the switchover experiment they will be emitted in the following TPR, and that the larger the emissions in the switchover, then the more featureless the following TPR. This was to be expected; there are similar amounts of sulphur dioxide adsorbed at each temperature, therefore a similar amount will be evolved in the switchover and temperature ramping.

The amounts of evolved gases never add up to the total amount of sulphur dioxide the sample was originally dosed with, indicating that a certain amount of it goes to form a compound which is stable above 900°C. Lox *et al.* (1989) also found this to be the case; they reported that, in their experiments, "26 % of the adsorbed sulphur dioxide cannot be desorbed at a temperature below 850 °C".

4.1.3.2 Ceria (CeO_{2-x})

Ceria, as mentioned previously ('Literature Survey'), is a special case in terms of sulphur dioxide adsorption in that it can change sulphites into sulphates as cerium's oxidation state changes from IV to III (Waqif *et al.* (1995)). Diwell *et al.* (1987) reported the release of hydrogen sulphide at ~650 °C for a TPR of ceria treated at 550 °C with sulphur dioxide[67].

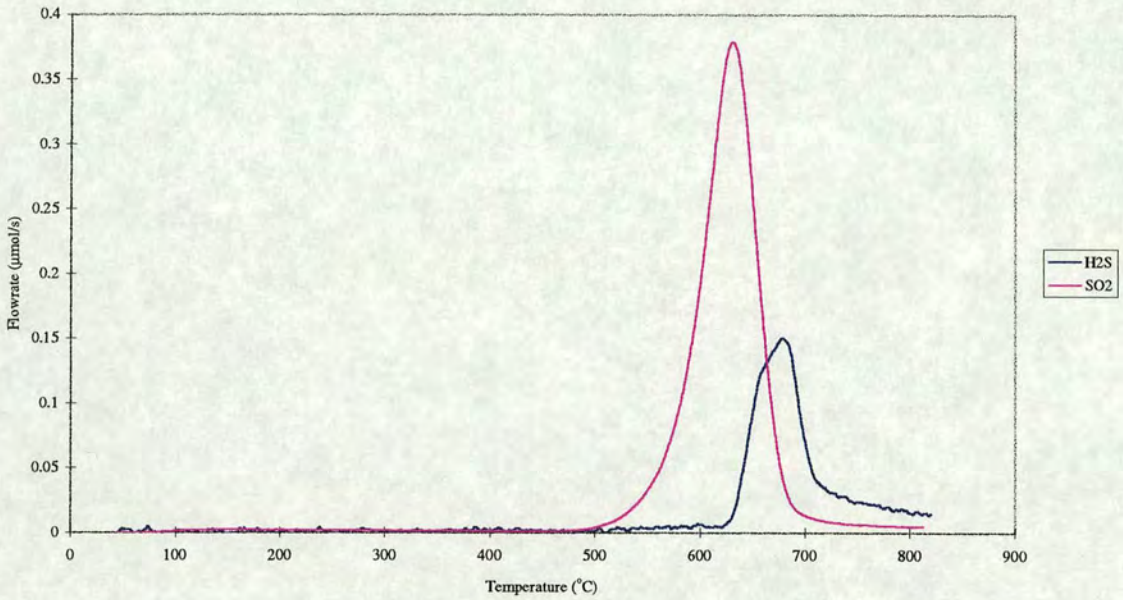

Figure 31: Standard TPR of Ceria

The ceria exhibited a relatively sharp sulphur dioxide peak, which occurred at a lower temperature than the smaller hydrogen sulphide peak. The maxima occurred at 638 °C and 678 °C for sulphur dioxide and hydrogen sulphide respectively. The curve for ceria was close to Gaussian, but is skewed towards higher temperature which, according to Falconer and Schwarz (1983) is indicative of a first order (or pseudo first order) reaction process.

The ceria adsorbed considerably more sulphur dioxide than alumina (38 µmol more of the sulphur dioxide it was exposed to (of a total of 85 µmol) despite a lower surface area). Ceria seems to have more "unaccounted for", i.e., stable above 900 °C, sulphur species than alumina, and its TPR peaks

---

[67] The sulphur dioxide dosing took place in nitrogen rather than oxidising conditions.

occur at higher temperatures. That ceria's TPR peak should occur at higher temperature than alumina is contrary to expectation, bearing in mind the thermal stabilities of the sulphates.[68]

The hydrogen consumption by ceria during the standard TPR can be seen below:

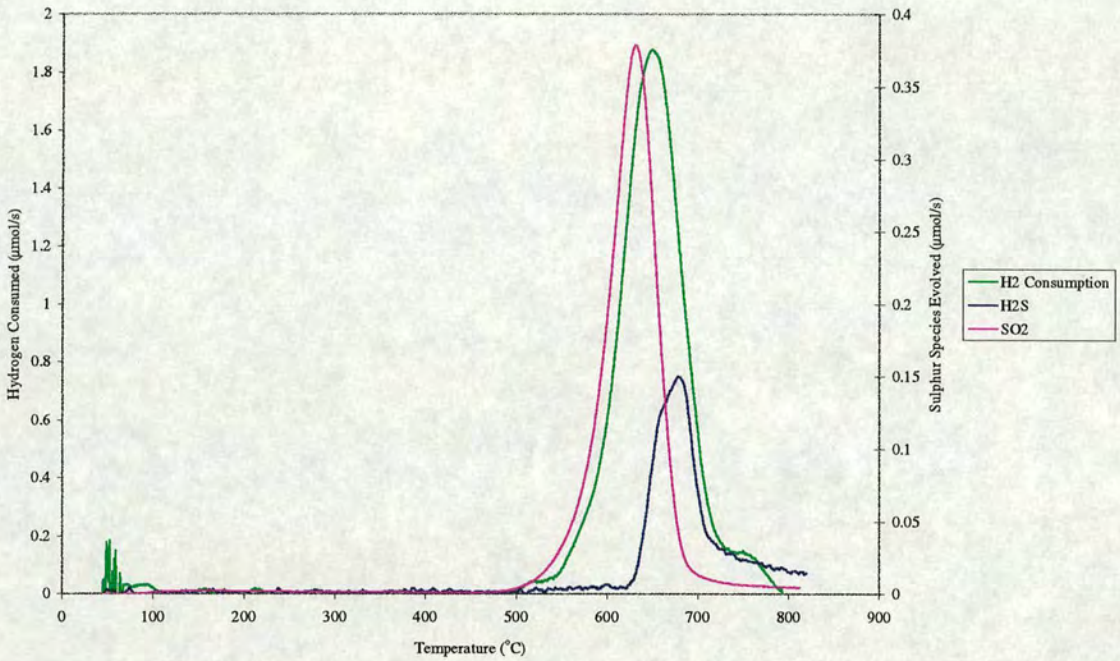

Figure 32: The Standard TPR of Ceria showing the Hydrogen Consumption

The number of moles of hydrogen consumed is approximately five times the number of moles of sulphur species evolved. The coincidence of the hydrogen consumption peak with the other peaks is clear. The factor of approximately five between the moles of sulphur species emitted and moles of hydrogen consumed may be informative. The factor can be used to assess the likelihood of specific reactions occurring, e.g.:

(i) $Ce(SO_4)_2 + 2\ H_2 \rightarrow CeO_2 + 2\ SO_2 + 2\ H_2O$

(ii) $2\ Ce(SO_4)_2 + 5\ H_2 \rightarrow Ce_2O_3 + 4\ SO_2 + 5\ H_2O$

(iii) $Ce_2(SO_4)_3 + 2\ H_2 \rightarrow CeO_2 + 3\ SO_2 + 2\ H_2O$

(iv) $Ce_2(SO_4)_3 + 3\ H_2 \rightarrow Ce_2O_3 + 3\ SO_2 + 3\ H_2O$

---

[68] Aluminium sulphate decomposes in a standard TPR at 830 °C, whereas cerium (IV) sulphate decomposes at 680 °C.

The stoichiometric ratios of these reactions are much lower than 5, making the consumption of hydrogen, which is clearly coincident with the emission of sulphur dioxide, difficult to explain. The decompositions of cerium sulphates to hydrogen sulphide have a stoichiometric ratio of ~4, which is closer, but the amount of hydrogen sulphide emitted here is clearly not enough to account for the hydrogen consumption. The only conclusion that can be drawn is that there is another hydrogen-consuming process occurring e.g. the reduction of ceria to cerium (III) oxide. This is quite likely bearing in mind ceria's role as an 'oxygen-storage component'., although it does not explain why the consumption is coincident with the emission of sulphur dioxide. Perhaps the two processes are linked by a surface reaction, or the water produced by either reaction is involved in the other.

The switchover emissions of hydrogen sulphide from ceria occur earlier and exhibit a greater peak height as the temperature increases.

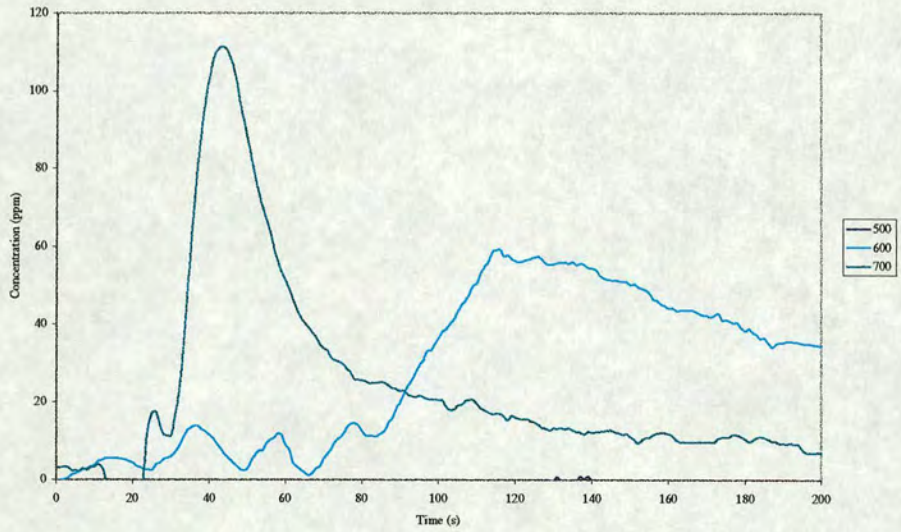

Figure 33: Hydrogen Sulphide Switchover Peaks on Ceria

The 400 and 500 °C switchovers exhibit no hydrogen sulphide. Switchover activity begins only at 600 °C, with a very long emission. The temperatures are in good agreement with the TPR spectrum, which exhibits no evolution of gases until after 500 °C.

The sulphur dioxide switchover peaks exhibit the same temperature dependency as those of hydrogen sulphide. The emissions of sulphur dioxide are very large compared to the hydrogen sulphide emissions. The evolution of sulphur dioxide at 700 °C is one of the largest seen in this research.

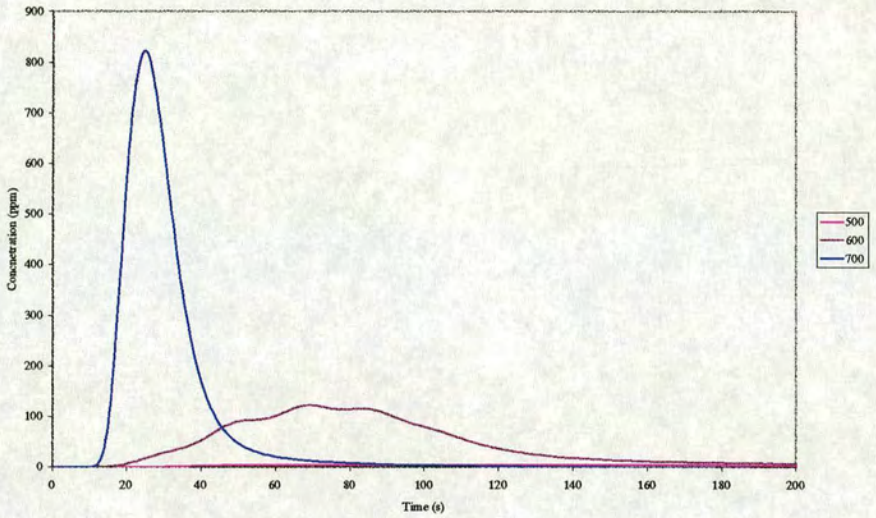

Figure 34: Sulphur Dioxide Switchovers on Ceria

4.1.3.3 P_{12} (Ceria - Alumina)

The effect, in terms of their reactions with sulphur dioxide, of adding ceria to alumina is addressed in the conclusions, but it is clear that the TPR is closer to that of ceria in the shape of its peaks and their relative sizes than it is to alumina. The sulphur dioxide peak shape has a similar shape to that for ceria, from which it may be inferred that it, too, represents a first order process. There is a pronounced shoulder in the hydrogen sulphide peak, which is due to the combination of the hydrogen sulphide TPR peaks of the two components.

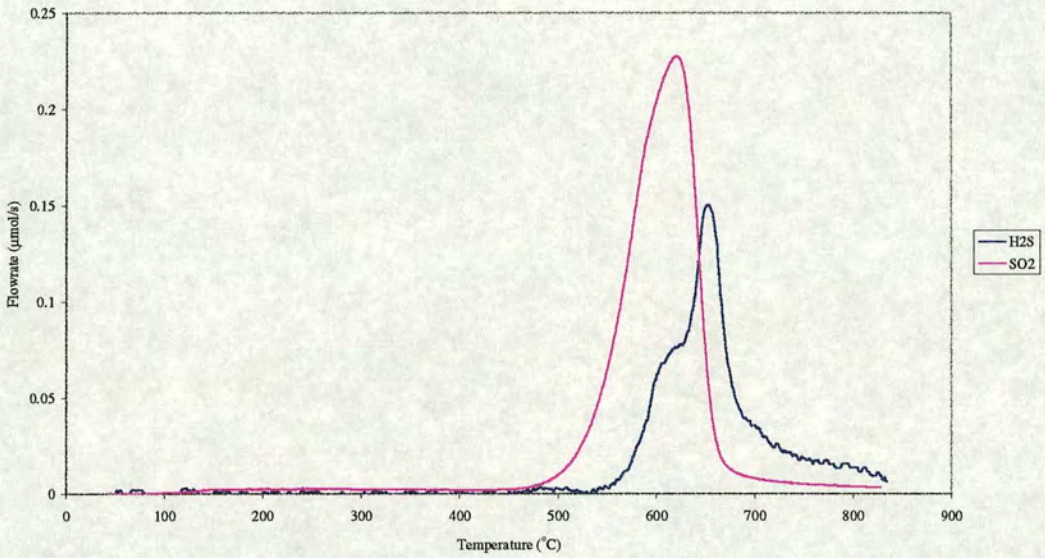

Figure 35: Standard TPR for P12

The peak maximum for the sulphur dioxide occurs at 627°C and that for hydrogen sulphide at 648°C. The peaks represent 24.6 and 14.5 µmol, respectively.

The switchovers observed on P_{12} are remarkably similar to those on ceria, if slightly smaller. The temperatures at which the switchovers occur and their shapes are approximately the same. The sulphur is, again, emitted predominantly as sulphur dioxide[69].

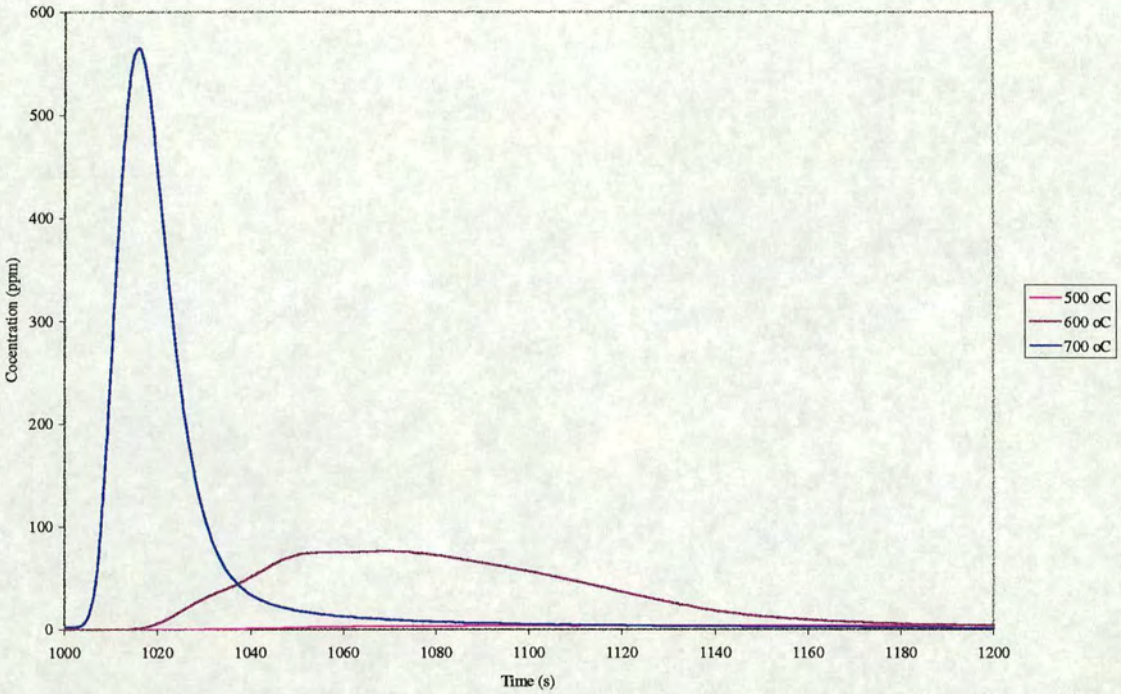

Figure 36: Sulphur Dioxide Switchovers on Ceria-Alumina

Similar trends are seen for all the undoped washcoat materials sulphur dioxide switchovers; with increasing temperature the peaks become sharper, earlier and higher. The 600 °C peak is usually very extended and the 500 °C peak insignificant. These observations are in agreement with the standard TPR spectra.

---

[69] The time on the x-axis of this graph represents the total time of the switchover experiment. 1000s is equivalent to the 0s in the previous switchover graphs. All the following switchover results will have this feature.

The hydrogen sulphide switchovers on P_{12} are small, but not negligible. They exhibit the same temperature dependence as the sulphur dioxide and, again, correlate well with the standard TPR. The shape and magnitude of the peaks is very similar to that from ceria.

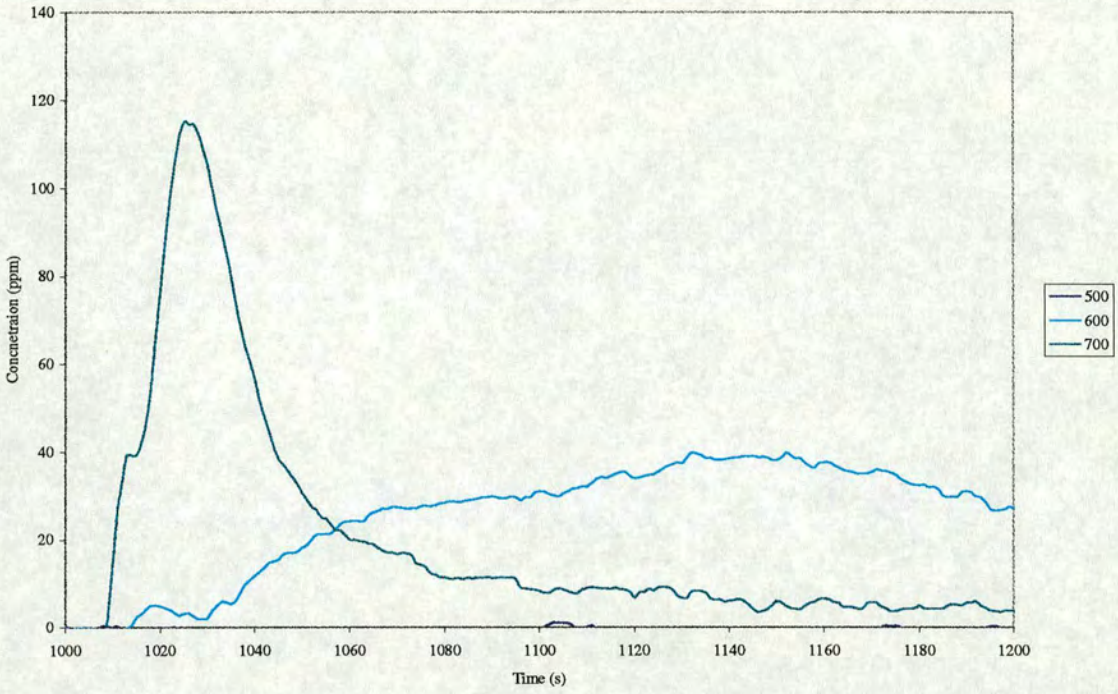

Figure 37: Hydrogen Sulphide Switchovers on Ceria-Alumina

The very high temperatures of desorption in the experiments using alumina and ceria take them outside the range of our DRIFTS equipment.

4.1.4 Platinised Analogues of the Washcoat Materials

4.1.4.1 Platinised Alumina

The comparison between alumina and its platinised analogue illustrates the effect of adding platinum to the washcoat. This is discussed more comprehensively in the conclusions, but there were obvious differences in both TPR and switchovers. The standard TPR of platinised alumina is shown below:

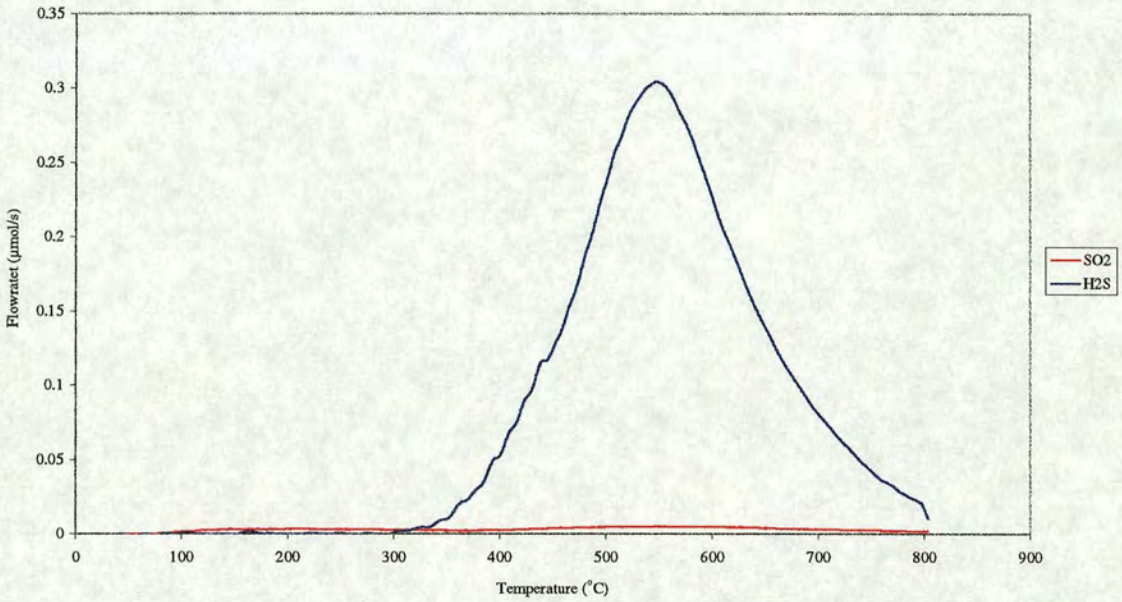

Figure 38: Standard TPR of Platinised Alumina

The amount adsorbed and emitted by the platinised sample in the TPR was much greater than that for the unplatinised sample. Alumina evolved 13.2 µmol of total sulphur species (out of 29.0 µmol adsorbed), whereas its platinised analogue evolved 74.0 µmol (out of 87.8 µmol adsorbed).

The temperature for the platinised alumina's hydrogen sulphide peak maximum was 547 °C; this should be compared to that of alumina, occurring at 643 °C. The platinisation had the effect of lowering the hydrogen sulphide peak maximum temperature by ~100 °C. The platinised sample adsorbed more sulphur dioxide and emitted a greater proportion of its stored sulphur as hydrogen sulphide (96 % as opposed to 74 %). The sulphur dioxide peak of the platinised alumina is extremely small and diffuse, in contrast to the well-defined peak of the alumina TPR.

The evolution of the hydrogen sulphide in the TPR occurred simultaneously with the consumption of hydrogen. The 'hydrogen consumption peak' was very similar in shape to that of the hydrogen sulphide, but represented a molar amount approximately 3.6 times greater than the hydrogen sulphide evolved. This is in agreement with the decomposition of aluminium sulphate to alumina (stoichiometric ratio 4). The same hydrogen consumption peak with the same molar ratio of hydrogen sulphide to hydrogen was observed in the TPR of alumina. This implies that a similar process occurred in both cases.

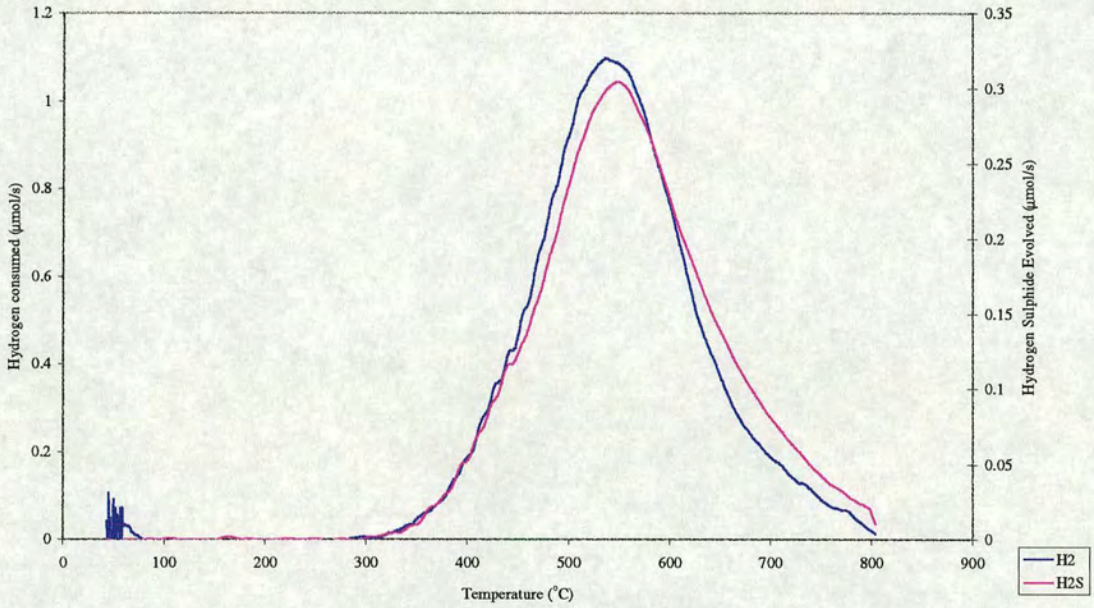

Figure 39: Standard TPR of Platinised Alumina showing Hydrogen Consumption

The switchover behaviour of platinised alumina differed significantly from that of the unplatinised. Whereas at 700 °C alumina produced a hydrogen sulphide peak of ~35 ppm, the platinised alumina hydrogen sulphide switchover peak reached ~420 ppm. The switchover peak was, again, seen to increase with temperature.

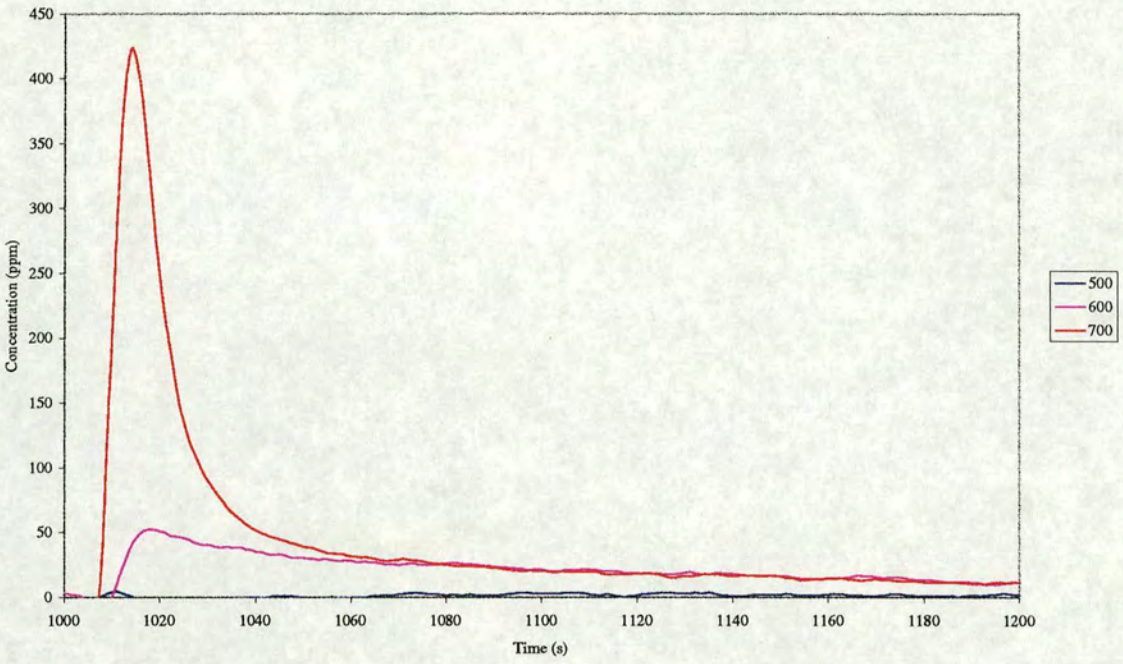

Figure 40: H_2S Switchover Peaks on Platinised Alumina

Platinised alumina adsorbed increasing amounts of sulphur dioxide over the range of switchover temperatures (this effect is small in comparison to the differences between switchover peaks). In comparison, alumina adsorbed less sulphur dioxide with increasing temperature.

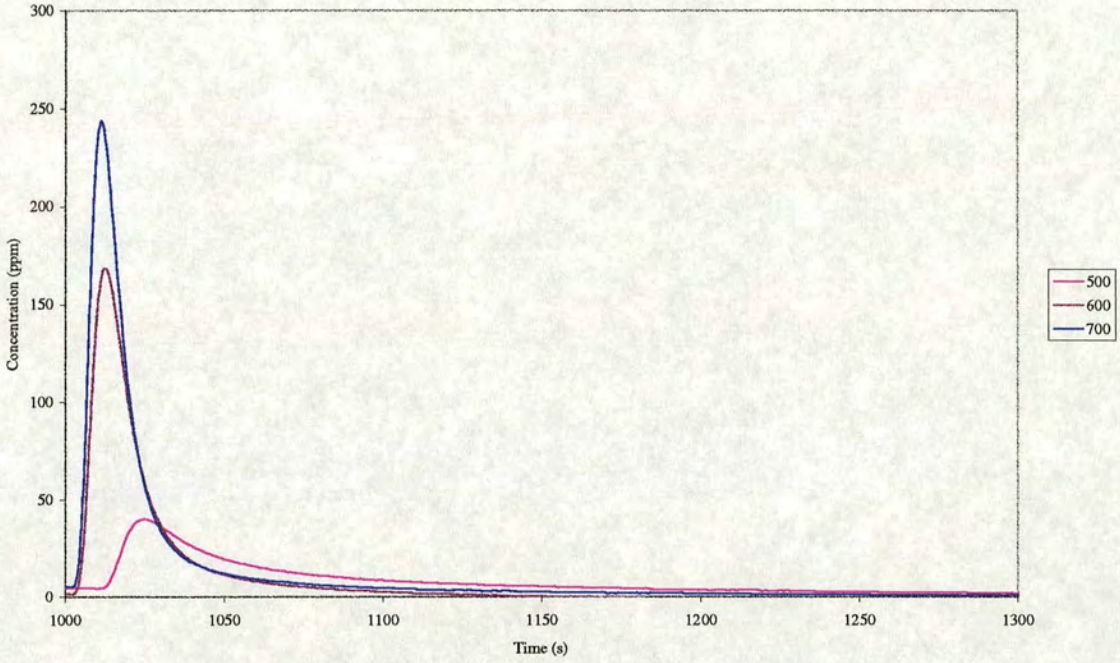

Figure 41: Sulphur Dioxide Switchovers on Platinised Alumina

The switchover emission of sulphur dioxide was greatly increased by the addition of platinum. The peak concentration at 700 °C was 245 ppm, whereas that for alumina was only ~50 ppm. The result is not as pronounced as it might seem, because the platinised alumina had adsorbed approximately 1.8 times as much sulphur dioxide during the dosing stage.

4.1.4.2 Platinised Ceria

The sample of platinised ceria gave many unusual results. This was due, in the main, to its very low surface area (~2.9 m^2/g), which must be taken into account in all results presented. Given that a monolayer coverage of sulphur dioxide is 7.0 µmol/m^2 (Fiederow *et al.* (1978)), then a 250 mg sample such as that used here will be exposed, in a standard switchover run, to approximately four times the amount of sulphur dioxide required for a monolayer. It should be noted that the surface areas of all other compounds used in this research have been found to be at least an order of magnitude greater than that of platinised ceria.

Despite the small amounts adsorbed and emitted, the TPR spectrum generated some useful information:

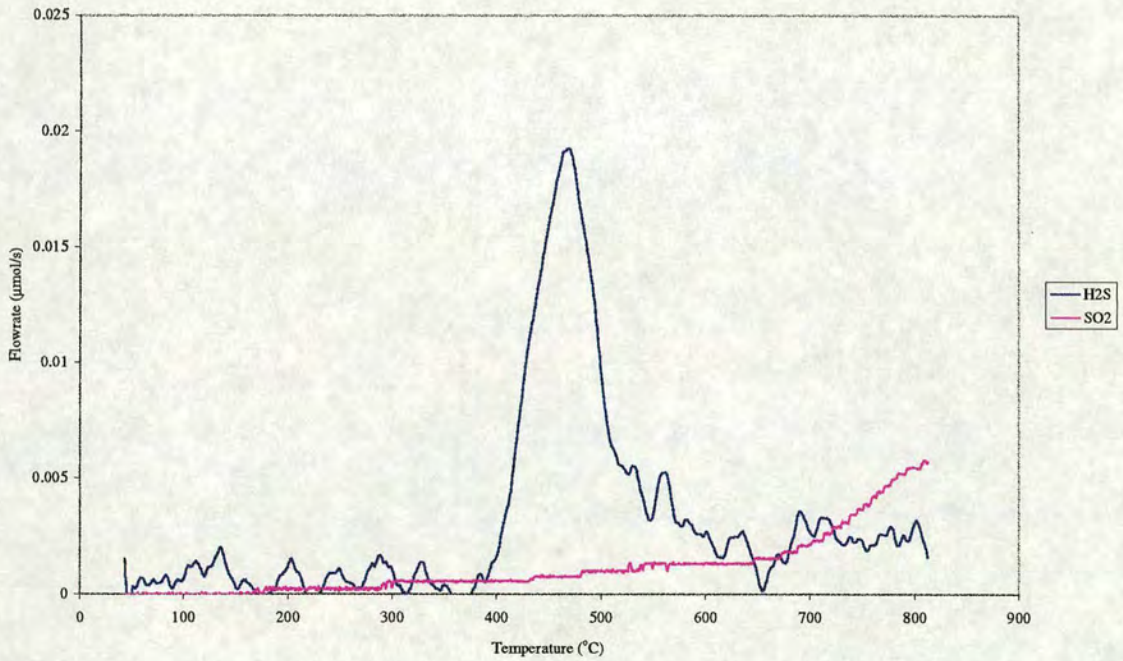

Figure 42: Standard TPR of Platinised Ceria

It should be noted that the apparent 'noise' of this spectrum is due to the small concentrations registered: the signal is too close to the level of the minimum resolution of the meter. The total amount of sulphur emitted was ~4.0 µmol, which, taking into account the very large error margins due to the noise, could represent the calculated monolayer coverage of ~5.0 µmol. The difference between this and the TPR of the unplatinised sample was, again, that the platinum acted to decrease the peak temperature (by ~ 140°C). The other salient feature of this TPR spectrum was the lack of a sulphur dioxide peak, where it had been the principal peak for ceria (this is observed in other comparisons of platinised and unplatinised samples).

Although very noisy, the platinised ceria switchovers did exhibit peaks of hydrogen sulphide:

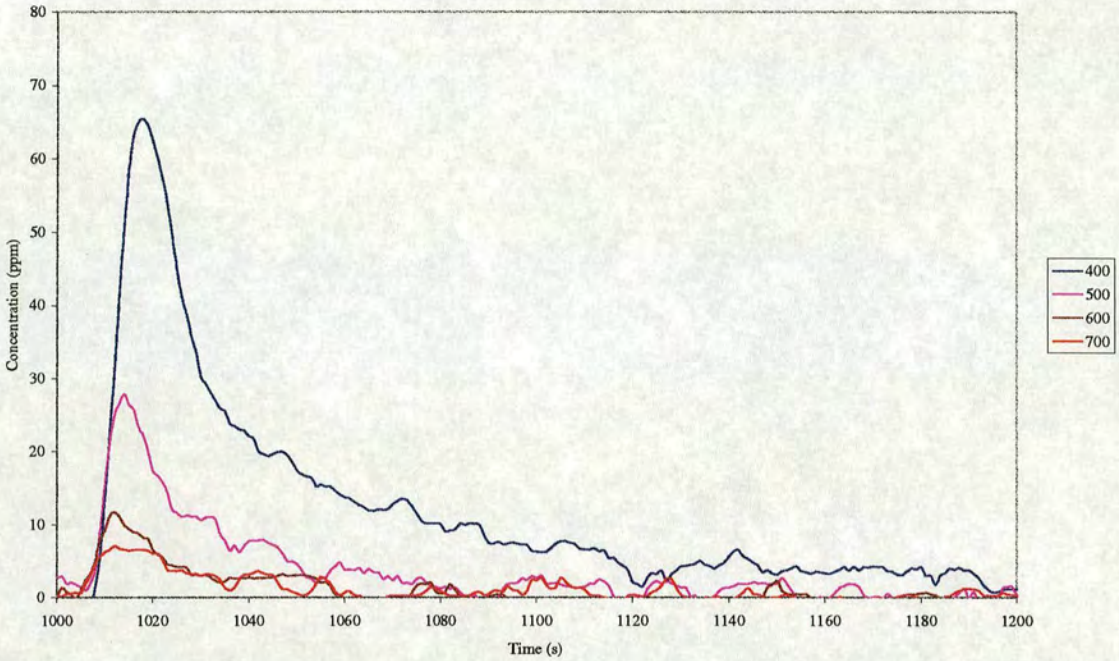

Figure 43: Hydrogen Sulphide Switchovers on Platinised Ceria

The amount of hydrogen sulphide emitted by the platinised ceria decreased with increasing temperature. The peak was largest at 400 °C. This differed from the switchover behaviour of any other component tested; all other switchover peaks increase with temperature and are usually insignificant at 400 °C. The effect may be due to the adsorption's dependence on temperature; the adsorption of sulphur dioxide by platinised ceria went through a maximum at approximately 500 °C. Nonetheless, the emission of species at 400 °C is not seen for any other component. It could be that adsorbate-adsorbate interactions have a role to play, as they are far more likely on this component, which may well be saturated on the surface.

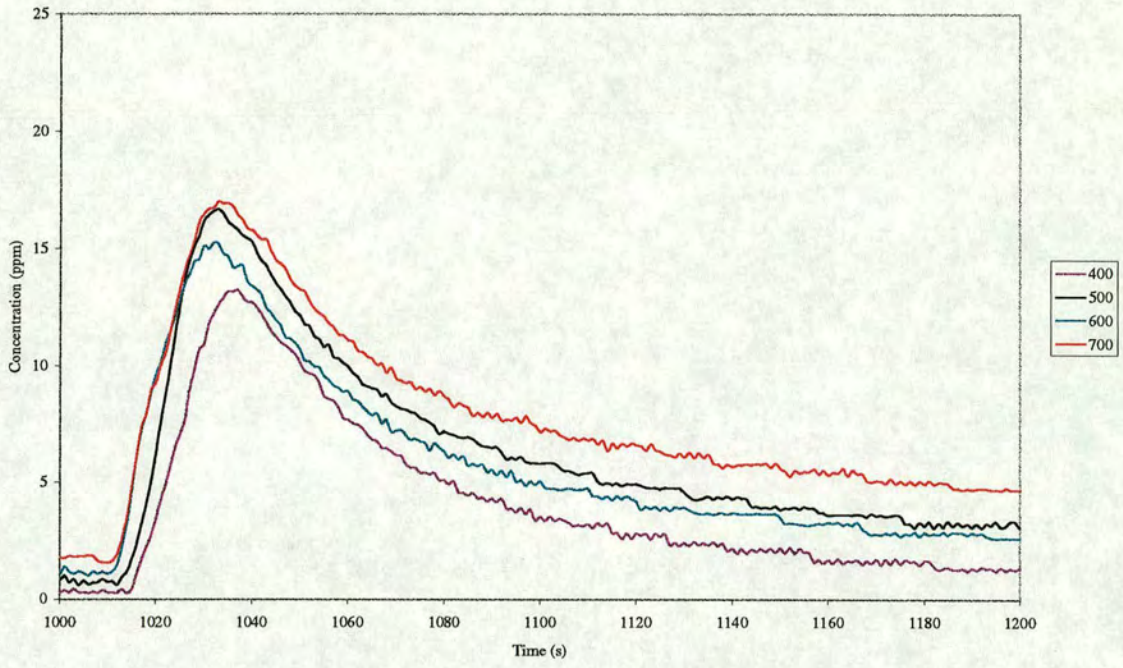

Figure 44: Sulphur Dioxide Switchovers on Platinised Ceria

The sulphur dioxide switchovers of platinised ceria are very curious; there is a small, but definite emission, which appears to have no clear temperature dependence.

It was thought that the temperature of the pretreatment may have been too high for this sample, and so the experiments were repeated with pretreatment to only 800 °C, but the characteristics of the switchovers and TPR were unchanged.

4.1.4.3 Platinised P_{12}

Platinised P_{12} is the formulation closest to that used in practice and, as such, exhibited the most activity in terms of switchover hydrogen sulphide production. The standard TPR is shown below;

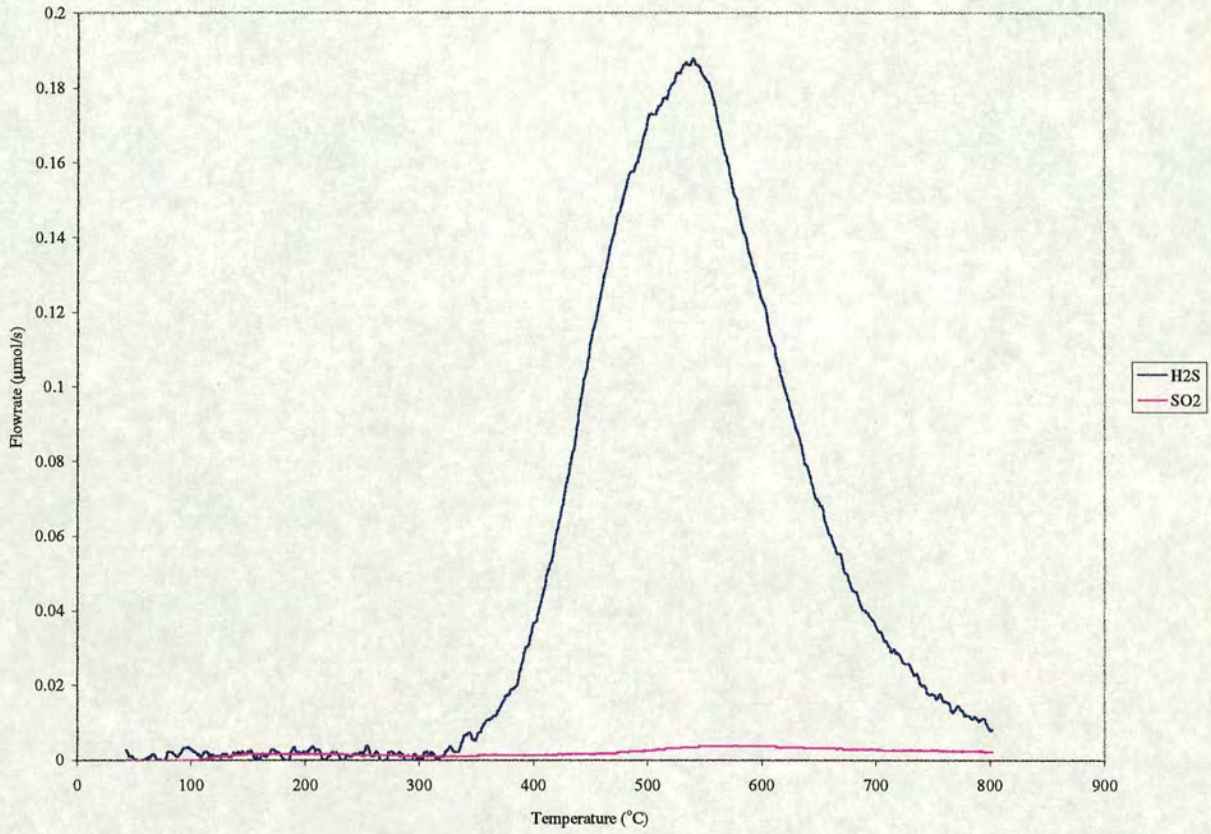

Figure 45: Standard TPR for Platinised P12

The spectrum was very similar to that of the platinised alumina; it had a similar shape and breadth and occurred at the same temperature. The major difference is a slight skew toward lower temperature. The peak was not quite as large as that of platinised alumina reflecting the fact that the platinised P_{12} did not adsorb as much sulphur dioxide as the platinised alumina.

In the standard TPR platinised P_{12} emitted almost all the sulphur as hydrogen sulphide; this is a feature of all the platinised analogues of the washcoat samples; platinisation diminishes the sulphur dioxide peak of the standard TPR. The hydrogen sulphide peak maximum occurred at 540°C and represented 54.1 µmol of the ~57 adsorbed (the very small sulphur dioxide peak accounted for the rest). This should be compared to the TPR of unplatinised P_{12}, where the hydrogen sulphide peak maximum occurred at 648 °C; again a decrease of ~100 °C.

During the TPR the hydrogen consumption peak correlated reasonably well with the hydrogen sulphide emission, if the values for the hydrogen sulphide spectrum were multiplied by a factor of ~4 (see graph below).

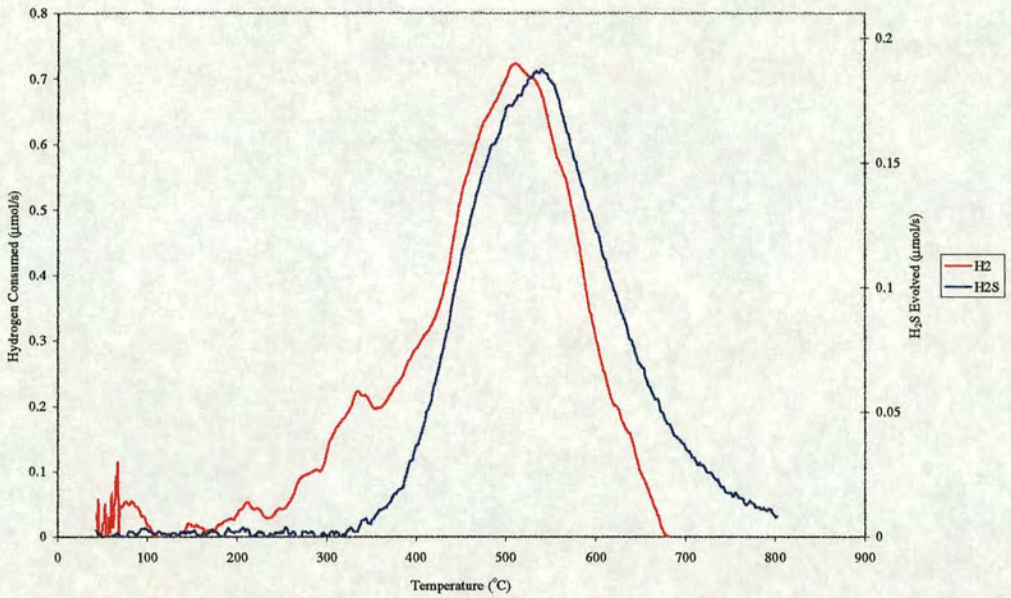

Figure 46:Standard TPR of Platinised P12 showing Hydrogen Consumption

Platinum addition caused the hydrogen sulphide switchovers of P_{12} to be greatly increased in size (see following chart). Hydrogen sulphide switchover peaks on platinised P_{12} were larger than any other seen. In these switchovers a significant amount of hydrogen sulphide was emitted at 500 °C. Although the peak height was very low, the emission continued for a long time.

The reactions which before the experiement would be believed to be the most likely over the course of the TPR procedure are, firstly, the formation of cerium (IV) sulphate[70] during oxidising conditions (500 °C, air, sulphur dioxide pulses) and, secondly, the decomposition of the sulphate during reducing conditions to form cerium (III) oxide (with all the sulphur emitted as hydrogen sulphide in this case):

$$2\ Ce(SO_4)_2 + 17\ H_2O \rightarrow Ce_2O_3 + 4\ H_2S + 13\ H_2O$$

Clearly the factor of 17:4 is very close to the factor of ~4 seen experimentally. Unfortunately, for the decomposition of a cerium sulphate to hydrogen sulphide, other possible reactions have hydrogen sulphide emission to hydrogen consumption ratios of ~4:

$$Ce(SO_4)_2 + 8\ H_2 \rightarrow CeO_2 + 2H_2S + 6H_2O$$

$$Ce_2(SO_4)_3 + 12\ H_2 \rightarrow 3\ H_2S + Ce_2O_3 + 9H_2O$$

The decomposition of aluminium sulphate to alumina with the emission of hydrogen sulphide is essentially the same as that for cerium (III) sulphate. Indeed, the TPR of platinised alumina also exhibits a stoichiometric ratio of approximately 4.

For this TPR, analysis of the stoichiometric ratios has not provided extra information, although it has ruled out some possibilities such as the decomposition of sulphites and the decomposition of cerium (III) sulphate to cerium (IV) oxide. However, it is likely that the decomposition of the cerium (III) sulphate is the reaction occurring, as there is evidence of its formation during the dosing stage of the procedure, in that heavily sulphur dioxide-treated samples are seen to be green in colour which is indicative of cerium (III) sulphate, rather than the cerium (IV) or aluminium sulphates.

---

[70] Ceria, as opposed to alumina, is generally believed to be the main cause of hydrogen sulphide emissions, as the emissions only became problematic with its incorporation into the washcoat.

The storage-release emissions (shown below) increase with temperature. This may have repercussions for the latest autocatalysts which are designed to combat 'cold start' by being positioned closer to the engine. They have to work at higher temperatures and the control of the stoichiometry is not as good, due to the decreased response time. These conditions should increase switchover peaks of hydrogen sulphide.

It is a feature of all these platinised analogues of the washcoat materials that they emitted considerably more hydrogen sulphide than the unplatinised. This was an expected feature; it is stated in the literature that only platinum-containing autocatalysts emit hydrogen sulphide. The platinised analogues also emit less sulphur dioxide (as a fraction of the total sulphur emitted).

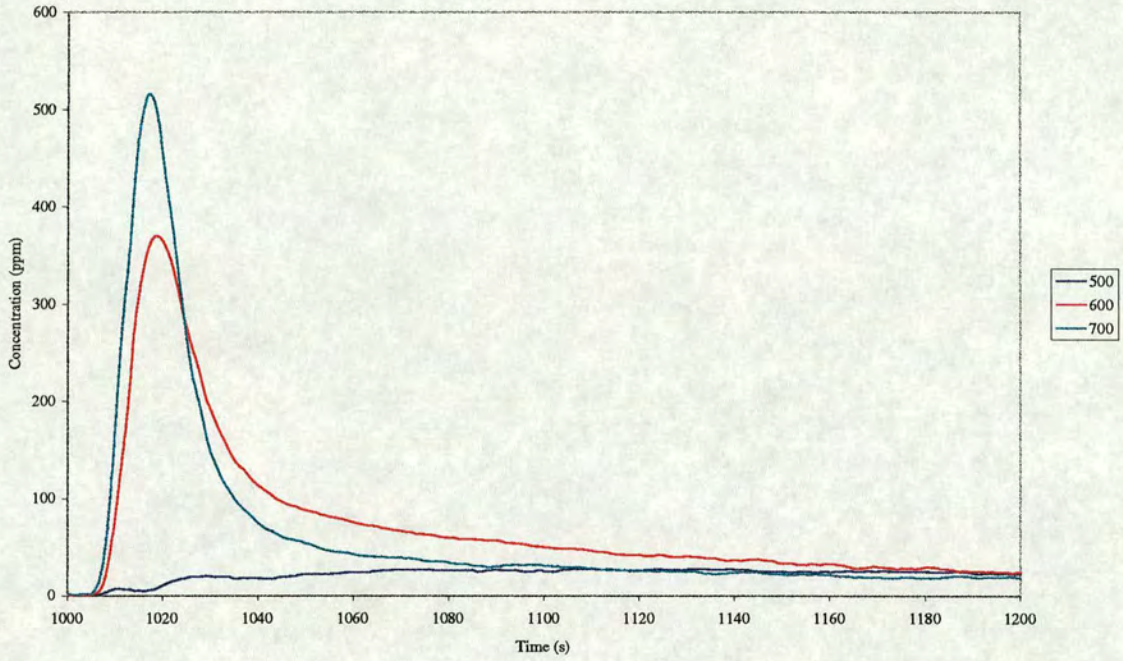

Figure 47: Hydrogen Sulphide Switchovers on Platinised P_{12}

The sulphur dioxide switchover peaks are shown below. At 500 °C and 600 °C the peaks are greater than those seen for unplatinised P_{12}. At 700 °C it appears that the unplatinised sample exhibits a larger switchover peak. It must be borne in mind that for the platinised sample a large proportion of the sulphur has been released as hydrogen sulphide, unlike the unplatinised sample, where very little was emitted as hydrogen sulphide.

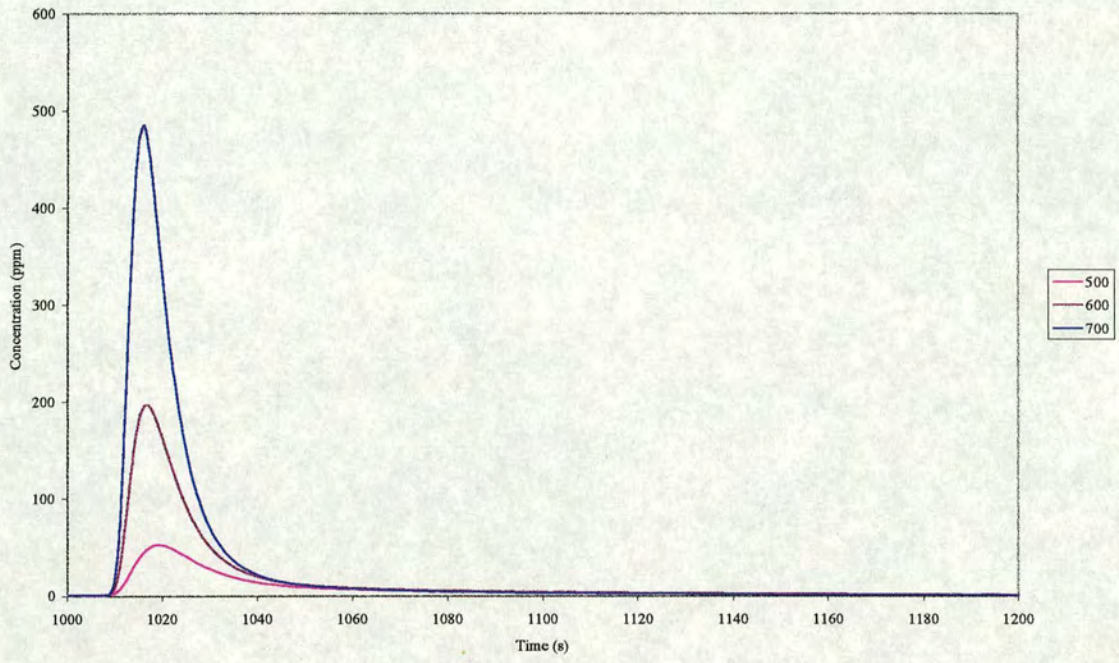

Figure 48: Sulphur Dioxide Switchovers on Platinised P_{12}

4.1.5 Barium - Doped Materials

The barium-doped samples were doped with a barium nitrate solution to 4.7 wt. % barium (as described in "Materials and Methods"). This was an equal molar amount to that used in the nickel (2.0 wt. %) and iron (1.9 wt. %) doping.

4.1.5.1 Barium – Doped P_{12}

The standard TPR of barium-doped P_{12} is shown below:

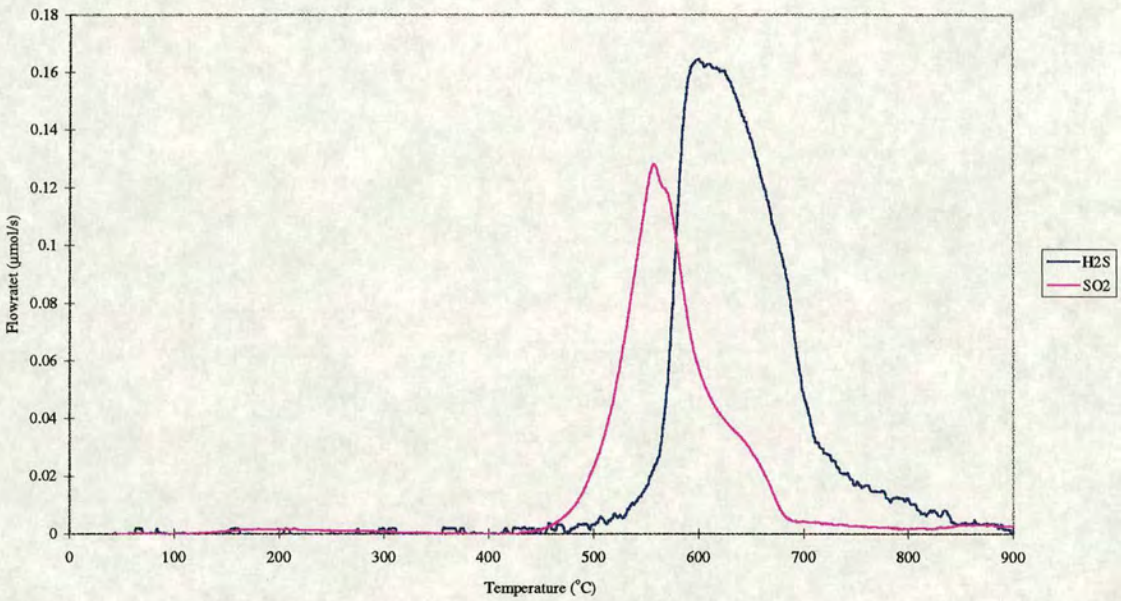

Figure 49: Standard TPR Barium-Doped P12

The TPR spectrum is unlike that of P_{12} indicating that the addition of barium has had a marked effect. The peak maxima of the sulphur dioxide and hydrogen sulphide traces occur at 565°C and 600°C and represent 16.4 and 22.8 µmol, respectively (total adsorbed 57.0 µmol). The relative amounts of sulphur dioxide and hydrogen sulphide emitted have been reversed by the addition of barium to the P_{12} formulation, i.e., the addition of barium to P_{12} leads to the emission of more hydrogen sulphide in the TPR.

The peculiar, skew shape of the hydrogen sulphide peak is seen in the hydrogen consumption peak, except multiplied by a factor of ~10 (see graph below). The factor of 10 is difficult to explain, it either implies;

1. the decomposition of a sulphur-containing species with considerably more oxygen than sulphur (as most of the hydrogen would be expected to become water), or
2. a species which adsorbs hydrogen, which seems unlikely, or
3. a species which has excess oxygen with which to form water with the hydrogen e.g. barium peroxide which can be formed by reaction with air at high temperature[71].

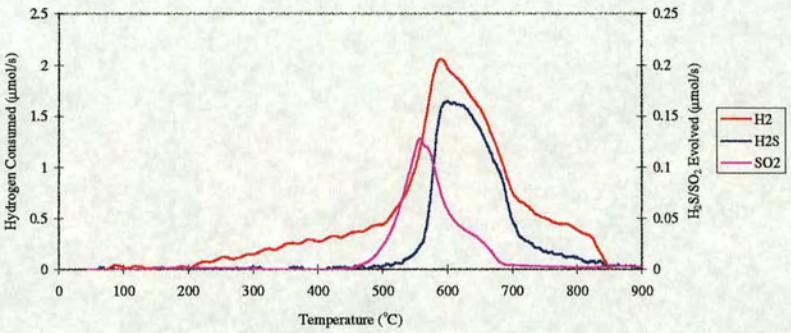

Figure 50: Standard TPR of Barium Doped P_{12} showing the Hydrogen Consumption

The peculiar shape of the hydrogen consumption peak is also seen when the hydrogen sulphide and sulphur dioxide peaks are added together. Therefore, it is likely that the same process which caused the gases to be evolved involved the consumption/conversion of hydrogen.

---

[71] Comprehensive Inorganic Chemistry states that "barium...can be oxidised with oxygen at temperatures of about 550 °C".

The hydrogen sulphide switchover peak increased in height and earliness with increasing temperature. The amount of hydrogen sulphide emitted as a fraction of the total sulphur emitted was relatively large for a non-platinised sample. This correlated with the relatively large amount of hydrogen sulphide seen in the standard TPR. In fact, the total amount of sulphur species emitted was relatively small, perhaps indicating the formation of a very stable species, such as barium sulphate for instance (the degree of adsorption of the sulphur dioxide is comparable to any similar experiment, e.g., P_{12}).

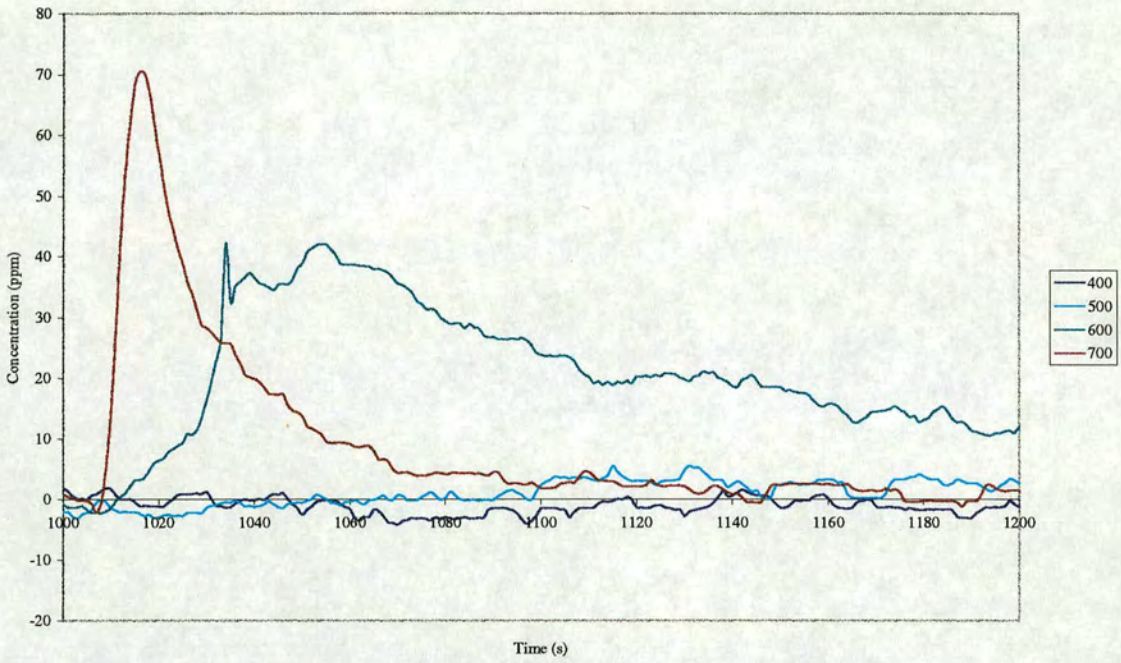

Figure 51: Hydrogen Sulphide Switchovers on Barium-Doped P12

The amount of sulphur dioxide emitted in the switchover (shown below) was considerably less than that emitted by the basic washcoat, P_{12}.

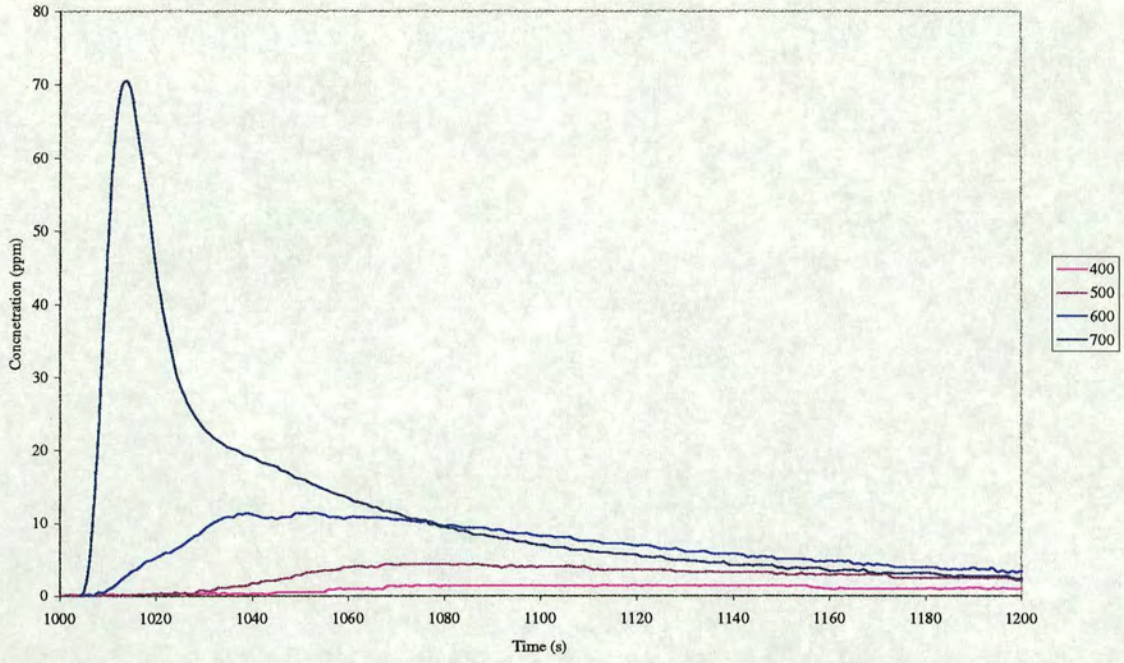

Figure 52: Sulphur Dioxide Switchovers on Barium-Doped P12

The sulphur dioxide peak increased with temperature in the same manner as that of the hydrogen sulphide. Adsorption also increased with temperature, as in most of the formulations in this research, although the differences in adsorption are small in comparison to the amount emitted. The peaks were very small compared to the iron and nickel doped P_{12} samples (both off-scale at 700 °C, i.e., over 930 ppm).

4.1.5.2 Barium – Doped Platinised P_{12}

The standard TPR of barium-doped platinised P_{12} is remarkably similar to that of platinised P_{12}. Whereas the TPR of the unplatinised sample was significantly changed by the addition of baria, its addition has had little effect on the platinised sample. The shape of the peak is very similar to that of platinised P_{12}, and virtually all the sulphur is emitted as hydrogen sulphide, which is a feature of all platinised samples.

The peak maxima occur at 590°C (hydrogen sulphide, representing 62.3 μmol) and 588°C (sulphur dioxide, representing 2.8 μmol). The sulphur dioxide peak is extremely small and, as such, is very poorly developed. The peak temperature has a large margin of error and would be seen to be considerably lower if fully developed.[72]

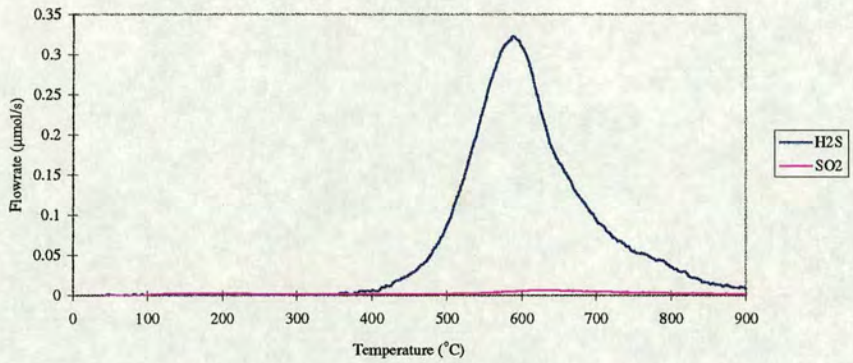

Figure 53: Standard TPR Barium Doped Platinised P12

It is noticeable in the TPR spectrum that there is a slight 'tail' in the hydrogen sulphide peak compared to the peak of platinised P_{12}. This is a feature in the TPR spectra of all the doped platinised P_{12} samples, although it is considerably more pronounced for the iron and nickel samples.

---

[72] See section 'Variable θ TPRs' to see development of a peak with increasing surface coverage.

Large hydrogen sulphide emissions are observed in switchover experiments with barium doped platinised P_{12}. The peaks are similar in magnitude to those observed in the platinised P_{12} experiments. The barium has had a very mild attenuating effect at most, in contrast to the effects of the nickel and iron. The sulphur species are predominantly emitted in the form of hydrogen sulphide; this is also unlike the behaviour of the iron and nickel doped species.

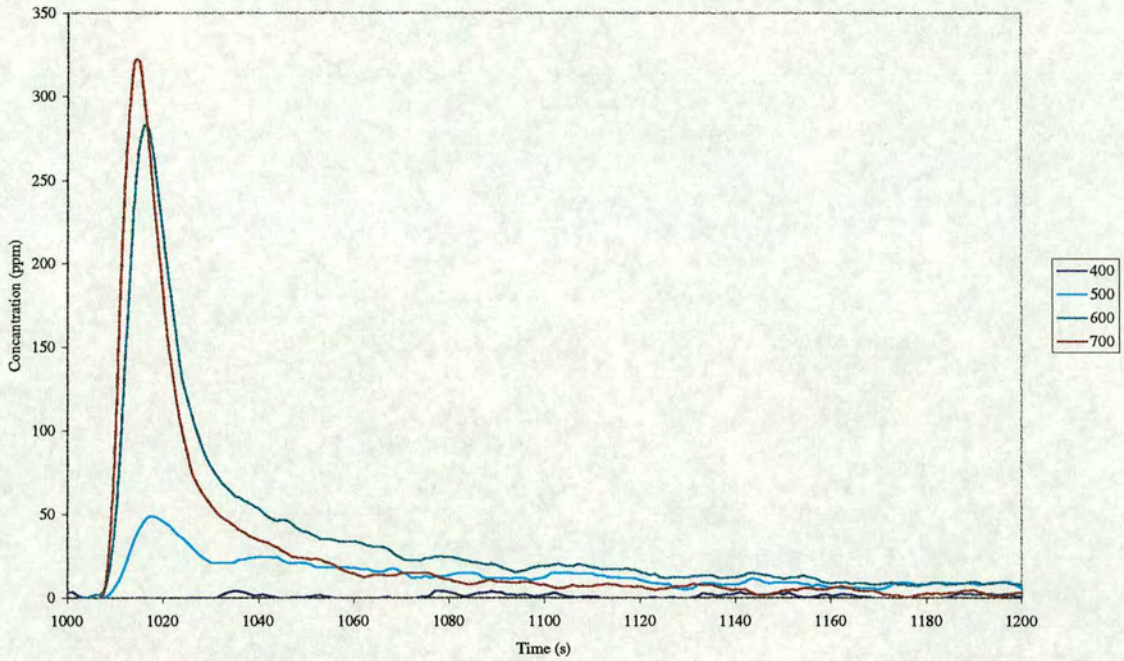

Figure 54: Hydrogen Sulphide Switchovers on Barium-Doped Platinised P12

The amount of sulphur dioxide produced upon switchover is relatively small, compared to the amounts emitted by the nickel and iron doped samples, perhaps because so much of the sulphur was emitted as hydrogen sulphide. The proportion of sulphur emitted from barium-doped platinised P_{12} as sulphur dioxide is lower than that for platinised P_{12}.

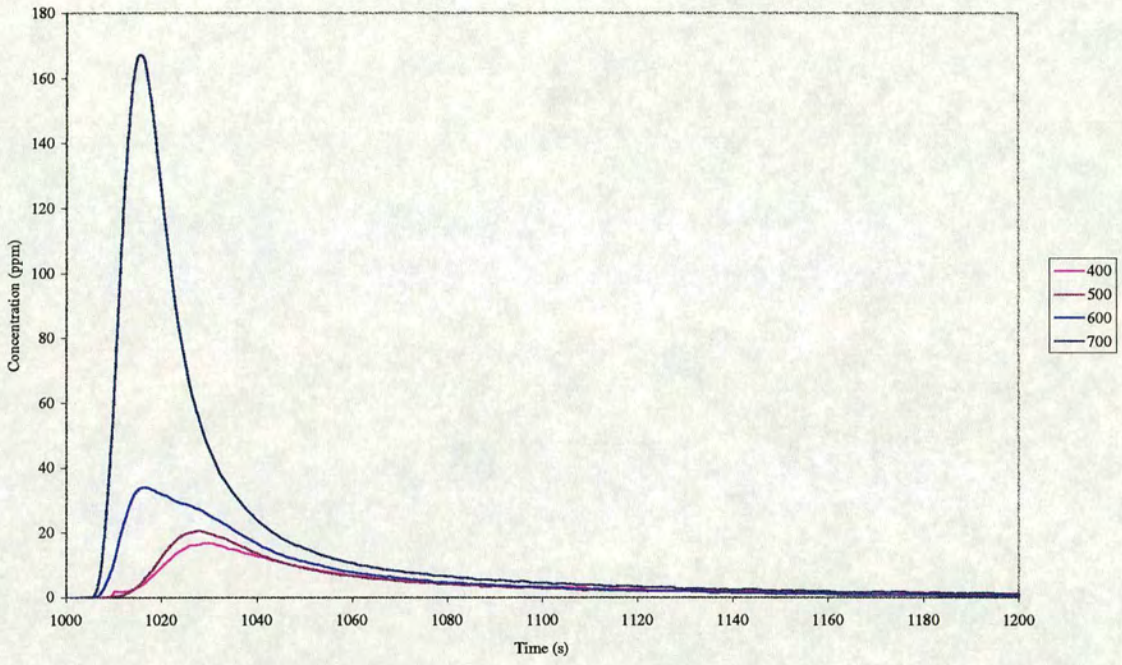

Figure 55: Sulphur Dioxide Switchovers on Barium-Doped Platinised P_{12}

4.1.6 Iron - Doped Materials

4.1.6.1 Iron – Doped P_{12}

In the standard TPR of iron-doped P_{12} the effect the addition of iron has had can be clearly seen. The temperatures of the peak maxima are seen to be very low at 474 °C (15.4 µmol) and 518 °C (24.8 µmol) for sulphur dioxide and hydrogen sulphide, respectively. This may well be a consequence of the formation of iron sulphates; TPRs performed in the course of this research on iron sulphates[73] show that they can decompose in hydrogen to sulphur dioxide below 500 °C. The shapes and relative proportions of the peaks are very different from that of P_{12}. The hydrogen sulphide peak has become the larger of the two peaks, and a 'tail' is evident at higher temperature.

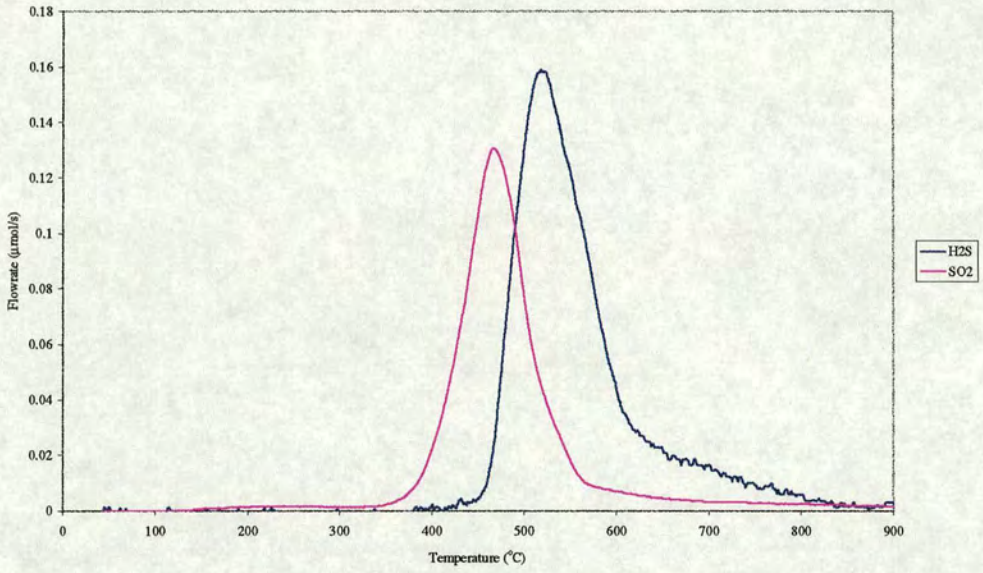

Figure 56: Standard TPR of Iron-doped P12

[73] See following section on 'TPRs of Pure Compounds'

The hydrogen consumption peak of the TPR is shown below. The consumption of hydrogen occurs at approximately the same temperature as the emission of the sulphur species (the peak maximum is between the two at 504 °C), and the sum of the hydrogen sulphide and sulphur dioxide peaks is very similar in shape to that of the hydrogen consumption peak.

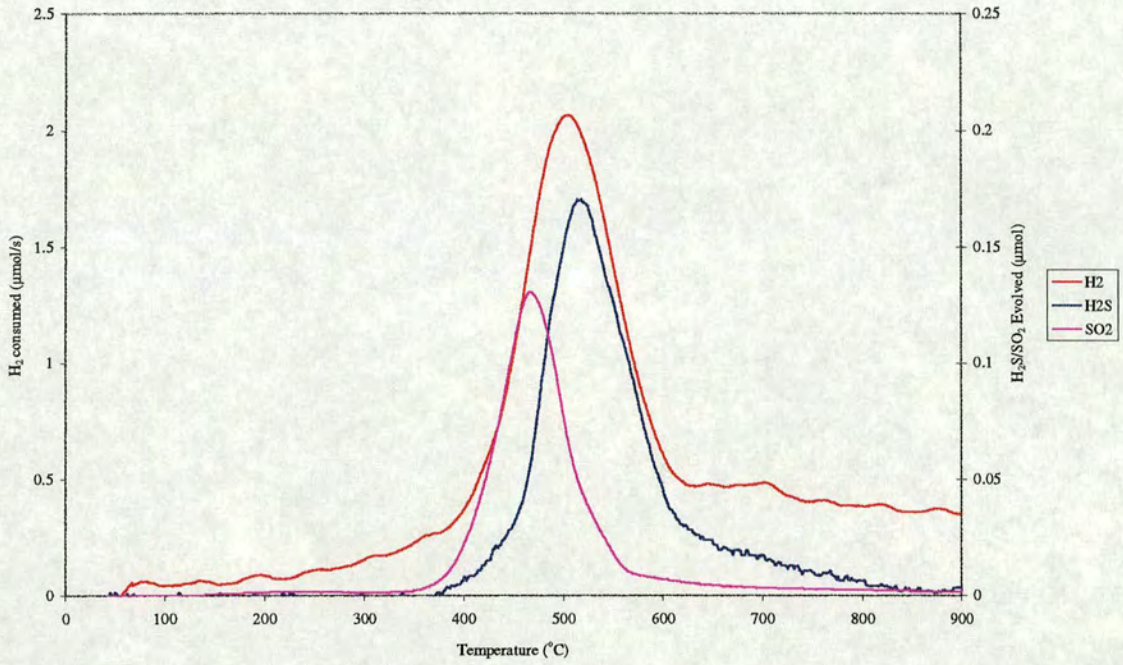

Figure 57: Standard TPR of Iron-Doped P_{12} showing Hydrogen Consumption

The temperatures at which the switchover peaks occurred were seen to correlate reasonably well with the TPR data. The peaks (predominantly sulphur dioxide) were seen at relatively low temperatures. The hydrogen sulphide switchovers were very small. This may be evidence of the hydrogen sulphide attenuating effect of iron as an additive, but as undoped P_{12} emits so little hydrogen sulphide in these experiments it is not conclusive. It should be pointed out that the 'double peak' in the graph below is not a real effect. The effect is due to having to remove a relatively large sulphur dioxide artefact from a relatively small hydrogen sulphide trace.

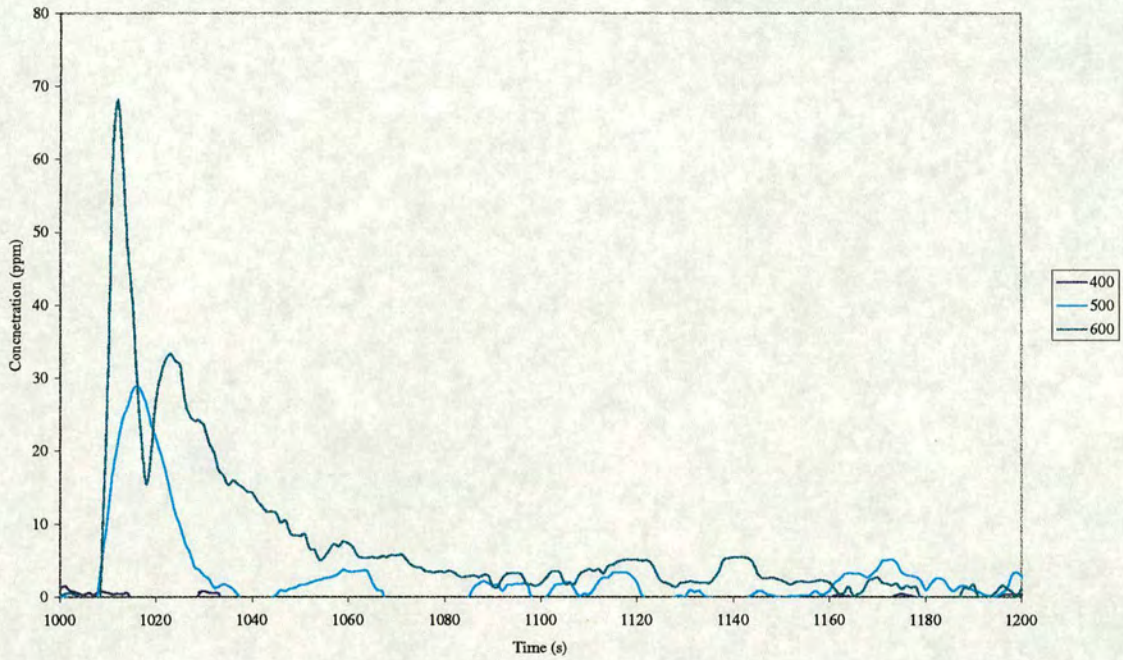

Figure 58: Hydrogen Sulphide Switchovers on Iron - Doped P12

The sulphur dioxide switchover peaks were seen to be very large. This resulted in the 600 °C switchover peak going slightly off-scale (i.e., over 930 ppm, see below) and the 700 °C peak (not shown) going considerably off-scale. This correlates with the sulphur dioxide peak of the standard TPR; 700 °C is over 100 °C beyond the point where virtually all sulphur dioxide has been emitted in the TPR. The hydrogen sulphide emission in the switchover experiments was very small. This may be because the hydrogen sulphide is 'scavenged' in the switchover or converted to sulphur dioxide by excess oxygen released by the iron[74], or it may be that the iron formed iron sulphate during the dosing stage (which decomposes with the release of sulphur dioxide).

Hydrogen sulphide emission is seen in the TPR, but not the switchover, presumably due to the different conditions. In the TPR; when the sample reaches emission temperature there is no available oxygen as the sample has been treated with reductant for a long time. This is not the case in the switchover experiments, where oxygen will still be available.

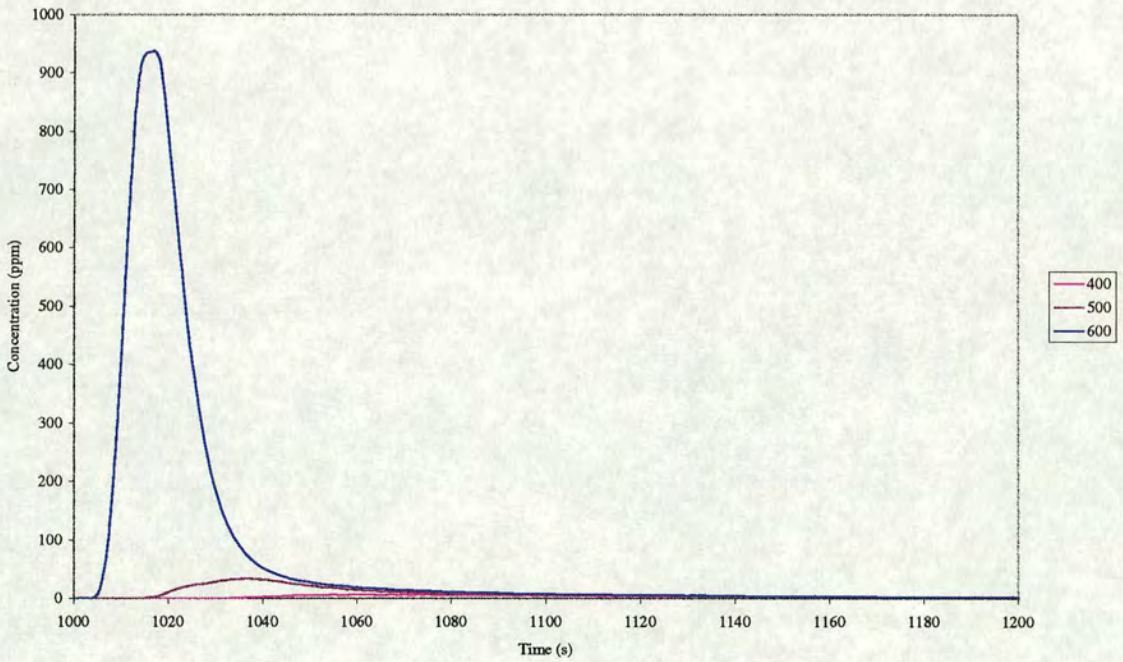

Figure 59: Sulphur Dioxide Switchovers on Iron-Doped P12

[74] See 'Literature Survey' for the proposed mechanisms by which hydrogen sulphide attenuators are believed to act.

4.1.6.2 Iron – Doped Platinised P_{12}

The standard TPR of iron-doped platinised P_{12} is shown below:

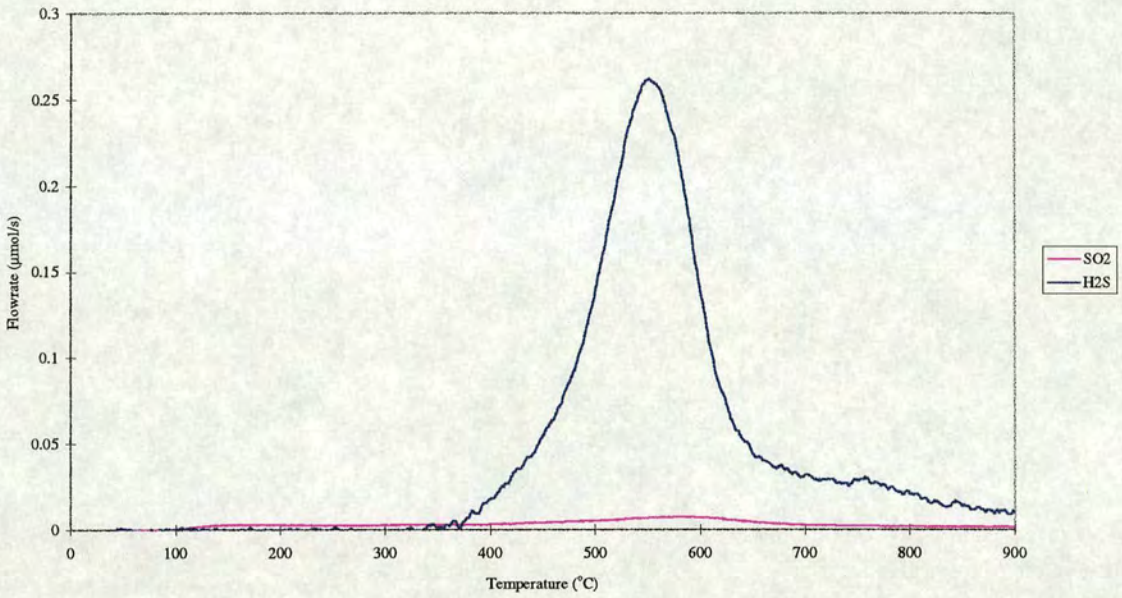

Figure 60 : Standard TPR Iron Doped Platinised P12

This TPR differs from that of platinised P_{12} in that it exhibits a distinct 'tail' in the hydrogen sulphide concentration at high temperatures. The trace can be divided into two distinct regions; firstly a lower temperature 'Gaussian' peak, similar to that seen in many other TPRs in this research, and, secondly, a higher temperature diffuse peak.

The main difference between this TPR and that of the unplatinised iron-doped P_{12} is that, as is seen in every comparison between the platinised and unplatinised samples, the sulphur dioxide peak has been greatly diminished. The peak maximum has been shifted to higher temperature by the addition of platinum to iron-doped P_{12}. Of all the formulations that were used in this research, only those of the iron-doped samples exhibited a higher temperature peak maximum in the platinised sample's TPR spectrum than in that of the unplatinised.

The TPR is shown below with the hydrogen consumption trace. There is excellent agreement between the temperatures of the maxima of these two peaks. The stoichiometric ratio between the peak amounts is approximately 5.0 which is consistent with the reduction of sulphates.

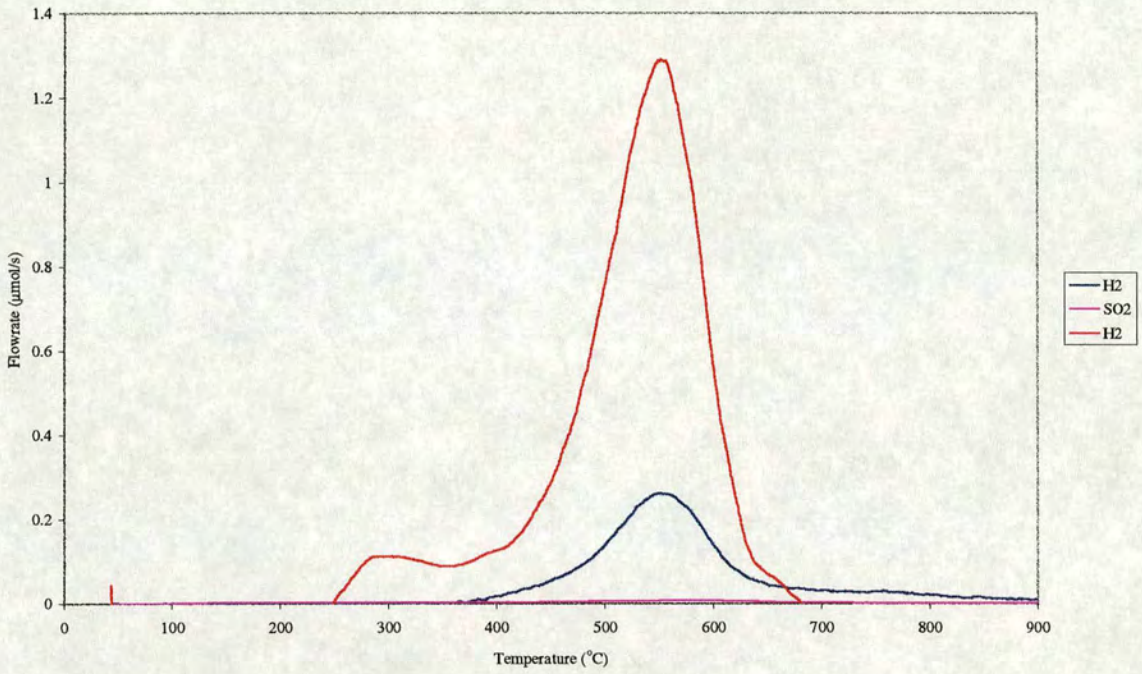

Figure 61: The Standard TPR of Iron-Doped Platinised P12 showing the hydrogen consumed

The hydrogen sulphide switchovers of iron-doped platinised P12 can be seen below. There is an increase in hydrogen sulphide emission with temperature, but the emissions are much smaller than for platinised P_{12} without iron-doping, i.e., the iron is an effective attenuating agent. This has been seen in practice (Bending *et al.* (1993)).

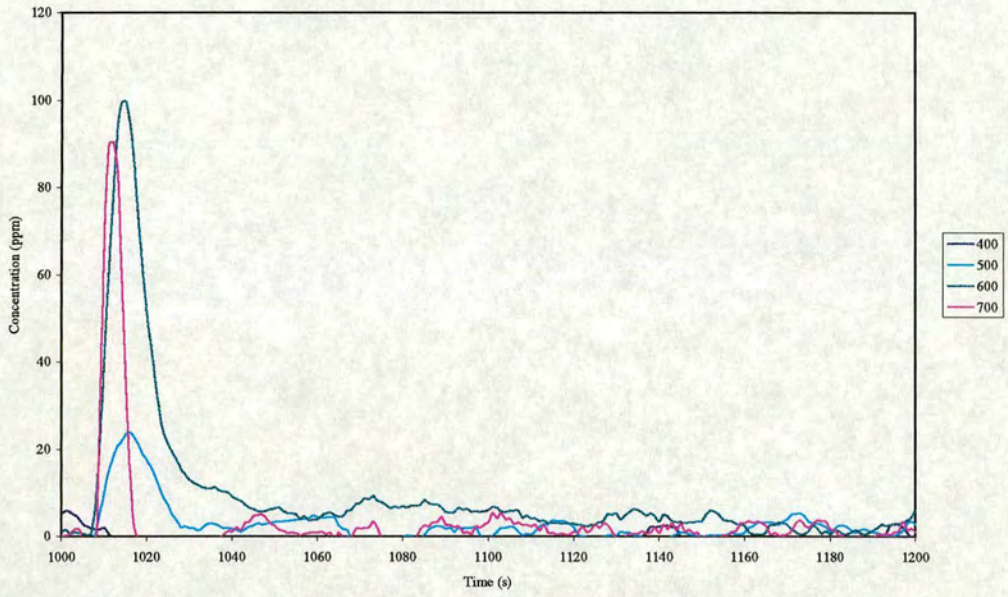

Figure 62: Hydrogen Sulphide Switchovers on Iron-Doped Platinised P12

The sulphur dioxide switchover peaks exhibited a clear increase in size with temperature. Most of the sulphur emitted by this component was in the form of sulphur dioxide illustrating its efficacy and perhaps its *modus operandi* as a hydrogen sulphide attenuating additive, i.e., that it causes sulphur species to be emitted as sulphur dioxide rather than hydrogen sulphide, perhaps by forming iron sulphates.

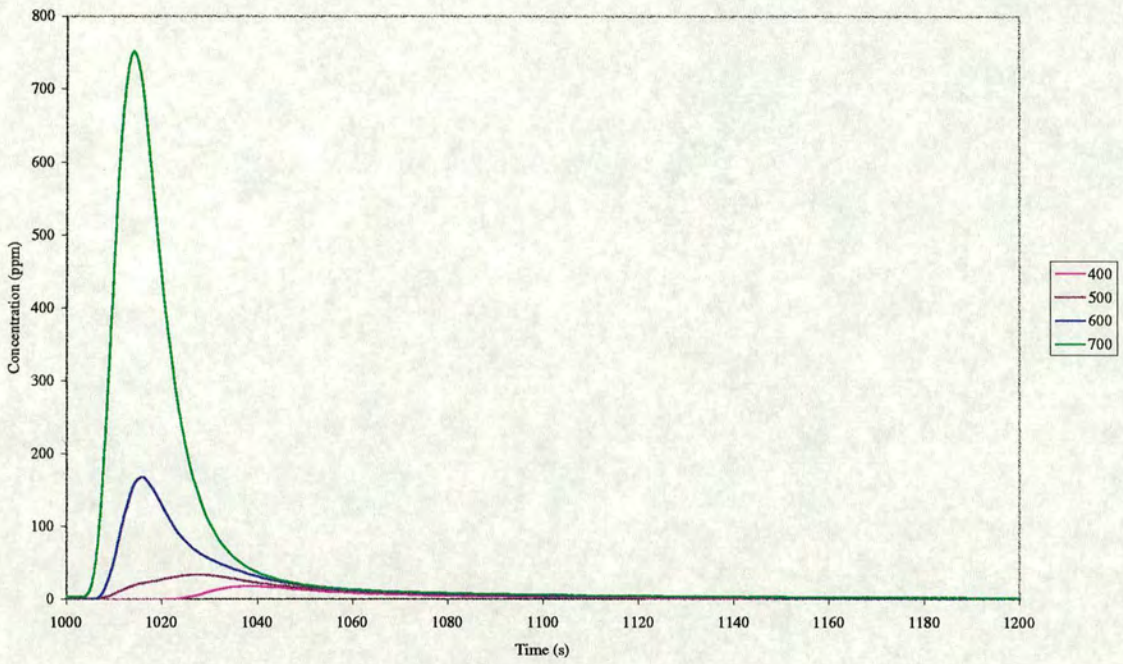

Figure 63: Sulphur Dioxide Switchover Peaks, Iron-Doped Platinised P12

4.1.7 Nickel - Doped Materials

Nickel is an important dopant to study, as it is successfully used in the USA to attenuate H_2S emissions, and would be used in Europe were it not for health concerns over nickel carbonyl emission. Hence, it is important to identify the salient differences between the results of nickel experiments and others; the main difference identified in the nickel experiments, apart from the expected reduced hydrogen sulphide switchover peaks, is the peculiar shape of the hydrogen sulphide TPR peak; there is a distinct 'tail'.

4.1.7.1 Nickel - Doped P_{12}

The standard TPR of nickel-doped P_{12} can be seen below. It exhibits a distinct 'tail' which is much more pronounced than those seen in the TPR spectra of iron- or barium-doped materials. The 'tail' was present in all TPR spectra of nickel-containing components in this research.

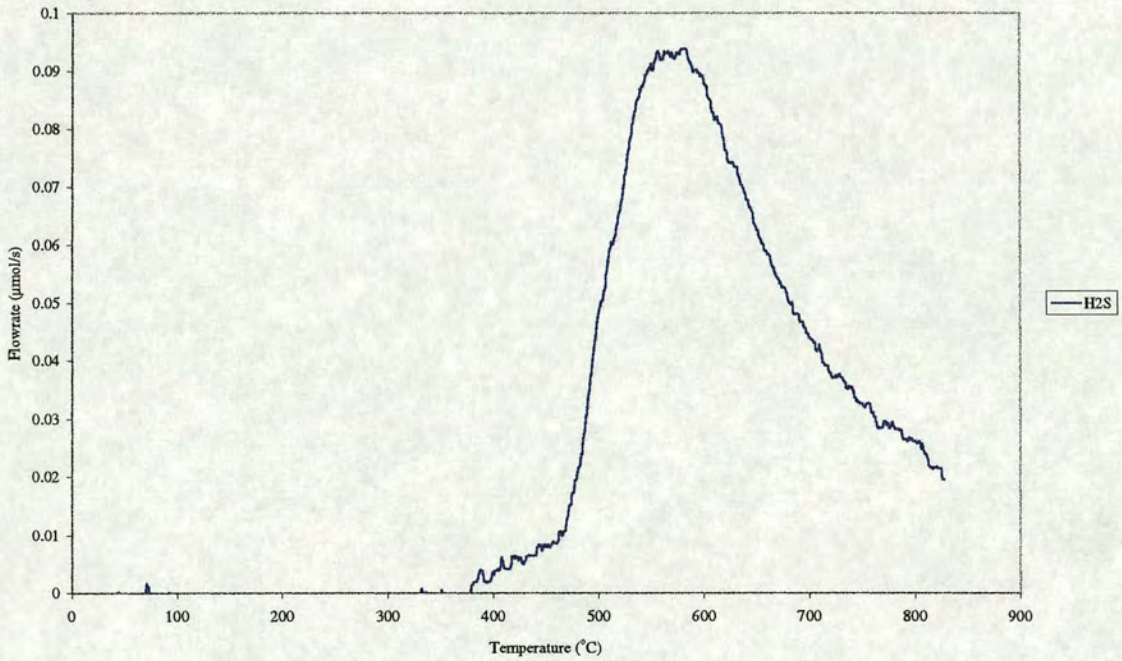

Figure 64: Standard TPR Nickel - Doped P12

The sulphur dioxide trace is not shown in this spectrum as it was insignificant (as it was in all TPRs on nickel-containing samples). The hydrogen sulphide 'tail' persists until after 800°C, indicating that some reducible species present is extremely thermally stable. It will be seen in section 4.2 that similar 'tails' are observed in the TPR spectra of nickel sulphides and sulphates.

The main hydrogen consumption peak in the TPR occurred prior to the emission of hydrogen sulphide peaking at 470 °C. This is an unusual feature; in almost all other TPR spectra it was observed that the hydrogen consumption occurred at the same time as emission of sulphur dioxide or hydrogen sulphide. This consumption of hydrogen could represent a number of processes, e.g.;

- Hydrogen storage
- The formation of nickel sulphide from the sulphate

The formation of the sulphide from the bulk sulphate can be seen in the following section. The TPR of the sulphate exhibits a sharp peak at approximately 500 °C, followed by a diffuse peak which persists to high temperature.

The tail in the hydrogen consumption peak correlates well with the hydrogen sulphide trace magnified by a factor of 4.

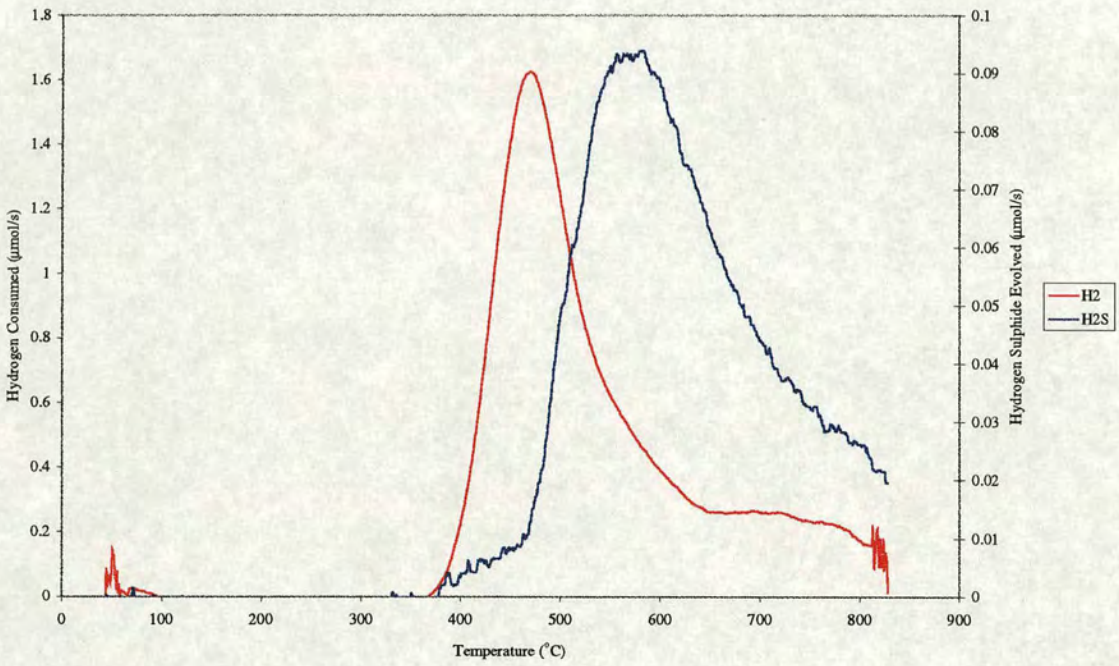

Figure 65: Hydrogen Consumption in the Standard TPR of Nickel-Doped P_{12}

In the chart below the hydrogen sulphide switchover peaks of nickel-doped P_{12} can be seen to be greatly attenuated. The peaks are persistent, emitting the hydrogen sulphide over a long time. This is an extremely useful feature of an attenuating agent; it does not matter that hydrogen sulphide is emitted, rather that it does not exceed the smell threshold. It is also a good feature that it does release the sulphur, whether in the form of sulphur dioxide or as hydrogen sulphide (in low concentrations), because a species which did not release would soon be saturated with the sulphur dioxide and no longer able to function.

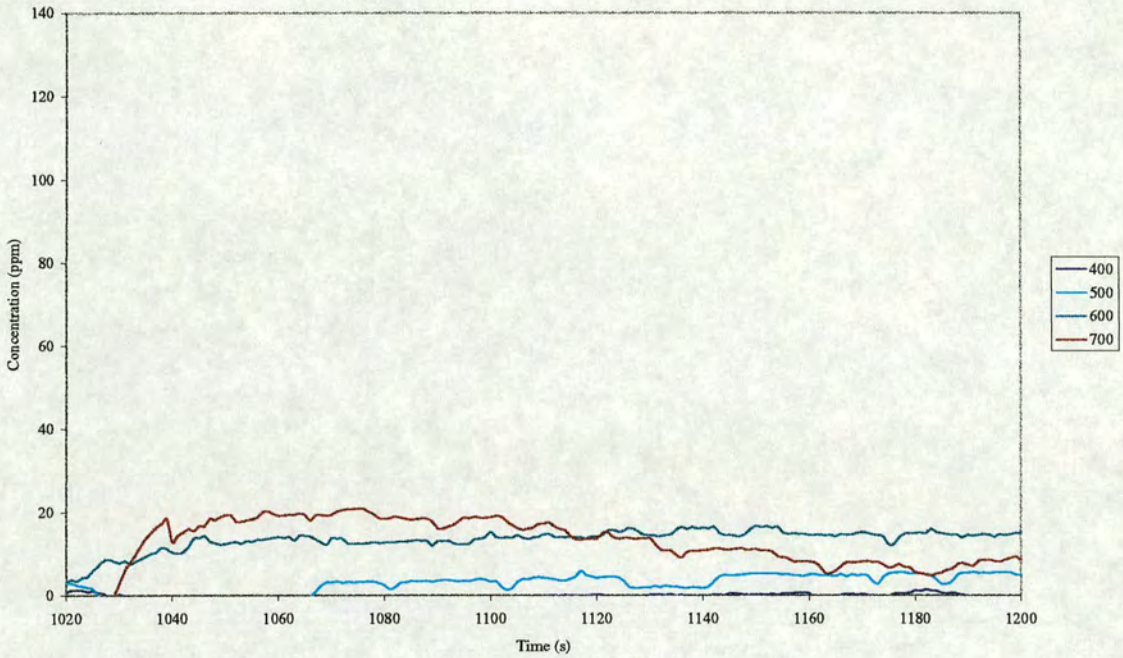

Figure 66: Hydrogen sulphide Switchovers on Nickel-Doped P12

The switchover peaks of both species are remarkably similar in behaviour to that of the iron-doped materials;

- Little hydrogen sulphide is emitted
- The emissions of sulphur dioxide are relatively large
- More sulphur dioxide is adsorbed at the dosing stage than by the P_{12}.

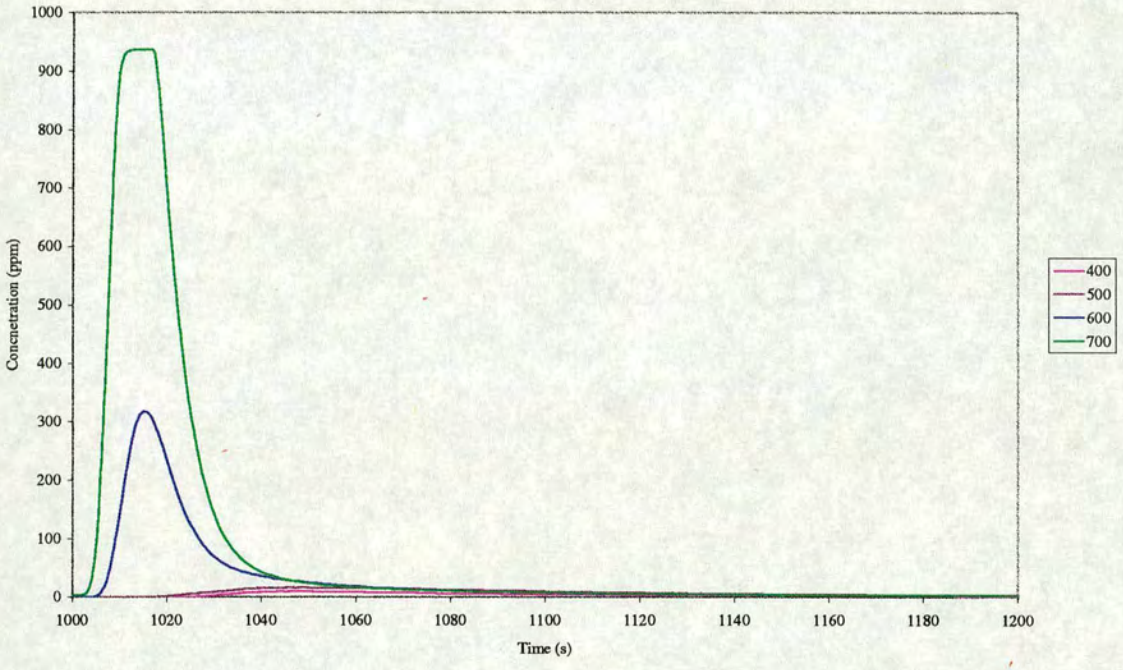

Figure 67: Sulphur Dioxide Switchovers on Nickel-Doped P_{12}

4.1.7.2 Nickel - Doped Platinised P_{12}

The standard TPR of nickel-doped platinised P_{12} exhibits a greater 'tailing' than the unplatinised sample. The platinisation has had the effect, as in most cases, of increasing the amount of sulphur dioxide adsorbed. This is generally thought to be due to the platinum's catalysing effect on the oxidation of sulphur dioxide to trioxide, the sulphur trioxide being more reactive than the dioxide. The effect observed in other comparisons between components and their platinised analogues, of diminished sulphur dioxide peak is not apparent here, because there was so little sulphur dioxide emitted in the TPR of the unplatinised sample.

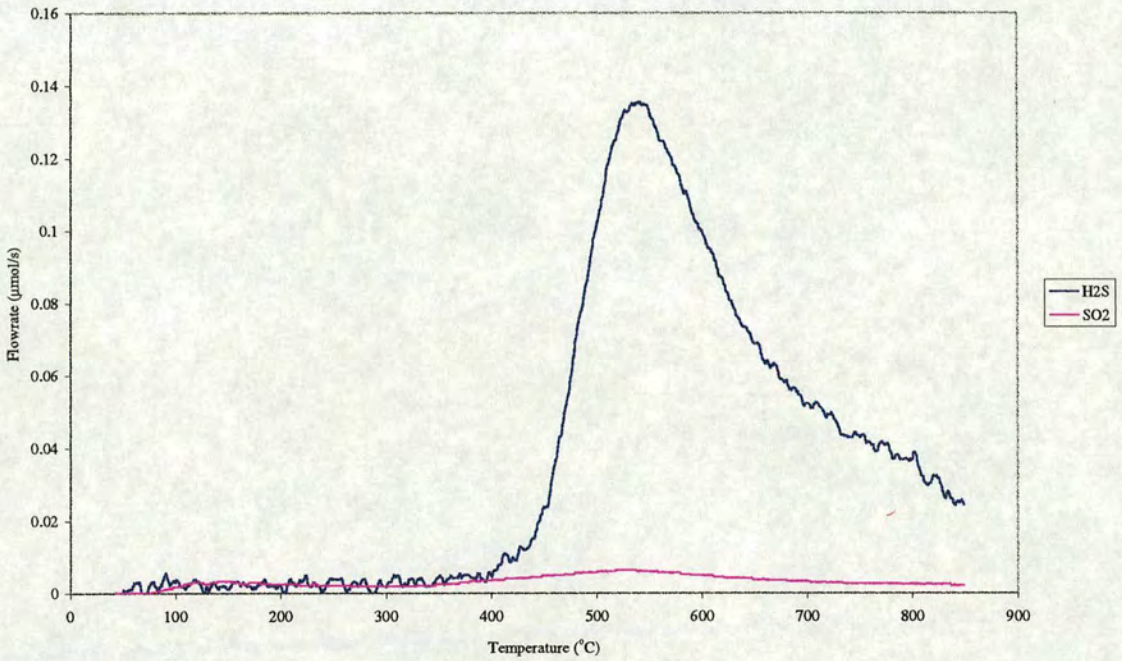

Figure 68: Standard TPR of Nickel Doped Platinised P12

The standard TPR of nickel-doped platinised P_{12} is shown below, with hydrogen consumption (note the different scales of the ordinate axes). As in the TPR of the unplatinised nickel-doped P_{12} there is significant consumption of hydrogen prior to any emission of hydrogen sulphide. This is much less pronounced here than was the case for the unplatinised sample. The latter part of the hydrogen consumption peak parallels the emission of the hydrogen sulphide.

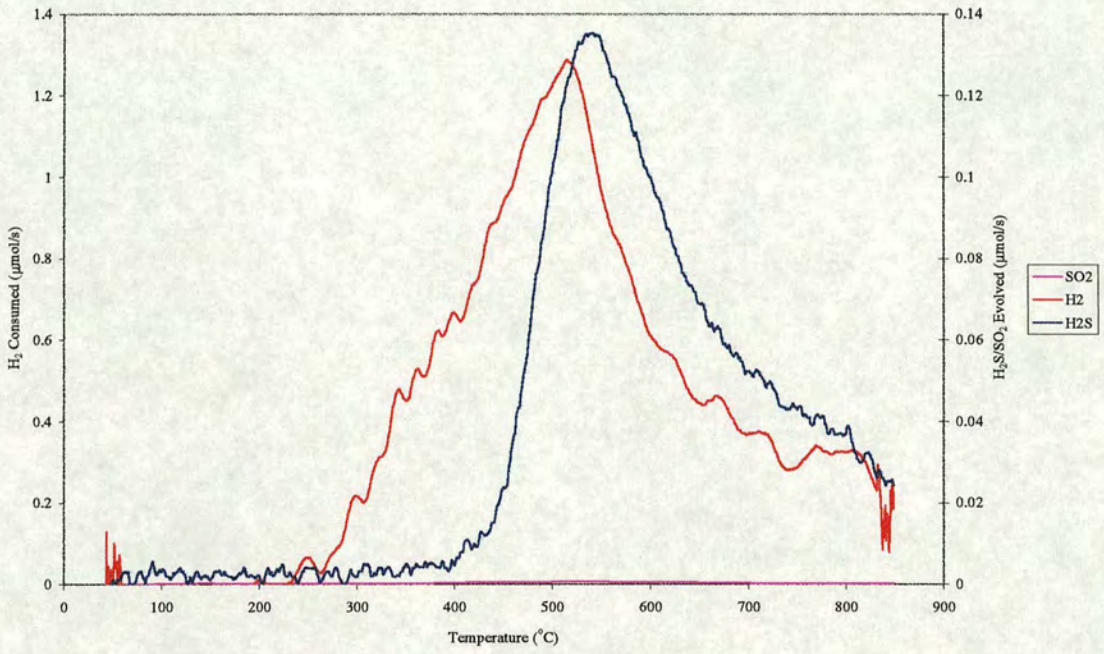

Figure 69: Standard TPR of Nickel-Doped Platinised P_{12} showing Hydrogen Consumption

The hydrogen sulphide switchover peaks have been drastically lowered by the addition of nickel to platinised P_{12}. It should be noted, however, that the hydrogen sulphide emissions are very prolonged and have a flat profile, as in nickel-doped P_{12}. Hydrogen sulphide emissions were observed in this research which lasted as long as 500 s, whilst remaining at a level of approximately 10 ppm.

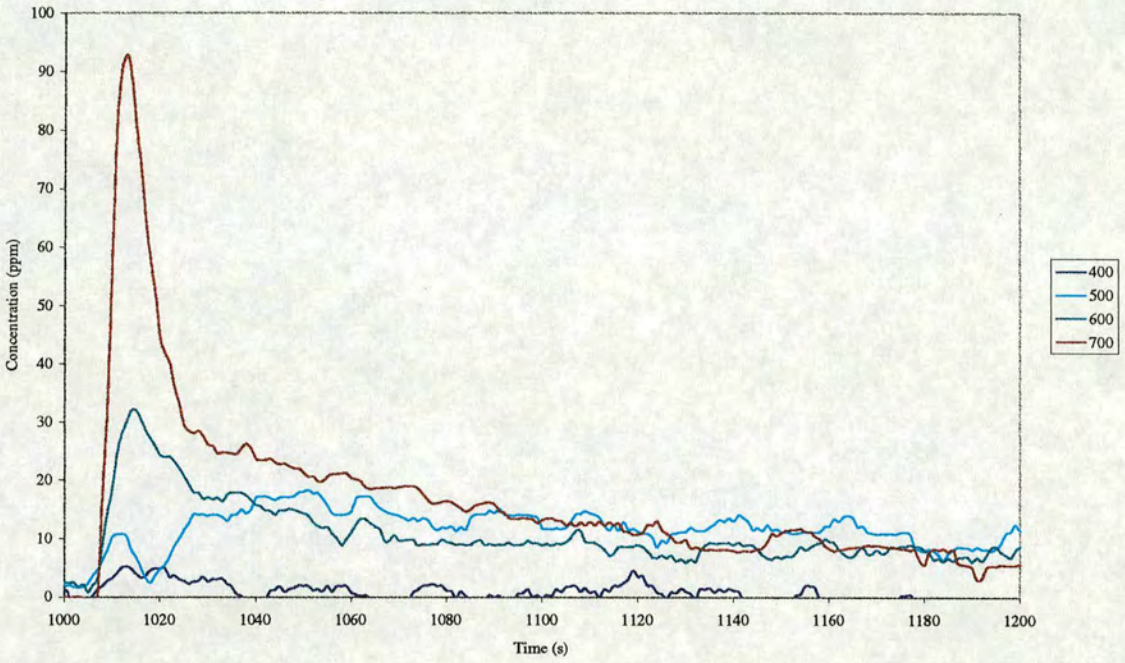

Figure 70: Hydrogen Sulphide Switchovers on Nickel-doped Platinised P12

The sulphur dioxide peaks were considerable, but were much smaller than those observed from the unplatinised sample. This could reflect the "hydrogen sulphide scavenging" of the nickel, in that it traps any hydrogen sulphide formed from sulphur dioxide by the action of the platinum and forms nickel sulphide, which releases the sulphur as hydrogen sulphide very slowly.

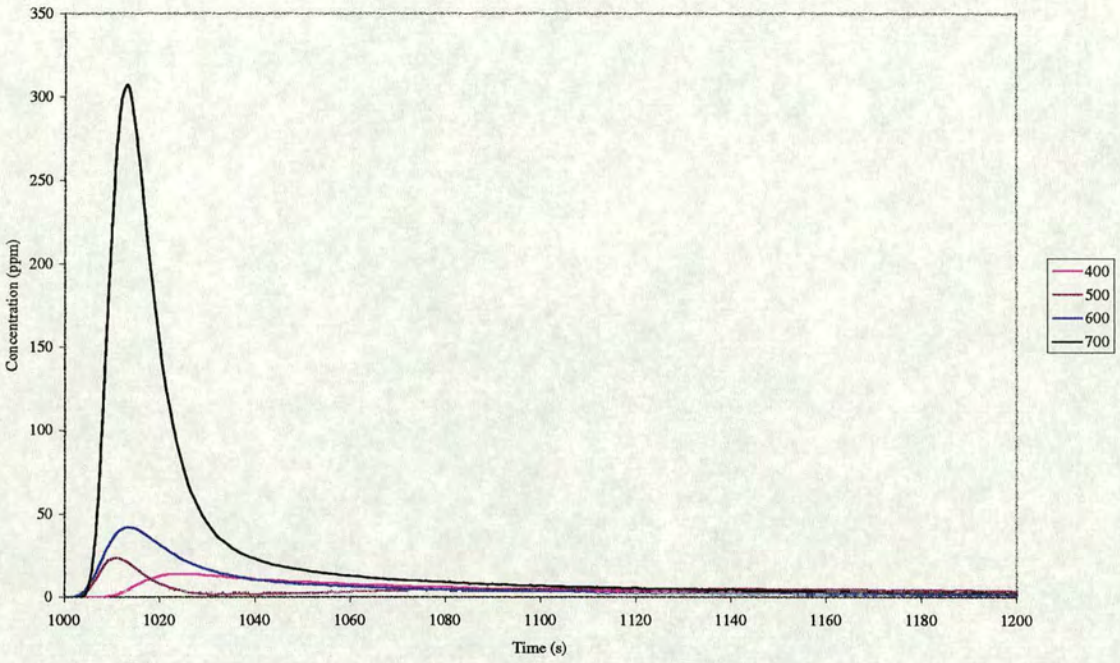

Figure 71: Sulphur Dioxide Switchover on Nickel-Doped Platinised P12

4.1.7.3 Nickel – Doped Alumina

Standard TPRs were performed on two samples of nickel–doped alumina, one with two percent nickel, the other with ten percent. This was to assess the effect of varying the nickel content on the TPR spectra. Again, the characteristic 'tail' on the hydrogen sulphide peak in the standard TPR was seen.

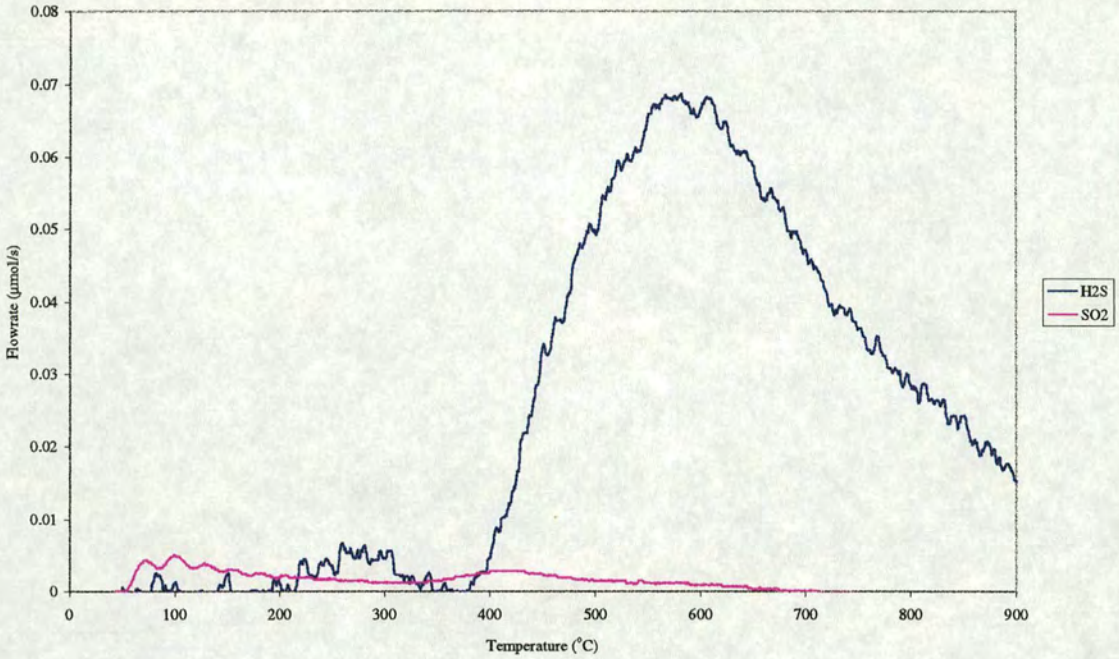

Figure 72: Standard TPR 2% Nickel Doped Alumina

The 2.0 wt.% nickel on alumina has a very similar TPR to that of 2.0 wt. % nickel P_{12}. The amounts of hydrogen consumed and hydrogen sulphide emitted are very similar at ~270 µmol and ~25 µmol, respectively. The fact that substrate change has not altered the TPR spectrum considerably indicates that the nickel is the dominant influence and the substrate is relatively unimportant, in the absence of platinum.

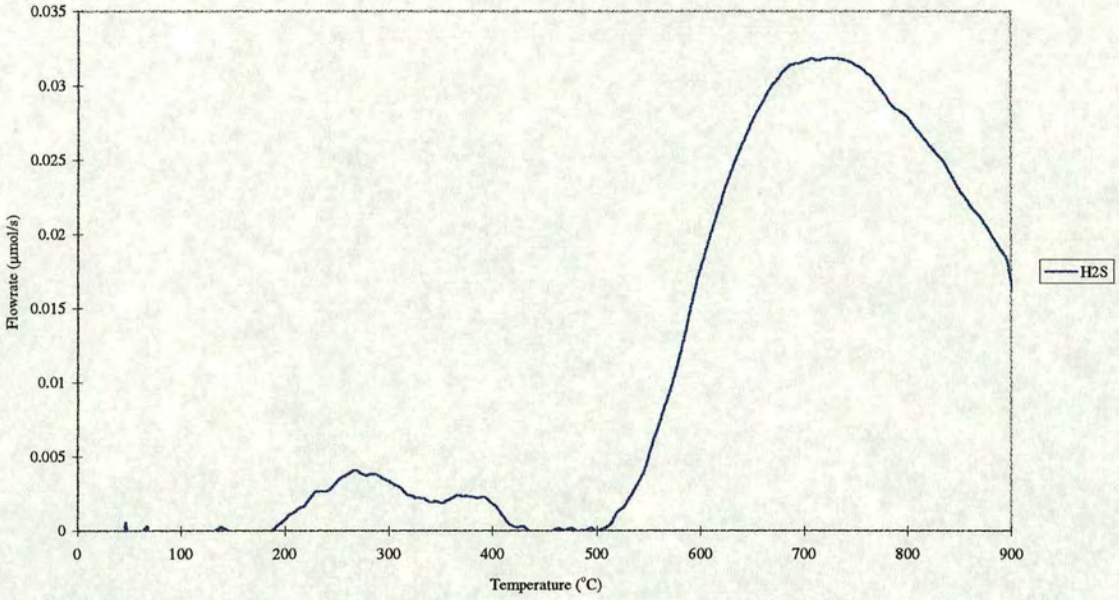

Figure 73: Standard TPR 10% Nickel Doped Alumina

During the TPR of 10 wt.% nickel on alumina ~440 µmol of hydrogen were consumed, but only ~12 µmol of hydrogen sulphide were emitted. The increase in the nickel content had the effect of pushing the hydrogen sulphide peak to higher temperatures and decreasing the size of the peak, indicating that the sulphur was bound more tightly.

4.1.8 Summary of TPR Data

The following table summarises the TPR peak data for sulphur dioxide and hydrogen sulphide evolution, and hydrogen consumption. It gives the peak temperatures and the amount of each gas evolved/consumed. The table also gives the half and three quarter widths of the peaks. It is from these widths that the desorption energies were calculated, as per the analyses presented in Falconer and Schwarz (1983). The error margin of the peak temperatures is +/- 5°C, due to the inherent errors in the thermocouple's measurement and measurement of the time lag between detector and reactor. The amounts are calculated by integrating the response by a simple trapezium rule method. Large errors are possible in the calculated amounts due to the choice of the baseline; a difference in baseline smaller than the resolution of the meter can result in considerable changes in the value calculated on that basis. This error becomes less significant the greater the amount evolved. For many of the peaks the two values of the desorption energy do not agree well. This is true for extremely small peaks, such as the sulphur dioxide peaks for nickel-doped materials, where the quality of the peak is poor, as it is so small. This is also true for the heavily 'tailed' peaks such as the nickel – doped alumina samples, as the two measures of peak width are rendered inconsistent by the tail. It should be noted that some of the data for very small peaks, particularly certain sulphur dioxide peaks, where virtually all sulphur was emitted as hydrogen sulphide (e.g, platinised alumina) is misleading, as the peaks are not fully developed. These are included for completeness. Data given as zero are information that could not be determined, usually meaning that there was no peak as such. This means either that the trace was flat or that it was continuously increasing, (meaning that the actual peak occurs at a temperature above the capability of this experimental system).

Comparison of the activation energy for platinised and unplatinised samples reveals that the energy of desorption has been decreased in the majority of cases, as would be expected. Comparison of the desorption energies of P_{12} and its doped analogues reveals that the doping has led to lower energies of desorption. The addition of nickel to alumina has also caused a decrease in the desorption energy, although the energy increases as the nickel content increases from two to ten per cent.

The symbols W1/2 and W3/4 represent the half- and three quarters widths of the peaks. The symbol $E_d(1^o)$ is the energy of desorption, assuming a first order desorption process (the further symbols 1/2 and 3/4 give the width from which this was determined). T_{max} is the temperature at which the peak maximum occurs. Examples of the formulae used in the calculations are given in Appendix 7.7.

	Gas	T_{max}	Max	Amount	W1/2	W3/4	E_d (1°)1/2	E_d (1°) 3/4
		°C	µmol/s	µmol	°C	°C	J/mol	J/mol
Alumina	SO_2	576	0.02	3	82	56	1.70E+05	1.57E+05
Alumina	H_2S	638	0.09	17	110	63	1.44E+05	1.61E+05
Alumina	H_2	628	0.37	88	122	53	1.26E+05	1.88E+05
Ceria	SO_2	633	0.38	32	57	35.5	2.82E+05	2.87E+05
Ceria	H_2S	681	0.15	14	53	38	3.37E+05	2.98E+05
Ceria	H_2	648	2.21	180	64	36	2.59E+05	2.93E+05
P12	SO_2	621	0.23	25	76	52	2.04E+05	1.89E+05
P12	H_2S	652	0.16	15	43	23	3.92E+05	4.67E+05
P12	H_2	627	1.84	280	85	55	1.84E+05	1.80E+05
Pt-Alumina	SO_2	548	0.01	3	338	211	3.38E+04	3.45E+04
Pt-Alumina	H_2S	549	0.31	74	176	102	7.06E+04	7.79E+04
Pt-Alumina	H_2	543	1.23	242	129.5	58	9.67E+04	1.40E+05
Pt-Ceria	SO_2	0	0.01	1	0	0	0.00E+00	0.00E+00
Pt-Ceria	H_2S	468	0.02	3	73	44	1.45E+05	1.53E+05
Pt-Ceria	H_2	0	0.99	162	0	0	0.00E+00	0.00E+00
Pt-P12	SO_2	578	0.00	2	347	192	3.54E+04	4.15E+04
Pt-P12	H_2S	540	0.19	46	185	115	6.53E+04	6.69E+04
Pt-P12	H_2	511	0.72	165	164	112	6.90E+04	6.38E+04
BaP12	SO_2	565	0.13	28	72	41	1.89E+05	2.12E+05
BaP12	H_2S	600	0.18	17	112	78	1.30E+05	1.18E+05
BaP12	H_2	591	2.06	479	134	84.5	1.05E+05	1.06E+05
FeP12	SO_2	474	0.13	16	74	46	1.45E+05	1.49E+05
FeP12	H_2S	518	0.17	25	98	59	1.22E+05	1.29E+05
FeP12	H_2	504	2.07	454	120	74.5	9.48E+04	9.71E+04
NiP12	SO_2	435	0.02	4	92	51	1.04E+05	1.20E+05
NiP12	H_2S	581	0.09	24	192.5	111.5	6.93E+04	7.66E+04
NiP12	H_2	470	1.62	268	100	59.5	1.05E+05	1.12E+05
BaPtP12	SO_2	631	0.01	3	221	114	6.71E+04	8.42E+04
BaPtP12	H_2S	590	0.32	62	127	71	1.11E+05	1.27E+05
BaPtP12	H_2	599	1.99	721	-499	88	2.42E+04	1.03E+05
FePtP12	SO_2	582.5	0.01	3	230.5	112.5	5.70E+04	7.62E+04
FePtP12	H_2S	551	0.26	45	105.5	65.5	1.23E+05	1.26E+05
FePtP12	H_2	550	1.52	274	109	62	1.18E+05	1.33E+05
NiPtP12	SO_2	536	0.01	3	322.5	161	3.46E+04	4.56E+04
NiPtP12	H_2S	541.5	0.14	36	176	96	6.92E+04	8.16E+04
NiPtP12	H_2	514	1.29	391	199.5	93.5	5.61E+04	7.82E+04
2% Ni Al	SO_2	416	0.00	1	156	87	5.56E+04	6.41E+04
2% Ni Al	H_2S	582	0.07	28	299	176.5	4.25E+04	4.62E+04
2% Ni Al	H_2	412	0.65	323	283	172.5	2.81E+04	2.95E+04
10% NiAl	SO_2	505	0.01	4	145	81	7.76E+04	8.91E+04
10% NiAl	H_2S	723	0.03	11	308	214.5	5.69E+04	5.13E+04
10% NiAl	H_2	484	2.27	0	119.5	69	9.02E+04	9.98E+04

Table 3: Summary of Matrix TPRs

4.2 Temperature-Programmed Reductions of Pure Compounds

TPRs were performed on a number of readily available sulphates and sulphides of the elements present in the autocatalyst formulation. This was for comparison with the TPRs performed on the sulphur dioxide-treated catalyst components; peaks occurring at similar temperatures to the catalyst, or with other similar characteristics (e.g. peak shape, peak order, similar molar ratios), would indicate that such species, or similar, had been formed. The reducing atmosphere was 5% hydrogen in nitrogen as in the 'standard' TPRs. The spectra were not expected to be entirely the same as those of the surface species, but it was hoped that similarities, or otherwise, in the shapes, orders or peak ratios would be informative.

The compounds were:

1. Aluminium sulphate
2. Cerium (III) sulphate
3. Cerium (IV) sulphate
4. Iron (II) sulphate
5. Iron (III) sulphate
6. Iron sulphide
7. Nickel sulphate
8. Nickel subsulphide
9. Barium sulphate

4.2.1 Aluminium Sulphate, $Al_2(SO_4)_3$

Pure aluminium sulphate, $Al_2(SO_4)_3$, provided by Aldrich, 99.99+% pure is a free-flowing white powder. It is hygroscopic, so the greatest efforts were made to ensure that it did not come into contact with ambient air. To this end, the container was opened inside a glove box[75] with a pure nitrogen atmosphere. A number of portions of the sulphate were measured out into sample vials which were then sealed with air-tight 'Nesco' film. The container was then sealed and the vials weighed to determine which contained the most appropriate mass of sulphate for the decomposition. The amount was then transferred to the reactor inside the glove box (under a nitrogen atmosphere) and the reactor sealed with 'Nesco' film until the moment of its connection to the catalyst test rig, which had already been flushed out with the 5% H_2 in N_2. As can be seen in the spectrum below, aluminium sulphate evolved sulphur dioxide in the TPR. The peak occurred at ~805°C, which is higher than any other sulphur dioxide peak for a pure compound seen in this research. In contrast to this, alumina emits its adsorbed sulphur species principally as hydrogen sulphide.

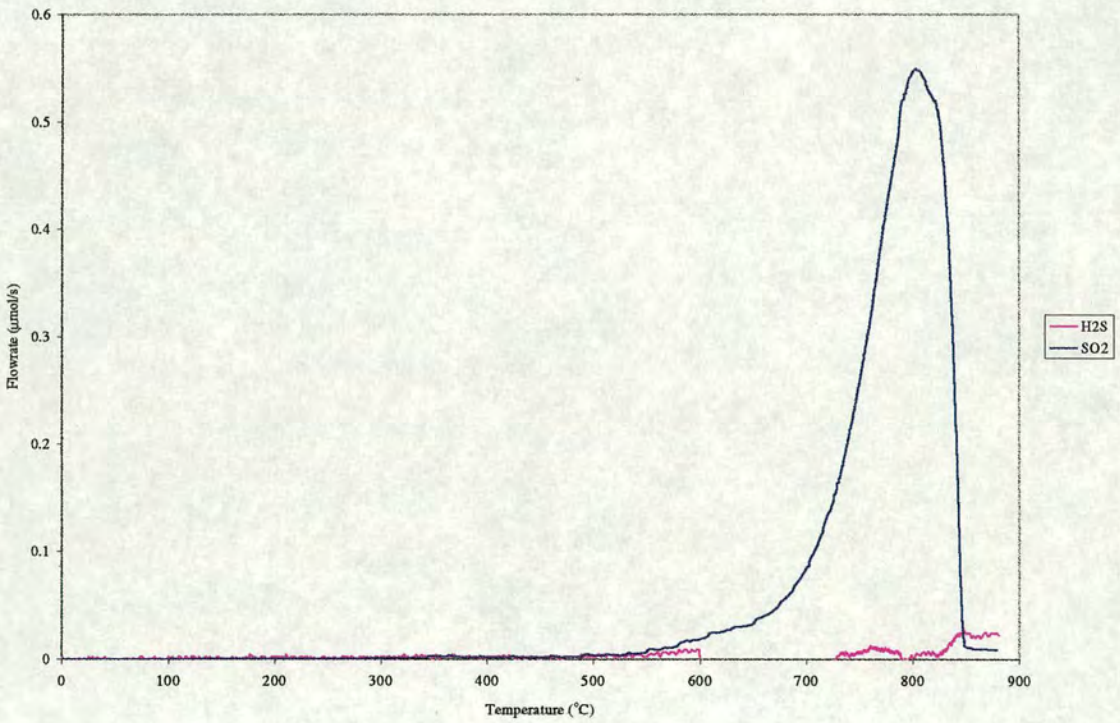

Figure 74: Aluminium Sulphate TPR

[75] See 'Materials and Methods' for a description of this glove box and its usage.

During the course of the experiment a 250 mg sample, (729 μmol) converted ~2130 μmol of hydrogen, which is close enough (within experimental error) to the calculated 2188 μmol of sulphur present to suggest that the reaction occurring was:

$$Al_2(SO_4)_3 + 3H_2 \rightarrow Al_2O_3 + 3SO_2 + 3H_2O$$

Additional evidence for the formation of alumina is the mass loss of the sample; a 250 mg sample lost 175 mg during the course of the heat treatment. This corresponds exactly with the formation of aluminium oxide (molecular mass: 102) from aluminium sulphate (342), a factor of 3.35 in both cases. The final form of the substance was a white powder, which also correlates with the formation of alumina.

Gottberg *et al.* (1990) state that aluminium sulphate decomposes at 600 °C. This may refer to the temperature at which it will decompose at constant temperature, nonetheless the results of this experiment seem to conflict with this claim.

There is a clear contrast here between the TPR of aluminium sulphate and sulphur dioxide-treated alumina. The TPR of sulphur dioxide treated alumina exhibited emission of sulphur predominantly as hydrogen sulphide rather than sulphur dioxide and this emission occurred at a much lower temperature (~650 °C).

4.2.2 *Cerium (III) Sulphate, $Ce_2(SO_4)_3$*

Cerium (III) sulphate has been cited as one of the most likely compounds to be formed as a sulphur storage medium. (Gidney (1996)). Over the course of the TPR the initially white crystalline material (supplied by Aldrich) became black. The measured mass loss over the course of the experiment was actually greater than that which would result from conversion of all the cerium sulphate into cerium (III) oxide. This was due to the difficulties of retrieving the sample from the reactor. In this case much of the product was in the form of a fine black powder, some of which may have become embedded in the sinter, or have blown through it.

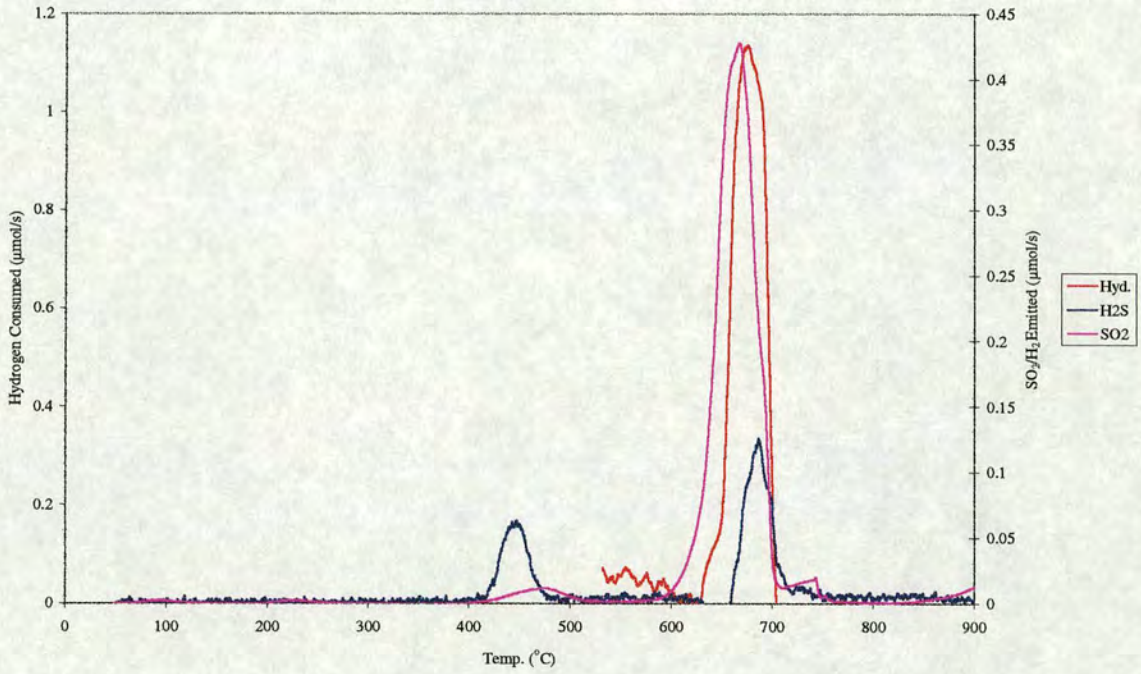

Figure 75: TPR of Cerium (III) Sulphate

The most striking feature of this TPR is the hydrogen sulphide double peak. The lower temperature peak could explain some of cerium's undoubted effect in increasing the hydrogen sulphide production by automobile catalytic converters. However, no similar peaks were ever seen in the TPRs of cerium-containing formulations, which is perhaps indication that the species decomposing in those TPRs was cerium (IV) sulphate. The two higher temperature peaks are, it will be seen in the following section, extremely similar to those occurring in the TPR of cerium (IV) sulphate. The hydrogen consumption peak corresponds very well with the sulphur dioxide peak and is approximately three times greater in size, corresponding to a reaction such as $Ce_2(SO_4)_3+3H_2 \rightarrow Ce_2O_3+3H_2O+3SO_2$. The peaks occur at 450 °C and 689 °C (hydrogen sulphide), 669 °C (sulphur dioxide) and 672 °C (hydrogen consumption).

4.2.3 Cerium (IV) Sulphate

The cerium sulphate evolved predominantly sulphur dioxide, the main peak occurring at ~680°C (see figure below). Another, smaller sulphur dioxide peak was observed, the peak maximum occurring at 380 - 390°C. This peak may correspond to a rearrangement of the compound. During the TPR, the sample underwent a colour change from its original bright yellow to a dark green, indicating reduction to cerium (III) oxide (see Weast (1982)). The hydrogen sulphide peak occurred at the higher temperature and was considerably smaller than the sulphur dioxide peak (representing 32 μmol, as opposed to the 109 μmol).

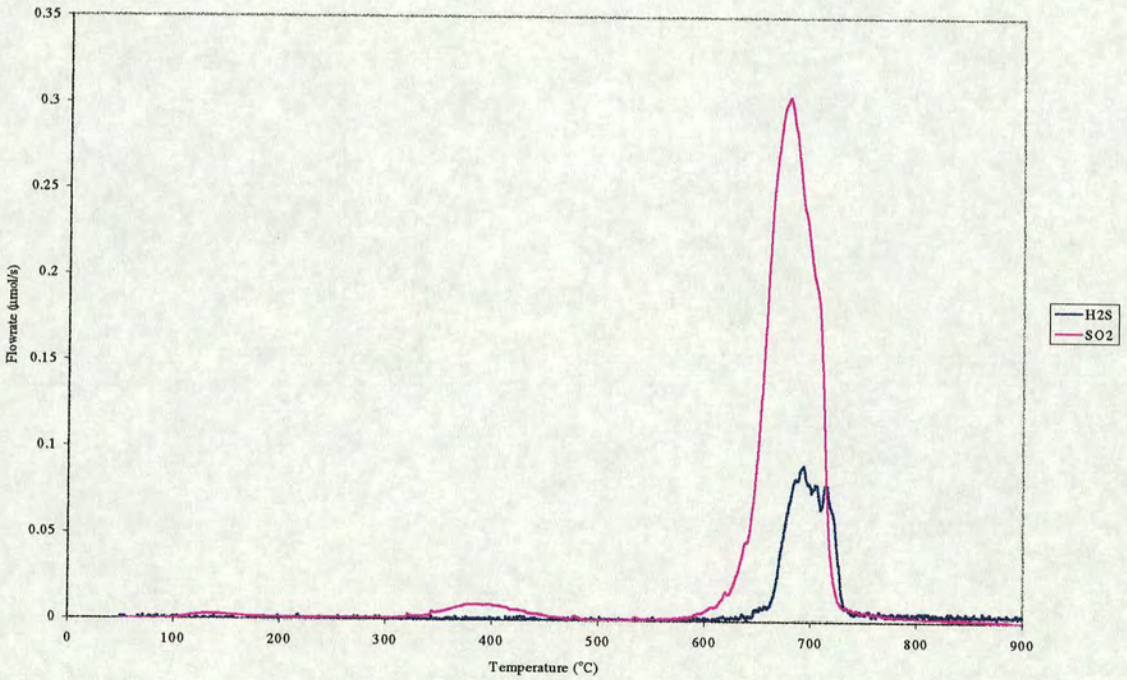

Figure 76: Cerium (IV) Sulphate TPR

4.2.4 Iron (II) Sulphate, $FeSO_4.7H_2O$

The TPR of iron (II) sulphate is shown below.

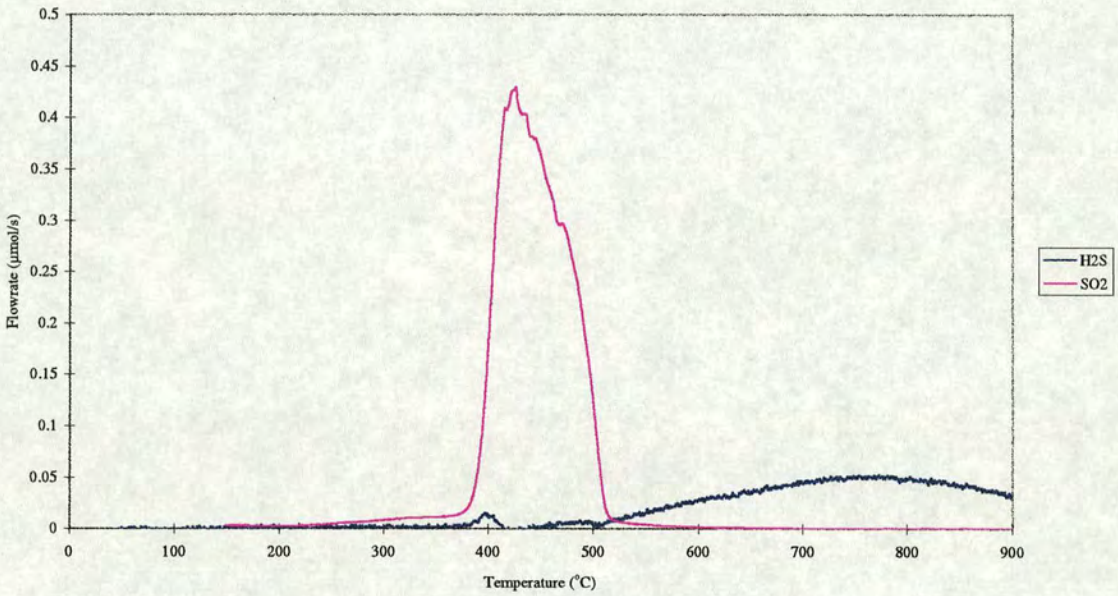

Figure 77: TPR Iron II Sulphate

The temperature at which this sulphate decomposed to sulphur dioxide was relatively low (peak maximum temperature was 426 °C). The high temperature diffuse hydrogen sulphide peak is similar to that formed by the TPR of iron sulphide (see TPR of FeS).

The low temperature of the sulphur dioxide peak has parallels with the results of experiments on the iron-doped components, particularly iron-doped P_{12}, which exhibit some of the lowest peak maximum temperatures seen in these experiments.

The 100 mg of sample used in this experiment contained 360 µmol of sulphur, approximately 218 µmol were emitted as sulphur dioxide. Of the remainder, 88 µmol were emitted as hydrogen sulphide by 900 °C, although it is obvious that the emission persisted to higher temperatures. The molar amount

of hydrogen consumed during this TPR is approximately a factor of 4 greater than the amount of sulphur dioxide evolved. It should be noted that the sample began to emit hydrogen sulphide immediately after the cessation of sulphur dioxide emission implying that the processes may be sequential.

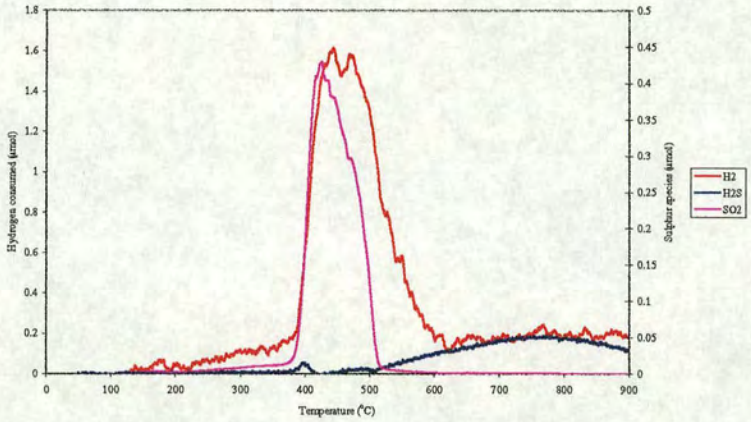

Figure 78: TPR of $FeSO_4$ showing Hydrogen Consumption

If the formation of a sulphide, such as FeS, took place, then the stoichiometry of the reaction would be thus:

$$FeSO_4 + 4H_2 \rightarrow FeS + 4H_2O$$

The FeS would decompose thus:

$$FeS+H_2 \rightarrow Fe+H_2S$$

However, this does not explain the emission of sulphur dioxide. If the sulphate decomposes directly to sulphur dioxide the reaction would proceed:

$$FeSO_4 + H_2 \rightarrow FeO + SO_2 + H_2O$$

This does not explain the factor of 4 between the hydrogen consumption and the sulphur dioxide emission.

The final weight of the sample was 25 mg indicating that it was close to full conversion to the metal (would be 20 mg). It was obvious from the unfinished hydrogen sulphide peak that the reaction was not complete at 900 °C. The final product was predominantly magnetic and metallic, whereas the initial substance was a pale green crystalline solid.

4.2.5 *Iron (III) Sulphate, $Fe_2(SO_4)_3.5H_2O$*

Iron (III) sulphate pentahydrate, supplied by Aldrich, is a pale brown crystalline solid. Its TPR results in the following spectrum.

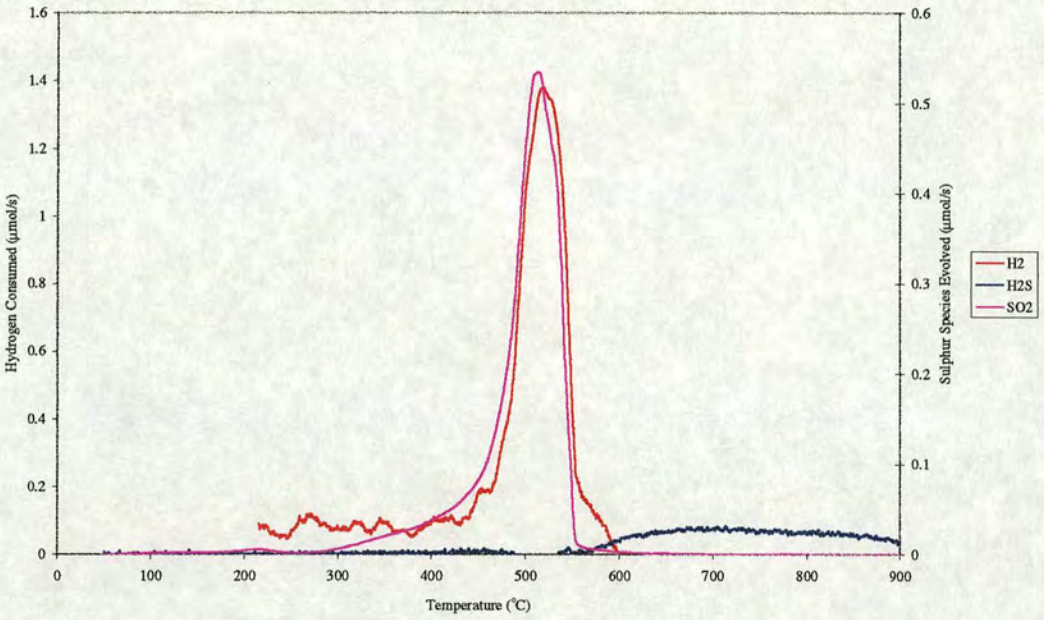

Figure 79: TPR of Iron (III) Sulphate

The TPR is similar to that of the iron (II) sulphate, in that the sulphur dioxide peak occurs first, and is much greater in size and much sharper than the higher temperature diffuse H_2S peak. The end of the sulphur dioxide peak and the beginning of the hydrogen sulphide peak are, again, coincident. The diffuse peak implies that a sulphide has been formed, which loses sulphur over a wide range of temperatures, as it has a low activation energy. The sulphate could be decomposing in various ways;

$$Fe_2(SO_4)_3 + 4H_2 \longrightarrow 2FeO + 3SO_2 + 4H_2O$$
$$Fe_2(SO_4)_3 + 10H_2 \longrightarrow 2FeS + SO_2 + 10H_2O$$
$$Fe_2(SO_4)_3 + 2H_2 \longrightarrow 2FeSO_4 + SO_2 + 2H_2O$$

H_2 is consumed and SO_2 emitted simultaneously (differing by a stoichiometric ratio of ~3), whereas H_2S emission is delayed. The sample was 120 µmol, emitting ~220 of its 360 µmol of sulphur as sulphur dioxide.

It seems that approximately a quarter of the sulphur is emitted as hydrogen sulphide. This agrees with a scheme whereby approximately a quarter of the moles of the compound decompose to the sulphide and the other 75 % decompose to the oxide, thereby consuming approximately 3 moles of hydrogen per mole of sulphur dioxide evolved, on average. The decomposition via the iron (II) sulphate seems

unlikely, as it was seen in the previous section that it decomposes with the evolution of sulphur dioxide at a lower temperature (peak ~425 °C) than iron (III) sulphate.

The final product was metallic and magnetic, indicating the formation of iron. The iron was probably formed in the following reaction:

$$FeS + H_2 \longrightarrow Fe + H_2S$$

The hydrogen consumption trace does not seem to correspond with this phenomenon, but this is probably because, due to the noise and the relatively low level of accuracy of the TCD, hydrogen consumption at this level would be difficult to distinguish.

4.2.6 Iron II Sulphide, FeS

The TPR spectrum is similar to the hydrogen sulphide peak observed in the iron sulphate TPRs, in that it is extremely broad and occurs at higher temperatures. This implied that iron sulphide-like species caused the broad, high temperature peaks in the sulphate TPRs and the 'tailing' in the TPRs of iron-doped materials.

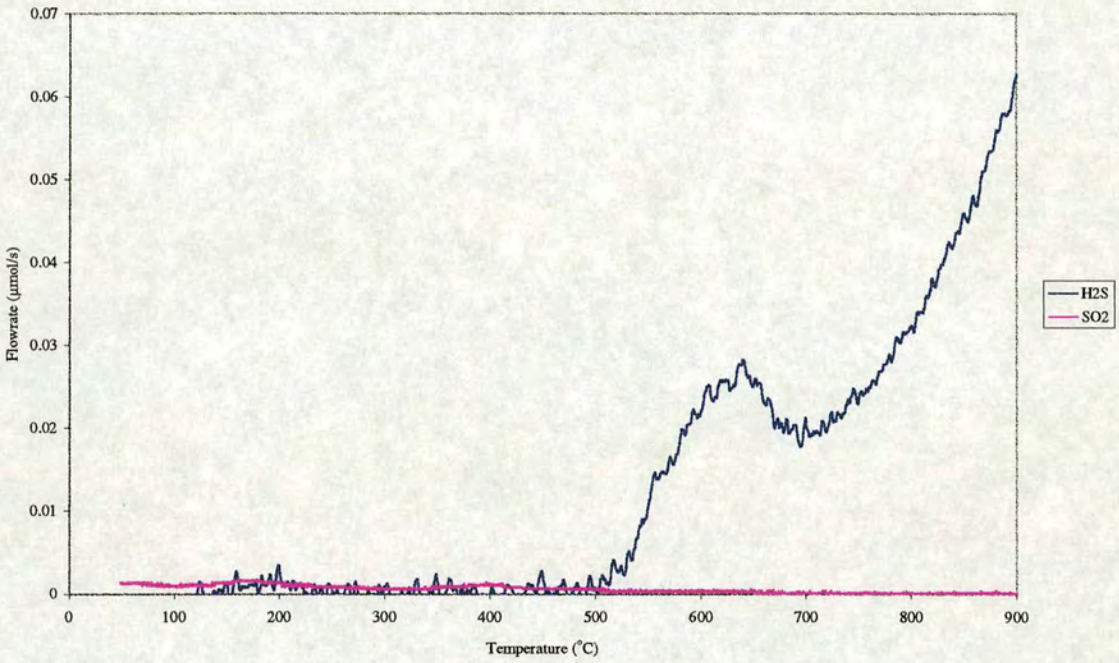

Figure 80: TPR of Iron (II) Sulphide

Clearly the decomposition of the sulphide is not complete by 900 °C; the second peak is still growing. The maximum of the first peak occurs at 642 °C. The substance, initially a dark grey, lustrous powder became more metallic during the course of the TPR. More thorough investigation of the TPR of this compound would require equipment which is able to maintain higher temperatures.

The hydrogen consumption in this experiment was impossible to distinguish from the noise of the TCD, as for the hydrogen sulphide trace of the previous TPR (Iron (III) sulphate).

4.2.7 *Nickel Sulphate, $NiSO_4.7H_2O$*

The TPR of nickel sulphate heptahydrate is remarkably similar to that of iron (III) sulphate, in that there is a sharp SO_2 peak at approximately 500°C, followed by a much more diffuse H_2S peak.

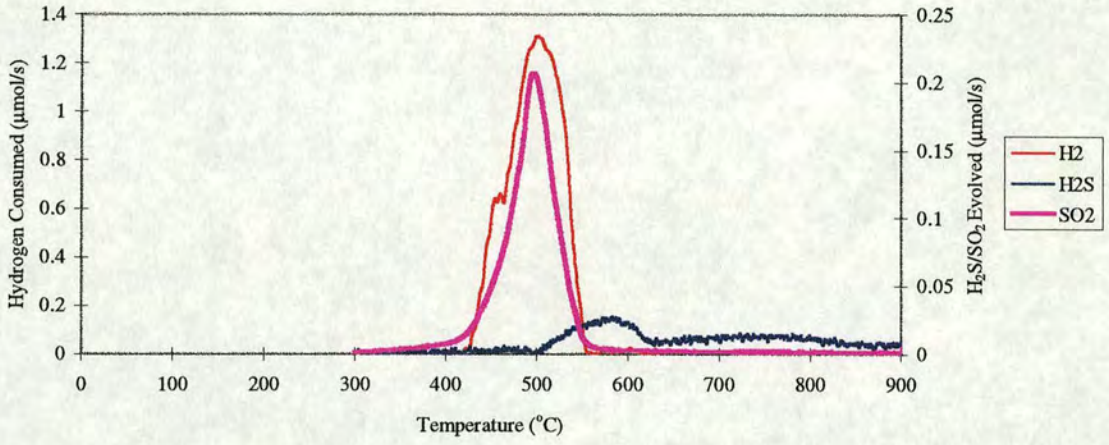

Figure 81: TPR of Nickel Sulphate

The initially blue crystalline solid becomes metallic and globular during the course of the TPR, indicating the formation of nickel. The mass loss was correct for the formation of nickel. The emission of hydrogen sulphide begins before that of sulphur dioxide ceases, unlike the iron sulphates. The hydrogen sulphide emission is, as for the iron sulphates, due to the decomposition of a nickel sulphide species. The TPR of the sulphide (following section) is remarkably similar to the hydrogen sulphide trace here, exhibiting the same two peaks. The stoichiometric ratio of the amount of SO_2 emitted in the main peak to H_2 consumed in that time is approximately 6, the peak maxima and peak shapes corresponding extremely well. The evolution of sulphur dioxide and consumption of hydrogen may well be due to reactions such as:

$$3NiSO_4 + 10H_2 \longrightarrow Ni_3S_2 + SO_2 + 10H_2O$$

$$NiSO_4 + H_2 \longrightarrow NiO + SO_2 + H_2O$$

The explanation may lie between these two reactions, as the stoichiometric ratios of hydrogen consumption to sulphur dioxide evolution lie on either side of the 6:1 ratio, at 10:1 and 1:1. The 'subsulphide' Ni_3S_2 is believed to be more likely to form than NiS (Golunski and Roth (1991)).

There was no detectable hydrogen consumption that corresponds with the hydrogen sulphide emission, which is also difficult to explain. This could indicate hydrogen storage, e.g., with the formation of a hydride[76]. The sulphides formed would decompose, thus:

$$NiS + H_2 \longrightarrow Ni + H_2S$$
$$Ni_3S_2 + 2H_2 \longrightarrow 3Ni + 2H_2S$$

[76] Nickel metal has the capability to absorb hydrogen, particularly when the metal is molten (Sidgwick (1952)).

4.2.8 *Nickel Sulphide, Ni_3S_2*

The TPR spectrum of nickel sulphide, shown below, exhibits features similar to that of the iron sulphide, in that the hydrogen sulphide peak extends to high temperature and is very broad. No sulphur dioxide peak was observed. The spectrum below is very similar to that seen in the TPR of nickel sulphate, particularly that it has two distinct regions, and to the hydrogen sulphide traces of standard TPRs of nickel doped materials.

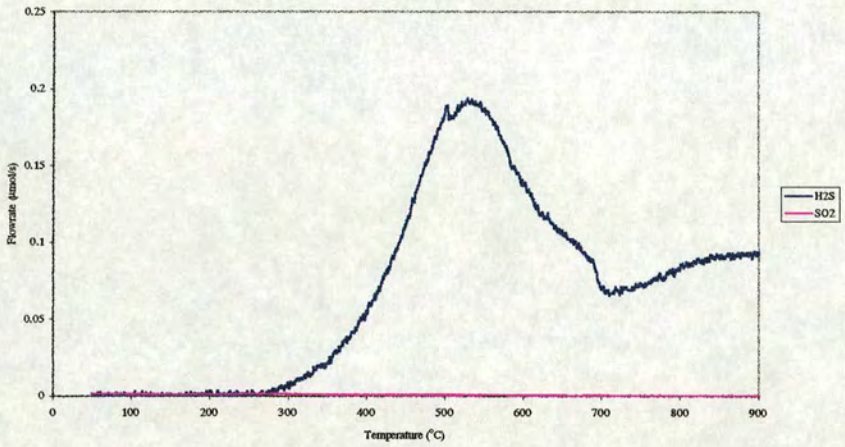

Figure 82: TPR of Nickel Sulphide

4.2.9 Barium Sulphate, $BaSO_4$

Barium sulphate's TPR exhibits no features whatsoever, indicating that no decomposition has taken place. Indeed the mass of sulphate and its appearance were unchanged by the TPR. It is known to be an extremely stable compound. The 'noise' of this spectrum is due to the extremely small scale of the y-axis.

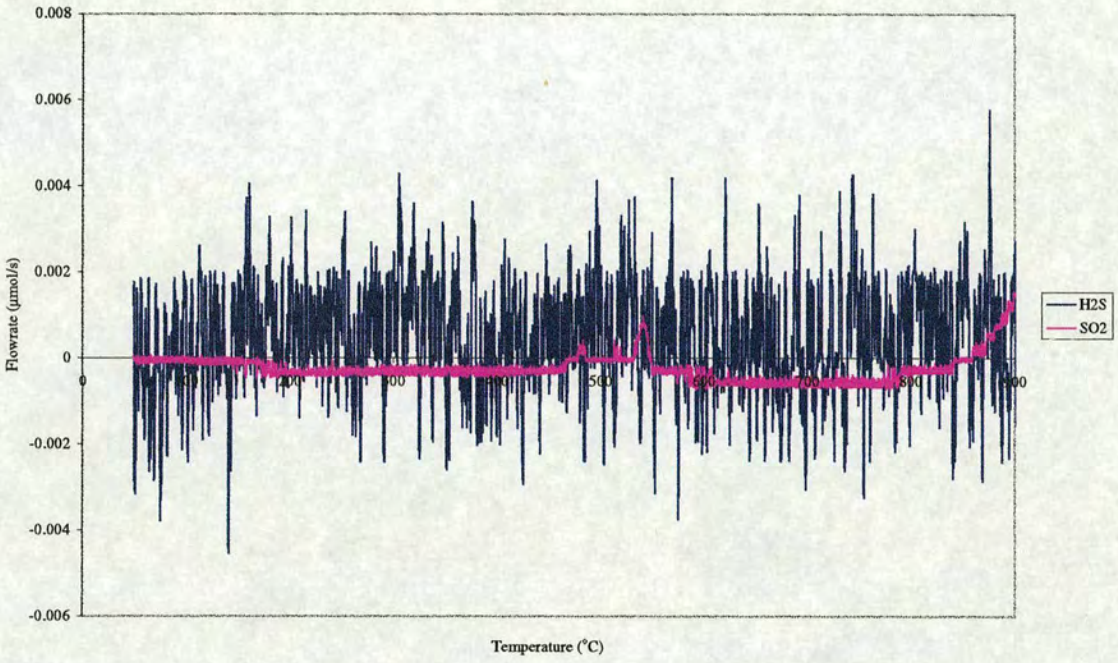

Figure 83: The Featureless TPR of Barium Sulphate

This indicates that bulk barium sulphate was not the substance formed by the reaction of sulphur dioxide with the barium-doped samples, as they exhibited peaks in the TPRs (as well as switchover activity).

4.2.10 Summary

The main points to be drawn from this study of TPRs of pure compounds are:

1. That the nickel and iron sulphates emit sulphur dioxide at around 500 °C in a relatively sharp peak.
2. The emission of hydrogen sulphide follows the sulphur dioxide peak in the TPR spectra for all the sulphates, except aluminium sulphate (which does not emit hydrogen sulphide).
3. Hydrogen consumption peaks correspond very well with all sulphur dioxide peaks.
4. Barium sulphate does not decompose in a hydrogen atmosphere up to 900 °C.
5. The TPR spectrum of cerium (IV) sulphate is very similar in form to that of sulphur dioxide treated ceria, displaced to a higher temperature by ~40 °C. This comparison contrasts with that between sulphur-dioxide treated alumina and aluminium sulphate, where the TPRs are very dissimilar.
6. Aluminium sulphate decomposes at a higher temperature (~125 °C higher) than cerium (IV) sulphate.
7. The hydrogen sulphide peaks in the TPRs of nickel and iron sulphide extend to high temperature and are very diffuse. This correlates with features of the TPRs of their respective sulphates, and those of the iron and nickel-doped washcoat materials. The hydrogen sulphide peak is more significant for the nickel compounds than for the iron compounds. This is reflected in the TPRs of the doped compounds; the 'tailing' of the TPR peak is much more pronounced for nickel-doped materials than for the iron-doped materials.

4.3 TPRs with Varying Surface Coverage (θ)

To assess the effect on the subsequent TPR of varying the dosage of sulphur dioxide and to explain the discrepancies between results obtained and those of Lundgren *et al.* (1995)[77], experiments were conducted on platinised P_{12} at 500 °C with varying dosages. The cumulative amounts emitted during the TPRs resulting from those various dosages are shown below:

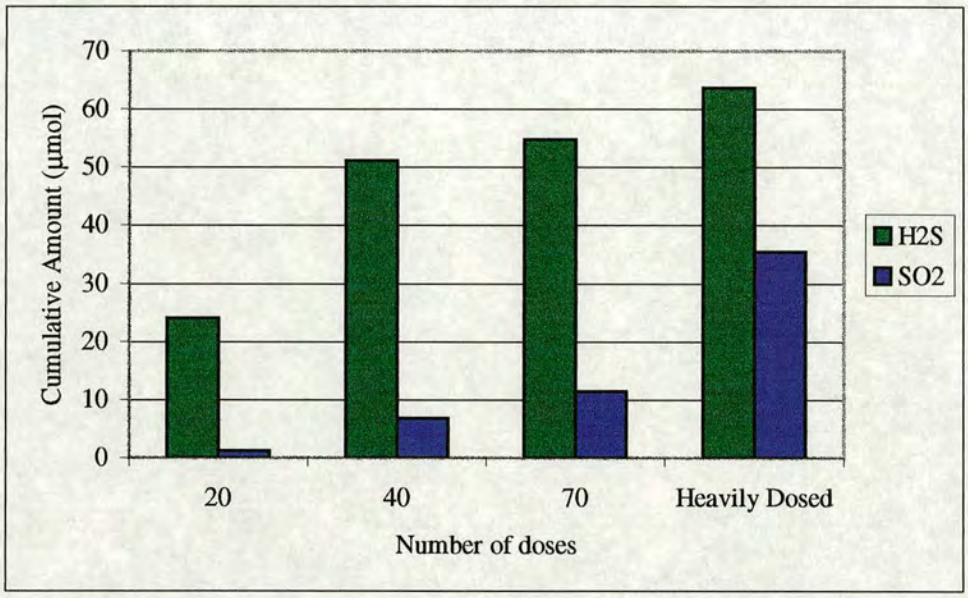

Figure 84: The Effect of Varying Sulphur Dioxide Treatment on the TPR of Platinised P_{12}

It seems that the sites responsible for hydrogen sulphide emission in the TPR are those which adsorb the sulphur dioxide first. These sites could be similar to the initial, strongly chemisorbed species seen by Chang (1978) on alumina. He also observed the formation of a second, more weakly chemisorbed set of sulphur dioxide sites, which may correspond to those which decompose to form sulphur dioxide at the lower temperature. The TPR of the most heavily sulphur dioxide-treated sample is very similar to those seen in Lundgren *et al.* (1995) resulting from sulphur dioxide adsorption on fully formulated catalysts. The 'heavy dosing' in experiment (d) was achieved by exposing the sample to a stream of sample gas (25% sulphur dioxide in nitrogen), intermittently with a dry air stream.

4.4 TPRs with Varying Linear Heating Rate (β)

To assess the effects of the linear heating rate, β, on the TPR spectrum a limited number of TPRs were conducted on platinised P_{12}.

(a) 10°C/min

(b) 25°C/min.

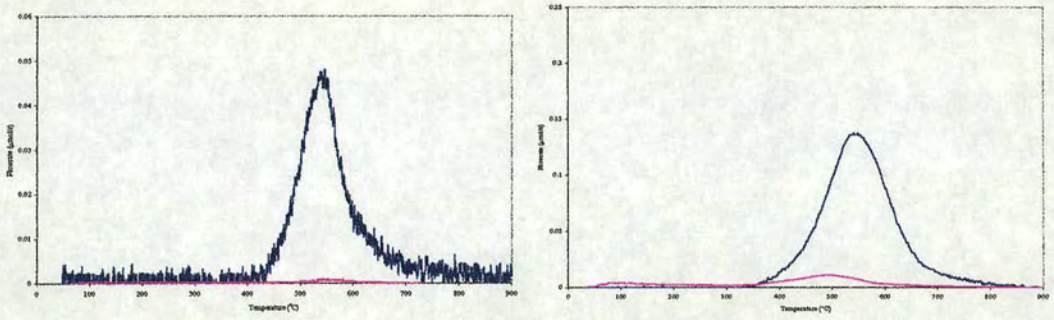

(c) 50°C/min

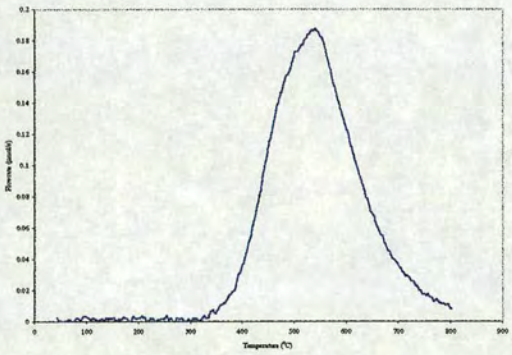

Figure 85: The Effect of Varying Heating Rate on the TPR of Platinised P12

The TPR spectra are very similar in shape and position. The peak maxima occur at the same temperature of 541 °C. Although the peak shapes are close to Gaussian, the half-widths vary. There is a clear trend of increasing breadth with increasing ramp rate; the half-widths are 84, 140 and 185 degrees.

Falconer and Schwarz (1983) state that the peak should increase in amplitude with increasing ramp rate and should take a shorter time to reach the peak maximum, and these conditions are achieved. However, they also state that the peak maximum temperature should increase and this is clearly not the

---

[77] The hydrogen TPRs of fresh, fully formulated catalysts presented in Lundgren *et al*, (1995) exhibit a much more pronounced sulphur dioxide peak. It was proposed that this was due to a greater sulphur dioxide dosage.

case. This may be due to the fact that this is not a simple desorption, but a process involving desorption and reaction.

4.5 Electron Microscopy and Related Techniques

4.5.1 SEM

The results of SEM analysis were disappointing. It seemed that the desired ability to observe the surface features produced by sulphur dioxide traetment were beyond the capability of the technique. Nonetheless, a number of SEM micrographs are included in the appendices to give some idea of the general topography of the oxide samples used.

4.5.2 Wavelength Dispersive Spectroscopy, WDS

Wavelength dispersive spectroscopy was performed on a number of heavily 'sulphated' samples at Johnson Matthey Technology Centre, Royston, Herts. The technique showed that particles heavily treated with sulphur dioxide exhibited a uniform distribution of sulphur atoms, i.e., the apparent dispersion of the sulphur mapped on to the topography of the catalyst chips. The apparent dispersion was the same as other species, such as oxygen, confirming that uniform distribution is indeed indicated by the apparent dispersion following the topography of the sample.

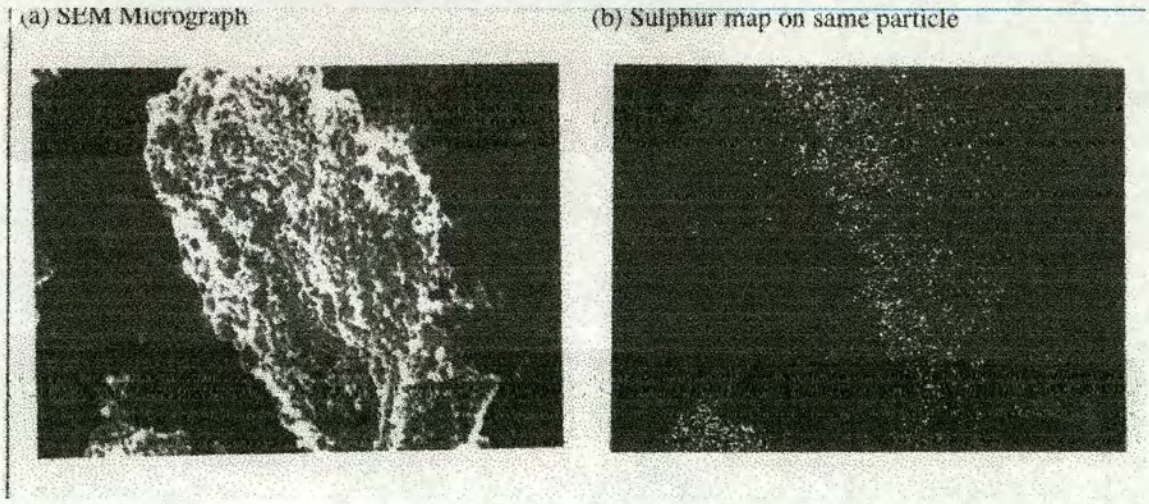

Figure 86: Sulphur Map on a Particle of Heavily Sulphur Dioxide Treated Platinised Alumina

A uniform distribution is to be desired, as it shows that the sulphur-adsorbing components were widely dispersed on the particle surface and that there was an equality of flow around the particle in the bed.

In image (a) on the following page there is a clear abrasion on the surface. In (b), the sulphur map of this chip, it can be seen that this abrasion corresponds to an area where sulphur is absent. This illustrates the fact that the adsorption of sulphur dioxide is predominantly a surface phenomenon.

(a)

(b)

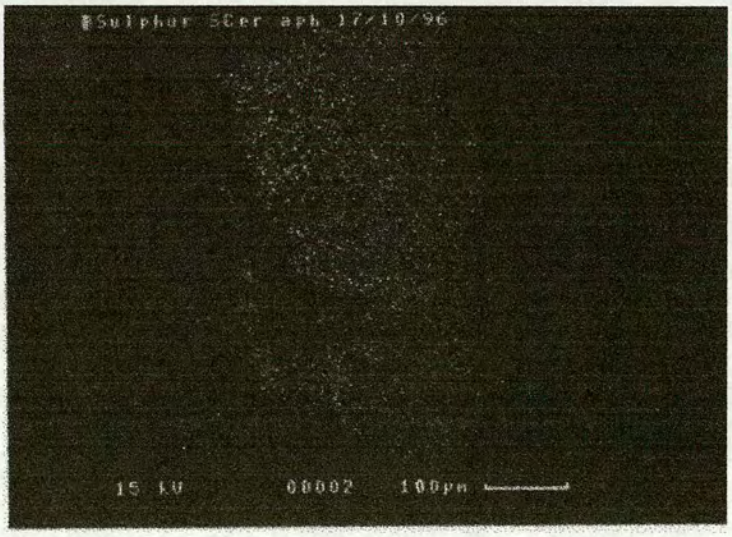

Figure 87: WDS Images

4.5.3 Backscattered electron imaging, BEI

Backscattered electron imaging generates a map of the atomic number of the sample in question (see 'Literature Survey'). In conjunction with WDS, it is conceivable that the sulphur adsorbed might be mapped onto the BEI image and a correlation between cerium or alumina found. In practice this proved too difficult.

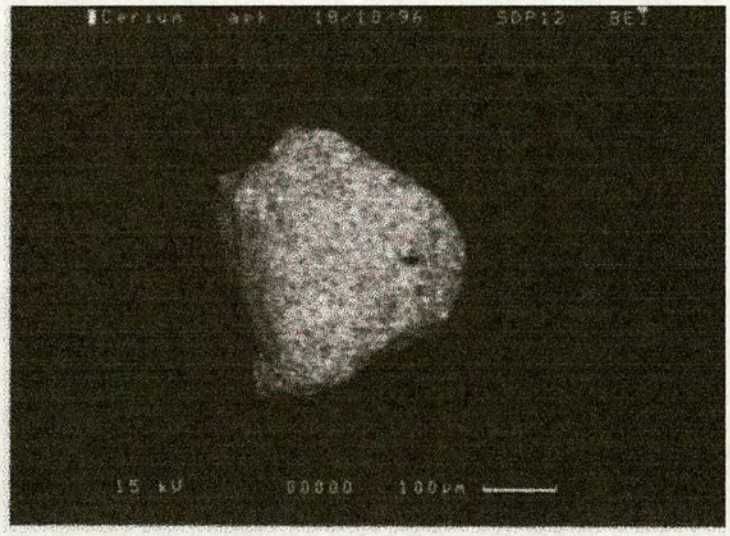

Figure 88: BEI Image

The darker areas of this chip represent cerium and the lighter areas alumina (the shape of the chip also has an influence).

4.6 DRIFTS

4.6.1 Preliminary Experiments

Experiments were conducted to test out the design of the cells used.

1. For commissioning purposes, sodium dithionate (NaS_2O_4) was decomposed under a nitrogen atmosphere. Sodium dithionate was chosen as it exhibited distinct S-O frequencies and because it decomposes at a relatively low temperature (190 °C, Sidgwick (1952)) which would cause fewer problems of temperature attainment and maintenance, and of temperature gradients within the sample[78]. It exhibits an obvious change in the infrared spectrum upon decomposition, as well as producing sulphur dioxide, which is readily seen in the gas spectrum[79]. In the experiments conducted the dithionate was seen to be totally decomposed by 210 °C, although the first changes in the DRIFTS spectrum were seen at ~200 °C. The discrepancy may well be due to the temperature gradient effects identified in the cell design (see 'Materials and Methods').
2. Sulphate-contaminated zinc hydroxide was heated under a nitrogen atmosphere. Zinc compounds were chosen because a great deal of research has been conducted in this laboratory on their infrared spectra and, therefore, the sulphate's frequencies could easily be distinguished.

4.6.2 Open Cup Experiments

A number of fresh and heavily sulphur dioxide-treated samples were analysed in the open cup (see 'Materials and Methods'). Samples of ceria, alumina and P_{12} and their platinised analogues were analysed.

The fresh samples were used as backgrounds to the Kubelka Munk spectra of the sulphur dioxide treated samples, but sulphur-containing species were never identified unambiguously. The fresh samples may not have been good backgrounds for these samples. It was decided that much better

---

[78] The difference between the temperature at the base and the surface is seen to increase with increasing temperature.

[79] This experiment incorporated a gas cell immediately after the DRIFTS cell. The infrared beam could be diverted through this cell rather than the DRIFTS by use of a system of mirrors that could be slid into place at any time. The experiment was a test of this system also.

results would be obtained by conducting *in situ* experiments using the spectrum of the sample immediately before dosing as the background.

4.6.3 In Situ DRIFTS Analysis

After the stages of development described in 'Materials and Methods', a DRIFTS environmental cell was made which was capable of reliably reaching and maintaining temperatures of greater than 500 °C[80]. It was the intention of this part of the research to identify the sulphur species formed on the catalyst surfaces by dosing the substances at ~500 °C. Switchover experiments were also performed. Due to the design features of the cell which were necessary to reach these high temperatures, the experiments had to be modified somewhat from those which had been performed on the 'catalyst test apparatus':

- The flow was considerably lower, at 100 cc/min. (higher flows would cause the sample surface to be disturbed).
- The cell design was not gas-tight, so it was impossible to monitor the evolved gas species quantitatively (the gas in was monitored though).
- The sample could not be pretreated in hydrogen as in experiments on the catalyst test apparatus, as the DRIFTS apparatus could not reach temperatures substantially higher than those at which dosing in air would be performed.

4.6.3.1 The DRIFTS Cell

The final incarnation of the DRIFTS cell has proved to be a great success for work at temperatures up to approximately 530 °C. This is an important result in itself. Unlike other high temperature cell designs, this cell has an extremely low gas space above it, so that the chances of detecting gaseous species are greatly decreased, it has a better flow pattern across the bed, with little chance of stagnation and, most importantly, it has some degree of pre-heating of the incoming gas, which is a design consideration which is often ignored. The extreme shallowness of the bed (or washcoat) is also an advantage as it lessens the chances of errors in temperature measurement.

---

[80] The maximum temperature achieved thus far is ~670 °C, although this is some way above a reliable working temperature.

4.6.3.2 In Situ Dosing Experiments

During dosing of alumina and platinised alumina with sulphur dioxide in air (replicating the conditions of the dosing stages of switchover and TPR experiments on the catalyst test apparatus), a broad absorbance, centred around 1350 cm^{-1}, was observed. This absorbance has been attributed to sulphate species.

The same experiments on ceria yielded two absorbances, at 1200 cm^{-1} and 1400-1340 cm^{-1}, which correlated extremely well with those reported by Waqif *et al.* (1997). These two absorbances are attributed by Waqif *et al.* to bulk and surface sulphates, respectively.

Experiments on platinised and unplatinised P_{12} have, as yet, yielded no *definite* sulphate absorbances, although work in this area is ongoing as part of a further research project (see 5.12 "proposals for Further Work").

Some of the spectra were problematic, as regions of the spectra were 'blacked out', alumina below 1000 cm^{-1} (as reported by Chang (1978)) and ceria below 800 cm^{-1} and at a region around 3300 cm^{-1}.

4.7 Operation of the 'Catalyst Test Rig' with Gas IR Analysis

The principal reason for operation of the catalyst test apparatus with on-line infrared analysis was to determine whether sulphur trioxide was emitted. The technique proved to be useful for a number of other reasons (see following section). The first task was to determine whether sulphur dioxide could be detected at the concentrations required. Nakamoto (1986) states that sulphur dioxide exhibits its three strongest peaks in the 1000-4000 cm^{-1} region as follows:

Vibration[81]	Frequency	Relative Intensity
ν_3	1361	1000
ν_1	1151	565
$\nu_1+\nu_3$	2500	20

Figure 89: IR Absorptions of Sulphur Dioxide

These peaks can be clearly seen in the following spectrum. This spectrum is from the calibration of the gas cell and therefore represents pure sulphur dioxide[82].

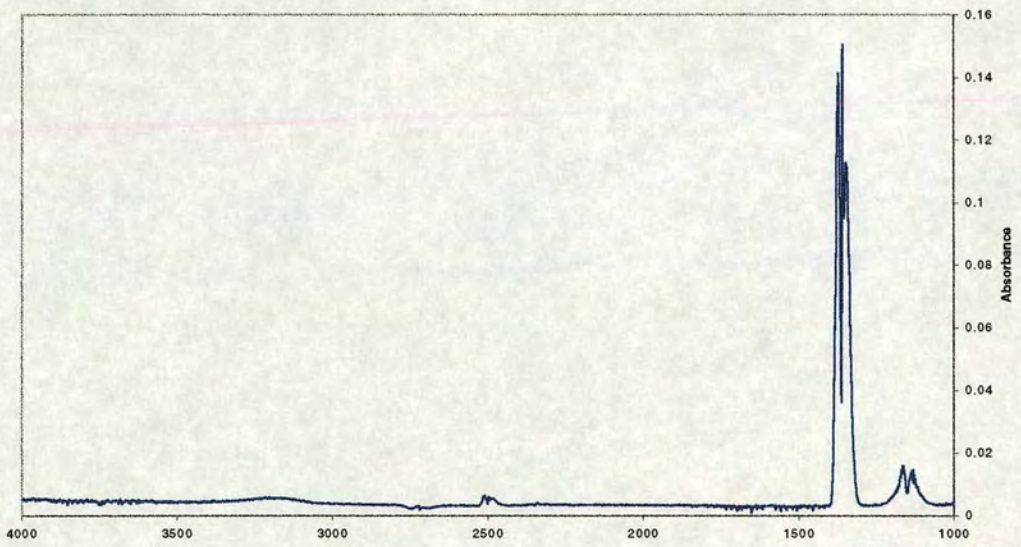

Figure 90: IR Spectrum of Sulphur Dioxide achieved using the gas cell

---

[81] These vibrations are described in the Literature Survey.
[82] The procedure involves complete evacuation of the system prior to input of sulphur dioxide.

4.7.1 Calibration for Sulphur Dioxide

To assess the feasibility of sulphur dioxide measurement using the gas cell described in 'Materials and Methods', a calibration was performed. The calibration should, theoretically, be linear, as the absorbance is proportional to the concentration. There are a number of reasons why this may be difficult to achieve in practice, such as the increasing significance of noise in the system as the concentration is decreased.

The calibration involved putting known amounts of sulphur dioxide at carefully measured pressures into the calibration apparatus described in 'Materials and Methods'. The correlation included data from a number of different fillings of the measured volume on different days. The results of the calibration showed that a good linear fit through the origin could be achieved. The linear fit was assessed for all three of the frequencies given above[83]. From the results, it was decided to use the ν_3 frequency for calibration as it gave the most reliable linear fit in the region of interest (>1000 ppm). The peaks were integrated using macros written for the Win-IR software. The calibration for peak heights was also calculated and this generated results of a similar linearity as those for peak areas.

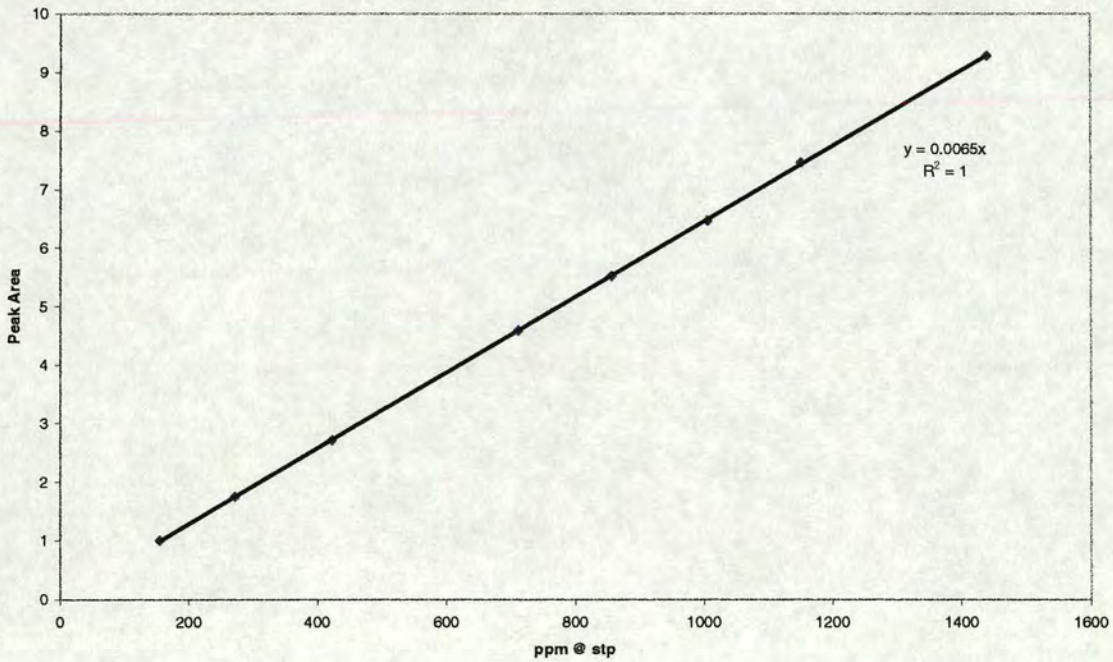

Figure 91: Calibration for Sulphur Dioxide v3 Peak Area[84]

[83] Integration limits: ν_1 1251.95 – 1046.51, ν_3 1426.53 – 1282.82, $\nu_1 + \nu_3$ 2554.06 – 2426.74

[84] The lower limit of this correlation is determined by the resolution of the pressure transducer.

The ν_1 peak was also calibrated and gave a very good linear fit, but it was observed in experiments that it became very difficult to discern at lower levels, as it was more diffuse than the ν_3 peak. Calibration by the $\nu_1 + \nu_3$ frequency became unreliable at ~2000 ppm

4.7.2 Time Resolved Experiments

It had to be ascertained whether time-resolved experiments were possible with the infrared spectrometer. To this end, standard pulses were passed through the gas infrared cell. The following spectra show a pulse of sulphur dioxide passing through the gas cell:

A. Growth of sulphur dioxide peak

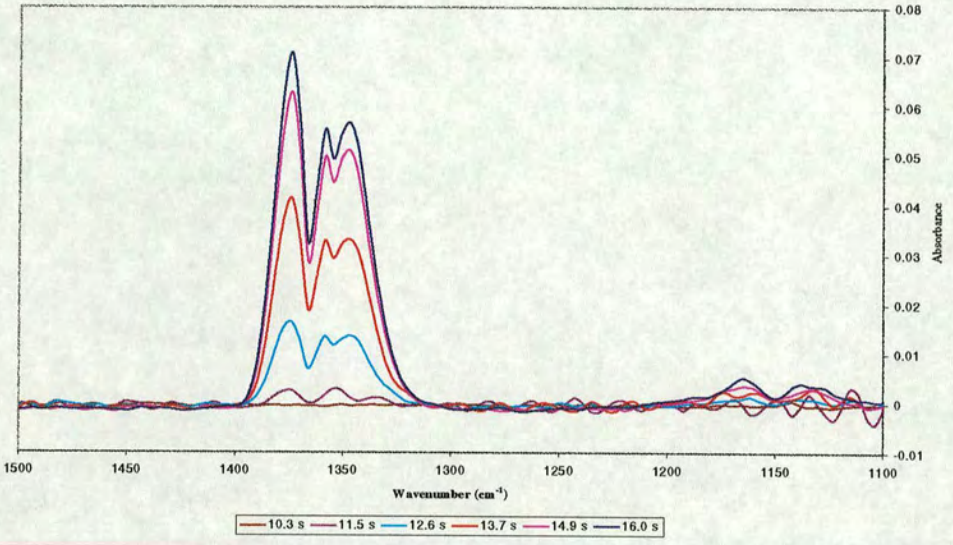

B. Peak diminishing.

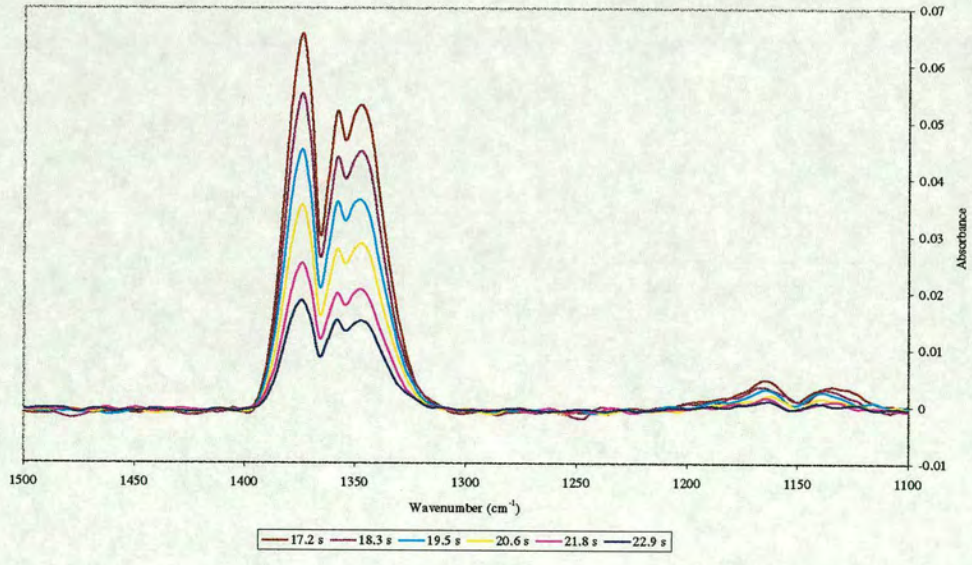

C. Integrated peak

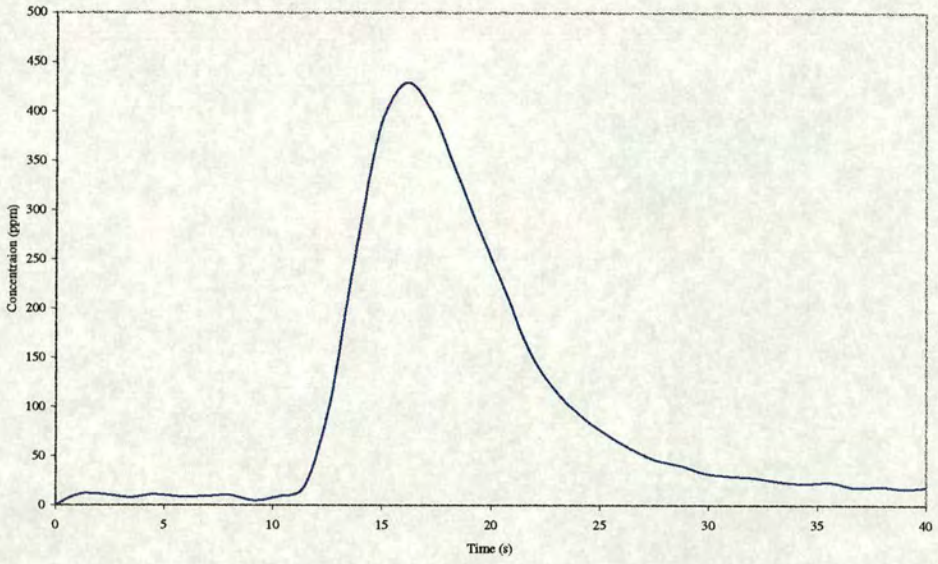

Figure 92: Standard Pulse of Sulphur Dioxide passing through the Gas IR cell[85]

The pulse is seen very clearly, with a degree of time resolution (~every second) comparable to that of the data logging used on the P.C. in the catalyst test rig. The peak shown in C is the result of integrating the ν_3 peak and multiplying by the coefficient determined in the calibration. The area of this peak, differed from that detected in the sulphur dioxide meter by ~5%.

4.7.3 Results

A set of experiments involving switchovers at 400 °C, 500 °C, 600 °C and 700 °C and a standard TPR was conducted on a number of samples[86]. A number of experimental phenomena were observable in the gas infrared spectrum:

- The emission of carbon monoxide during certain pretreatments.
- The creation of water during switchovers, enabling the extent of its artefact on the sulphur dioxide meter to be measured more accurately during this period.
- Sulphur dioxide was observed both as the remainder of a pulse during the dosing portion of an experiment and as a product of switchover and TPR runs.

---

[85] Flowrate 800 cc/min.

The important results of these experiments were:

1. No evidence of the presence of sulphur trioxide was seen in any of these runs. This is in agreement with the findings of other researchers, e.g., Lox *et al.* (1989).
2. The degree to which the water produced artefacts in the sulphur dioxide concentration was quantified, and shown to be relatively insignificant
3. The hydrogen consumption was shown to correlate with the production of water, as expected.
4. The technique of using infrared spectrum 'real-time' monitoring of the outflows of these experiments was shown to be useful and accurate.
5. An unknown species was emitted by nickel-doped platinised P_{12} at ~880 °C in its TPR. This species exhibited two peaks of similar intensity, a triplet centred at 1186 cm^{-1}, and a doublet centred at 1337 cm^{-1}. The two peaks were due to the same species, as they appeared and disappeared simultaneously. The vibrations are in the correct region for some form of SO vibration, and, indeed, overlap with the sulphur dioxide photometers detection frequency. The most likely explanation is some form of SO_2XY species. Possibilities (based on the frequencies of absorption) include sulfonate esters, sulfonyl chlorides and sulfonamides[87]. A search for frequencies due to various sulphur oxyacids proved fruitless. It should be pointed out that this effect was relatively minor and would affect the sulphur mass balances very little.

The unknown species seems unlikely to be a sulfonamide, as there would be corresponding absorptions at 3335 and 1615 cm^{-1}, which are not in evidence. The formation of the other species is difficult to envisage, as there appear to be no sources for the chlorine and the carbon, for the sulfonyl chlorides and sulfonate esters, respectively.

---

[86] P_{12}, platinised P_{12} and nickel-doped platinised P_{12}.
[87] These species all exhibit absorptions at 1175 cm^{-1} and 1335 cm^{-1} according to the Aldrich Library of IR Spectra.

4.8 Characterisation

4.8.1 Surface Area Analysis

Surface area analysis was performed on a number of samples at Johnson Matthey technology centre Royston, Herts. and in the University of Edinburgh Department of Chemistry.[88] To summarise the results:

	BET Surface Area (m^2/g)	
	Fresh	Sulphur Dioxide Treated
Alumina	168.9	143.7
Ceria	114.6	86.3
P12	137.6	107.6
Pt-Alumina	178.0	154.0
Pt-Ceria	2.9	2.9
Pt-P12	116.9	61.9
Ni P12	118.6	
Ba P12	116.7	
Fe P12	117.6	
Ni Pt P12	115.4	
Ba Pt P12	113.0	
Fe Pt P12	115.2	

Table 4: Surface Areas of Fresh and Sulphated Samples

[88] With help from Ron Brown.

Heavy sulphur dioxide treatment decreases the BET surface area, the greatest decrease occurring for platinised P_{12}. The surface area of platinised ceria is markedly lower than all other formulations. The surface areas of the ceria sample before and after treatment agree very well with the values given by Waqif *et al.* (1997), of 115 m^2/g and 80 m^2/g, their samples also originating from Rhone-Poulenc. The surface area of the fresh samples remained the same during pretreatment. The pretreated surface area is the most important value, as it is in this state that the samples were exposed to the sulphur dioxide.

4.8.2 XRPD Analysis

XRPD was performed on freshly prepared and heavily sulphated samples of platinised and unplatinised alumina, ceria and P_{12}. The powder photographs produced (see appendices) demonstrated that the process of platinisation, had not changed the phases within the compound, even if, as in the case of ceria, it had significantly altered the surface area; the photographs of ceria, alumina and P_{12} were indistinguishable from the powder photographs of their platinised counterparts. The diffractograms of ceria and γ-alumina correlated extremely well with those of ceria[89] and γ-alumina, respectively, in the JCPDS database. The diffractogram of P_{12} correlated with a mixture of these two.

As expected, XRPDs of sulphated samples did not yield any peaks that could be assigned to any phases containing sulphur. This was expected, because it was believed that there was not enough sulphur present to be detected by this technique, i.e., that the sulphur species did not form a distinct phase.

There were some differences between 'fresh' and 'sulphated' samples. The question was whether these differences were actually due to the sulphur dioxide treatment or some other part of the process, particularly the extreme conditions of the pretreatment. A search of the database revealed no sulphur compounds which could account for the differences between the compounds, so the likelihood is that they are due to changes in the structure of the washcoat.

The XRPDs of the sulphated ceria samples differ slightly from those of unsulphated ceria, but still correspond very well to the ceria diffractogram in the database. The main differences were a much

---

[89] "Cerianite", CeO_2

more distinct peak at ~67° (which does not correlate with the database ceria diffractogram) and a new peak at ~46°. These differences could not be attributed with any degree of certainty to any sulphur-containing compound or, indeed, any other likely species.

The sulphated alumina sample XRPDs had no significant differences from their unsulphated counterparts, indicating that the sulphation and the heat treatments have no effect on the bulk crystal structure of γ-alumina.

The most substantial differences occurred between the XRPDs of the P_{12} samples and their sulphated counterparts. The comparison of P_{12} and its sulphur dioxide treated analogue shows that there are entirely new peaks at 23.5°, 41.5° and 60° and that some of the peaks have changed in size. The same features were seen in the comparison of the platinised P_{12} and its sulphur dioxide treated analogue, except that the new peaks were much more pronounced and new peaks again were in evidence at 54.5°, 70.5°, 80.5° and 85°. These new peaks can be discerned in the XRPD of the sulphated P_{12}, but are not significant features. The peaks could not be matched up to sulphur-containing species, but there was a strong correlation between the new peaks and the XRPD of cerium aluminium oxide[90] ($CeAlO_3$). The XRPD of this species correlates with all the new peaks above and with the greatly increased sizes of others, all other peaks in the diffractograms correlate with the original alumina or ceria peaks. This implies that the heating and reduction of these compounds has caused them to interact to form a new crystal phase and that this interaction is facilitated by the presence of platinum. This may explain the particularly large decrease in the surface area of platinised P_{12} upon use.

---

[90] Also known as aluminium cerium oxide

5. Discussion

5.1 Simulating the Hydrogen Sulphide Storage-Release Mechanism

The first conclusion to draw from the results of this research is that a simplified system, such as the catalyst test apparatus, can be used to simulate the storage and release of sulphur species on automobile catalytic converter washcoat components. This is a validation of the design of the apparatus and experiments. Also, this research has shown that hydrogen sulphide 'spikes' are produced by certain components by the simple expedient of changing the atmosphere to a reducing gas, after exposure to sulphur dioxide during oxidising conditions.

In all the systems investigated in the course of this research, the phenomena observed have been seen to agree with observed fact;

- Switchover 'spikes' have been observed in the expected temperature range.
- Dopants which are used in practice to attenuate hydrogen sulphide emissions have been observed to have the anticipated effect. This is not a trivial achievement; other researchers (Yamada *et al.* (1990) and Harkonen *et al.* (1990)) have been unable to replicate the proven hydrogen sulphide attenuating effects of nickel or iron additives in the laboratory.

5.2 Temperature of Activity

The storage-release experiments conducted give an idea of the temperatures required for hydrogen sulphide switchover peaks to be significant. In most cases the temperature of activity is seen to correlate with the TPR peaks of the standard TPR. There are no instances of switchover peaks at a temperature below that at which significant emissions are seen in the standard TPR for that component. However, the TPR does not necessarily predict which gas will be desorbed in the switchover. This is due to the fact that the conditions during a TPR differ from those occurring in the switchover; the most important factor is likely to be the availability of oxygen, which will be considerably greater in the switchover than the standard TPR.

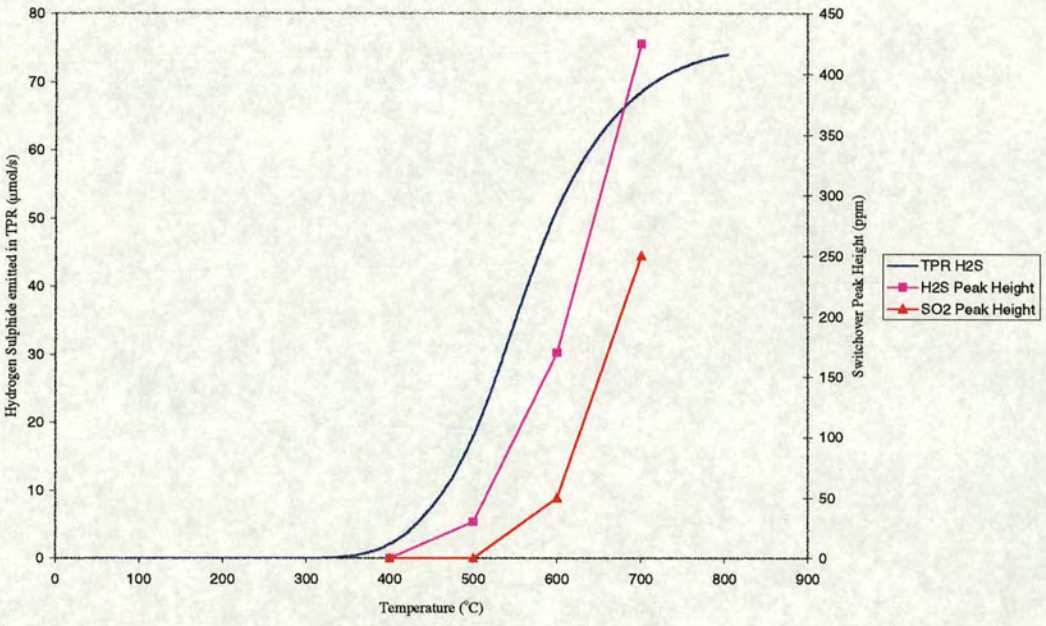

Figure 93: Comparison of TPR Cumulative Peak and Switchover Peak Temperatures for Platinised Alumina

Nickel-doped P_{12} emits the sulphur in the TPR solely as hydrogen sulphide, whereas large sulphur dioxide emissions are seen in the switchovers. In the TPR there is a large consumption of hydrogen prior to the emission of hydrogen sulphide. This hydrogen consumption does not correspond to a sulphur dioxide emission. This may represent the consumption of much of the available, stored oxygen[91] (to form water), leaving the reduced sulphur unable to be emitted as sulphur dioxide, due to the lack of available oxygen.

[91] Some of it in the form of nickel sulphate, being reduced to the sulphide.

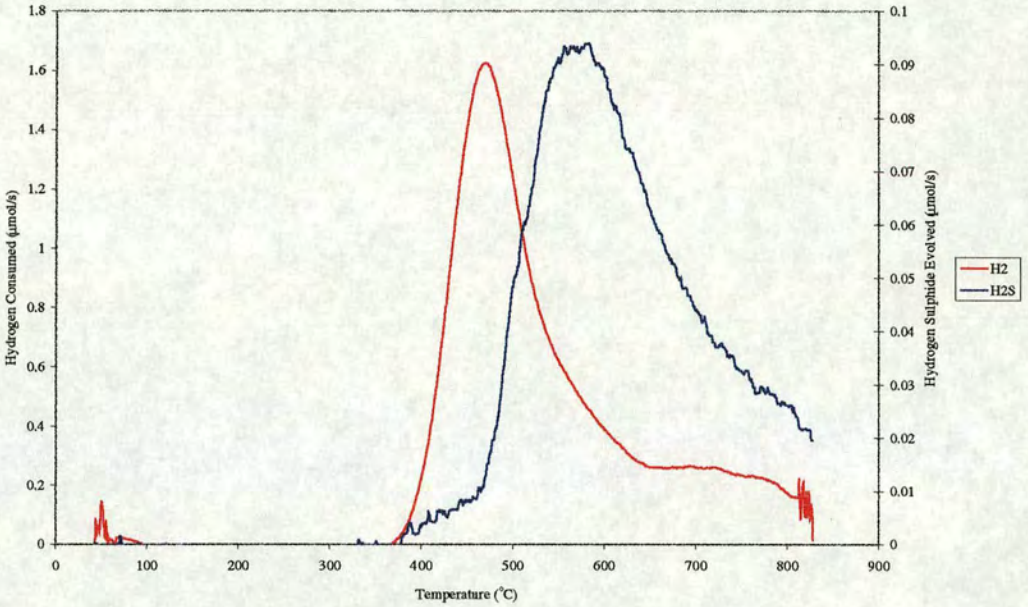

Figure 94: Nickel doped P_{12} TPR showing Hydrogen Consumed

'Conventional wisdom' has it that temperatures of greater than 500°C are required for hydrogen sulphide spikes (e.g., Gidney (1996)). This correlates well with the temperatures of activity seen in this system.

Sulphur dioxide storage-release emissions were observed to occur at lower temperatures than hydrogen sulphide emissions. This agrees with the temperatures at which their respective peaks occurred in standard TPRs; sulphur dioxide peaks *always* occurred at lower temperature than hydrogen sulphide peaks. These two desorptions may represent different sites; a higher energy, more stable site leading to desorption as hydrogen sulphide and a lower energy site leading to sulphur dioxide desorption. The hydrogen sulphide site has been observed to 'fill up' first during dosing (see section 4.3). These different sites have been observed before in, e.g., Lundgren *et al.* (1991).

5.3 The Co-oxidation of Carbon Dioxide with Sulphur Dioxide

Carbon dioxide is present in the air supply used during the sulphur dioxide storage stage of experiments. It was observed that carbon dioxide concentration remained constant during all sulphur dioxide dosing runs, indicating that very little[92], if any carbon dioxide, was adsorbed. Further evidence that carbon dioxide was not adsorbed is the absence of significant carbon dioxide peaks in standard TPRs or post-switchover TPRs. No emission of CO was observed in any runs, nor of COS in any of the runs performed with infrared gas analysis.

Hedges and Yeh (1992) report that the rate at which sulphur dioxide is adsorbed by a ceria/alumina sorbent is unaffected by the carbon dioxide concentration in the range 0 – 15 %. This agrees with the findings of this work, in that, it is an indication that carbon dioxide has no effect on the adsorption of sulphur dioxide, which it would be likely to were it adsorbed.

Further research is currently underway to look into the co-oxidation of carbon dioxide and sulphur dioxide, at these temperatures (~500 °C) and at lower temperatures, with a range of different oxides.

5.4 Combining Alumina and Ceria

It is important to know whether the effect of adding ceria to alumina is purely additive, i.e., whether it can be regarded as a pure mixture, with a pure mixture of its ingredients' properties, or whether the mixture behaves more like one of its components than the other. Diwell *et al.* (1987) postulate that the alumina stabilises the surface area of the ceria, thereby retarding the decomposition of cerium (III) sulphate. If this were the case, then higher temperatures would be required for the same switchover peak from P_{12} than ceria, and higher temperature peak maxima would be observed in the TPR. In these experiments it has been observed that the peak maximum temperatures of P_{12}'s peaks are actually slightly lower than those of ceria.

---

[92] It is possible that undetectable (below the meter's resolution) amounts were adsorbed continuously, which could add up to a significant amount. Switchovers conducted in DRIFTS equipment at 500 °C have shown a peak at 2000 cm^{-1} which *may* be platinum carbonyl during switchover.

Ceria adsorbs considerably more sulphur dioxide than alumina. In a standard TPR ceria adsorbs ~70% of the sulphur dioxide it is exposed to, whereas alumina adsorbs ~15 %. In comparison P_{12} adsorbs over 80%. It seems as if mixing the two has increased the capability for sulphur dioxide sorption.

The TPR of P_{12} has features of both alumina's and ceria's TPRs. The sharpness of the peaks is similar to that of ceria, but the relative sizes of the hydrogen sulphide peak to the sulphur dioxide peak is slightly greater than that for ceria, indicating (as the decreased temperature and the shoulder at lower temperature do) that the characteristics of P_{12} are not entirely due to ceria. It is clear from the charts below that P_{12}'s TPR characteristics are predominantly due to the influence of ceria.

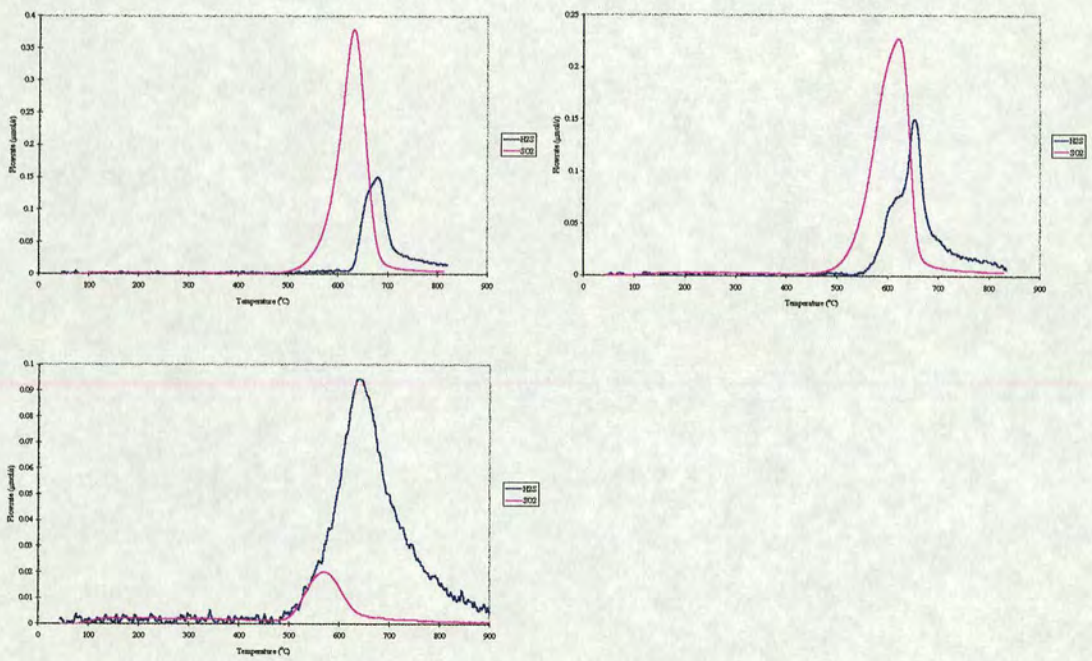

Figure 95: Standard TPRs, from top left Ceria, P_{12} and alumina (pink SO_2, blue H_2S)

Alumina's only switchover peak of H_2S was a small one (~50 ppm) at 700°C. Ceria exhibited considerably larger switchover peaks, particularly of sulphur dioxide. P_{12}'s storage-release behaviour is very similar to that of ceria; the same peak shapes are seen in the sulphur dioxide switchovers of both.

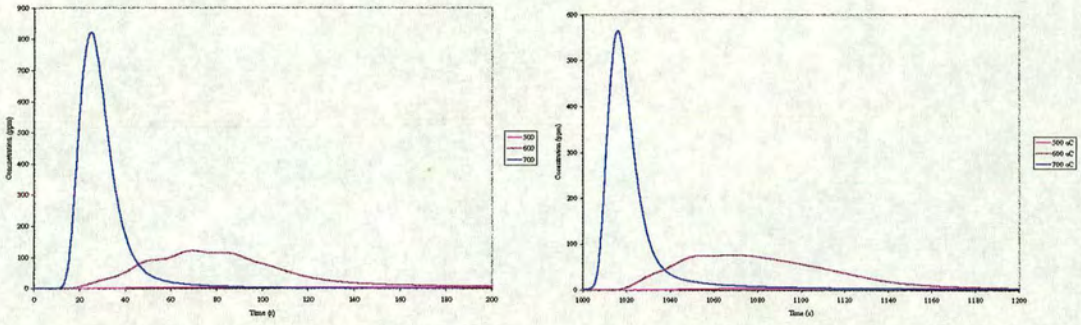

Figure 96(a)Ceria (b) P_{12}

The hydrogen sulphide switchover peaks are also remarkably similar.

In summary: although, ceria makes up only 21.1 wt. % of a P_{12} washcoat (less as a molar percentage) it has the greater effect on the storage-release behaviour of P_{12} with sulphur species. Indeed P_{12}'s behaviour is extremely close to that of ceria and quite unlike that of alumina in almost all respects.

5.5 *Effect of Platinum*

Platinum catalyses the formation of hydrogen sulphide by the storage-release mechanism. It is seen to lower the temperature at which switchover peaks occur[93]. The effect is illustrated in the histogram below:

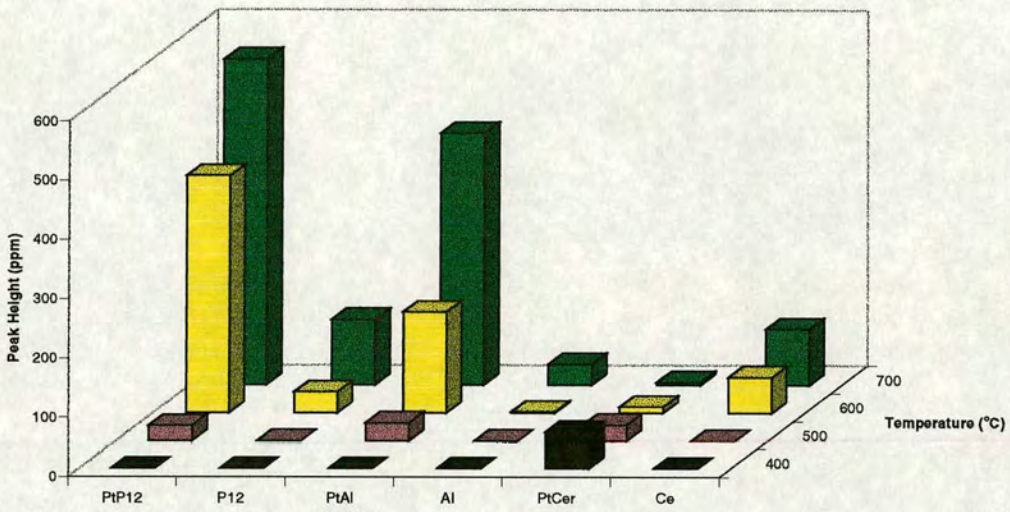

Figure 97: The Effect of Platinum on Hydrogen Sulphide Switchover Peaks

The catalytic effect can be seen between alumina and platinised alumina, and P_{12} and its platinised analogue at 500, 600 and 700 °C.

The distinctive behaviour of platinised ceria in most respects is attributed to its extremely low surface area (ceria ~80 m^2/g, platinised ceria ~3 m^2/g). However, it is difficult to explain the 400 °C hydrogen sulphide switchover peak produced by platinised ceria and the fact that the hydrogen sulphide peaks decrease in magnitude with increasing temperature. It is true that the hydrogen sulphide peak in platinised ceria's standard TPR occurred at a temperature below 500 °C, so this observation may be

consistent with the extremely low temperature of the switchover. The decreasing peak size may indicate that the form in which the platinised ceria stores the sulphur becomes more stable, the higher the dosing temperature. The unusual behaviour must be due to the addition of platinum, as the unplatinised sample exhibited the usual trend of increasing peak height with temperature. It may be that platinum has lowered the temperature at which the ceria loses surface area. Waqif *et al.* (1997) reported that (unplatinised) ceria calcined at 400 °C has a surface area of 115 m^2/g, whereas that calcined at 850 °C has surface area of ~5 m^2/g, very similar to that of this sample of platinised ceria.

Platinum is also seen to lower the peak maximum temperature of the H_2S peak in all TPRs (in the absence of other additives), indicating, again, that it is a catalyst for the release or formation of hydrogen sulphide. The following graph shows that the peak maximum for alumina and P_{12} is decreased by approximately 100°C, by the addition of platinum.

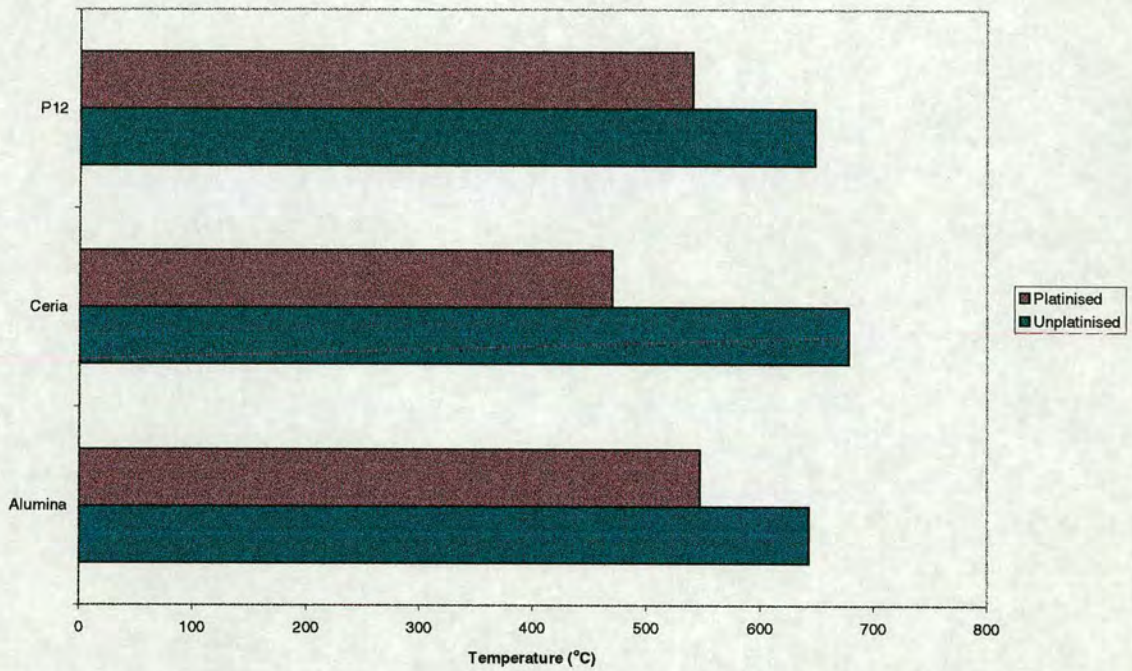

Figure 98: Effect of Platinum on Hydrogen Sulphide TPR Peak Maximum Temperature

This finding agrees extremely well with the observations of Lox *et al.* (1989) who found that, for a 'fully formulated catalyst', "the maximum in the hydrogen sulfide formation occurs at a temperature of about 100°C lower than without the presence of platinum group metals". The particularly large

---

[93] Or to increase the amount of hydrogen sulphide emitted, at a given temperature.

difference seen between the peak maximum temperature of ceria and its platinised analogue may well be overemphasised, due to the relatively small peak exhibited by platinised ceria in the TPR spectrum.

Addition of platinum always leads to a greater proportion of the adsorbed sulphur species being emitted as hydrogen sulphide, regardless of doping by other materials. P_{12} exhibits this trait well;

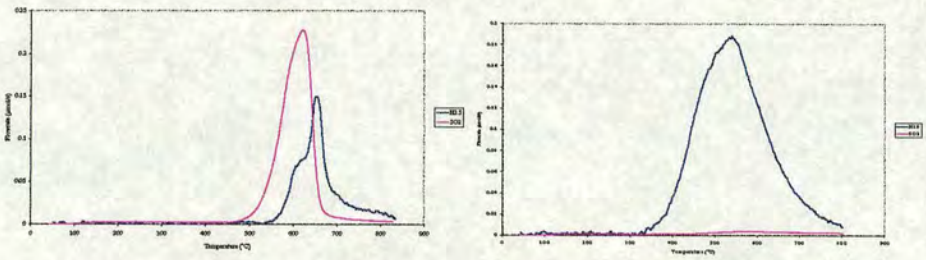

Figure 99 (a) TPR of P_{12} (b) TPR of Platinised P_{12}

The sulphur dioxide peak in the spectum of P_{12} (66 % of the emitted sulphur species) becomes insignificant (<5%) upon addition of 0.5 wt. % platinum to the formula. The effect is seen in many other comparisons of standard TPRs of component mixtures with and without platinum.

It can be seen that platinum is not necessary for hydrogen sulphide production in the TPR, but that it lowers the temperatures at which it occurs. It has been stated (Warr *et al.* (1994)) that platinum is necessary for hydrogen sulphide production. Clearly, this is not entirely true, but it is true that it is the presence of platinum that causes hydrogen sulphide emissions to reach problematic levels in real driving conditions.

The platinum has a role to play in the storage of the sulphur dioxide. A comparison of the adsorption of sulphur dioxide by alumina and platinised alumina shows this plainly; unplatinised alumina adsorbs only ~15 % of the sulphur dioxide it is exposed to, whereas platinised alumina adsorbs closer to 85 %. Other comparisons do not illustrate this as well, perhaps because all other formulations contain ceria, which is able to adsorb large amounts of sulphur dioxide.

The probable mechanism by which platinum takes part in the storage of the sulphur species is by converting the sulphur dioxide to the more reactive sulphur trioxide during oxidising conditions. It is unlikely that the platinum stores any of the sulphur itself, as it has been calculated (Diwell *et al.* (1987)) that there are no stable platinum-sulphur species at these temperatures in oxidising conditions. Instead, the extremely reactive sulphur trioxide reacts with alumina or ceria near to the platinum (i.e., a

'spillover effect). No sulphur trioxide was detected in the course of these experiments (this agrees with the results of Lox *et al.* (1989)).

The hydrogen sulphide is formed on or by the more thermally stable site. There are other forms, which do not require the presence of platinum in which sulphur dioxide can be stored, which will release the sulphur as sulphur dioxide.

5.6 *The Effect of Nickel*

The extent to which nickel attenuates hydrogen sulphide emissions is clearly demonstrated by the histogram below.

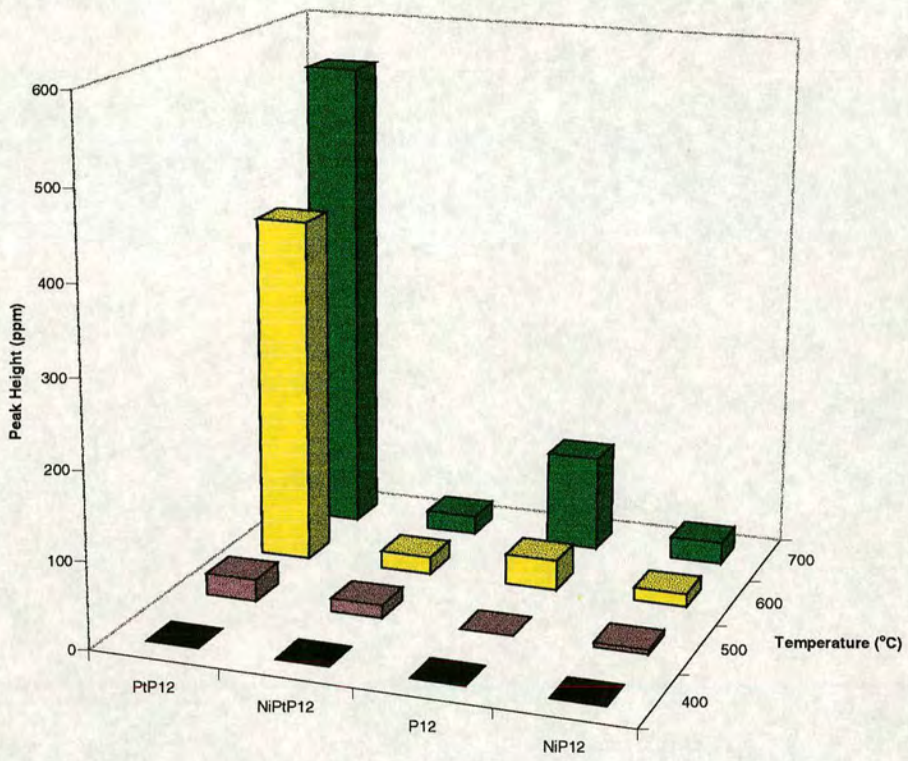

Figure 100: Hydrogen Sulphide Emission Attenuation by Nickel Addition

These results are a validation of the experimental design, in that the compounds in the rig behave as they have been observed to in practice; nickel addition does attenuate hydrogen sulphide emissions in practice. This histogram also illustrates the temperature dependence of the storage-release reaction, i.e., there is a slight increase in attenuated peak height with increasing temperature.

With the standard TPR and the pure nickel compound TPRs we can begin to build a picture of exactly which reactions are responsible for nickel's attenuating effect. In the TPR of nickel sulphide it can be seen that this compound emits hydrogen sulphide over a wide range of temperature. This is a useful attribute of an attenuating additive, because in a storage-release mechanism this will lead to slower emission of H_2S. It is, after all, the peak concentration of the H_2S which is the most important factor – not the total amount emitted. The characteristic tail of the TPR of any nickel doped component is due

to sulphide species such as this. Slow release of the hydrogen sulphide was observed in the 'switchover' experiments conducted on nickel-doped platinised P_{12}. The hydrogen sulphide was emitted at a low concentration for a long time at 500°C. This is part of nickel's attenuating effect.

The tailing effect can clearly be seen in the following comparison of platinised P_{12} with its nickel-doped analogue. Although the peak maximum occurs at a similar temperature, the peak is clearly skewed toward high temperature.

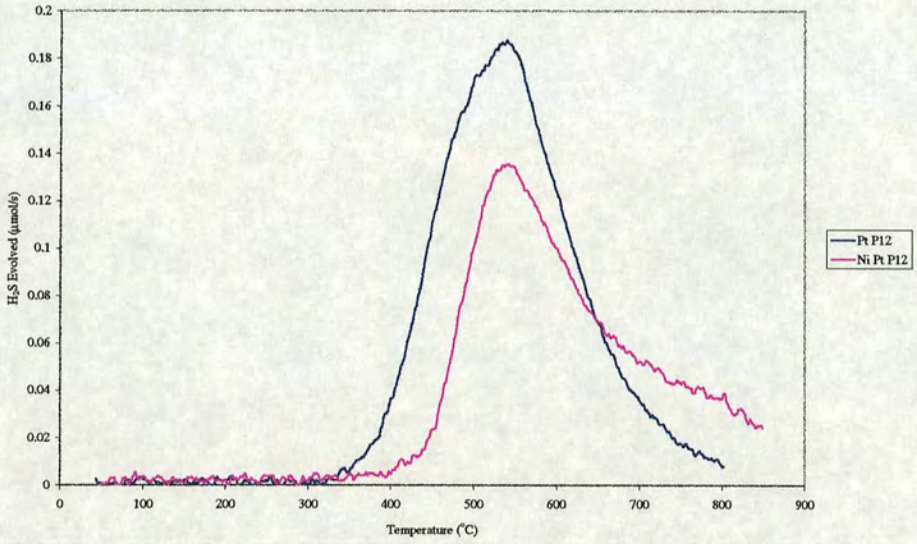

Figure 101: The Effect of adding Nickel to Platinised P_{12}

The following graphs demonstrate that the pronounced tailing effect is seen in all the nickel-doped components' TPRs.

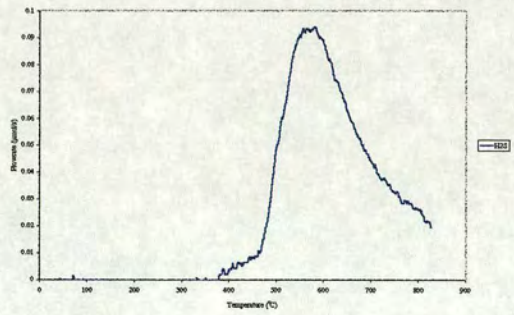

(a)

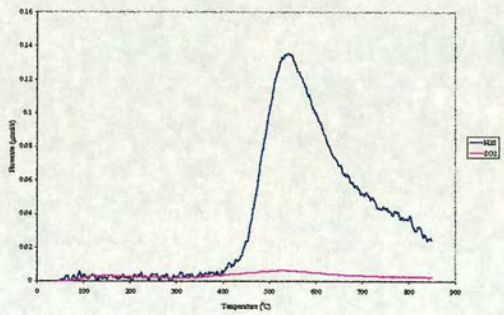

(b)

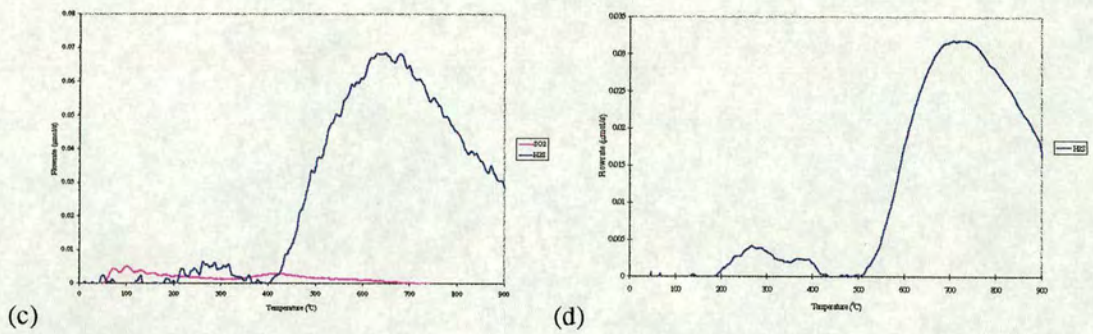

Figure 102 : Standard TPRs of Nickel-Doped Components (a)P_{12}, (b)Platinised P_{12} (c)Alumina (2 wt. %) (d) 10 wt. % illustrating the characteristic tail.

During switchover runs, most of the sulphur was emitted as sulphur dioxide. This implies the formation of a nickel sulphate species. In the TPR, nickel sulphate is reduced to nickel sulphides to produce the characteristic diffuse higher temperature peak, as well as decomposing to sulphur dioxide.

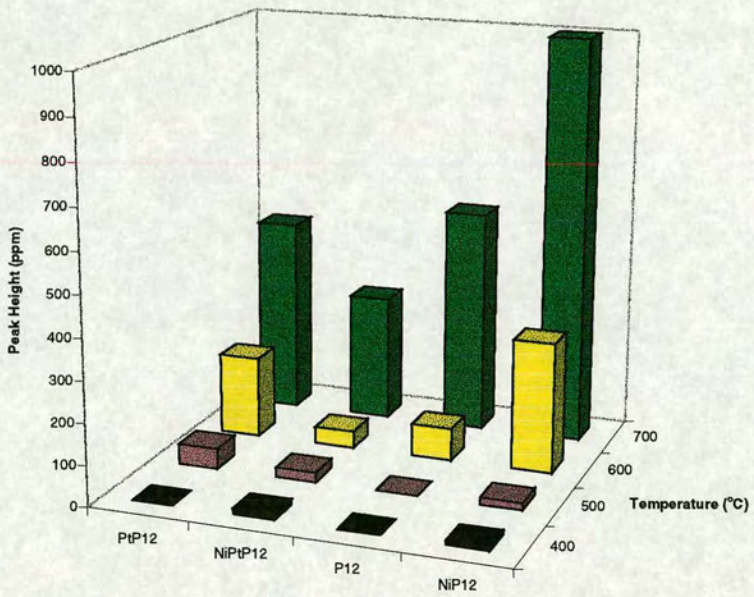

Figure 103: Sulphur Dioxide Switchover Peak Heights

The amount of sulphur dioxide emitted upon switchover by the nickel-doped platinised P_{12} is less than that of the platinised P_{12}, but as a proportion of the total sulphur species emitted by the sample it is considerably more:

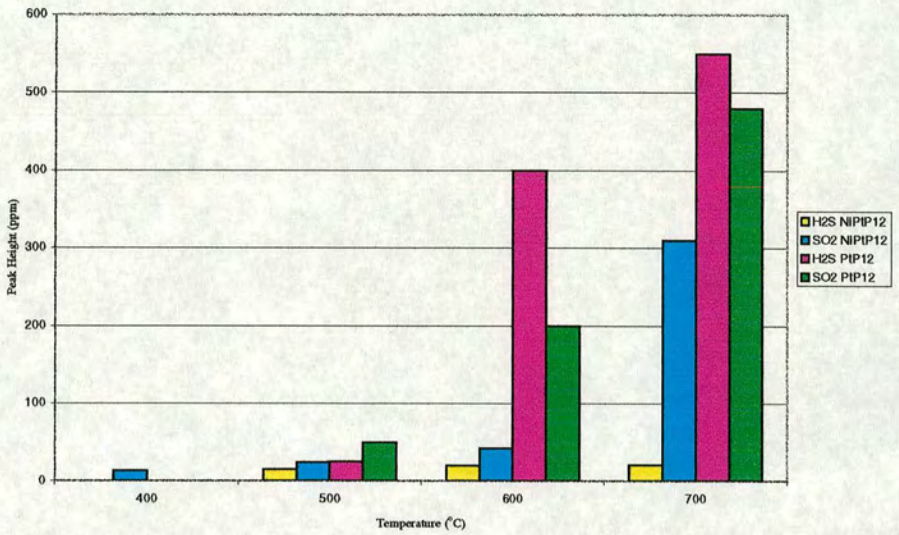

Figure 104: A Comparison of the Sulphur Dioxide and Hydrogen Sulphide Peak Heights of Platinised P_{12} with and without Nickel

The *modus operandi* of the nickel as a hydrogen sulphide attenuating agent is, principally, to cause the sulphur to be emitted as sulphur dioxide, but also to slow the rate of emission of any hydrogen sulphide produced.

5.7 *The Effect of Iron*

Iron has also been demonstrated to attenuate hydrogen sulphide emissions. Indeed, a 'modified form' (Bending *et al.* (1993)) is used in practice. The following histogram illustrates the effect on hydrogen sulphide switchovers of adding iron to the samples in these experiments:

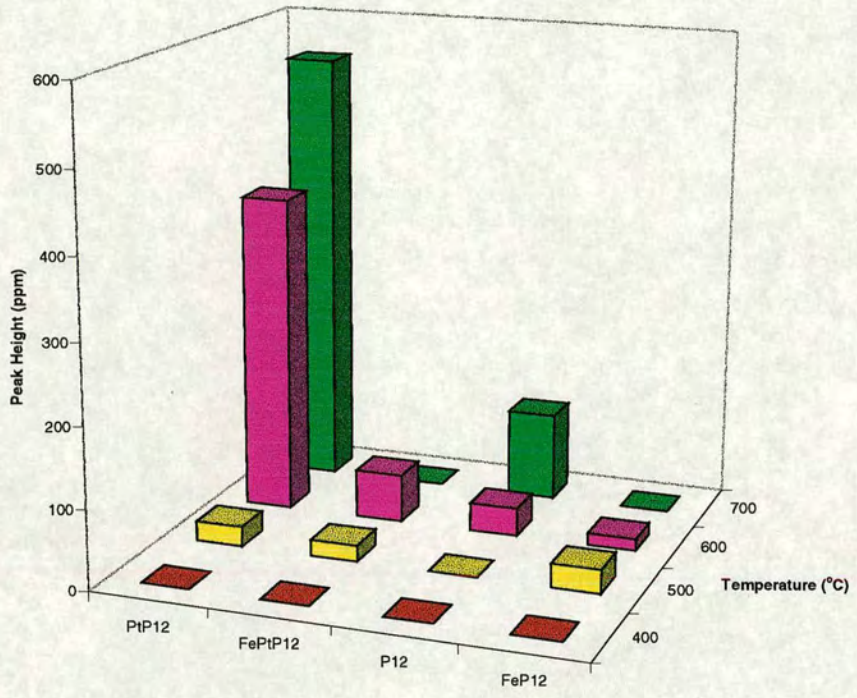

Figure 105: The Effect of Iron Doping on Hydrogen Sulphide Switchover

Iron's attenuating effect is clearly demonstrated. Bending *et al.* (1993) claimed that unmodified iron oxide could provide a similar level of control to nickel. Their assertion has been borne out in this research.

This effect could be explained by the formation of iron sulphates and sulphides. The TPR spectra of the iron sulphates and sulphides have many characteristics in common with those of nickel;

- The early sharp SO_2 peak and following diffuse H_2S peak of the sulphates.
- The high temperature diffuse H_2S peak of the sulphide.

The same general trends can be observed for iron's sulphur dioxide switchovers that were observed for nickel:

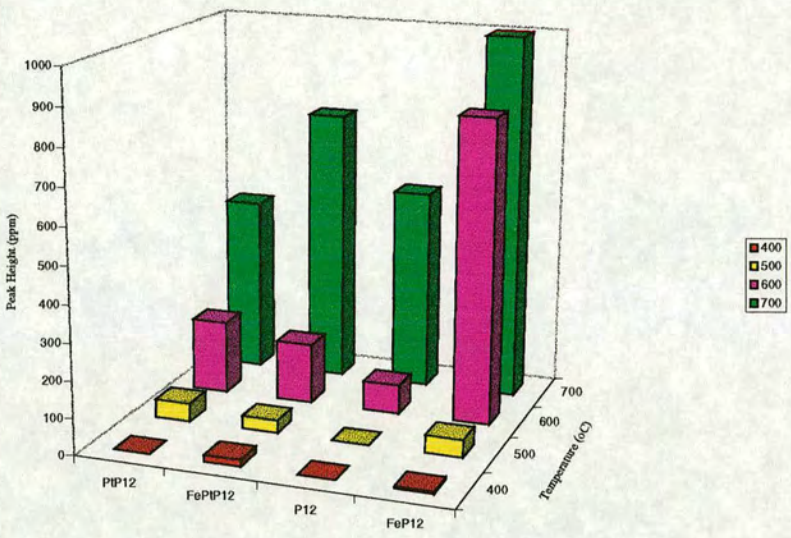

Figure 106 : Sulphur Dioxide Switchovers with and without Iron-Doping

The largest sulphur dioxide peak is, as for nickel, that from the metal-doped unplatinised sample. All the sulphur dioxide switchovers of the iron-doped components at 600 and 700 °C are large in comparison with their hydrogen sulphide counterparts, indicating that the iron also attenuates by causing the converter to produce sulphur dioxide in preference to hydrogen sulphide.

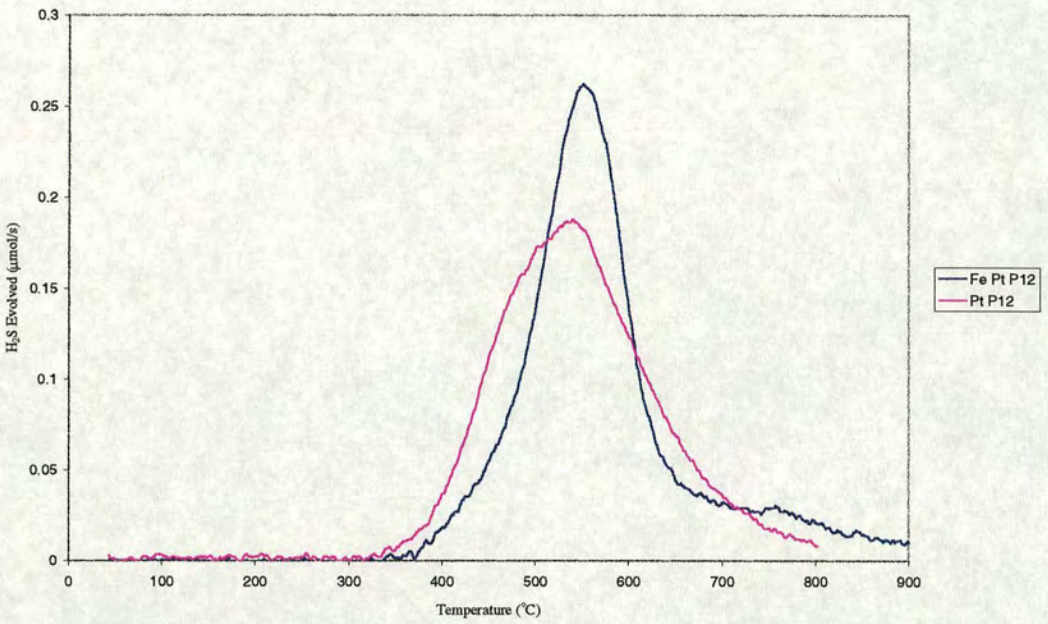

Figure 107: Comparison of the Standard TPRs of Platinised P12 and its Iron-Doped Analogue

Comparison of the standard TPR of platinised P_{12} with its iron-doped analogue reveals similar peak maximum temperatures, although the peak of the TPR of the iron-doped material is considerably sharper. There is distinct tailing of the iron-doped component's trace, although this is nowhere near as pronounced as that observed for nickel-doped components.

5.8 The Effect of Barium

The following graph illustrates the effect addition of barium to the formulation:

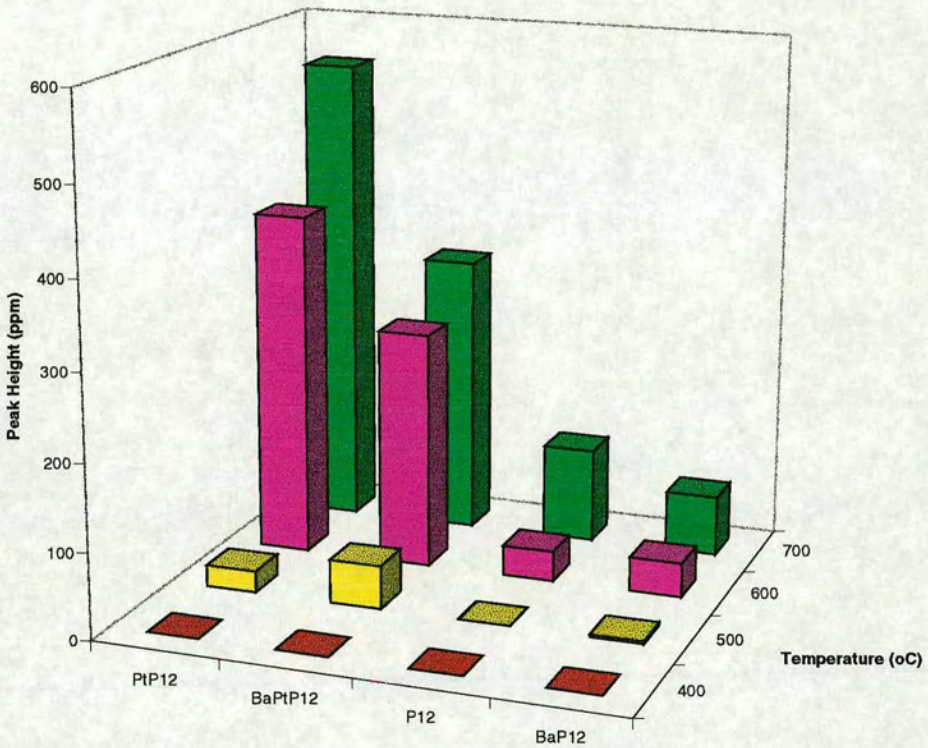

Figure 108: The Effect of Barium Doping on Hydrogen Sulphide Switchovers

Clearly, the barium has a moderate attenuating effect on the switchover peaks. Barium oxide was identified as a possible additive by Yamada *et al.* (1990), as it satisfied their thermodynamic criteria for a successful additive, but it was shown to actually increase hydrogen sulphide switchover peaks in their tests. The findings presented here conflict with the results of Yamada *et al.*, but do not recommend baria as a suitable candidate for a hydrogen sulphide attenuating agent, as the degree of activity is not great enough. Indeed, in terms of the proportion of the total amount of species emitted the hydrogen sulphide emitted by barium-doped samples is actually greater than those without barium.

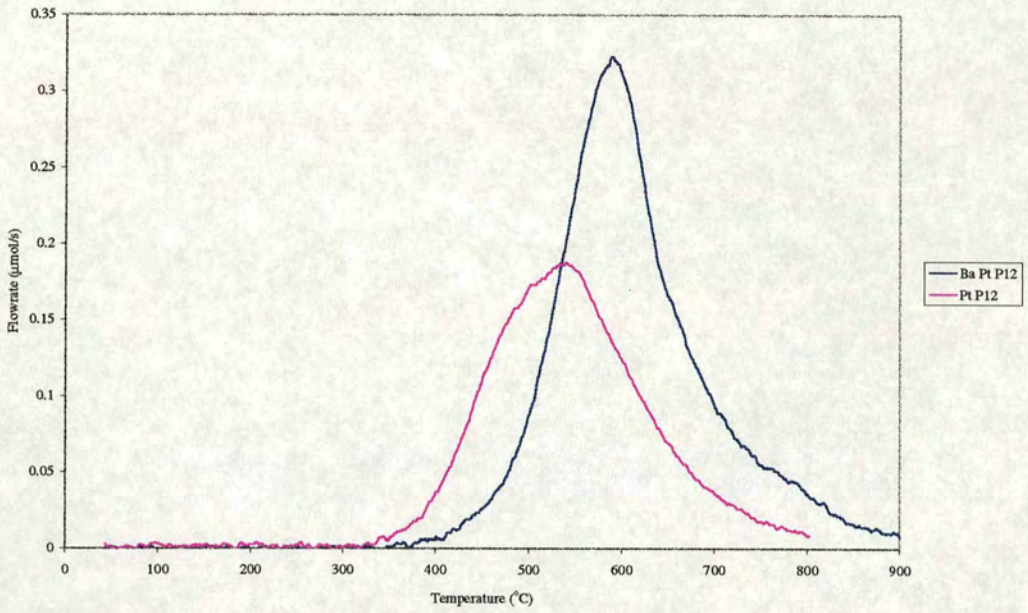

Figure 109: Comparison of Platinised P_{12} TPR with that of its Barium-Doped Analogue

The peak in the barium-doped sample's spectrum occurs at a considerably higher temperature than that for the undoped. This may explain barium's moderate attenuating effect (it emits considerably less sulphur dioxide and hydrogen sulphide than the platinised P_{12}).

The peak in the TPR of barium doped platinised P_{12} is considerably larger than that of P_{12}, as it adsorbed much more of the sulphur dioxide to which it was exposed. All three additives seemed to activate the formulations toward adsorption of sulphur dioxide. All the formulations doped with iron, nickel or barium adsorbed more sulphur dioxide than their undoped counterparts.

5.9 In Situ DRIFTS Research

The majority of the work that went into this area was in the development of an environmental DRIFTS cell which could reach temperatures high enough to be of use for work on the storage-release of sulphur compounds on automobile catalytic converters. That development work was ultimately successful, and a number of species have been identified on ceria and alumina samples. Thus far the HTEC has reliably reached and maintained temperatures of up to 530 °C, although it has been to higher temperatures than this for short periods of time. The cell design has advantages over others in that it preheats the incoming gases and has a flat upper window such that the gases flow over the sample in a laminar manner.

At 500 °C sulphates have been seen to form on the surfaces of alumina, platinised alumina and ceria. So, it seems likely that sulphates are the form in which the sulphur is stored on the autocatalyst surface.

An interesting effect was discovered whilst performing switchover experiments with deuterium replacing the hydrogen as reductant. On platinised alumina, when both hydroxyl and –OD groups are formed on the surface, upon switching the environment to nitrogen the –OD group will take as much as nine times longer to disappear. The form in which these groups are desorbed is unknown as yet, but the effect is currently under investigation.

5.10 Criteria for Choosing Additives for Hydrogen Sulphide Emission Attenuation

Yamada *et al.* (1990) chose two criteria to assess the viability of an oxide as an attenuating agent. Firstly, they stated that the species should not form sulphates during stoichiometrically net oxidising conditions, and, secondly, that they should trap hydrogen sulphide during stoichiometrically net reducing conditions. These criteria were flawed, as iron oxide is a proven attenuator and yet did not meet these criteria[94]. Nickel did meet these criteria, but so did other compounds which were then shown, experimentally, *not* to function well as hydrogen sulphide attenuating additives. The first

---

[94] They also showed, experimentally, that it did not function well as an attenuator.

assumption, that the species should not form sulphates may well be wrong. In this research it has appeared that the ability of the additive to adsorb sulphur dioxide during oxidative conditions and release it as such during reducing conditions is a significant part of its functionality, and perhaps explains why the iron- and nickel-doped samples adsorbed more sulphur dioxide. Nickel and iron doped platinised components have both been observed to emit significant amounts of sulphur dioxide upon switching to reducing conditions following dosing with sulphur dioxide in oxidising conditions. This is indicative of sulphate decomposition.

Chemical criteria[95] for choosing additives have been arrived at by the study of iron- and nickel-doped materials, which are proven attenuators in the field. The criteria should be predictive.

- The TPR of its sulphate/sulphite should exhibit a relatively low temperature (around 500 °C) large sulphur dioxide peak, implying the ability to desorb the sulphur mostly as sulphur dioxide in reducing conditions. The thermodynamic stabilities of the sulphates may be very important: those of nickel, iron, copper and manganese are very similar (Phillips and Williams (1962)[96]) and all are proven attenuators[97].

- The hydrogen sulphide peak of the TPR (representing the decomposition of a sulphide) should be diffuse and occur at higher temperatures. This is the key to nickel and iron's abilities to attenuate hydrogen sulphide emission. This is not the case for barium and, consequently, it is not a good attenuator.

---

[95] There are many other criteria that must be fulfilled as detailed in the 'Literature Survey'.
[96] II p. 511
[97] Manganese and copper have proved impractical, due to precious metal interactions and volatility, respectively.

5.11 Reaction Kinetics

The energy of desorption of the sulphur species from the oxide after adsorption at 500 °C has been estimated from their standard TPR spectra. Some of the curves exhibit distinct first order characteristics. The desorption of sulphur dioxide from ceria (below) exhibits a characteristic first order shape (Falconer and Schwarz (1983)). As there is an excess of hydrogen present, it may be that it is actually pseudo-first order. Indeed, the hydrogen consumption peak correlates very well with this peak.

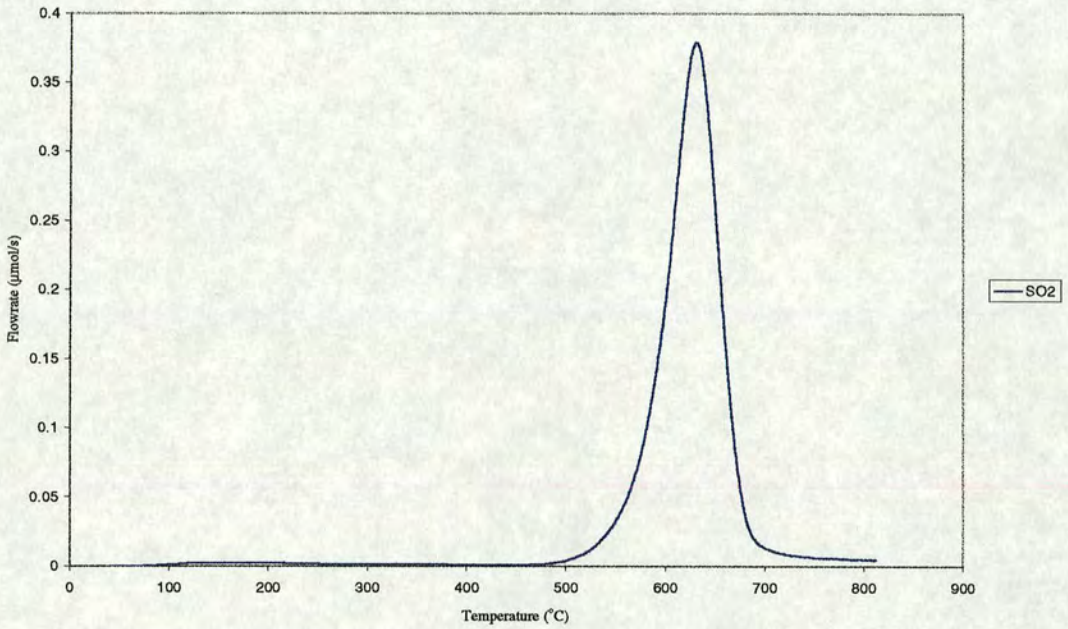

Figure 110: Sulphur Dioxide Desorption by Ceria (Standard TPR)

In the summary of the standard TPR results it can be seen that the agreement between the two values[98] estimated for the energy of desorption of sulphur dioxide from ceria have a good degree of agreement (282 and 287 kJ/mol). Platinised alumina exhibits a much more symmetrical peak for its desorption of hydrogen sulphide. A symmetrical peak is indicative of a second order process. The half and three quarter width estimations for a second order process for platinised alumina correlate reasonably well (99.8 and 108.2 kJ/mol). It is difficult to suggest a feasible second order reaction, especially

[98] The half-width value and the three-quarter-width value.

considering that hydrogen is in great excess and would therefore participate in a pseudo-first order manner.

5.12 Proposals for Further Work

5.12.1 Other Reductants

Exhaust gas mixtures contain a number of other reductants, principally carbon monoxide and hydrocarbons. Research by Lundgren *et al.* (1995) has shown that there are large differences between TPRs performed with H_2 and those in methane. The main difference was that with hydrocarbons as the reductants, sulphur dioxide peaks do not appear. Kim and Juskelis (1996) performed similar TPRs to those in this work, with propane as the reductant. Their work on ceria shows that the TPR peak temperatures are higher when propane is used than when hydrogen is used. Many workers (e.g., Gidney (1996)) have claimed that hydrogen is the most likely reductant, mainly on grounds of its relative abundance.

5.12.2 Other Catalysts

It has been demonstrated that platinum has an important role in the production of H_2S. The results of using other PGMs, such as palladium, for instance, would be informative. This topic has been investigated to some extent by Engler *et al.* (1991) who have examined sulphur storage and release on ceria and alumina impregnated with Rh, Pt and Pd. Brisley *et al.* (1995) claim that high palladium loading catalysts "offer improved H_2S attenuation compared to current platinum rhodium catalysts with additives". No research similar to this has been performed on other prospective PGMs for automobile catalytic converter.

5.12.3 Experimental Systems

5.12.3.1 Microreactors

A battery of microreactors would be ideal for further work in this field. A design similar to the catalyst test rig, but incorporating computer-controlled flows and switching between reactors is envisaged. Coherent sets of experiments could then be performed automatically.

This would enable faster 'sweeps' of prospective additives at various loadings. Instrumentation would be more complex leading to a greater cost and 'dead-time' initially, but once established the system envisaged would produce results at a much greater rate.

From this point of view a reactor with a fixed external heating system would be preferable, as it would speed up reactor replacement, which was one of the most time-consuming procedures in this work.

5.12.3.2 Gas Detection

The gas detection systems used in this research were far from ideal. The detection overlaps between water and sulphur dioxide in the infrared and hydrogen sulphide and sulphur dioxide in ultraviolet made analysis of results fraught with difficulty. Further work in this area should involve more reliable detection systems;

Infrared Gas Analysis: The technique of using an infrared gas cell and scanning the entire available IR spectrum very rapidly (~every second) has been used to a limited extent in this work, and can distinguish between sulphur dioxide and water. Unfortunately, it does not have the same degree of resolution as the gas meters used and analysis of results can be very time-consuming. The main failing of this technique for research in this area is that it cannot detect hydrogen sulphide to any useful degree, and that infrared spectroscopy is unable to detect homonuclear diatomic molecules, such as hydrogen.

Mass Spectrometry: Although mass spectrometry was believed to be incompatible with sulphur-containing gases for reasons of the contamination of the filament, it has been used by other researchers to detect both sulphur dioxide and hydrogen sulphide (e.g., Lox *et al.* (1989)). The greatest advantage of mass spectrometry would be that it could monitor any substance required, usually without problems of ambiguity.

Gas meters: If research very similar to this were to be conducted, then a different arrangement of meters could be used which would not have the interference problems of those used in this research;

- A fluorescence based analyser for both sulphur dioxide and hydrogen sulphide could be used, such as that used by Harkonen *et al.* (1990).[99] The meter would have automatic cross-sensitivity correction between the two gases and no problems of overlap with water.
- An ultraviolet-based meter could be used to detect the sulphur dioxide (e.g Hartmann and Braun Radas 2 for sulphur dioxide) and NDIR for hydrogen sulphide detection (e.g Gidney (1990), the Siemens 'Ultramat'). It is unlikely that the hydrogen sulphide frequency would overlap with that of water, but it would certainly be possible that the sulphur dioxide ultraviolet detection frequency could overlap with hydrogen sulphide. Nonetheless, the problem would be simplified to some extent, if the previous option were not available.

5.12.4 Higher Temperature TPRs

It has been shown by Lox *et al.* (1989) that some TPR peaks may occur at temperatures above 900 °C. Furthermore, there are clear examples in this research of peaks, particularly the hydrogen sulphide peak of nickel doped substances, which extend beyond 900 °C. To investigate these regions, further developments in the design of the reactor would be necessary.

5.12.5 DRIFTS Research

More comprehensive DRIFTS research is currently underway as part of a research project into the co-oxidation of carbon dioxide and sulphur dioxide on a range of oxides, over a range of temperatures (ambient to >500 °C). This will include oxides of relevance to this research.

---

[99] Monitor Labs.

6. References

Amenomiya, Y. and Cvetanovic, R.J., "Applications of a TPD Technique to Catalyst Studies" Adv. Cat., 17, 103 (1971).

Amenomiya, Y. and Cvetanovic, R.J., "Application of Flash-Desorption Method to Ctalyst Studies. I. Ethylene-Alumina System", 67, J. Phys. Chem., 144 – 147 (1963).

Aris R., Lee S-Y, "The Distribution of Active Ingredients in Supported Catalysts Prepared by Impregnation" Catal. Rev. - Sci. Eng., 27(2), 207 - 340 (1985).

Atkins P. W., "Physical Chemistry", Oxford University Press (1997).

Banwell C. N., "Fundamentals of Molecular Spectroscopy", 3rd Ed., McGraw-Hill, London (1983).

Barefoot R., Env. Sci & Tech., 31, 309 (1997).

Beck D.D. and Sommers J.W., "Impact of Sulfur on Three-Way Catalysts : Comparison of Commercially Produced Pd and Pt-Rh Monoliths", *Catalysis and Automotive Control III,* Studies in Surface Science and Catalysis, 96, 721 - 748, (1995).

Beckwith P., Bennet P. J., Brisley R.J., Goodfellow C. L. and Wilkins A., "The Effect of Three-Way Catalyst Formulation on Sulphur Tolerance and Emissions from Gasoline Fuelled Vehicles", SAE 940310 (1994).

Bending R. G., Albert M. R., D'Aniello M. J., Golunski S.E., Diwell A.F. and Truex T.J., "Nickel-Free H_2S Control Technology for European Applications", SAE 930777 (1993).

Berben P. H., Kappers M. J. and Geus J. W., "An FT-IR Study of adsorption of Sulfur Dioxide on Alpha and Gamma-Alumina", Mikrochimica Acta, II, 15-18 (1988).

Bond G. C., "Catalysis by Metals", Academic Press, New York and London (1962)

Bowker M., Houghton H., Waugh K. C., Giddings T. and Green M., "Crystal Plane Dependence of Adsorption and Reaction on Zinc Oxide", J.Cat., 84, 252 - 255 (1983).

Bowker M., Houghton H. and Waugh K. C., "Mechanisms and Kinetics of Methanol Synthesis on Zinc Oxide" J.Chem.Soc. (Faraday Trans.), 77, 3023 - 3036 (1981).

Brenner A. and Hucul D.A., "Experimental errors in the Application of TPD to Practical Catalysts" J.Cat., 56, 134 - 138 (1979).

Brown P., "Alarm at Killer traffic fumes", The Guardian, Jan. 14th 1998.

Brisley R.J., Chandler G.R., Jones H.R., Anderson P.J., Shady P.J, "The Use of Palladium in Advanced Catalysts" SAE Technical Paper Series, 950259 (1995).

Cadle S. H. and Murawa P.A, SAE 780200 (1978)

Calvert J.G., Heywood J.B., Sawyer R.F. and Seinfeld J.H., "Achieving Acceptable Air Quality : some Reflections on Controlling Vehicle Emissions", Science, 261, 37 - 45 (1993)

Chang C.C., "Infrared studies of Sulphur dioxide on γ-Alumina", J.Cat., 53, 374 - 38, (1978).

Chem. & Ind. "Hot Cats", Chem. & Ind., 21st Oct. 1996.

Chopey N. P., Ondrey G. and Parkinson G., "Microreactors Find New Niches", Chemical Engineering, Mar. 1997, 30 – 33.

Coghlan A., "Clean burn", New Scientist, 11th April 1998.

Dalla Lana I. G., Karge H. G. and George Z., "Adsorption of Sulphur Dioxide", J. Phys. Chem., 97, 8005 (1993).

Datta A., Cavell R.G., Tower R.W. and George Z.M., "Claus Catalysis. 1. Adsorption of SO_2 on the Alumina Catalyst Studied by FTIR and EPR Spectroscopy", J. Phys. Chem., 89, 443 - 449 (1985).

Delgass W.W., Haller G.L., Kellerman R., Lunsford J.H., "Spectroscopy in Heterogeneous Catalysis", Academic Press (1979).

Dettling J.C., Hwang H.S., Pudick S. and Tauster S.J., "Control of H_2S emissions from High-Tech TWC Converters", SAE 900506 (1990).

Diwell A.F., Hallett C. and Taylor J.R., "The Impact of Sulphur Storage on Emissions from Three-Way Catalysts", SAE 872163 (1987).

Diwell A.F., Golunski S.E., Taylor J.R. and Truex T.J., "The Role of Sulphate Decomposition in the Emission and Control of H_2S from Autocatalysts", Stud. Surf. Sci. and Catalysis, Catalysis and Automotive Pollution Control II, 417 – 423 (1991).

Engler B., Koberstein E., Lindner D. and Lox E., "The Influence of Three-Way Catalyst Parameters on Secondary Emission", Stud. Surf. Sci. and Catalysis, CAPOC II (1991).

Ernest M.V., "Development of Beaded Three-Way Catalysts with reduced H_2S Emissions", SAE Technical Paper Series, 892042 (1989).

Falconer J. L. and Schwarz J. A., "TPD and Reaction: Applications to Supported Catalysts" Catal.Rev., 25(2), 141 - 227 (1983).

Fiederow R., Dalla Lana I. G. and Wanke S. E., "Adsorption of Sulfur Dioxide on Heat Treated γ-Aluminas at Room Temperature", J. Phys. Chem., 82, No. 23, p2474 (1978).

Fierain W., "The Value of Spent Exhaust Catalysts", Catalysis and Automotive Control II, Studies in Surface Science and Catalysis, 115 – 123 (1991).

Fierro G., LoJacuno M., Inversi M., Porta P., Lavecchia R. and Cioci F., "A Study of Anomalous TPR Profiles of Cu2O, CuO and Cuo-ZnO Catalysts", J. Cat., 148, 709 - 721 (1994).

Flegler S. L., Heckman J. W. and Klompare K. L., "Scanning and Transmission Electron Microscopy. An Introduction", Freeman (1993).

Forzatti E. and Tronconi P., "Experimental Criteria for Diffusional Limitations during TPD from Porous Catalysts" J.Cat., 93, 197 - 200 (1985).

Ghardashkani S. and Cooper D.A. "A Thermogravimetric Study of the Reaction Between Sulfur Dioxide and Calcium Oxide", Thermochimica Acta, 161, 327 - 337 (1990).

Gidney J.T., "The Effect of Drive Cycle, Gas Temperature, catalyst Formulation and loading and Engine Fuelling Strategy on H_2S and SO_2 Emissions", Johnson Matthey Internal Report, (1996).

Golunski S. and Roth S., "Identifying the Functions of Nickel in the Attenuation of H_2S Emissions from 3-way Automotive Catalysts", Cat. Today, 9, No. 1-2, 105-112 (1991).

Goodsel A.J., Low M.J.D. and Takezawa N., "Reactions of Gaseous Pollutants with Solids. II. Infrared Study of sorption of SO_2 on MgO", Env. Sci. Tech., 6, 268 - 273 (1972).

Gorte R.J., "Design parameters for TPD from Porous Catalysts", J.Cat., 75, 164 (1982).

Gottberg I., Högberg E. and Weber K., "Sulphur Storage and Hydrogen Sulphide Release from a from a Three-Way Catalyst Equipped Car", SAE 890491, (1989).

Griffiths P. R. and de Haseth J. A., "Fourier Transform Infrared Spectrometry", John Wiley & Sons Inc. (1986).

Gross G.P., Biller W.F., Greene D.F., Kearby K.K., U.S. Patent 3370914.

Harkonen M.A., Salanne S., Rantakyla T-K and Pohjola V.J., "Prevention of Hydrogen Sulphide formation on Three-Way Catalysts", SAE 900498 (1990).

Harrison B., "Catalysis: Fundamentals and Practice", Lecture given at EPSRC Summer School (1997).

Hartmann & Braun, "Operating Instructions Uras 10 E / Uras 10 P NDIR Industrial Photometer".

Heck R.M. and Farrauto R.J., "Catalytic Air Pollution Control: Commercial Technology", van Nostrand ISBN 0-442-01782-0 (1993).

Hedges S.W. and Yeh J.T., "Kinetics of Sulfer Dioxide on Supported Cerium Oxide Sorbents", Env. Prog., 11(2), 98 - 103 (1992).

Henk M.G., White J.J. and Denison G.W., "Sulfur Storage and Release from Automotive Catalysts", SAE Technical Paper series, 872134 (1987).

Henssler H., "The Evolution of the EEC Regulations on Vehicle Emissions", Catalysis and Automotive Pollution Control II, Elsevier, Amsterdam (1991).

Herz R. K., Kiela J. B. and Marin S. P., "Adsorption effects During TPD of CO from Supported Platinum" J.Cat., 73, 66 (1982).

Hutchings G., "Principles of Heterogeneous Catalysis", Catalysis: Fundamentals and Practice, EPSRC Summer School, 1997.

Ibok E.E. and Ollis D.F., "TPD from Porous Catalysts: Shape Index Analysis", J.Cat., 66, 391 - 400 (1980).

Iwasawa K, Acc. Chem. Res., 30, 103 (1997)

Johnson Matthey, "Cutting Diesel vehicle Pollution", leaflet available from Johnson Matthey catalytic Systems Division, Orchard Road, Royston, Herts. (1994).

Joy G. C., Lester G. R. and Molinaro F. S., "The Influence of Sulfur Species on the Laboratory Performance of Automotive Three Component Control Catalysts", SAE Technical Paper Series, 790943 (1979).

Karge H.G. and Dalla Lana I.G., "Infrared studies of SO_2 Adsorption on a Claus Catalyst by Selective Poisoning of Sites", J. Phys. Chem., 88, 1538 - 1543 (1984).

Kent S. A., Katzer J. R. and Manogue W. H., "Infrared Spectroscopic Investigation of the Adsorption and Reactions of SO_2 on CuO", Ind. Eng. Chem., Fundam., 16, No. 4 (1977).

Khulbe K. C. and Mann R. S., "ESR Studies of SO_2 and H_2S Adsorption on Alumina and Alumina-Supported Mo and Mo-Co", J. Cat., 51, 364-371 (1978).

Kim G. and Juskelis M.V., "Catalytic Reduction of SO_3 Stored in SO_x Transfer Catalysts – A Temperature-Programmed Reaction Study", Stud. Surf. Sci. and Cat., 101, 137 – 142 (1996).

Kirchner T. and Eigenberger G., "Optimization of the Cold-Start Behaviour of Automotive Catalysts Using an Electrically Heated Pre-Catalyst", Chem. Eng. Sci., 51, No. 10, 2409 – 2418 (1996).

Kortum G., "Reflectance Spectroscopy. Principles, Methods, Applications", Springer – Verlag (1969).

Levenspiel O., "Chemical Reaction Engineering", Wiley (1962).

Li X.S., Xin Q., Guo X.X., Grange P. and Delmon B., "Reversible Hydrogen adsorption on MoS_2 studied by TPD and TPR", J. Cat., 137, 385 - 393 (1992).

Low M. J. D., Goodsel A.J. and Takezawa N., "Reactions of Gaseous Pollutants with Solids. I. Infrared Study of the Sorption of SO_2 on CaO", Env. Sci. Tech., 5, 1191 -1195 (1971).

Lox E.S, Engler B.H. and Koberstein E., "Development of Scavenger-Free Three-Way Automotive Emission Control Catalysts with Reduced Hydrogen Sulfide Formation", SAE 890795 (1989).

Lundgren S., Spiess G., Hjortsberg O., Jobson E., Gottberg I., Smedler G., "Sulphur Adsorption and Desorption on Fresh and Aged Ce Containing Catalysts", Catalysis and Automotive Pollution Control III Studies in Surface Science and Catalysis, 96, Elsevier (1995).

Machiels, C.J., "Development of a Pulse Reactor with On-line MS Analysis to Study the Oxidation of Methanol".

Mackenzie D., "Off to a dirty start", New Scientist, 20th Sept. 1997.

Mayotte S.C., Lindhjem C.E., Rao V., Sklar M.S., " Reformulated Gasoline Effects on exhaust Emissions : Phase I : initial Investigation of Oxygenate, Volatility, Distillation and Sulphur effects", SAE 941973 (1994)

Mitchell M.B., Sheinker V.N. and White M.G., "Adsorption and Reaction of Sulfur Dioxide on Alumina and Sodium-Impregnated Alumina", J. Phys. Chem., 100, No. 18 (1996).

Modell M. and Reid R. C., "Thermodynamics and it Applications", Prentice Hall Inc. (1974).

Monti D.A.M. and Baiker A., "TPR : Parametric Sensitivity and Estimation of Kinetic Parameters" J.Cat., 83, 323 - 335 (1983).

Nakamoto K., "Infrared and Raman Spectra of Inorganic and Coordination Spectra", 4th edition, Wiley (1986).

Pearce F., "Devil in the diesel", New Scientist 25th Oct. 1997.

Pelovski Y., Pietkova W., Gruncharov I., Pacewska B. and Pysiak J., "Investigations of Thermal Decomposition of Aluminium Sulphate by the EMF Method", Thermochimica Acta, 205, 283 -287 (1992).

Phillips and Williams, "Inorganic Chemistry", II, Clarendon Press.

Pringle T. J., "Novel Routes to Potential Packed Bed Absorbents for the Desulphiding Reaction", PhD Thesis, University of Edinburgh (1998).

Radojevic M., "Opportunity NOx", Chemistry in Britain, March 1998.

Rieck J.S., Suarez W. and Kubsh J.E., "Development of Non-Nickel Additives for Reducing Hydrogen Sulfide Emissions from Three-Way Catalysts", SAE Paper 892095 (1989).

Saur O., Bensitel M., Mohammed Saad A. B., Lavalley J. C., Tripp C. P. and Morrow B. A., "Adsorption of Sulphur Dioxide", J. Cat., 99, 104 (1986).

Schleyer C.H., Dunker A.M., Yarwood G., Cohen J.P. and Pollack A.K., "Effect of Fuel Sulphur Content on Predicted Ozone for Years 2005/2010 - Auto/Oil Air Quality Improvement research Program", SAE 932728 (1993).

Schoonheydt R.A. and Lunsford J.H., "Infrared Spectroscopic Investigation of the Adsorption and Reactions of SO_2 on MgO", J. Cat., 26, 261 - 271 (1972).

Sellers H. and Shustorovich E., "Chemistry of Sulfur Oxides on Transition metal surfaces: BOC-MP analysis", J. Mol. Cat. A – Chemical, 119, No. 1-3, 367-375 (1997)

Sharp D.W.A., "The Penguin Dictionary of Chemistry", Penguin (1983).

Sidgwick N. V., "Chemical Elements and Their Compounds", O.U.P (1952)

Sohail K., "Reaction of Sulphur Containing Gases with Zinc Oxide Absorbents", PhD. Thesis., University of Edinburgh (1992).

Subramanian S., Kudia R.J and Chattha M.S., "Treatment of Natural Gas Vehicle Exhaust", SAE Technical Paper Series, 930223 (1993).

Summers J.C., White J.J. and Williamson W.B., "Durability of Palladium only Three-Way Automotive Emission Control Catalysts", SAE 890794 (1989).

Truex T.J., Windawi H., Ellgren P.C., "The Chemistry and Control of H_2S Emissions in Three-Way Catalysts", SAE 872162 (1987).

Twigg M. V., "Catalyst Handbook", Wolfe Publishing (1989).

Vanhove D., "Catalyst testing at a lab scale in mild oxidation: Can you control the reaction temperature?", App. Cat. A: Gen., 138, 215 – 234 (1996).

Viala A., "Effets sur la sante des polluants atmospheriques emis par les vehicules automobiles", Quel Environnement, 351, 25 -27 (1989).

Walker P. M. B., "Chambers Science and Technology Dictionary", Chambers (1988).

Waqif M., Saad A.M., Bensitel M., Bachelier J., Saur O. and Lavalley J-C., "Comparative Study of SO_2 adsorption on Metal Oxides", 88(19), 2931 - 2936 (1992).

Waqif M., Bazin P., Saur O., Lavalley J. C., Blanchard G. and Touret O., "Study of ceria sulfation", App. Cat. B: Env., 11, 193 – 205 (1997).

Warr K (ed.), "The Three-Way Catalytic Converter", The Open University, Physical Chemistry, S342 (1994).

Weast R. C. (ed.), "Handbook of Chemistry and Physics", CRC Press, p E-2 (1981).

Westerterp K.R., van Swaaij W.P.M. and Beenackers A.A.C.M., "Chemical Reactor Design and Operation", Wiley (1987).

White J.J., Carroll J.N., Liss W.E., Brady M.J., Burkmyre W.M. and Church M., "Natural Gas Converter Performance and Durability", SAE 930222 (1993).

Wotring W. T., Meguerian G. H., Gandhi H. S., McCuiston F. D. and Piken A. G., "50,000 Mile Vehicle Road Test of Three-Way and NOx Reduction Catalyst Systems", SAE Technical Paper Series, 780608 (1978).

Yamada T., Kayano K. and Funabiki M., "Development of Non-Ni Low H_2S Pt/Rh/CeO_2 TWC Catalyst", SAE 900611 (1990).

Ziolek M., Kujawa J., Saur O., Aboulayt A. and Lavalley J.C., "Influence of sulfur dioxide adsorption on the surface properties of metal oxides", J. Molecular Catalysis A: Chemical, 112, 125 – 132 (1996).

7. Appendices

7.1 X-Ray Powder Diffractograms

A number of XRPDs and salient comparisons can be seen on the following pages (the species in italics represent the library peaks plotted on the XRPDs):

1. γ–Alumina, *γ–alumina*
2. Sulphated γ–alumina, *γ–alumina*
3. Platinised alumina, *γ–alumina*
4. Sulphated platinised alumina, *γ–alumina*
5. Ceria, *cerianite(CeO_2)*
6. Sulphated ceria, *cerianite(CeO_2)*
7. Platinised ceria, *cerianite(CeO_2)*
8. P_{12}, *cerianite(CeO_2), γ–alumina*
9. Platinised P_{12}, P_{12}
10. Sulphated P_{12}, sulphated platinised P_{12}
11. Sulphated platinised P_{12}, *cerium aluminate ($CeAlO_3$)*

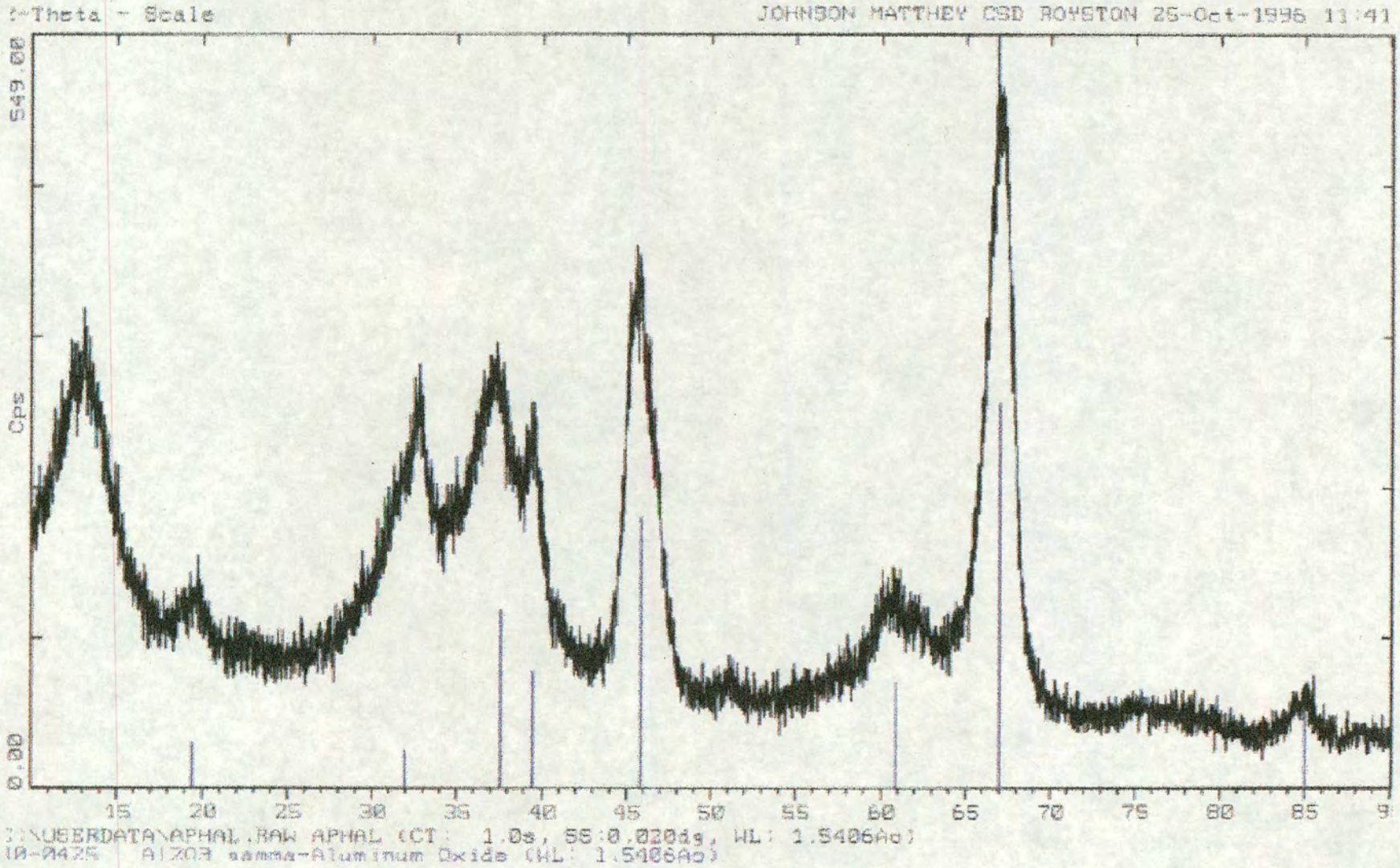
?~Theta ~ Scale
JOHNSON MATTHEY CSD ROYSTON 25-Oct-1996 11:41
649.00
Cps
0.00
15
20
25
30
35
40
45
50
55
60
65
70
75
80
85
9
?:\USERDATA\APHAL.RAW APHAL (CT: 1.0s, SS:0.020dg, WL: 1.5406Ao)
10-0425 Al2O3 gamma-Aluminum Oxide (WL: 1.5406Ao)

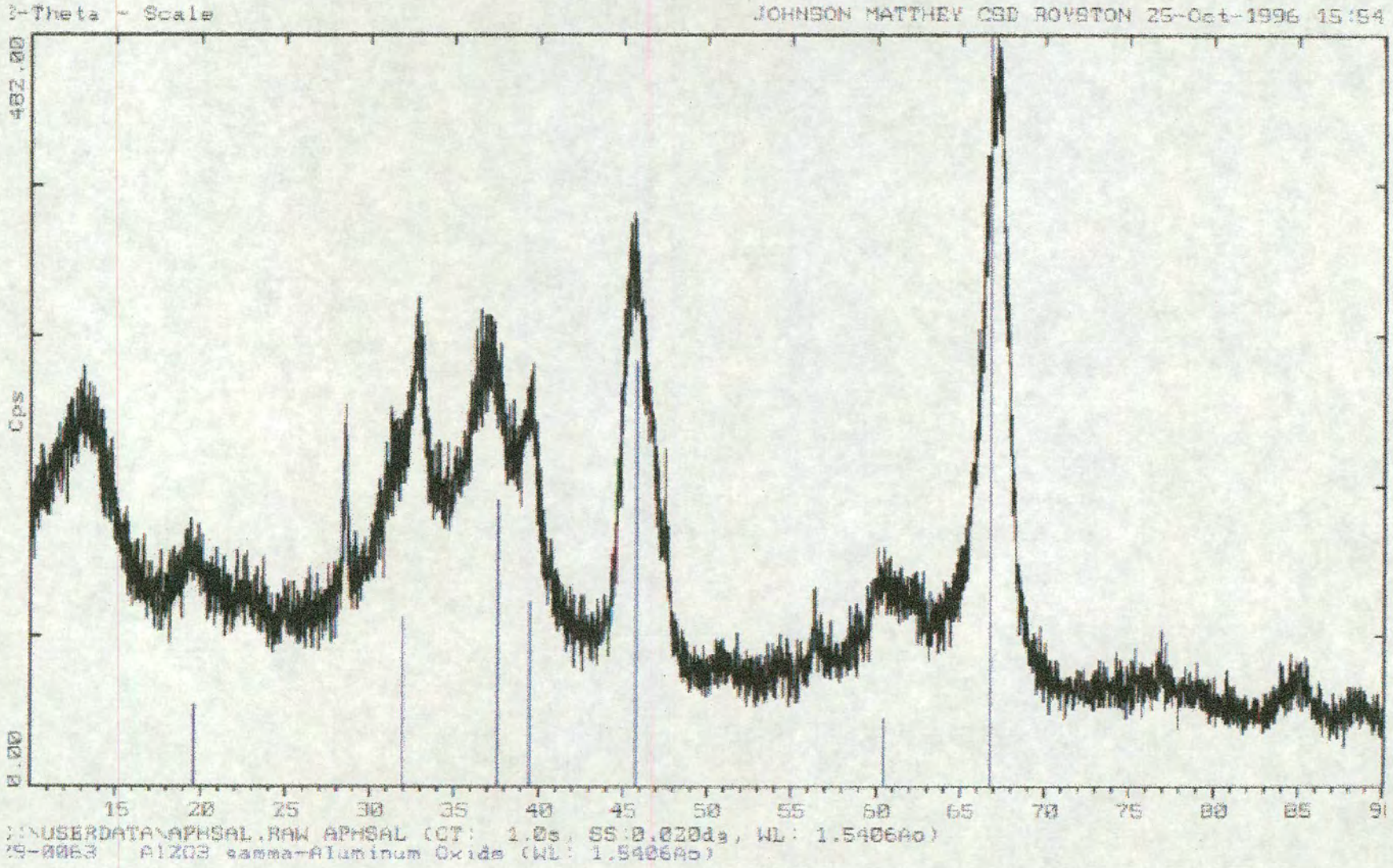
2-Theta - Scale
JOHNSON MATTHEY CSD ROYSTON 25-Oct-1996 15:54
482.00
Cps
0.00
15
20
25
30
35
40
45
50
55
60
65
70
75
80
85
C:\USERDATA\APHSAL.RAW APHSAL (CT: 1.0s, SS:0.020d, WL: 1.5406Ao)
29-0063 Al2O3 gamma-Aluminum Oxide (WL: 1.5406Ao)

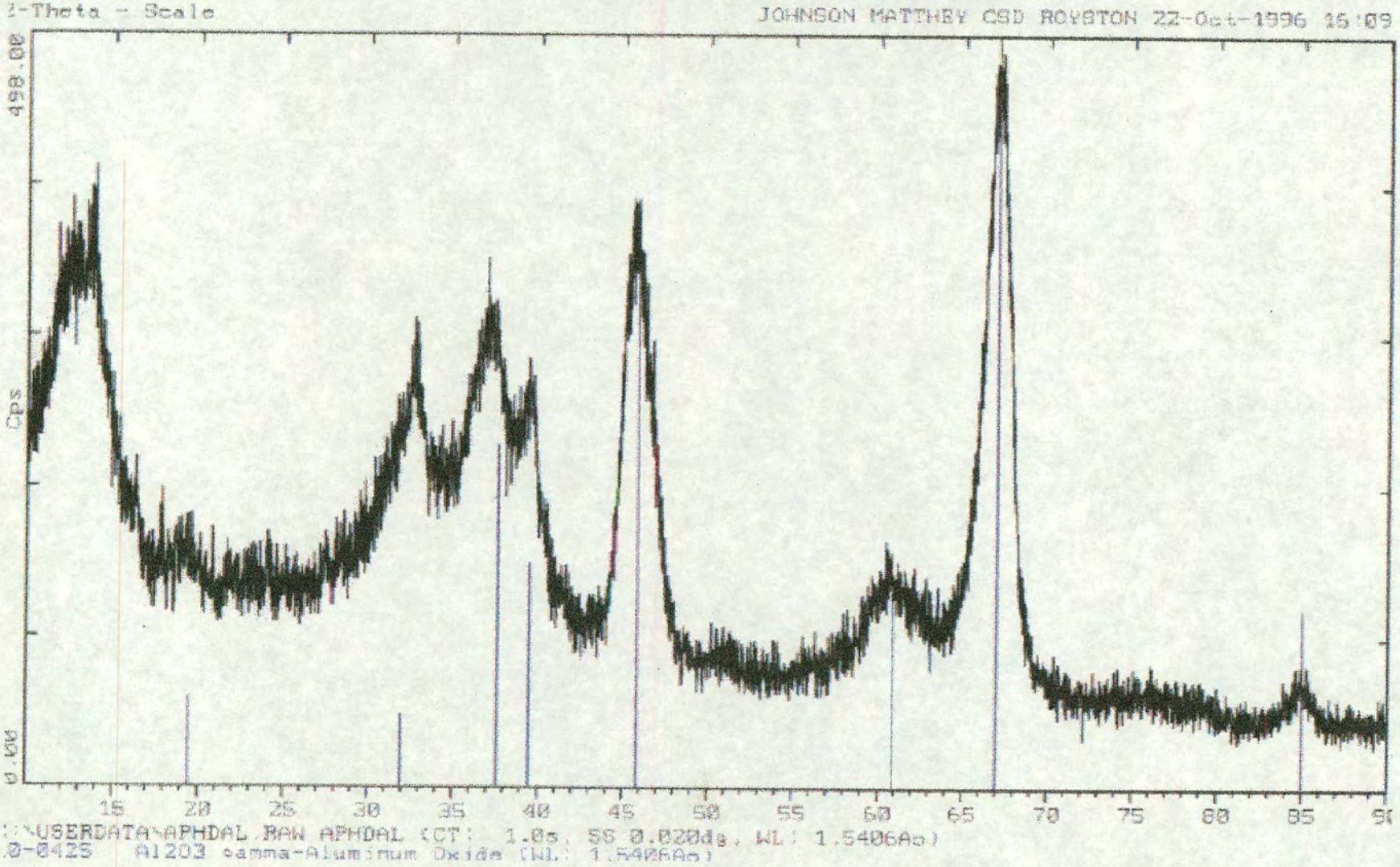
2-Theta - Scale
JOHNSON MATTHEY CSD ROYSTON 22-Oct-1996 15:09
458.00
Cps
0.00
15
20
25
30
35
40
45
50
55
60
65
70
75
80
85
90
:\USERDATA\APHDAL.RAW APHDAL (CT: 1.0s, SS 0.020d, WL: 1.5406Ao)
0-0425 Al2O3 gamma-Aluminum Oxide (WL: 1.5406Ao)

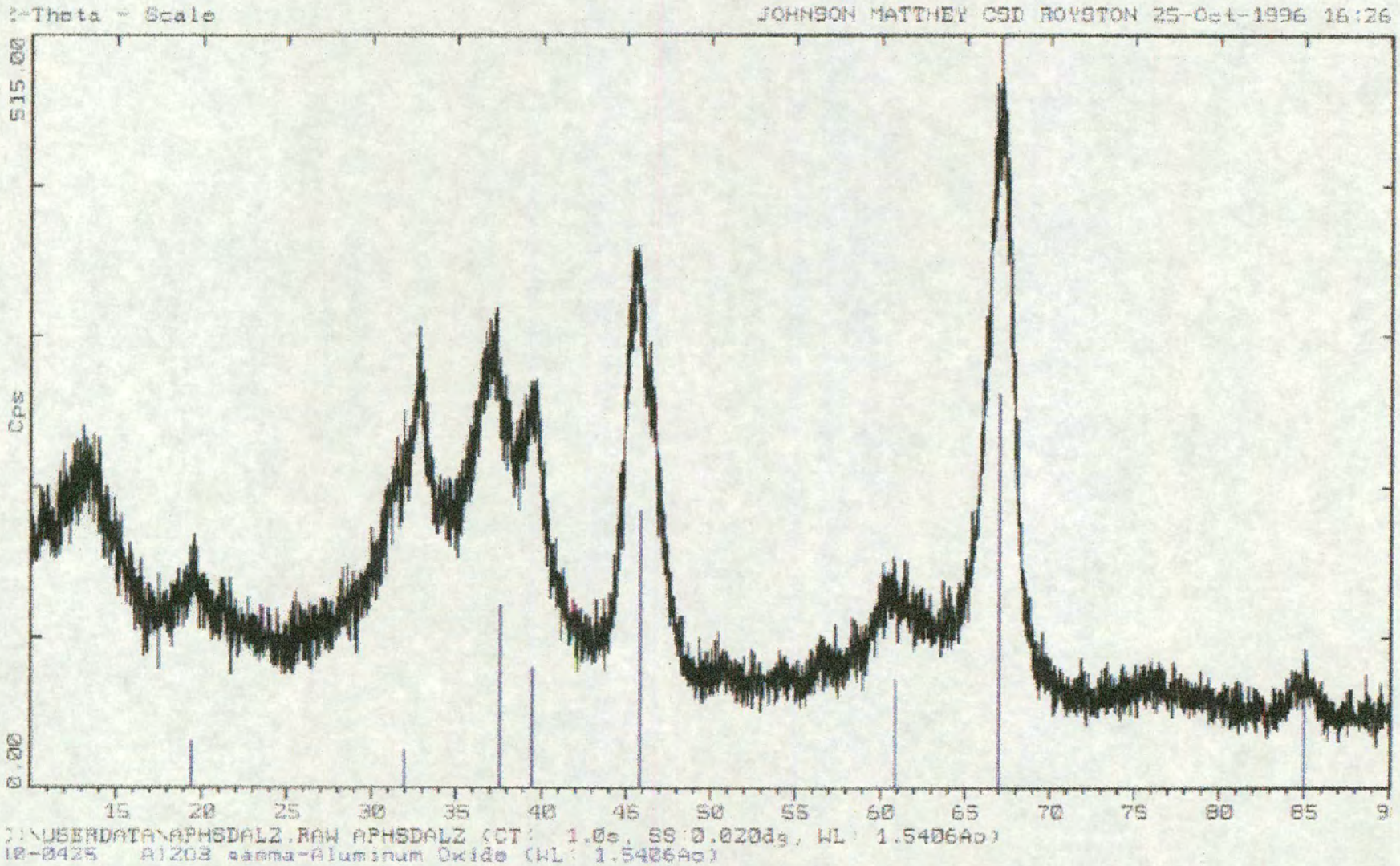
2~Theta ~ Scale
JOHNSON MATTHEY CSD ROYSTON 25-Oct-1996 16:26
15.00
Cps
0.00
15
20
25
30
35
40
45
50
55
60
65
70
75
80
85
C:\USERDATA\APHSDALZ.RAW APHSDALZ (CT: 1.0s, SS:0.020deg, WL: 1.5406Ao)
10-0425 Al2O3 gamma-Aluminum Oxide (WL: 1.5406Ao)

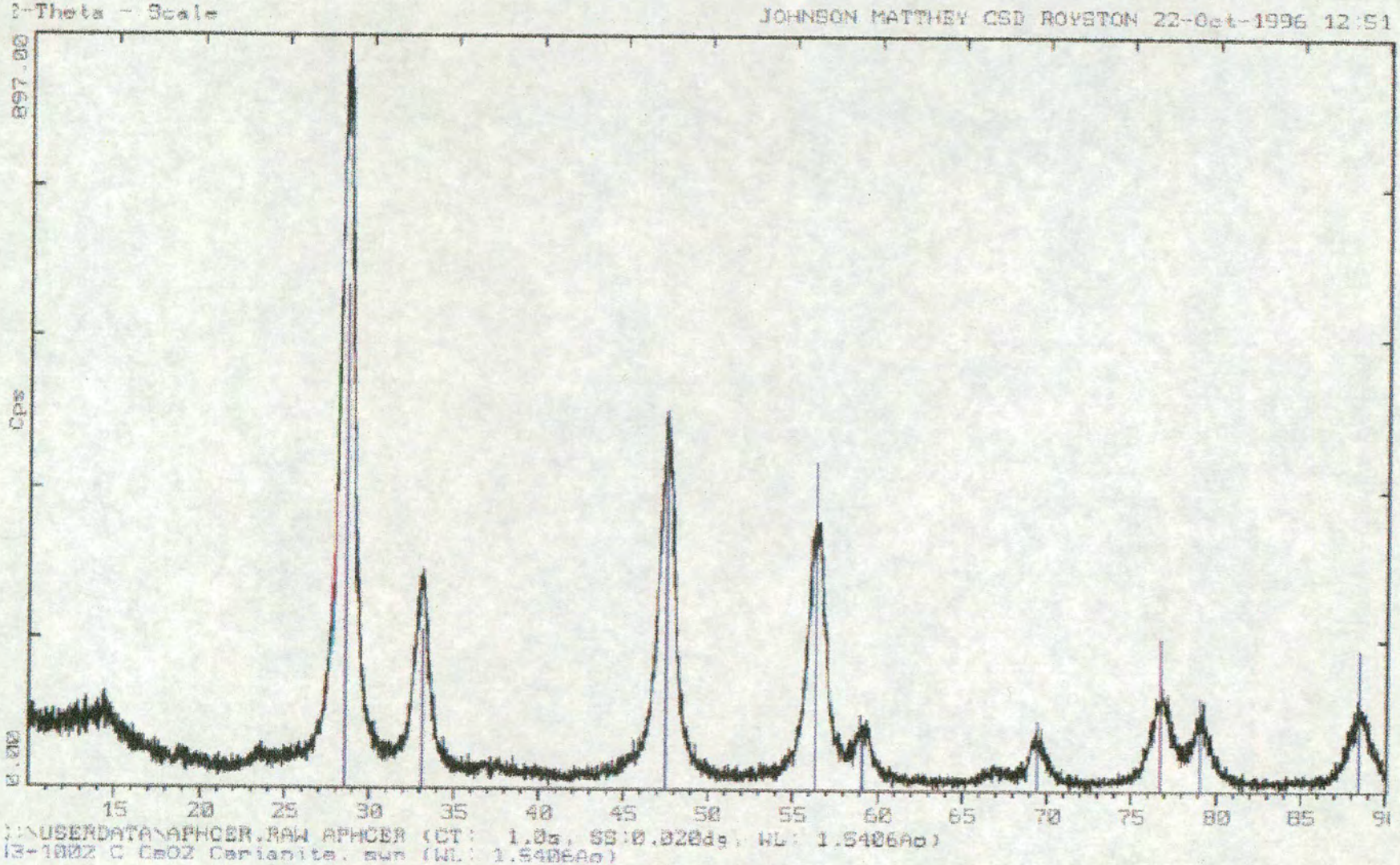
2-Theta - Scale
JOHNSON MATTHEY CSD ROYSTON 22-Oct-1996 12:51
897.00
Cps
0.00
15
20
25
30
35
40
45
50
55
60
65
70
75
80
85
C:\USERDATA\APHCER.RAW APHCER (CT: 1.0s, SS:0.020dg, WL: 1.5406Ao)
03-1002 C CeO2 Cerianite, syn (WL: 1.5406Ao)

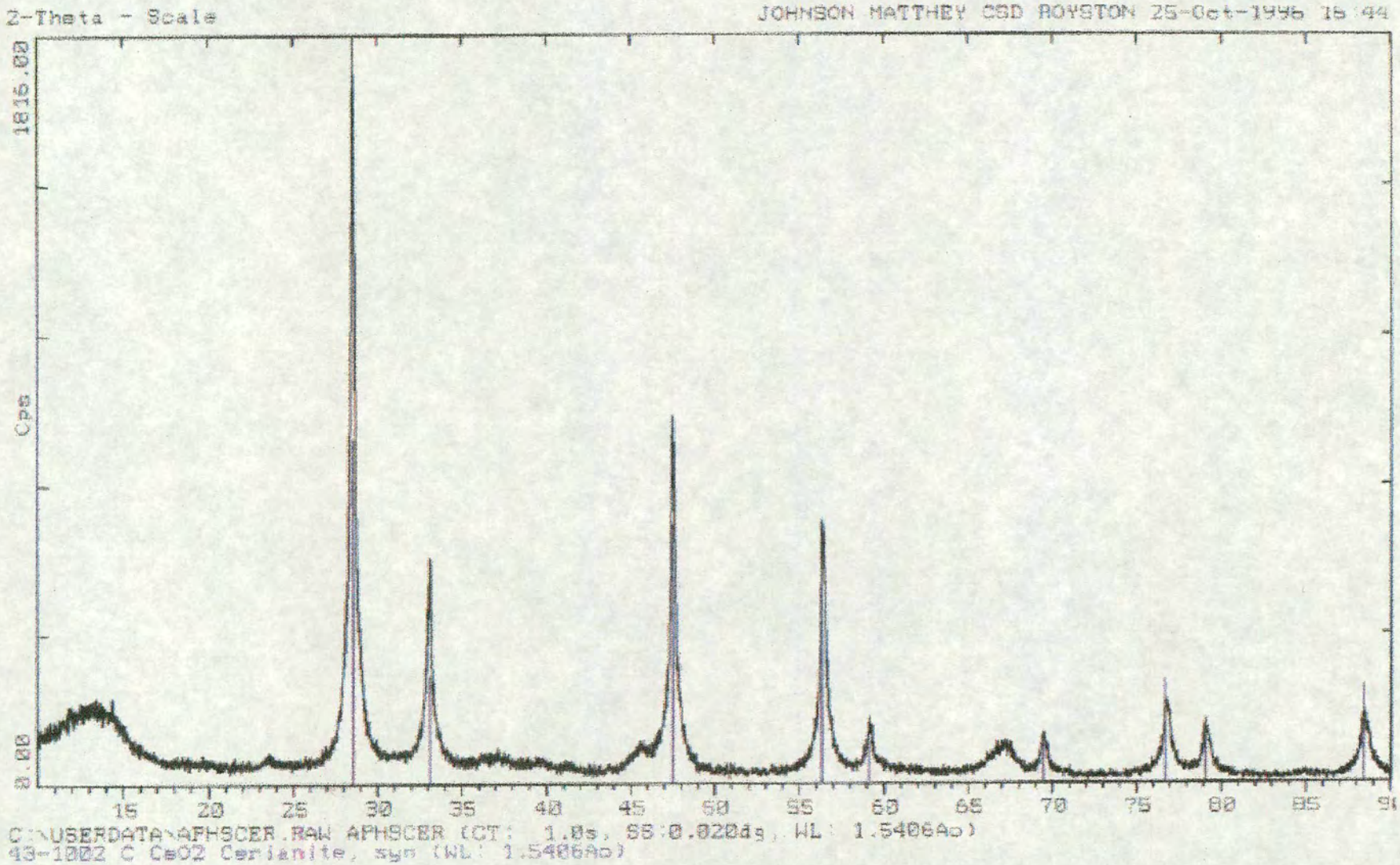
2-Theta - Scale
JOHNSON MATTHEY CSD ROYSTON 25-Oct-1996 16:44
1815.00
Cps
0.00
15
20
25
30
35
40
45
50
55
60
65
70
75
80
85
C:\USERDATA\APHSCER.RAW APHSCER (CT: 1.0s, SS:0.020dg, WL: 1.5406Ao)
43-1002 C CeO2 Cerianite, syn (WL: 1.5406Ao)

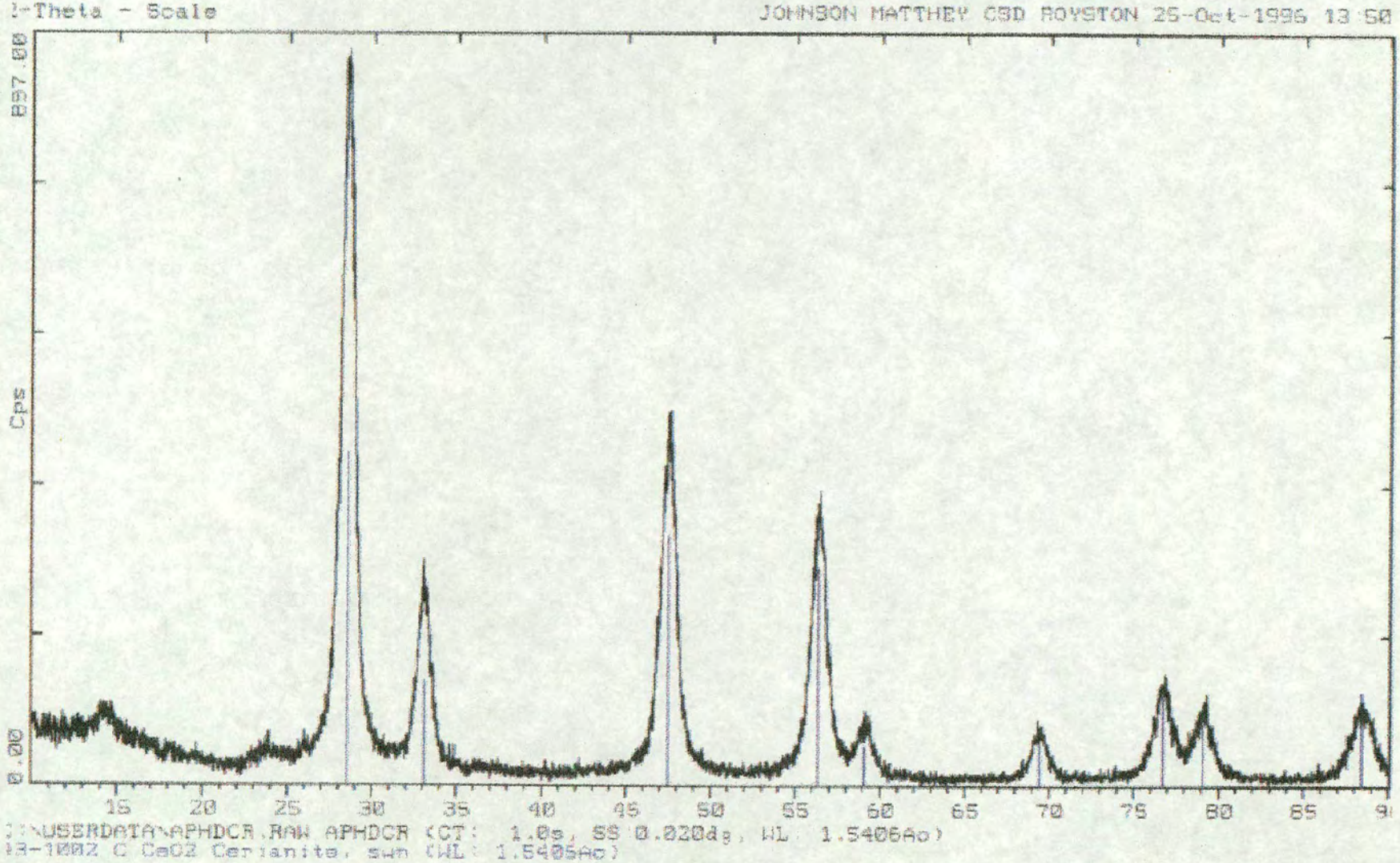
?-Theta - Scale
JOHNSON MATTHEY CSD ROYSTON 25-Oct-1996 13:50
857.00
Cps
0.00
15
20
25
30
35
40
45
50
55
60
65
70
75
80
85
9
):\USERDATA\APHDCR.RAW APHDCR (CT: 1.0s, SS 0.020d$, WL: 1.5406Ao)
43-1002 C CeO2 Cerianite, syn (WL: 1.5405Ac)

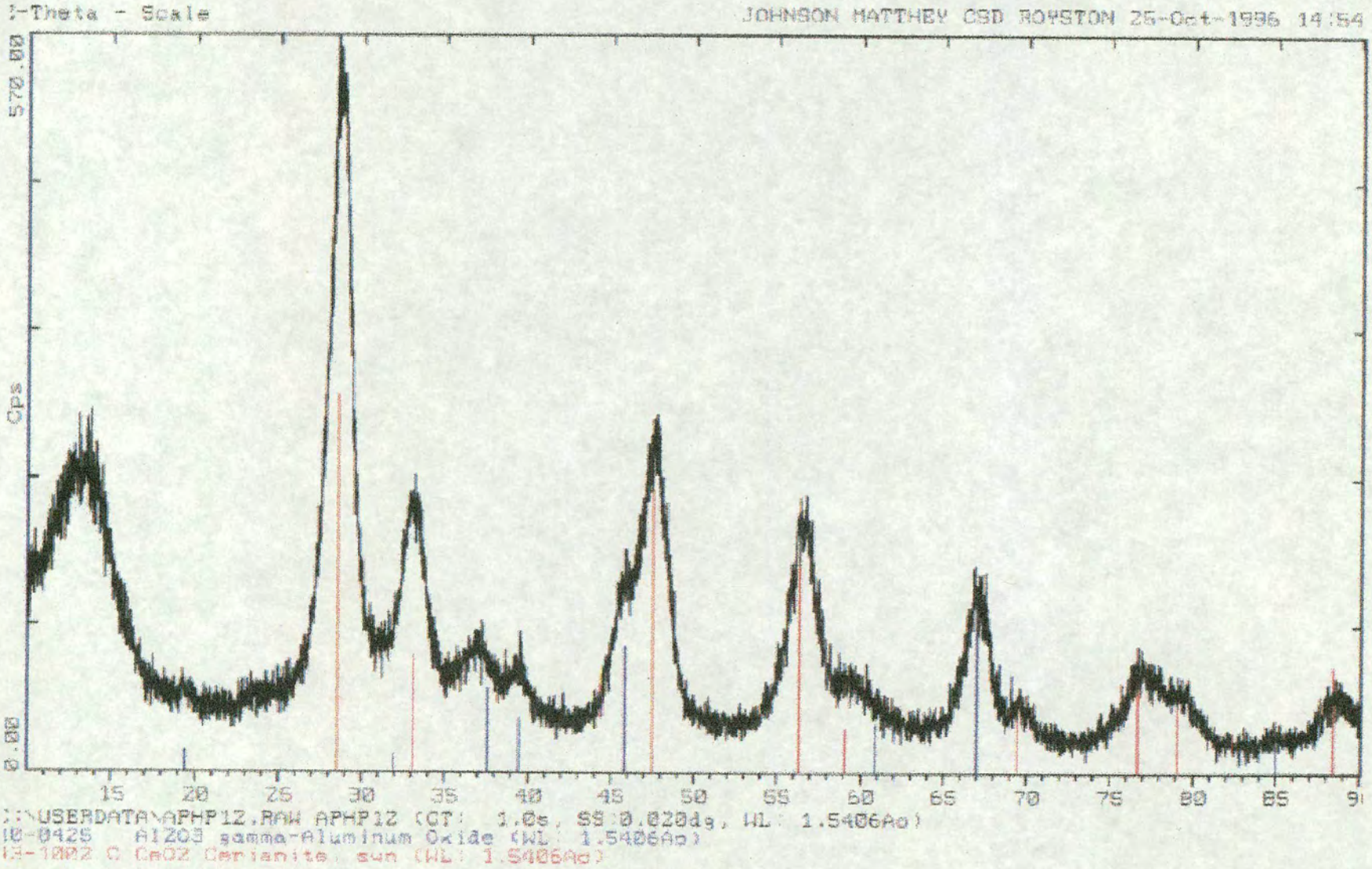
?-Theta - Scale
JOHNSON MATTHEY CSD ROYSTON 25-Oct-1996 14:54
80.00
Cps
0.00
15
20
25
30
35
40
45
50
55
60
65
70
75
80
85
C:\USERDATA\APHP12.RAW APHP12 (CT: 1.0s, SS:0.020d, WL: 1.5406Ao)
10-0425 Al2O3 gamma-Aluminum Oxide (WL: 1.5406Ao)
43-1002 C CeO2 Cerianite, syn (WL: 1.5406Ao)

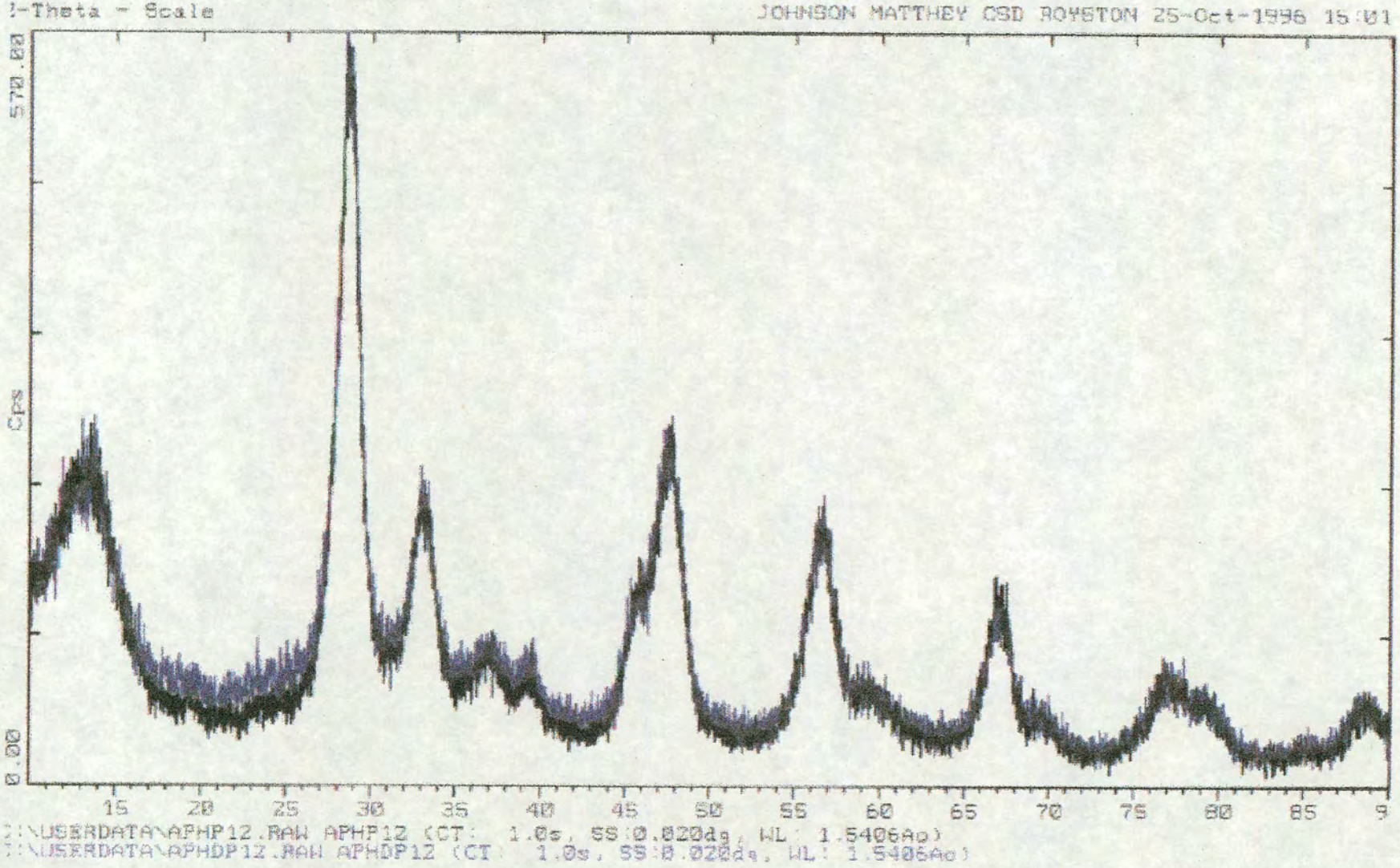
2-Theta - Scale
JOHNSON MATTHEY CSD ROYSTON 25-Oct-1996 15:01
Cps
15
20
25
30
35
40
45
50
55
60
65
70
75
80
85
C:\USERDATA\APHP12.RAW APHP12 (CT: 1.0s, SS:0.020dg, WL: 1.5406Ao)
C:\USERDATA\APHDP12.RAW APHDP12 (CT: 1.0s, SS:0.020dg, WL: 1.5406Ao)

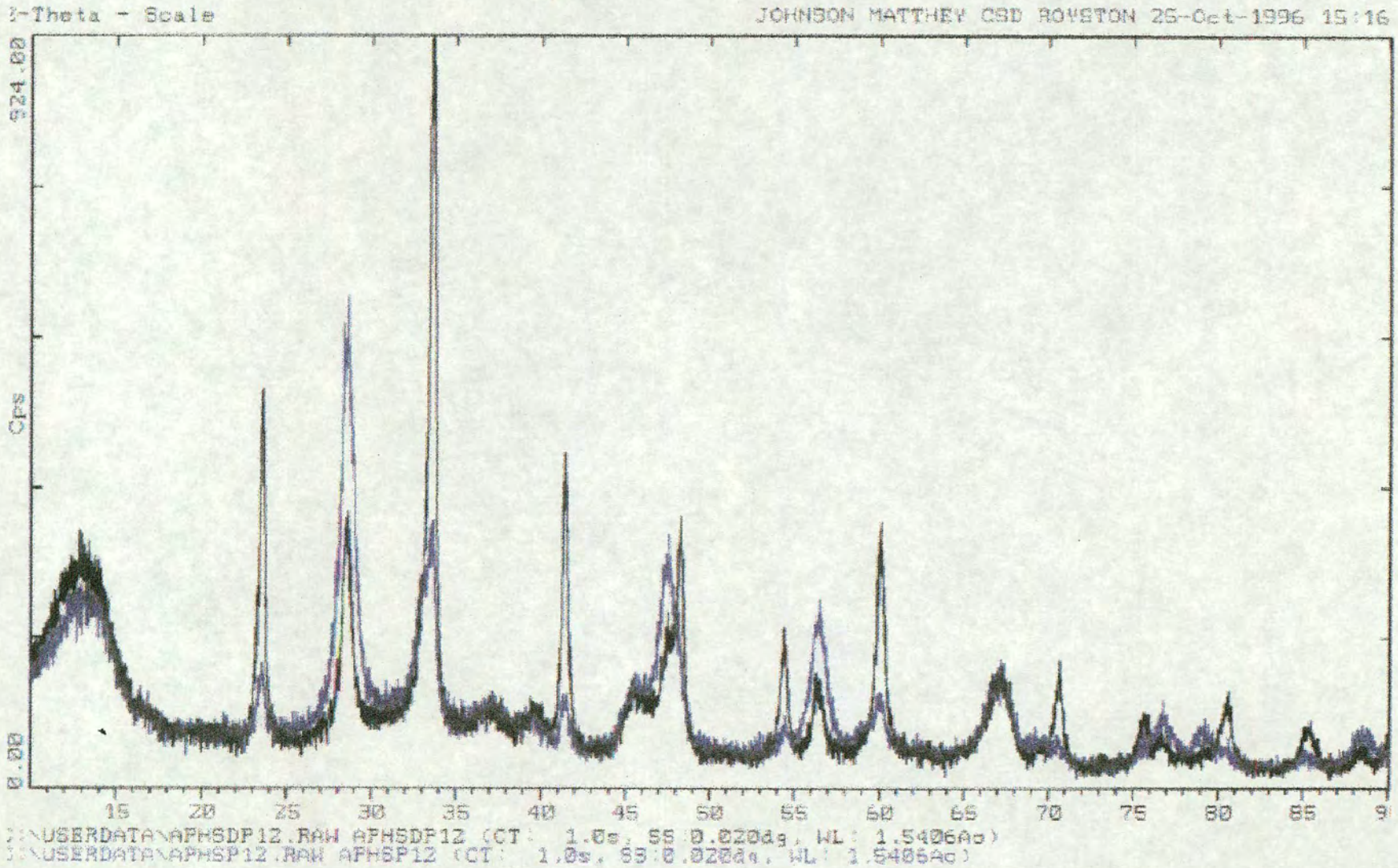
2-Theta - Scale
JOHNSON MATTHEY CSD ROYSTON 25-Oct-1996 15:16
524.00
Cps
0.00
15
20
25
30
35
40
45
50
55
60
65
70
75
80
85
C:\USERDATA\APHSDP12.RAW APHSDP12 (CT: 1.0s, SS:0.020dg, WL: 1.5406Ao)
C:\USERDATA\APHSP12.RAW APHSP12 (CT: 1.0s, SS:0.020dg, WL: 1.5406Ao)

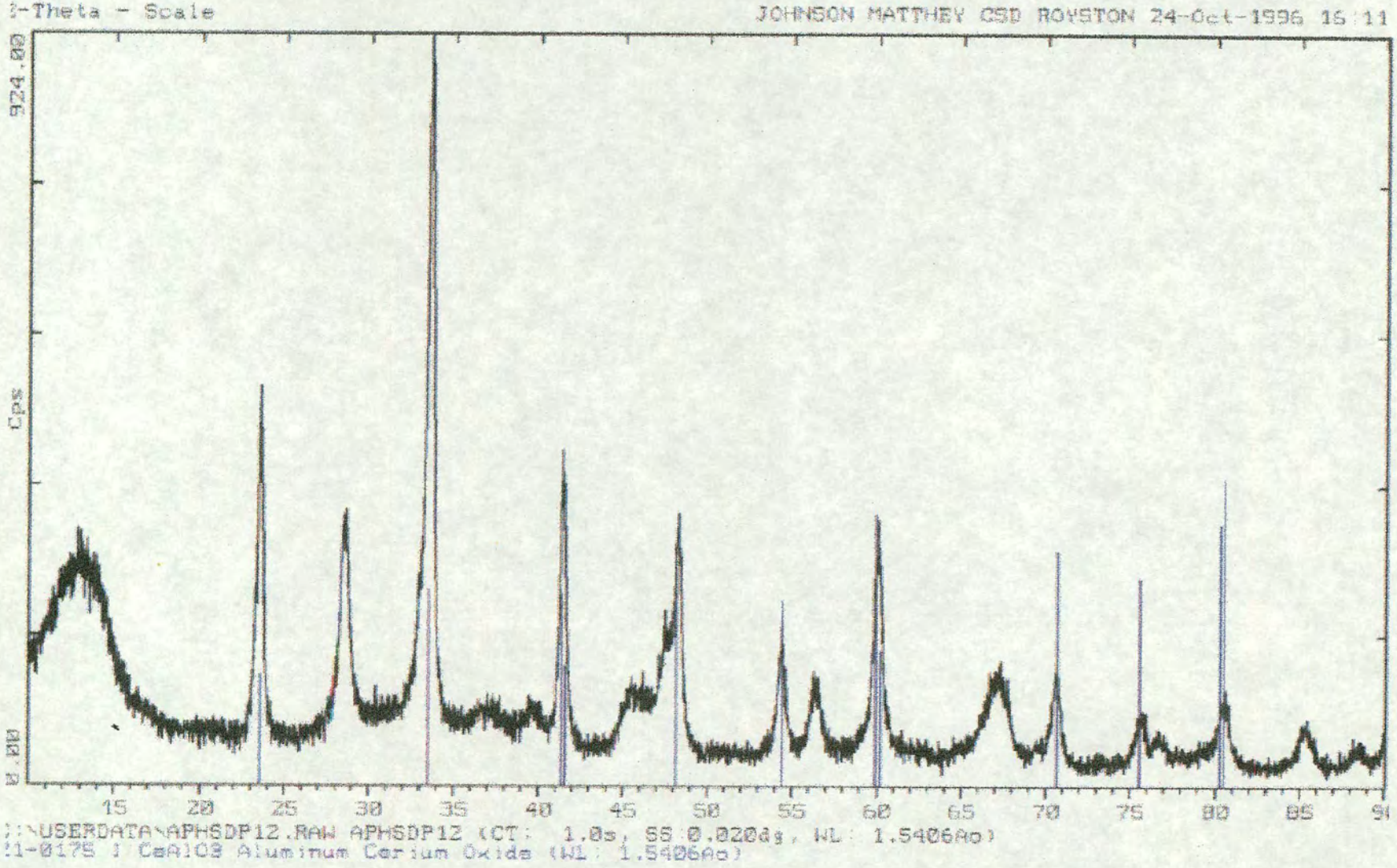
?-Theta - Scale
JOHNSON MATTHEY CSD ROYSTON 24-Oct-1996 15:11
924.00
cps
88.0
15
20
25
30
35
40
45
50
55
60
65
70
75
80
85
90
;:\USERDATA\APHSDP12.RAW APHSDP12 (CT: 1.0s, SS:0.0204s, WL: 1.5406Ao)
?1-0175 I CeAlO3 Aluminum Cerium Oxide (WL: 1.5406Ao)

7.2 The Theory of Temperature Programming

Temperature programmed experiments are usually performed with a linear heating schedule, thus:

$T=T_o+\beta t$

Where T_o is the initial temperature, T, the temperature at time, t, and β is the linear ramp rate. Ideally (i.e. without significant diffusional or convective effects[100]) for a single reactant, the mass balance can be written:

$$u\frac{\partial C_g}{\partial z} = -V_m \frac{\partial \vartheta}{\partial t}$$

..and..

$$-\frac{\partial \vartheta}{\partial t} = R_d - R_a$$

where C_g is the gas phase concentration, z is the distance through the bed, u the interstitial velocity, V_m is the number of moles of surface sites per unit volume, θ is the fractional coverage (dimensionless), R_d is the rate of desorption (in s^{-1}) and $R_{a,}$ the rate of desorption.

Readsorption can be an extremely important factor in temperature-programmed experiments. If differential bed conditions can be assured, then the first equations of this appendix can be reduced to[101]:

$$-\frac{d\vartheta}{dt} = k_d(\vartheta)\vartheta^n - k_a C_g(1-\vartheta)^p$$

$$FC_g = V_c V_m k_d(\vartheta)\vartheta^n - V_c V_m k_a C_g(1-\vartheta)^p$$

Which can be combined to give:

$$-\frac{d\vartheta}{dt} = \frac{F}{\beta}\left(\frac{k_d(\vartheta)\vartheta^n}{F + V_c V_m k_a (1-\vartheta)^p}\right)$$

---

[100] This can be achieved by good design, and confirmed by testing

[101] (θ) denoting a function of θ

Hence, for no readsorption ($F>>V_cV_mk_a(1-\theta)^p$):

$$-\frac{d\vartheta}{dt}=\frac{\nu_n(\vartheta)}{\beta}e^{-\frac{E_d}{RT}}\vartheta^n$$

..and for free readsorption ($F<<V_cV_mk_a(1-\theta)^p$):

$$-\frac{d\vartheta}{dt}=\frac{F}{V_cV_m\beta}\frac{\nu_n(\vartheta)}{\nu_a}e^{-\frac{\Delta H(\vartheta)}{RT}}\frac{\vartheta^n}{(1-\vartheta)^p}$$

Using an Arrhenius form for the rate constant, with the activation energy and pre-exponential factors expressed as functions of surface coverage.

The analysis becomes somewhat more complex for TPR. Indeed, Falconer and Schwarz state that "a complete theoretical description to explain TPR of single and multiple reactants is unlikely". Nonetheless, some of the analysis techniques reviewed in Falconer and Schwarz have been applied to the results of the TPRs, generating the table in section 4.1.8. The results of assuming first order desorption are given in section 4.1.8. First order is assumed, as the excess of hydrogen present may render the kinetics pseudo first order (second order can also be calculated), but it is difficult to say whether the figures generated are meaningful, as the order is unknown. The principal aim of the temperature programmed experiments is to compare the standard TPRs produced by the various formulations in the matrix in terms of reduction temperature and peak characteristics.

Analytical techniques to determine the reaction order from the peak shapes have proved unsuccessful, although some peaks are, qualitatively, similar to first or second order peak shapes.

7.3 Scanning Electron Micrographs

Although SEM did not prove particularly informative, a number of micrographs are included here to illustrate the porosities and size distributions of various components that were used in the course of this research. The following list details the micrographs shown on the next 6 pages:

1. P_0 alumina in powder form (upper) and ceria in powder form (lower)
2. P_{12} powder form
3. Platinised P_{12} in powder form (upper) and platinised ceria in powder form
4. Sulphur dioxide treated platinised P_{12} in the form of chips (upper) and sulphur dioxide treated platinised alumina, also in the form of chips (lower)
5. Barium carbonate (both)
6. Iron (III) oxide (both)

A number of components were prepared at the beginning of this project, but were ultimately not used, although SEM micrographs were taken. The barium carbonate and iron oxide micrographs are samples of these. They illustrate that the microscopic form of these catalyst components can vary considerably more than that of alumina and ceria (and their platinised and sulphur dioxide-treated analogues). The barium carbonate exhibits no visible porosity at this magnification, whereas the iron oxide is clearly very porous. The iron oxide is in the form of hollow, holed spheres; this is due to the spray-drying method employed in its production.

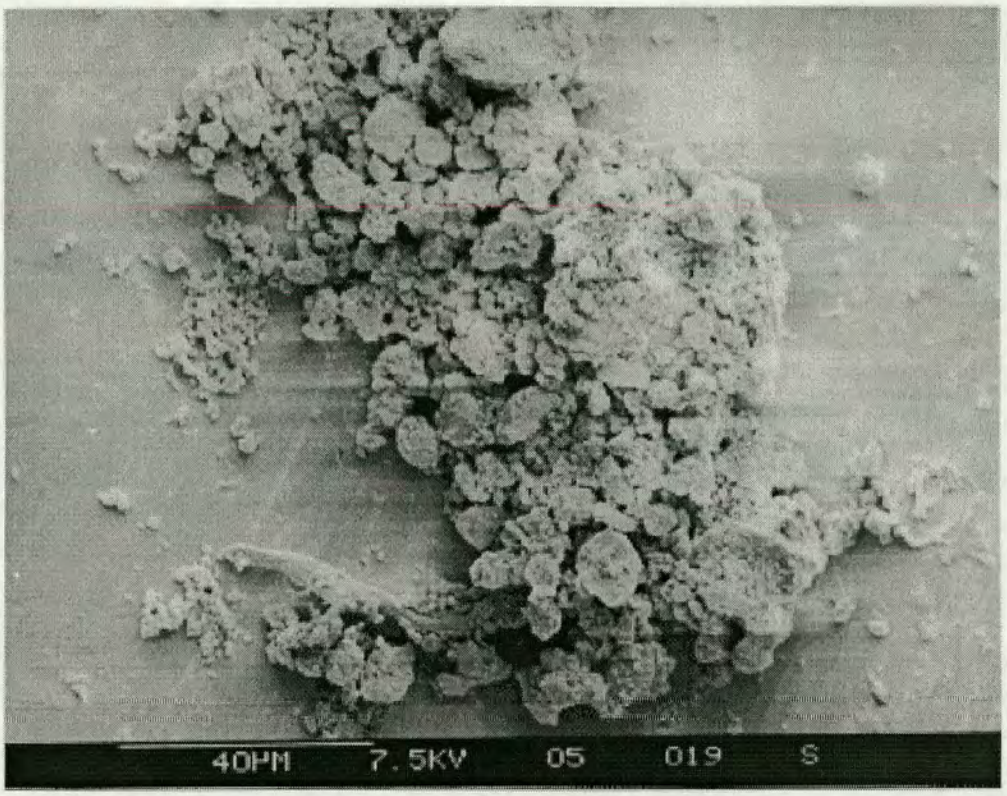
40PM 7.5KV 05 019 S

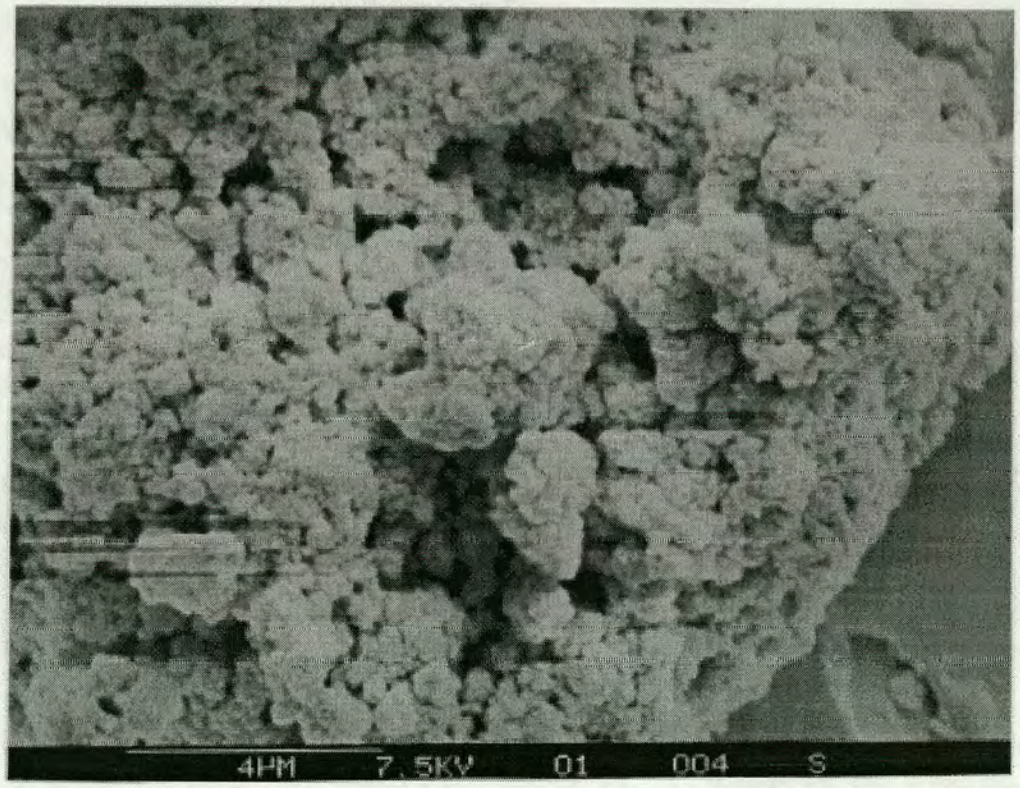
4PM 7.5KV 01 004 S

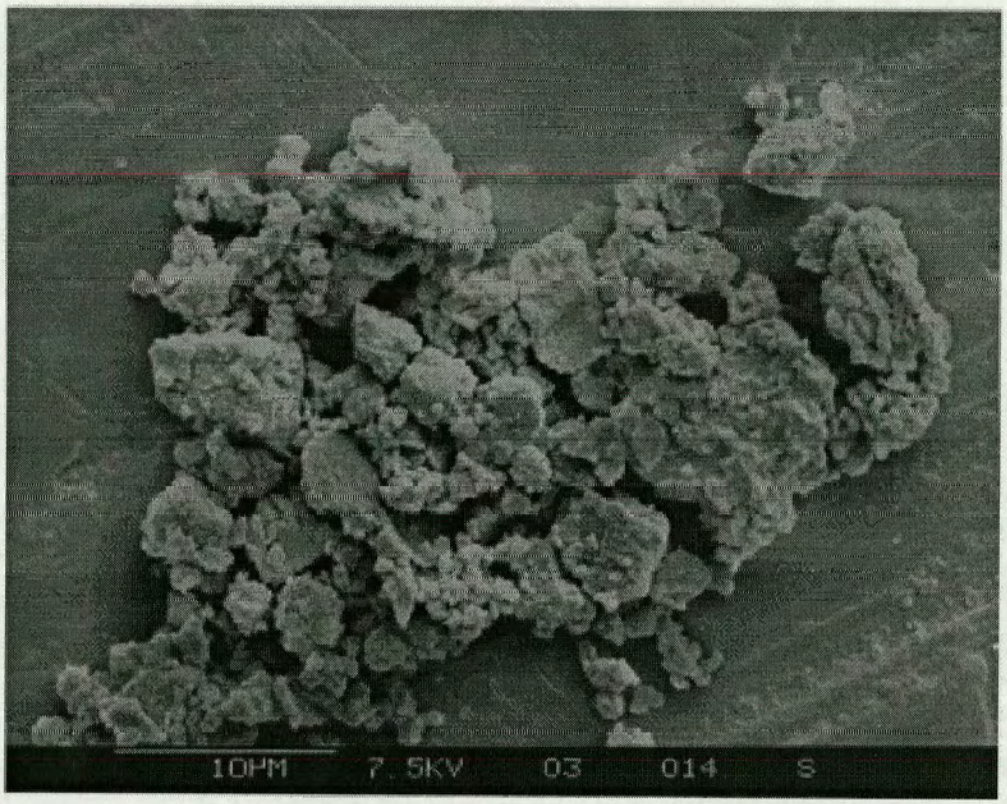
10PM
7.5KV
03
014
S


10PM 7.4KV 01 004 S

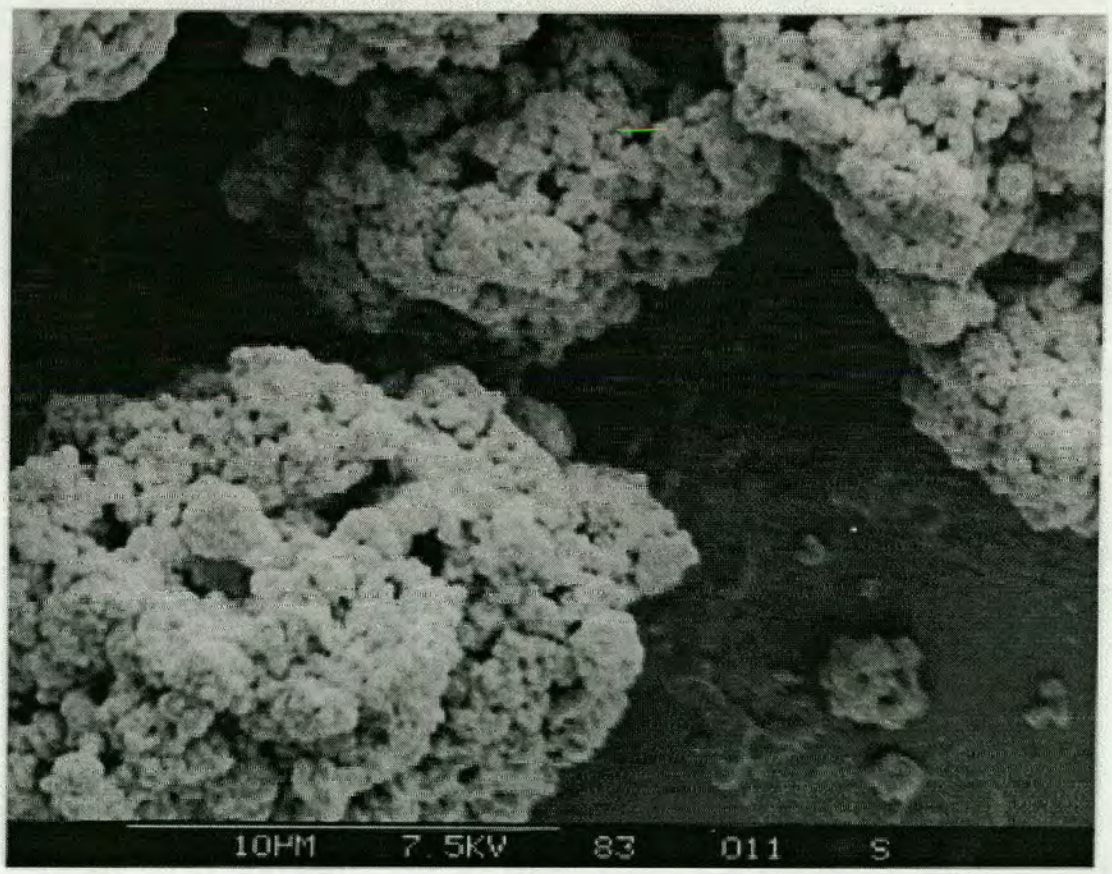
10PM 7.5KV 83 011 S

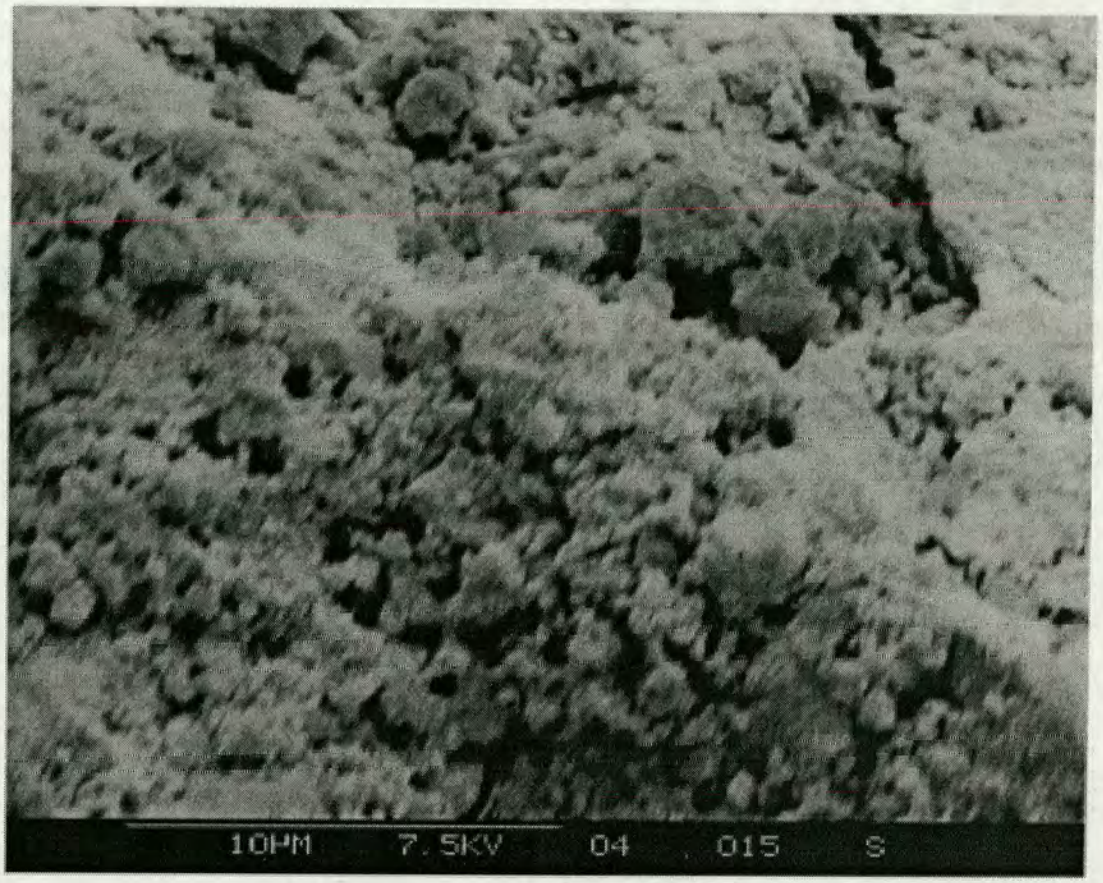
10UM 7.5KV 04 015 S

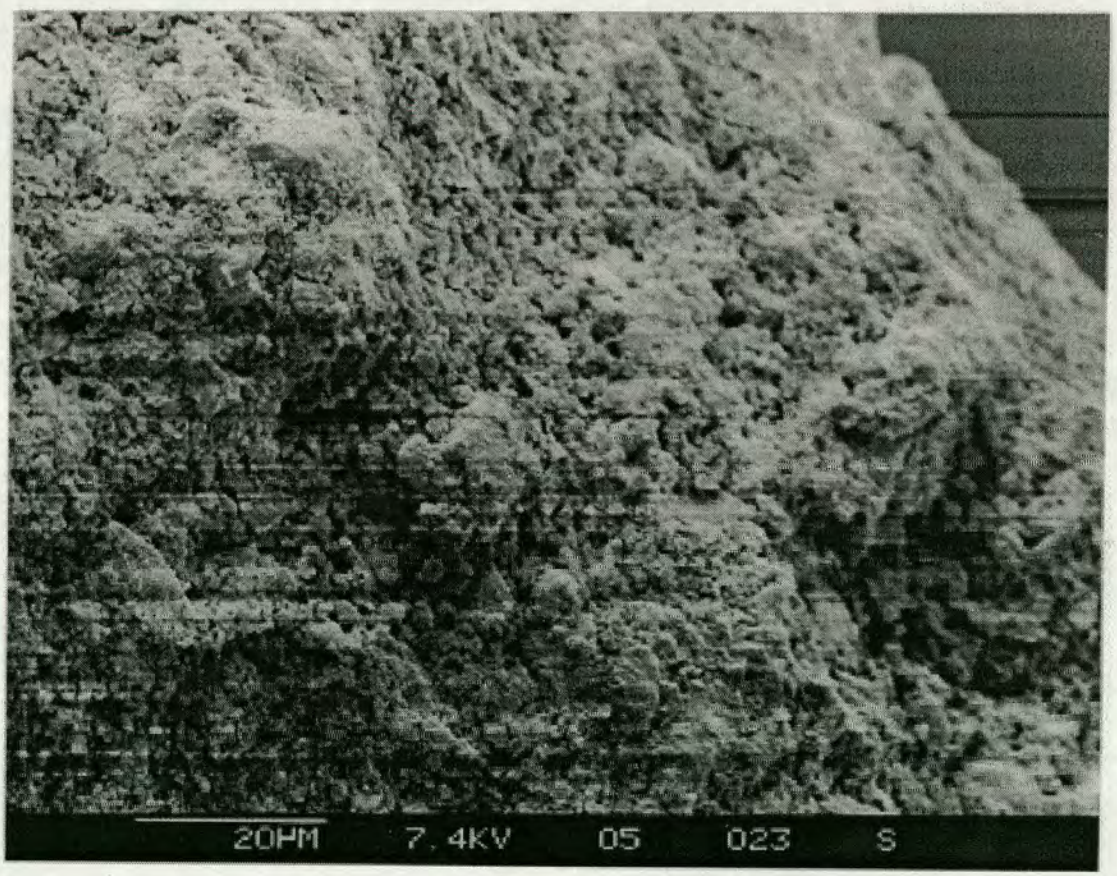
20UM 7.4KV 05 023 S

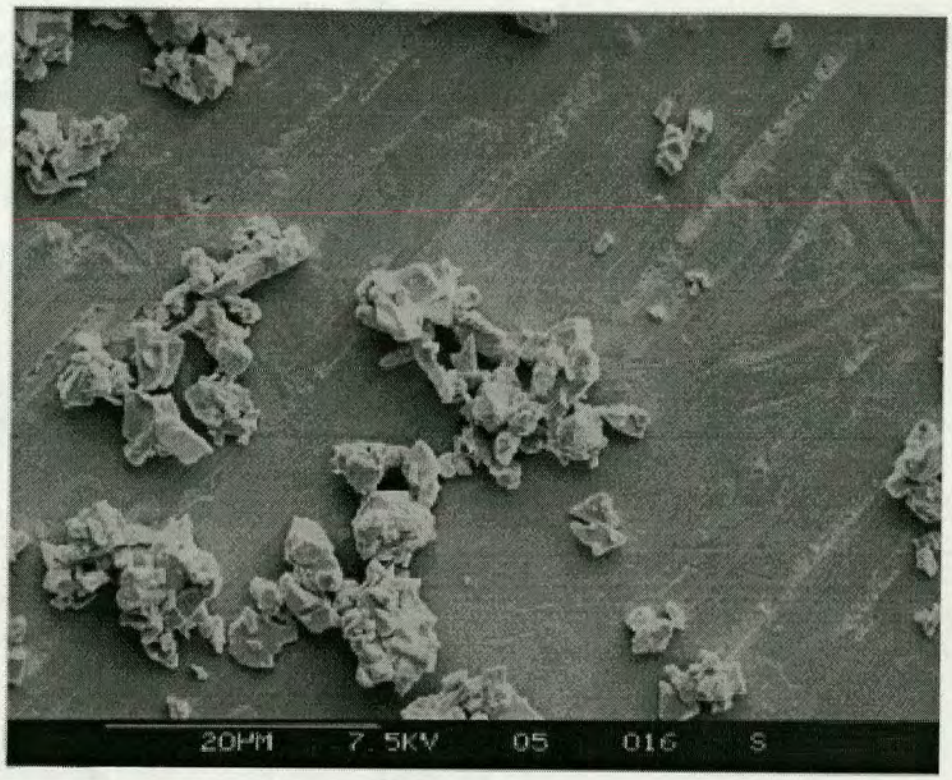
20UM 7.5KV 05 016 S

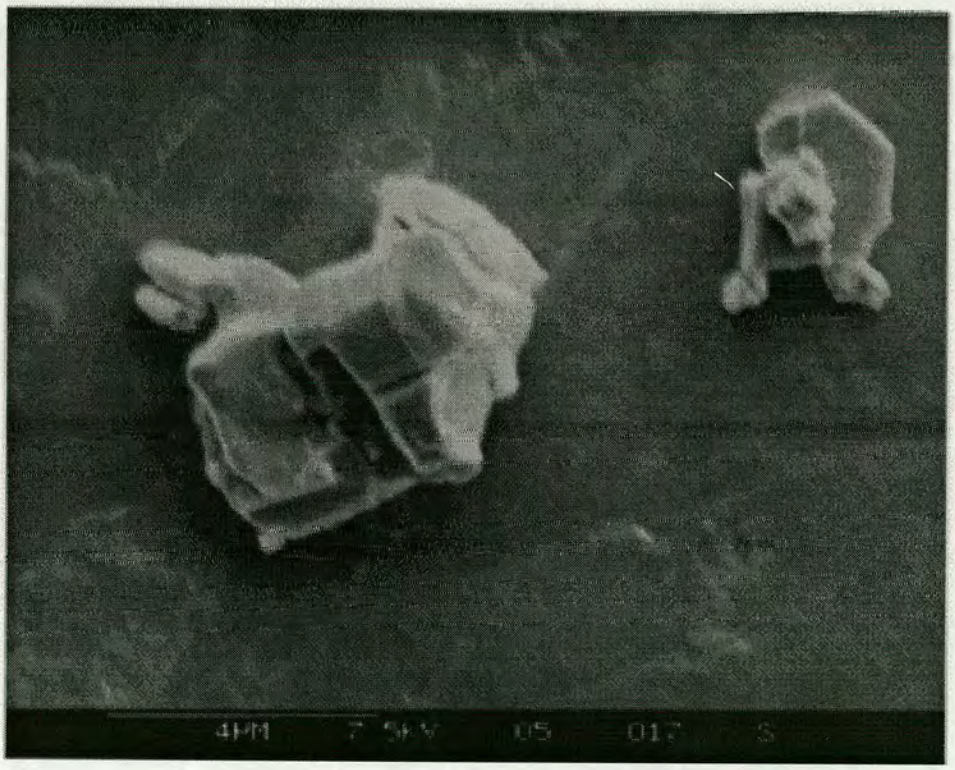
4UM 7.5KV 05 017 S

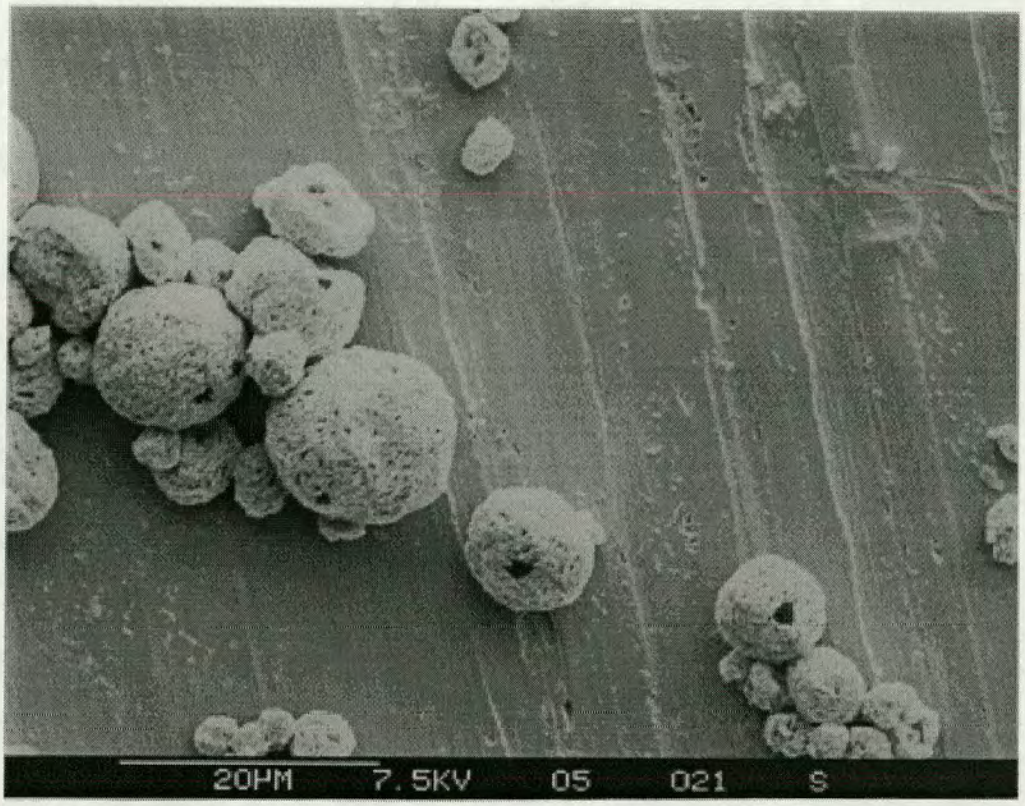
20PM 7.5KV 05 021 S

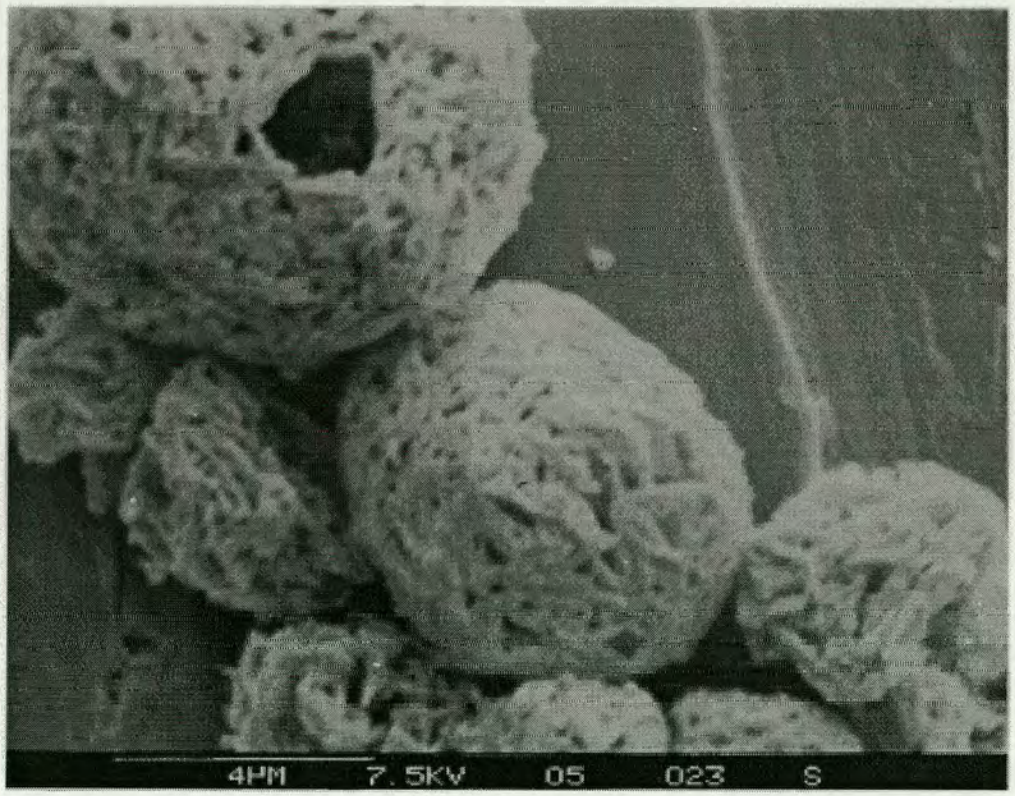
4PM 7.5KV 05 023 S

7.4 Errors

All temperatures quoted for the catalyst test apparatus were within +/-1°C of the Eurotherm temperature controller set-point temperature. The temperatures quoted have proved to be very reproducible.

Temperatures quoted in the DRIFTS work were within +/- 10 °C, because the temperature of the DRIFTS apparatus was not controlled by the Eurotherm, but by the voltage setting of the variac and tended to fluctuate continuously, perhaps due to voltage fluctuations. The Eurotherm controller could not be used to control the temperature of the DRIFTS rig, as it tended to put the system through temperature gradients which were too steep, resulting in unsustainable rates of expansion of components of the HTEC.

The resolution of the photometers was 5 ppm (hydrogen sulphide), 2 ppm (carbon monoxide and sulphur dioxide) and 1 ppm (carbon dioxide). The URAS 10E photometer is subject to non-linearity errors of up to 2 % of span, which correspond to possible inaccuracies of up to 10, 16 and 4 ppm for the CO_2, SO_2 and CO readings. Analysis of the steady state readings reveals that drifts are negligible on the time scale of a typical experiment. Standard deviations in 'constant' values were found to be 2.3 ppm for hydrogen sulphide, 0.64 ppm for sulphur dioxide and 0.0211 vol. % for the TCD.

The three measured flowrates through the TCD, URAS 10E and Radas 2 were correct to 1, 5 and 10 cc/min respectively, leading to a maximum +/-16 cc/min. error for the total flowrate. The flows were constantly monitored by rotameters, which were initially calibrated against soap-film meters, and checked at regular intervals, and when flows deviated from the set-points. The possible calibration errors were considerably smaller than the rotameter reading errors quoted above.

In many experiments in reactor engineering it is possible to test the flow of a non-reactive tracer through the packed bed and compare the response to the dispersion model. In the case of a non-isothermal, reactive system, an extremely large amount of data would be required to even establish an empirical model. Such a model was not the objective of this research. Instead the following policies were adopted:

1. All experiments have been duplicated at least once. Certain experiments have been repeated several times. The results have assured a high degree of reliability in the system. Peak shapes and temperatures proved to be freely reproducible.

2. A large number of experiments were to be performed (all repeated at least once with satisfactory correlation between experiments) to create a matrix of experimental results from which direct comparisons can be made.

7.5 Reaction Equilibria

This appendix gives the equilibrium data for a number of reactions specified in this text. Twigg (1989) gives a number of values for the $SO_2 + 1/2\ O_2 \rightarrow SO_3$ reaction, e.g.;

Temperature (K)	K_p ($atm^{1/2}$)
700	287.7
800	34.75
900	6.730
1000	1.816

Hence, experimental work was conducted with sulphur trioxide detection by infrared gas analysis, which ultimately showed that sulphur trioxide is not produced, probably due to its adsorption by the sample.

A number of other gas phase reactions are possible. The thermodynamic feasibility of the reaction $COS+H_2O \rightarrow H_2S+CO_2$ was calculated at a number of relevant temperatures. In the experiments performed here this reaction is only ever likely to occur during a switchover, as this is the only occasion where carbon dioxide and hydrogen sulphide are both present. However, experiments performed with infrared gas analysis have shown that COS is never emitted and this is probably due to the small amounts of both gases and the presence of water. The data below shows that the equilibrium is also against the formation of COS.

T(K)	400	500	600	700	800	900	1000	1100
$\Delta g^o/T$	-82.7	-65.7	-54.3	-46.1	-40.0	-35.2	-31.5	-28.5
K_p	20932	2701	683	255	122.3	69.3	44.3	30.9

The water-gas shift reaction, $CO_2+H_2 \rightarrow CO+H_2O$, must also be considered. No significant amounts of carbon monoxide were observed, and this is due to the fact that, again, the circumstances occur only fleetingly, during a switchover, although the thermodynamics may be favourable (K_p is highest, at~ 1, for a 700 °C switchover (Modell and Reid (1974)).

Other reactions which should be considered are:

- $H_2 + ½ O_2 \rightarrow H_2O$. Again this occurs only briefly, but is responsible for the appearance of water during switchover experiments. The thermodynamics of this reaction, as expected, are extremely favourable ($K_p > 10^9$ $atm^{-1/2}$)
- $CO + ½ O_2 \rightarrow CO_2$ is extremely favourable at these temperatures ($K_p > 10^9$ $atm^{-1/2}$) which may also help to explain the absence of CO.
- $1/3 SO_2 + 2/3 H_2S \rightarrow ½ S_2$ (g) + $2/3 H_2O$, the Claus reaction) is slightly favoured at higher temperature ($K_p \sim 1.9$ $atm^{3/2}$ at 700 °C), but the relatively large amount of water and the ppm levels of SO_2 and H_2S (which are seldom around at relatively high concentrations simultaneously) may act against the formation of S_2(g). To the author's knowledge, the production of sulphur gas (or liquid) has never been reported from automobile catalytic converters.

7.6 Data Logging and Valve Operation Software

The following pages list the C programs that were written to perform the various tasks required in the experimental runs. The purposes of these are detailed in section 3.1.8.

1. observe.c

```
/*
   ------------------------------------------------------------------
------------
   Program: observe.c
   Release: 1
   Author: A.P. Harvey
   Last Update: 21-05-95
   Purpose: To receive the readouts from the H2S meter, TCD,
temperature
   controller and 4-way gas meter and to send all these to a data
file,
   without operating the GIV at all. Data points every 10s or when
SO2
   value deviates from previous one by specified amount.
   ------------------------------------------------------------------
------------
*/

#include <stdio.h>
#include <time.h>
#include <stdlib.h>
#include <string.h>

#include "pclface.h"
/*
   ------------------------------------------------------------------
------------
   Main Program
   ------------------------------------------------------------------
------------
*/

int main ( int argc, char *argv[] )
{
  long int count[9] = {0,0,0,0,0,0,0,0,0};/* Creating and
initialising*/
  long int i,x;
  time_t init,now,temp;              /* variables */
  int register in = 0;
  int Result,ThisChannel,NextChannel;
  double value[9], oldSO2 = 0.0, oldH2S = 0.0;

  /* Data file format */
  char *FORMAT = "%li\t%.2f\t%.2f\t%.2f\t%.2f\t%.3f\t%.3f\n";
  FILE *resultsfile;

  InitialiseCard( );
  InitInputs(3,8,0);  /* (FirstChannel, LastChannel, ChannelGain) */

  switch (argc)       /* Puts result data to results.dat by default
*/
```

```
{                    /* if no filename specified */
    case 1:
     resultsfile = fopen("results.dat","w");
     break;
    case 2:
     resultsfile = fopen(argv[1],"w");
     break;
    default:
     printf("Wrong number of arguments\n");
     printf("Usage:  1: getnumb     \n");
     printf("        2: getnumb [filename]\n");
     exit (1);
}

fprintf ( resultsfile, "#Time\tH2S\tCO2\tCO\tSO2\tO2\tTCD\n" );

clrscr();   /* Clears screen */

time (&init);

while (1)  /* Loops until 0 returned */
{
   if ( kbhit ())  /* Stops program if ESC pressed */
    if ((in = getch()) == '\x1B')
       return(0);

   time(&temp);
   time(&now);

   for (i=0;i<9;++i)  /* Sets totals and counts back at zero */
   {
    value[i] = 0.0;
    count[i] = 0;
   }


   while(difftime(now,temp)<1)
   {
    /* Reads each value in and puts it into the variable
'Result'*/
    GetNextInput( &Result, &ThisChannel, &NextChannel);

    switch(ThisChannel)   /* Adds values to their respective
variables */
    {
       case 3:                          /* Ch. 3 is H2S */
          value[3] += (double)Result;  /* Running total */
          count[3]++;                  /* Number of readings */
          break;
       case 4:
          value[4] += (double)Result;  /* CO2 */
          count[4]++;
          break;
       case 5:
          value[5] += (double)Result;  /* CO */
          count[5]++;
          break;
       case 6:
          value[6] += (double)Result;  /* SO2 */
          count[6]++;
          break;
       case 7:
```

```
            value[7] += (double)Result;  /* O2 */
            count[7]++;
            break;
         case 8:
            value[8] += (double)Result;  /* TCD output */
            count[8]++;
            break;
       }
       time(&now);
      }

      for ( i=3; i<9; ++i)    /* Calculates average reading on each
channel */
       value[i] /= count[i];

      value[3] -= 205;        /*  Linear relationships of the form
y=mx+c  */
      value[3] /= 0.3261;     /*  between the analogue output from the
meter */
      value[4] -= 204.0;      /*  and the actual gas concn. reading
*/
      value[4] /= 1.634;      /*  First values are c, second are m
*/
      value[5] -= 205;
      value[5] /= 0.8152;
      value[6] -= -203.0;
      value[6] /= -0.935;
      value[7] -= 203;
      value[7] /= 32.73;
      value[8] -= 0.669;
      value[8] /= 5.514;

      time(&now);
      x = difftime(now,init);/* converts into integer */

      /* Sets the form of the readout */
      gotoxy(1,4); /* position */
      printf("\nGas\t\tH2S\tCO2\tCO\tSO2\tO2\tTCD\t\t\n\n");
      printf("Reading\t\t%.2f\t%.2f\t%.2f\t%.2f\t%.3f\t%.3f
\t\n\n",
             value[3],value[4], value[5], value[6], value[7],
value[8]);
      printf("Units\t\tppm\tppm\tppm\tppm\tvol%\tvol%\t\t\n\n");
      printf("Reading Number\t\t%i\t\t\t\t",x);


      /* Takes data point every 10s or if specified value deviates
from the
      previous by a given amount */

      if (x%10==0 || (oldSO2 - value[6])>1 || (-oldSO2 + value[6])>1
||
                 (oldH2S - value[3])>2.5 || (-oldH2S + value[3])>2.5)
      {
       /* Writes line of data to file */
       fprintf( resultsfile, FORMAT,x, value[3], value[4], value[5],
                               value[6], value[7], value[8]);
       /* Prints the message 'Data Point' every time data is taken */
       printf("   Data Point\t\n");
      }
      else
       printf ("            \t\n");
```

```
      printf ("\n(Press ESC to quit)");

      oldSO2 = value[6];    /* Updates old SO2 reading */
      oldH2S = value[3];
   }
}
```

2. obstpr.c

```
/*
   ------------------------------------------------------------------
------------
   Program: obstpr.c
   Release: 1
   Author: A.P. Harvey
   Last Update: 21-05-95
   Purpose: To receive the readouts from the H2S meter, TCD,
temperature
   controller and 4-way gas meter and to send all these to a data
file,
   without operating the GIV at all. Data points every 10s or when
SO2
   value deviates from previous one by specified amount.
   ------------------------------------------------------------------
------------
*/

#include <stdio.h>
#include <time.h>
#include <stdlib.h>
#include <string.h>

#include "pclface.h"
/*
   ------------------------------------------------------------------
------------
   Main Program
   ------------------------------------------------------------------
------------
*/

int main ( int argc, char *argv[] )
{
  long int count[9] = {0,0,0,0,0,0,0,0,0};/* Creating and
initialising*/
  long int i,x;
  time_t init,now,temp;              /* variables */
  int register in = 0;
  int Result,ThisChannel,NextChannel;
  double value[9], oldSO2 = 0.0, oldH2S = 0.0;

  /* Data file format */
  char *FORMAT = "%li\t%.2f\t%.2f\t%.2f\t%.2f\t%.3f\t%.3f\n";
  FILE *resultsfile;

  InitialiseCard( );
  InitInputs(3,8,0);  /* (FirstChannel, LastChannel, ChannelGain) */
```

```
  switch (argc)       /* Puts result data to results.dat by default
*/
  {                   /* if no filename specified */
     case 1:
      resultsfile = fopen("results.dat","w");
      break;
     case 2:
      resultsfile = fopen(argv[1],"w");
      break;
     default:
      printf("Wrong number of arguments\n");
      printf("Usage:  1: getnumb     \n");
      printf("        2: getnumb [filename]\n");
      exit (1);
  }

  fprintf ( resultsfile, "Time\tH2S\tCO2\tCO\tSO2\tO2\tTCD\n");

  clrscr();   /* Clears screen */

  time (&init);

  while (1)  /* Loops until 0 returned */
  {
     if ( kbhit ())  /* Stops program if ESC pressed */
      if ((in = getch()) == '\x1B')
         return(0);

     time(&temp);
     time(&now);

     for (i=0;i<9;++i)  /* Sets totals and counts back at zero */
     {
      value[i] = 0.0;
      count[i] = 0;
     }


     while(difftime(now,temp)<1)
     {
      /* Reads each value in and puts it into the variable
'Result'*/
      GetNextInput( &Result, &ThisChannel, &NextChannel);

      switch(ThisChannel)   /* Adds values to their respective
variables */
      {
         case 3:                          /* Ch. 3 is H2S */
            value[3] += (double)Result;   /* Running total */
            count[3]++;                   /* Number of readings */
            break;
         case 4:
            value[4] += (double)Result;   /* CO2 */
            count[4]++;
            break;
         case 5:
            value[5] += (double)Result;   /* CO */
            count[5]++;
            break;
         case 6:
            value[6] += (double)Result;   /* SO2 */
```

```
            count[6]++;
            break;
         case 7:
            value[7] += (double)Result;  /* O2 */
            count[7]++;
            break;
         case 8:
            value[8] += (double)Result;  /* TCD output */
            count[8]++;
            break;
       }
       time(&now);
      }

      for ( i=3; i<9; ++i)     /* Calculates average reading on each
channel */
       value[i] /= count[i];

      value[3] -= 205;        /*  Linear relationships of the form
y=mx+c  */
      value[3] /= 0.3261;     /*  between the analogue output from the
meter */
      value[4] -= 204.0;      /*  and the actual gas concn. reading
*/
      value[4] /= 1.634;      /*  First values are c, second are m
*/
      value[5] -= 205;
      value[5] /= 0.8152;
      value[6] -= -203.0;
      value[6] /= -0.935;
      value[7] -= 203;
      value[7] /= 32.73;
      value[8] -= 0.669;
      value[8] /= 5.514;

      time(&now);
      x = difftime(now,init);/* converts into integer */

      /* Sets the form of the readout */
      gotoxy(1,4); /* position */
      printf("\nGas\t\tH2S\tCO2\tCO\tSO2\tO2\tTCD\n\n");
      printf("Reading\t\t%.2f\t%.2f\t%.2f\t%.2f\t%.3f\t%.3f   \n\n",
             value[3],value[4], value[5], value[6], value[7],
value[8]);
      printf("Units\t\tppm\tppm\tppm\tppm\tvol%\tvol%\n\n");
      printf("Reading Number\t\t%i",x);


      /* Takes data point every 10s or if specified value deviates
from the
      previous by a given amount */

      /*if (x%10==0 || (oldSO2 - value[6])>1 || (-oldSO2 +
value[6])>1 ||
                  (oldH2S - value[3])>2.5 || (-oldH2S + value[3])>2.5)
      {*/
       /* Writes line of data to file */
       fprintf( resultsfile, FORMAT,x, value[3], value[4], value[5],
                              value[6], value[7], value[8]);
       /* Prints the message 'Data Point' every time data is taken */
       printf("   Data Point\n");
      /*}
```

```
      else
       printf ("                                \n");*/

      printf ("\n(Press ESC to quit)");

      oldSO2 = value[6];   /* Updates old SO2 reading */
      oldH2S = value[3];
   }
}
```

3. 3way.c

```
/*
   ------------------------------------------------------------------
------------
   Program: 3way.c
   Release: 1
   Author: A.P. Harvey
   Last Update: 14-05-97
   Purpose: To try out the new 3-way solenoid for red->ox and v.v.
switching.
   ------------------------------------------------------------------
------------
*/

#include <stdio.h>
#include <time.h>
#include <stdlib.h>
#include <string.h>

#include "pclface.h"
/*
   ------------------------------------------------------------------
------------
   Main Program
   ------------------------------------------------------------------
------------
*/

int main ( int argc, char *argv[] )
{
  long int count[9] = {0,0,0,0,0,0,0,0,0};/* Creating and
initialising*/
  long int i,x;
  time_t init,now,temp;              /* variables */
  int register in = 0;
  int Result,ThisChannel,NextChannel;
  double value[9], oldSO2 = 10.0;
  char c;

  /* Data file format */
  char *FORMAT = "%li\t%.2f\t%.2f\t%.2f\t%.2f\t%.3f\t%.2f\n";
  FILE *resultsfile;

  InitialiseCard( );
  InitInputs(3,8,0);  /* (FirstChannel, LastChannel, ChannelGain) */
```

```
  switch (argc)       /* Puts result data to results.dat by default
*/
  {                   /* if no filename specified */
     case 1:
      resultsfile = fopen("results.dat","w");
      break;
     case 2:
      resultsfile = fopen(argv[1],"w");
      break;
     default:
      printf("Wrong number of arguments\n");
      printf("Usage:  1: getnumb     \n");
      printf("        2: getnumb [filename]\n");
      exit (1);
  }

  clrscr();   /* Clears screen */

  time (&init);


  gotoxy(1,4);
  printf("Press A for Air, H for 5% H2 in N2 flow\n\n");
  scanf ("%c",&c);
  printf("%c",c);


  /* Screen display */
  gotoxy (1,4);
  if ( c=='a'||c=='A')
  {
      printf("\nAir Flowing\n\nESC to stop this program");
      DigitalOutput(0,0);
  }

  if ( c=='h'||c=='H')
  {
      printf ("\n5% Hydrogen in Nitrogen Flowing\n\nESC to stop this
program");
      DigitalOutput(8,0);
  }

  while (1)  /* Loops until 0 returned */
  {
     if ( kbhit ())  /* Stops program if ESC pressed */
     {
      if ((in = getch()) == '\x1B')
      {
         return(0);
      }
     }

  }
}
```

4. flush.c

```
/*
```

```
   ------------------------------------------------------------------
------------
   Program: flush.c
   Release: 1
   Author: A.P. Harvey
   Last Update: 20-08-96
   Purpose: To flush out the sample loop with sample gas.
   ------------------------------------------------------------------
------------
*/

#include <stdio.h>
#include <time.h>
#include <stdlib.h>
#include <string.h>

#include "pclface.h"
/*
   ------------------------------------------------------------------
------------
   Main Program
   ------------------------------------------------------------------
------------
*/

int main ( int argc, char *argv[] )
{
  long int count[9] = {0,0,0,0,0,0,0,0,0};/* Creating and
initialising*/
  long int i,x;
  time_t init,now,temp;              /* variables */
  int register in = 0;
  int Result,ThisChannel,NextChannel;
  double value[9], oldSO2 = 10.0;

  /* Data file format */
  char *FORMAT = "%li\t%.2f\t%.2f\t%.2f\t%.2f\t%.3f\t%.2f\n";
  FILE *resultsfile;

  InitialiseCard( );
  InitInputs(3,8,0);  /* (FirstChannel, LastChannel, ChannelGain) */

  switch (argc)       /* Puts result data to results.dat by default
*/
  {                   /* if no filename specified */
     case 1:
      resultsfile = fopen("results.dat","w");
      break;
     case 2:
      resultsfile = fopen(argv[1],"w");
      break;
     default:
      printf("Wrong number of arguments\n");
      printf("Usage:  1: getnumb     \n");
      printf("        2: getnumb [filename]\n");
      exit (1);
  }

  clrscr();   /* Clears screen */
  gotoxy(1,4);
  printf("Press Esc to stop flush\r");
```

```
  time (&init);

  DigitalOutput(0,0); /* De-activates GIV */

  while (1)  /* Loops until 0 returned */
  {
     if ( kbhit ())  /* Stops program if ESC pressed */
     if ((in = getch()) == '\x1B')
     {
         DigitalOutput(0,0);
         return(0);
     }

     DigitalOutput(5,0);
  }
}
```

5. 1pulse.c

```
/*
   ------------------------------------------------------------------
------------
   Program: 1pulse.c
   Release: 1
   Author: A.P. Harvey
   Last Update: 1-06-95
   Purpose: To receive the readouts from the H2S meter, TCD,
temperature
   controller and 4-way gas meter and to send all these to a data
file.
   Modification: 1 pulse after 100s ( to observe baseline drift ),
and
   no other action. Data points every 10s then every 1s during pulse
obs.
   ------------------------------------------------------------------
------------
*/

#include <stdio.h>
#include <time.h>
#include <stdlib.h>
#include <string.h>

#include "pclface.h"
/*
   ------------------------------------------------------------------
------------
   Main Program
   ------------------------------------------------------------------
------------
*/

int main ( int argc, char *argv[] )
{
  long int count[9] = {0,0,0,0,0,0,0,0,0};/* Creating and
initialising*/
  long int i,x;
  time_t init,now,temp;              /* variables */
```

```
  int register in = 0;
  int Result,ThisChannel,NextChannel;
  double value[9], oldSO2 = 10.0;
  int n=0;

  /* Data file format */
  char *FORMAT = "%li\t%.2f\t%.2f\t%.2f\t%.2f\t%.3f\t%.2f\n";
  FILE *resultsfile;

  InitialiseCard( );
  InitInputs(3,8,0);  /* (FirstChannel, LastChannel, ChannelGain) */

  switch (argc)       /* Puts result data to results.dat by default
*/
  {                   /* if no filename specified */
     case 1:
      resultsfile = fopen("1pulse.dat","w");
      break;
     case 2:
      resultsfile = fopen(argv[1],"w");
      break;
     default:
      printf("Wrong number of arguments\n");
      printf("Usage:  1: getnumb     \n");
      printf("        2: getnumb [filename]\n");
      exit (1);
  }

  clrscr();   /* Clears screen */

  time (&init);

  DigitalOutput(0,0); /* De-activates GIV (exact position is
known(?))*/

  while (1)  /* Loops until 0 returned */
  {
     if ( kbhit ())  /* Stops program if ESC pressed */
      if ((in = getch()) == '\x1B')
         return(0);

     time(&temp);
     time(&now);

     for (i=0;i<9;++i)  /* Sets totals and counts back at zero */
     {
      value[i] = 0.0;
      count[i] = 0;
     }


     while(difftime(now,temp)<1)
     {
      /* Reads each value in and puts it into the variable
'Result'*/
      GetNextInput( &Result, &ThisChannel, &NextChannel);

      switch(ThisChannel)   /* Adds values to their respective
variables */
      {
         case 3:                          /* Ch. 3 is H2S */
            value[3] += (double)Result;  /* Running total */
```

```
            count[3]++;                    /* Number of readings */
            n++;
            break;
         case 4:
            value[4] += (double)Result;  /* CO2 */
            count[4]++;
            break;
         case 5:
            value[5] += (double)Result;  /* CO */
            count[5]++;
            break;
         case 6:
            value[6] += (double)Result;  /* SO2 */
            count[6]++;
            break;
         case 7:
            value[7] += (double)Result;  /* O2 */
            count[7]++;
            break;
         case 8:
            value[8] += (double)Result;  /* TCD output */
            count[8]++;
            break;
       }
       time(&now);
      }

      gotoxy (1,4);       /* Sets position of readout */

      for ( i=3; i<9; ++i)     /* Calculates average reading on each
channel */
       value[i] /= count[i];

      value[3] -= 205;         /* Linear relationships of the form
y=mx+c */
      value[3] /= 0.3261;       /* between the analogue output from
the meter */
      value[4] -= 204.0;       /* and the actual gas concn. reading */
      value[4] /= 1.634;       /* First values are c, second are m */
      value[5] -= 205;
      value[5] /= 1.246;
      value[6] -= -203.0;
      value[6] /= -0.937;
      value[7] -= 203;
      value[7] /= 32.73;

      time(&now);
      x = difftime(now,init);  /* converts time into integer */

      /* Sets the form of the readout */
      printf("\nGas\t\tH2S\tCO2\tCO\tSO2\tO2\tTCD(Hyd.) \n\n");
      printf("Reading\t\t%.2f\t%.2f\t%.2f\t%.2f\t%.3f\t%.2f\n\n",
            value[3],value[4], value[5], value[6], value[7],
value[8]);
      printf("Units\t\tppm\tppm\tppm\tppm\tvol%\tvol%\n\n");
      printf("Reading Number\t\t%i\n\n",x);
      printf("Counts per second\t%i",n);

      /* Takes data point every 10s before 100s and every second
thereafter.
      First 100s examining drift, then pulse at 100s, then
examination of
```

```
      pulse shape */

      if ( x%10==0 || x>50)
      {
       /* Writes line of data to file */
       fprintf( resultsfile, FORMAT,x, value[3], value[4], value[5],
                              value[6], value[7], value[8]);
       /* Prints the message 'Data Point' every time data is taken */
       printf("   Data Point\n");
      }
      else
       printf ("                                \n");

      printf ("\n(Press ESC to quit)");

      oldSO2 = value[6];   /* Updates old SO2 reading */


      if ( x == 50)    /* Pulse at 50s */
       DigitalOutput(6,0);
      else if ( x == 42 )
       DigitalOutput(4,0);
      else if ( x == 46 )
       DigitalOutput(0,0);
      else if ( x == 48 )
       DigitalOutput(5,0);
      else if ( x == 52 )
       DigitalOutput(0,0);


      n = 0;

  }
}
```

6. nonavge.c

```
/*
   ------------------------------------------------------------------
------------
   Program: nonavge.c
   Release: 1
   Author: A.P. Harvey
   Last Update: 4-09-95
   Purpose: As per 1pulse.c, but testing out the merits of using the
last
   reading rather than an average over the last second. This should
be
   particularly important when analysing peak shapes.
   ------------------------------------------------------------------
------------
*/

#include <stdio.h>
#include <time.h>
#include <stdlib.h>
#include <string.h>
```

```
#include "pclface.h"
/*
   ------------------------------------------------------------------
------------
   Main Program
   ------------------------------------------------------------------
------------
*/

int main ( int argc, char *argv[] )
{
  long int count[9] = {0,0,0,0,0,0,0,0,0};/* Creating and
initialising*/
  long int i,x;
  time_t init,now,temp;              /* variables */
  int register in = 0;
  int Result,ThisChannel,NextChannel;
  double value[9], oldSO2 = 10.0;

  /* Data file format */
  char *FORMAT = "%li\t%.2f\t%.2f\t%.2f\t%.2f\t%.3f\t%.2f\n";
  FILE *resultsfile;

  InitialiseCard( );
  InitInputs(3,8,0);  /* (FirstChannel, LastChannel, ChannelGain) */

  switch (argc)       /* Puts result data to results.dat by default
*/
  {                   /* if no filename specified */
     case 1:
      resultsfile = fopen("1pulse.dat","w");
      break;
     case 2:
      resultsfile = fopen(argv[1],"w");
      break;
     default:
      printf("Wrong number of arguments\n");
      printf("Usage:  1: getnumb     \n");
      printf("        2: getnumb [filename]\n");
      exit (1);
  }

  clrscr();   /* Clears screen */

  time (&init);

/*  DigitalOutput(0,0);*/ /* De-activates GIV (exact position is
known)*/

  while (1)  /* Loops until 0 returned */
  {
     if ( kbhit ())  /* Stops program if ESC pressed */
      if ((in = getch()) == '\x1B')
         return(0);

     time(&temp);
     time(&now);

     for (i=0;i<9;++i)  /* Sets totals and counts back at zero */
     {
      value[i] = 0.0;
      count[i] = 0;
```

```
      }


      while(difftime(now,temp)<1)
      {
       /* Reads each value in and puts it into the variable
'Result'*/
       GetNextInput( &Result, &ThisChannel, &NextChannel);

       switch(ThisChannel)   /* Adds values to their respective
variables */
       {
          case 3:                          /* Ch. 3 is H2S */
             value[3] = (double)Result;  /* Running total */
             count[3]++;                  /* Number of readings */
             break;
          case 4:
             value[4] = (double)Result;  /* CO2 */
             count[4]++;
             break;
          case 5:
             value[5] = (double)Result;  /* CO */
             count[5]++;
             break;
          case 6:
             value[6] = (double)Result;  /* SO2 */
             count[6]++;
             break;
          case 7:
             value[7] = (double)Result;  /* O2 */
             count[7]++;
             break;
          case 8:
             value[8] = (double)Result;  /* TCD output */
             count[8]++;
             break;
       }
       time(&now);
      }

      gotoxy (1,4);       /* Sets position of readout */


/* averaging commented out */
/*      for ( i=3; i<9; ++i)     Calculates average reading on each
channel
       value[i] /= count[i]; */

      value[3] -= 205;         /* Linear relationships of the form
y=mx+c */
      value[3] /= 0.3261;       /* between the analogue output from
the meter */
      value[4] -= 204.0;       /* and the actual gas concn. reading */
      value[4] /= 1.634;       /* First values are c, second are m */
      value[5] -= 204;
      value[5] /= 1.246;
      value[6] -= -203.00;
      value[6] /= -0.937;
      value[7] -= 203.00;
      value[7] /= 32.73;

      time(&now);
```

```
      x = difftime(now,init);  /* converts time into integer */

      /* Sets the form of the readout */
      printf("\nGas\t\tH2S\tCO2\tCO\tSO2\tO2\tTCD(Hyd.) \n\n");
      printf("Reading\t\t%.2f\t%.2f\t%.2f\t%.2f\t%.3f\t%.2f\n\n",
             value[3],value[4], value[5], value[6], value[7],
value[8]);
      printf("Units\t\tppm\tppm\tppm\tppm\tvol%\tvol%\n\n");
      printf("Reading Number\t\t%i",x);

      /* Takes data point every 10s before 100s and every second
thereafter.
      First 100s examining drift, then pulse at 100s, then
examination of
      pulse shape */

      if ( x%10==0 || x>100)
      {
       /* Writes line of data to file */
       fprintf( resultsfile, FORMAT,x, value[3], value[4], value[5],
                             value[6], value[7], value[8]);
       /* Prints the message 'Data Point' every time data is taken */
       printf("   Data Point\n");
      }
      else
       printf ("                              \n");

      printf ("\n(Press ESC to quit)");

      oldSO2 = value[6];   /* Updates old SO2 reading */


      if ( x == 100)    /* Pulse at 100s */
       DigitalOutput(2,0);
      else if ( x == 75 ) /* Sample loop filling position at 75s*/
       DigitalOutput(1,0);

  }
}
```

7. switch.c

```
/*
   ------------------------------------------------------------------
------------
   Program: switch.c
   Release: 1
   Author: A.P. Harvey
   Last Update: 14-05-97
   Purpose: To receive the readouts from the H2S meter, TCD,
temperature
   controller and 4-way gas meter and to send all these to a data
file.
   To test out new solenoid.
   Latest alteration to include 3-way solenoid for automatic
switchover.
   ------------------------------------------------------------------
------------
```

```
*/

#include <stdio.h>
#include <time.h>
#include <stdlib.h>
#include <string.h>

#include "pclface.h"
/*
   ------------------------------------------------------------------
------------
   Main Program
   ------------------------------------------------------------------
------------
*/

int main ( int argc, char *argv[] )
{
  long int count[9] = {0,0,0,0,0,0,0,0,0};/* Creating and
initialising*/
  long int i,x;
  time_t init,now,temp;              /* variables */
  int register in = 0;
  int Result,ThisChannel,NextChannel;
  double unaver = 0.0, realH2S, value[9], oldSO2, oldH2S, oldtcd;

  /* Data file format */
  char *FORMAT = "%li\t%.2f\t%.2f\t%.2f\t%.2f\t%.3f\t%.3f\n";
  FILE *resultsfile;

  InitialiseCard( );
  InitInputs(3,8,0);  /* (FirstChannel, LastChannel, ChannelGain) */

  switch (argc)       /* Puts result data to results.dat by default
*/
  {                   /* ie no filename specified */
     case 1:
      resultsfile = fopen("results.dat","w");
      break;
     case 2:
      resultsfile = fopen(argv[1],"w");
      break;
     default:
      printf("Wrong number of arguments\n");
      printf("Usage:  1: getnumb     \n");
      printf("        2: getnumb [filename]\n");
      exit (1);
  }

  fprintf (resultsfile, "#Time\tH2S\tCO2\tCO\tSO2\tO2\tTCD\n");

  clrscr();   /* Clears screen */

  time (&init);

  DigitalOutput(0,0); /* De-activates GIV */

  while (1)  /* Loops until 0 returned */
  {
     if ( kbhit ())  /* Stops program if ESC pressed */
      if ((in = getch()) == '\x1B')
         return(0);
```

```
     time(&temp);
     time(&now);

     for (i=0;i<9;++i)  /* Sets totals and counts back at zero */
     {
      value[i] = 0.0;
      count[i] = 0;
     }


     while(difftime(now,temp)<1)
     {
      /* Reads each value in and puts it into the variable
'Result'*/
      GetNextInput( &Result, &ThisChannel, &NextChannel);

      switch(ThisChannel)   /* Adds values to their respective
variables */
      {
         case 3:              /* Ch. 3 is H2S */
            realH2S = (double)Result;     /* unaveraged */
            value[3] += (double)Result;   /* Running total */
            count[3]++;                   /* Number of readings */
            break;
         case 4:
            value[4] += (double)Result;   /* CO2 */
            count[4]++;
            break;
         case 5:
            value[5] += (double)Result;   /* CO */
            count[5]++;
            break;
         case 6:
            unaver = (double)Result;       /* UNAVERAGED */
            value[6] += (double)Result;   /* SO2 */
            count[6]++;
            break;
         case 7:
            value[7] += (double)Result;   /* O2 */
            count[7]++;
            break;
         case 8:
            value[8] += (double)Result;   /* TCD output */
            count[8]++;
            break;
      }
      time(&now);
     }

     for ( i=3; i<9; ++i)    /* Calculates average reading on each
channel */
      value[i] /= count[i];

     value[3] -= 205;       /*  Linear relationships of the form
y=mx+c  */
     value[3] /= 0.3261;    /*  between the analogue output from the
meter */
     realH2S -= 205;
     realH2S /= 0.3261;
     value[4] -= 204.0;     /*  and the actual gas concn. reading
*/
```

```
      value[4] /= 1.634;      /*  First values are c, second are m
*/
      value[5] -= 205;
      value[5] /= 0.8152;
      value[6] -= -203.0;
      value[6] /= -0.935;
      unaver -= -203.0;
      unaver /= -0.935;
      value[7] -= 203;
      value[7] /= 32.73;
      value[8] -= 1.000;
      value[8] /= 5.514;

      time(&now);
      x = difftime(now,init); /* converts time into integer */

      /* Sets the form of the readout */
      gotoxy(1,4); /* position */
      printf("\nGas\t\tH2S\tCO2\tCO\tSO2\tO2\tTCD\n\n");
      printf("Reading\t\t%.2f\t%.2f\t%.2f\t%.2f\t%.3f\t%.3f   \n\n",
             realH2S,value[4], value[5], unaver, value[7], value[8]);
      printf("Units\t\tppm\tppm\tppm\tppm\tvol%\tvol%\n\n");
      printf("Reading Number\t\t%i",x);


      /* Takes data point every 10s or if specified value deviates
from the
      previous by a given amount */

      if (x%10==0 || (oldSO2 - value[6]) >1 || (-oldSO2 + value[6])>1
        || (oldH2S - value[3]) >1 || (-oldH2S + value[3]) >1 ||
x>=1000
        || (oldtcd - value[8]) >0.05 || (-oldtcd + value[8]) >0.05 )
      {
       /* Writes line of data to file */
       fprintf( resultsfile, FORMAT,x, value[3], value[4], value[5],
                              value[6], value[7], value[8]);
       /* Prints the message 'Data Point' every time data is taken */
       printf("   Data Point\n");
      }
      else
       printf ("                                \n");

      printf ("\n(Press ESC to quit)");

      oldSO2 = value[6];   /* Updates old SO2 reading */
      oldH2S = value[3];   /* Updates old H2S reading */
      oldtcd = value[8];

      if ( x<=1000)
      {
       if ( x == 1)       /* 0s sample gas shutoff */
             DigitalOutput(0,0);
       else if ( x == 12 )
             DigitalOutput(4,0);
       else if ( x == 16)
             DigitalOutput(0,0);
       else if ( x%100 == 19 ) /* Goes to sample loop filling
position */
             DigitalOutput(5,0);  /* every 100s for 1s before
injection */
       else if ( x%100 == 20 )
```

```
            DigitalOutput(6,0); /* Injection */
       else if ( x%100 == 21 )
            DigitalOutput(0,0); /* Shutoff */
      }
      else
      {
       DigitalOutput(8,0);
      }
   }
}
```

8. ambpulse.c

```
/*
   ------------------------------------------------------------------
------------
   Program: ambpulse.c
   Release: 1
   Author: A.P. Harvey
   Last Update: 17-05-96
   Purpose: To receive the readouts from the H2S meter, TCD,
temperature
   controller and 4-way gas meter and to send all these to a data
file.
   Modification: 1 pulse after 100s ( to observe baseline drift ),
and
   no other action. Data points every 10s then every 1s during pulse
obs.

   Differs from 1pulse.c in that sample loop is allowed to reach
ambient P.
   ------------------------------------------------------------------
------------
*/

#include <stdio.h>
#include <time.h>
#include <stdlib.h>
#include <string.h>

#include "pclface.h"
/*
   ------------------------------------------------------------------
------------
   Main Program
   ------------------------------------------------------------------
------------
*/

int main ( int argc, char *argv[] )
{
  long int count[9] = {0,0,0,0,0,0,0,0,0};/* Creating and
initialising*/
  long int i,x;
  time_t init,now,temp;              /* variables */
  int register in = 0;
  int Result,ThisChannel,NextChannel;
  double value[9], oldSO2 = 10.0;
```

```
   int n=0;


   /* Data file format */
   char *FORMAT1 = "%c\t%c\t%c\t%c\t%c\t%c\t%c";
   char *FORMAT = "%li\t%.2f\t%.2f\t%.2f\t%.2f\t%.3f\t%.2f\n";
   FILE *resultsfile;

   InitialiseCard( );
   InitInputs(3,8,0);  /* (FirstChannel, LastChannel, ChannelGain) */

   switch (argc)       /* Puts result data to results.dat by default
*/
   {                   /* if no filename specified */
      case 1:
       resultsfile = fopen("1pulse.dat","w");
       break;
      case 2:
       resultsfile = fopen(argv[1],"w");
       break;
      default:
       printf("Wrong number of arguments\n");
       printf("Usage:  1: getnumb     \n");
       printf("        2: getnumb [filename]\n");
       exit (1);
   }

   fprintf (resultsfile,"#Time\tH2S\tCO2\tCO\tSO2\tO2\tTCD\n");

   clrscr();   /* Clears screen */

   time (&init);

  DigitalOutput(0,0); /* De-activates GIV (exact position is
known(?))*/

  while (1)  /* Loops until 0 returned */
  {
     if ( kbhit ())  /* Stops program if ESC pressed */
      if ((in = getch()) == '\x1B')
         return(0);

     time(&temp);
     time(&now);

     for (i=0;i<9;++i)  /* Sets totals and counts back at zero */
     {
      value[i] = 0.0;
      count[i] = 0;
     }


    while(difftime(now,temp)<1)
    {
     /* Reads each value in and puts it into the variable
'Result'*/
     GetNextInput( &Result, &ThisChannel, &NextChannel);

     switch(ThisChannel)   /* Adds values to their respective
variables */
     {
```

```
            case 3:                              /* Ch. 3 is H2S */
               value[3] += (double)Result;       /* Running total */
               count[3]++;                       /* Number of readings */
               n++;
               break;
            case 4:
               value[4] += (double)Result;       /* CO2 */
               count[4]++;
               break;
            case 5:
               value[5] += (double)Result;       /* CO */
               count[5]++;
               break;
            case 6:
               value[6] += (double)Result;       /* SO2 */
               count[6]++;
               break;
            case 7:
               value[7] += (double)Result;       /* O2 */
               count[7]++;
               break;
            case 8:
               value[8] += (double)Result;       /* TCD output */
               count[8]++;
               break;
         }
         time(&now);
        }

        gotoxy (1,4);       /* Sets position of readout */

        for ( i=3; i<9; ++i)     /* Calculates average reading on each
channel */
         value[i] /= count[i];

        value[3] -= 205;         /* Linear relationships of the form
y=mx+c */
        value[3] /= 0.3261;       /* between the analogue output from
the meter */
        value[4] -= 204.0;       /* and the actual gas concn. reading */
        value[4] /= 1.634;       /* First values are c, second are m */
        value[5] -= 205;
        value[5] /= 1.246;
        value[6] -= -203.0;
        value[6] /= -0.937;
        value[7] -= 203;
        value[7] /= 32.73;

        time(&now);
        x = difftime(now,init);  /* converts time into integer */

        /* Sets the form of the readout */
        printf("\nGas\t\tH2S\tCO2\tCO\tSO2\tO2\tTCD(Hyd.) \n\n");
        printf("Reading\t\t%.2f\t%.2f\t%.2f\t%.2f\t%.3f\t%.2f\n\n",
               value[3],value[4], value[5], value[6], value[7],
value[8]);
        printf("Units\t\tppm\tppm\tppm\tppm\tvol%\tvol%\n\n");
        printf("Reading Number\t\t%i\n\n",x);
        printf("Counts per second\t%i",n);

        /* Takes data point every 10s before 50s and every second
thereafter.
```

```
      First 50s examining drift, then pulse at 50s, then examination
of
      pulse shape */

      if ( x%10==0 || x>50)
      {
       /* Writes line of data to file */
       fprintf( resultsfile, FORMAT,x, value[3], value[4], value[5],
                              value[6], value[7], value[8]);
       /* Prints the message 'Data Point' every time data is taken */
       printf("   Data Point\n");
      }
      else
       printf ("                                \n");

      printf ("\n(Press ESC to quit)");

      oldSO2 = value[6];   /* Updates old SO2 reading */


      if ( x == 50)    /* Pulse at 50s */
       DigitalOutput(2,0);
      else if ( x == 42 )
       DigitalOutput(4,0);
      else if ( x == 46 )
       DigitalOutput(0,0);
      else if ( x == 48 )
       DigitalOutput(1,0);
      else if ( x == 52 )
       DigitalOutput(0,0);


      n = 0;

   }
}
```

9. sol-try.c

```
/*
   ------------------------------------------------------------------
------------
   Program: sol-try.c
   Release: 1
   Author: A.P. Harvey
   Last Update: 21-05-95
   Purpose: To receive the readouts from the H2S meter, TCD,
temperature
   controller and 4-way gas meter and to send all these to a data
file.
   To test out new solenoid.
   ------------------------------------------------------------------
------------
*/

#include <stdio.h>
#include <time.h>
#include <stdlib.h>
```

```
#include <string.h>

#include "pclface.h"
/*
   ------------------------------------------------------------------------
------------
   Main Program
   ------------------------------------------------------------------------
------------
*/

int main ( int argc, char *argv[] )
{
  long int count[9] = {0,0,0,0,0,0,0,0,0};/* Creating and
initialising*/
  long int i,x;
  time_t init,now,temp;              /* variables */
  int register in = 0;
  int Result,ThisChannel,NextChannel;
  double unaver = 0.0, realH2S, value[9], oldSO2, oldH2S, oldtcd;

  /* Data file format */
  char *FORMAT = "%li\t%.2f\t%.2f\t%.2f\t%.2f\t%.3f\t%.3f\n";
  FILE *resultsfile;

  InitialiseCard( );
  InitInputs(3,8,0);  /* (FirstChannel, LastChannel, ChannelGain) */

  switch (argc)       /* Puts result data to results.dat by default
*/
  {                   /* if no filename specified */
     case 1:
      resultsfile = fopen("results.dat","w");
      break;
     case 2:
      resultsfile = fopen(argv[1],"w");
      break;
     default:
      printf("Wrong number of arguments\n");
      printf("Usage:  1: getnumb     \n");
      printf("        2: getnumb [filename]\n");
      exit (1);
  }

  fprintf ( resultsfile ,"#Time\tH2S\tCO2\tCO\tSO2\tO2\tTCD\n");

  clrscr();   /* Clears screen */

  time (&init);

  DigitalOutput(0,0); /* De-activates GIV */

  while (1)  /* Loops until 0 returned */
  {
     if ( kbhit ())  /* Stops program if ESC pressed */
      if ((in = getch()) == '\x1B')
         return(0);

     time(&temp);
     time(&now);

     for (i=0;i<9;++i)  /* Sets totals and counts back at zero */
```

```
      {
       value[i] = 0.0;
       count[i] = 0;
      }


      while(difftime(now,temp)<1)
      {
       /* Reads each value in and puts it into the variable
'Result'*/
       GetNextInput( &Result, &ThisChannel, &NextChannel);

       switch(ThisChannel)   /* Adds values to their respective
variables */
       {
          case 3:              /* Ch. 3 is H2S */
             realH2S = (double)Result;     /* unaveraged */
             value[3] += (double)Result;  /* Running total */
             count[3]++;                  /* Number of readings */
             break;
          case 4:
             value[4] += (double)Result;  /* CO2 */
             count[4]++;
             break;
          case 5:
             value[5] += (double)Result;  /* CO */
             count[5]++;
             break;
          case 6:
             unaver = (double)Result;       /* UNAVERAGED */
             value[6] += (double)Result;  /* SO2 */
             count[6]++;
             break;
          case 7:
             value[7] += (double)Result;  /* O2 */
             count[7]++;
             break;
          case 8:
             value[8] += (double)Result;  /* TCD output */
             count[8]++;
             break;
       }
       time(&now);
      }

      for ( i=3; i<9; ++i)    /* Calculates average reading on each
channel */
       value[i] /= count[i];

      value[3] -= 205;        /*  Linear relationships of the form
y=mx+c  */
      value[3] /= 0.3261;     /*  between the analogue output from the
meter */
      realH2S -= 205;
      realH2S /= 0.3261;
      value[4] -= 204.0;      /*  and the actual gas concn. reading
*/
      value[4] /= 1.634;      /*  First values are c, second are m
*/
      value[5] -= 205;
      value[5] /= 0.8152;
      value[6] -= -203.0;
```

```
      value[6] /= -0.935;
      unaver -= -203.0;
      unaver /= -0.935;
      value[7] -= 203;
      value[7] /= 32.73;
      value[8] -= 1.000;
      value[8] /= 5.514;

      time(&now);
      x = difftime(now,init); /* converts time into integer */

      /* Sets the form of the readout */
      gotoxy(1,4); /* position */
      printf("\nGas\t\tH2S\tCO2\tCO\tSO2\tO2\tTCD\n\n");
      printf("Reading\t\t%.2f\t%.2f\t%.2f\t%.2f\t%.3f\t%.3f   \n\n",
             realH2S,value[4], value[5], unaver, value[7], value[8]);
      printf("Units\t\tppm\tppm\tppm\tppm\tvol%\tvol%\n\n");
      printf("Reading Number\t\t%i",x);


      /* Takes data point every 10s or if specified value deviates
from the
      previous by a given amount */

      if (x%10==0 || (oldSO2 - value[6]) >1 || (-oldSO2 + value[6])>1
              || (oldH2S - value[3]) >1 || (-oldH2S + value[3])>1)
      {
       /* Writes line of data to file */
       fprintf( resultsfile, FORMAT,x, value[3], value[4], value[5],
                              value[6], value[7], value[8]);
       /* Prints the message 'Data Point' every time data is taken */
       printf("   Data Point\n");
      }
      else
       printf ("                                \n");

      printf ("\n(Press ESC to quit)");

      oldSO2 = value[6];   /* Updates old SO2 reading */
      oldH2S = value[3];   /* Updates old H2S reading */
      oldtcd = value[8];

      if ( x == 1) /* 0s sample gas shutoff */
       DigitalOutput(0,0);
      else if ( x == 12 )
       DigitalOutput(4,0);
      else if ( x == 16 )
       DigitalOutput(0,0);
      else if ( x%100 == 19 ) /* Goes to sample loop filling position
*/
       DigitalOutput(5,0);  /* every 100s for 1s before injection */
      else if ( x%100 == 20 )
       DigitalOutput(6,0); /* Injection */
      else if ( x%100 == 21 )
       DigitalOutput(0,0); /* Shutoff */

  }
}
```

7.7 Peak Width Analysis

The TPR peak data presented in section 4.2 were analysed by the method of 'Peak Width Analysis' detailed in Falconer and Schwarz (1983), assuming a first order desorption process (the calculations can easily be performed assuming second order desorption, but the results of this have not been presented here as they generate no further useful information).

The equations used were:

(i) $$\frac{E_d}{RT_{max}} = -1 + \left[1 + \frac{5.832T_{max}^2}{W_{1/2}^2}\right]^{1/2}$$

(ii) $$\frac{E_d}{RT_{max}} = -1 + \left[1 + \frac{2.353T_{max}^2}{W_{3/4}^2}\right]^{1/2}$$

Clearly, all the data required were the temperature of the peak maximum and either the half or three quarters width.

Example: For the desorption of sulphur dioxide by ceria T_{max} = 633 °C, W1/2 = 57 °C and W3/4 = 35.5°C. Hence :

$$E_d(1°)1/2 = RT_{max}\left[-1 + \left[1 + \frac{5.832T_{max}^2}{W_{1/2}^2}\right]^{1/2}\right] = 282 \text{ kJ/mol}$$

$$E_d(1°)3/4 = RT_{max}\left[-1 + \left[1 + \frac{2.353T_{max}^2}{W_{3/4}^2}\right]^{1/2}\right] = 287 \text{ kJ/mol}$$

Analysis of these calculations, assuming an error of +/- ~5 °C on any given temperature measurement, shows that the greatest errors stem from the widths rather than the peak temperature as they are the result of two separate measurements and are thus theoretically prone to errors of +/- 10 °C. For the

calculations given above, the variation in E_d can theoretically be as much as 20 % of the value stated for the half width calculation and 30 % for the three quarter width calculation. This gives some idea of the sensitivity of this technique to the width measurement, particularly for smaller values (as these are). This sensitivity may help to explain some of the discrepancies between the two estimates given in the table in 4.2.